Analysis of skeleton in a mouse model of Rett syndrome

Dr Bushra Kamal
MBBS

Thesis submitted in fulfilment of the requirement for the degree of Doctor of Philosophy
Institute of Neuroscience and Psychology
College of Medical, Veterinary and Life Science
University of Glasgow
Glasgow, G12 8QQ
UK

Acknowledgement

“In the name of Allah Almighty, the most merciful, the most beneficent”

Man is a wonderful creature; he sees through the layers of fat (eyes), hears through a bone (ears) and speaks through a lump of flesh (tongue) - Ali ibn Abi Talib

I owe my deepest gratitude to my supervisors Dr Stuart Cobb and Prof. Anthony Payne for their continuous guidance, advice and constructive criticism. I am also extremely grateful to Prof. Elizabeth Tanner for the exciting learning opportunities, she has provided over the period of 3 years.

I am very thankful to David Russell, Dr Robert Wallace for all their technical assistance and fruitful collaboration.

I have been fortunate to know and work with fantastic people over the past few years. Special thanks go to Dr Mark Bailey, Dr John Shaw-Dunn, Prof William Cushley, Prof David Maxwell, Dr Stuart Macdonald, Dr Katherine price, Dr Paul Rea, Paul Ross, for their kind help and support during the last four years.

I am indebted to Dr Kamal Gadalla, Lesley MacInnes, Elaine Wales, Henry Gu, Thishnapha Vudhironarit, Daniela Minchella, Eva Laura Bogaerts and Sophie Hall for their constant help and personal support during the writing period of this thesis.

My deepest respect, great love and gratitude to my mother **Shaeen Begum**, the most loving, kind, patient and intelligent woman I will ever know. This thesis is dedicated to her. Finally, special thanks and great love goes to my lovely sister Dr Sabin Kamal and dearest, sweet brother Mr Mustafa Kamal without their constant love, prayers and support this whole journey of PhD would have not been possible.

Abstract

Rett Syndrome (RTT) is an X-linked genetic disorder and a major cause of intellectual disability in girls. Mutations in the methyl-CpG binding protein 2 (*MECP2*) gene, are the primary cause of the disorder. Despite the dominant neurological phenotypes that characterise RTT, *MECP2* is expressed ubiquitously throughout the body and a number of peripheral phenotypes such as growth retardation (reduced height and weight), skeletal deformities (scoliosis/kyphosis), reduced bone mass and low energy fractures are also common yet under-reported clinical features of the disorder.

In order to explore whether MeCP2 protein deficiency results in altered structural and functional properties of bone and to test the potential reversibility of any such defects, I have conducted series of histological, imaging and biomechanical tests of bone using an accurate genetic (functional knockout) mouse model of RTT. Initial experiments using a GFP reporter mouse line demonstrated the presence of MeCP2 in bone cells and the effective silencing on the gene in functional knockout mice. Different aspects of the study were conducted in different types of bone tissues that were especially suited for individual assays. For instance, biomechanical three point bending tests were conducted in long bone (femur) whilst trabecular geometry measures were measured in spinal vertebrae.

Both hemizygous *Mecp2*$^{stop/y}$ male mice in which *Mecp2* is silenced in all cells and female *Mecp2*$^{stop/+}$ mice in which *Mecp2* is silenced in ~50% of cells as a consequence of random X-chromosome inactivation (XCI), revealed, lighter and smaller long bones and significant reductions in cortical bone mechanical properties (~ 39.5% reduction in stiffness, 31% reduction in ultimate load and 37% reduction in Young's modulus respectively in *Mecp2*$^{stop/y}$ male mice; %) and material properties (microhardess reduced 12.3% in *Mecp2*$^{stop/y}$ male mice and 14% in*Mecp2*$^{stop/+}$ female mice) as compared to age wild type control mice. Micro structural analysis conducted using µCT also revealed a significant reduction in cortical (54% reduction in cortical thickness, 30% in bone volume, 20% in total area, and 38% in marrow area) and trabecular (~30% in trabecular thickness) bone parameters as compared to age matched wild-type controls MeCP2-deficent mice. Histological analysis using Sirius red staining as a marker of collagen

revealed a ~25% reduction in collagen content in MeCP2 deficient mice as compared to age matched wild type controls.

In experiments designed to establish the potential for reversal of MeCP2-related deficits, unsilencing of *Mecp2* in adult mice by tamoxifen-induced and cre-mediated excision of a stop cassette located at the endogenous Mecp2 locus (male; *Mecp2*$^{stop/y}$*, CreER* and female; *Mecp2*$^{+/stop}$, *CreER*), resulted in a restoration of biomechanical properties towards the wild-type levels. Specifically, Male *Mecp2*$^{stop/y}$*, CreER* mice displayed improvement in mechanical properties (stiffness 40%, ultimate load 10%, young's modulus 61% and micro hardness 12%) and structural bone parameter (trabecular thickness 80%) as compared to *Mecp2*$^{stop/y}$ male mice. Female *Mecp2*$^{+/stop}$, *CreER*, displayed a significant improvement (19%) in microhardess measures as compared to Mecp2 deficient mice.

Overall, the results of my studies show that MeCP2-deficiency results in overt, but potentially reversible, alterations in the biomechanical integrity of bone and highlights the importance of targeting skeletal phenotypes in considering the development of pharmacological and gene-based therapies for Rett Syndrome.

Table of Contents

List of Figures

List of Tables

Author's Declaration

I declare that the work presented in this thesis is entirely my own with all exceptions being clearly indicated or/ and properly cited in the context.

Signature.....

Bushra Kamal

The work has not been presented in part or alone for any other degree programme. Some of the work contained here has been submitted in part to be published:

Bushra Kamal, David Russell, Anthony Payne, Diogo Constante, K. Elizabeth Tanner, Hanna Isaksson, Neashan Mathavan, Stuart R. Cobb, (October 2014) *"Bio-material properties of bone in a mouse model of Rett Syndrome".* Bone Journal, 71, pp 106-114. (doi:10.1016/j.bone.2014.10.008).

Abbreviations

AAV	Adeno-associated virus
ANOVA	Analysis of variance
B-ALP	Bone specific alkaline phosphatase
BMC	Bone mineral content
BMD	Bone mineral density
BMP	Bone morphogenic protein
BSU	Basic structural unit
Ca	Calcium
CAM	Calmodulin
CP	Cerebral Palsy
CpG	Cytosine-guanine dinucleotides
COX	Cycloxygenase
CTD	C terminal domain
CTRs	Calcitonin recptors
CTX	C – terminal telopeptide cross links
CX	Connexion
DNA	4’,6-diamindino-2-phenylindole
DXA	Dual-energy X-ray absorptiometry
ECM	Extracellular matrix

EDTA	Ethylenediaminetetraacetic acid
ERK	Extracellular signal regulated kinase
FAK	Focal adhesion kinase
GFP	Green fluorescent protein
HDAC1	Histone deacetylase inhibitor
MAP	Mitogen activated protein
M-CSF	Macrophage colony stimulating factor
ID	Inter domain
KO	knock out
MBD	Methyl binding domain
MECP2	Human Methyl-CpG-binding protein 2 gene
Mecp2	Mouse Methyl-CpG-binding protein 2 gene
MeCP2	Human Methyl-CpG-binding protein 2 protein
Mecp2	Mouse Methyl-CpG-binding protein 2 protein
MECP2_e1	Methyl-CpG-binding protein 2 isoform e1
MECP2_e2	Methyl-CpG-binding protein 2 isoform e2
NLS	Nuclear localising signal
NO	Nitric oxide
NTD	N- terminal domain

OC	Osteocalcin
ODF	Osteoclast differentiation factors
OI	Osteogenesis imperfecta
OPG	Osteoprotegerin
PBS	Phosphate buffer solution
PGE2	Prostaglandin E2
PINP	N- terminal propeptides of collagen type 1
PTH	Parathyroid hormone
RANK	Receptor activator of nuclear factor- $_{k}$B
RANKL	Receptor activator of nuclear factor- $_{k}$B ligand
RNA	Ribonucleic acid
ROI	Region of interest
RTT	Rett syndrome
SA-CAT	Stretch activated cation channel
SAXS	Small-angle X-ray scattering
SD	Standard deviation
SUV39H	Suppressor of variegation 3-9 homolog1
SEM	Scanning electron microscopy
TGF-β	Tissue growth factor-β

TRAP	Tartrate-resistant acid phosphatase
TRANCE	Tumour necrosis factor related activation induced cytokine
TRD	Transcription repression domain
VEGF	Vascular endothelial growth factor
XCI	X chromosome inactivation
µCT	X-ray microtomgraphy

Chapter 1

General Introduction

Andrea Rett, an Austrian physician, first noticed Rett syndrome (RTT) in 2 young girls as they sat in the waiting room of his clinic. He observed that the children were making the same repetitive hand-washing motions. In 1966, he conducted a comparative review of 22 young females exhibiting similar symptoms and compulsive stereotyped behaviours (Rett, 1966). He proposed the unusual brain atrophy of RTT affected girls is linked to the hyper ammonia in childhood. Later on after a gap of 17 years (in 1983) similar finding were described by Hagberg et al (Hagberg et al., 1983). Dr Hagberg highlighted the findings presented by Andrea Rett including the classical normal growth followed by developmental delay, autism, gait abnormalities, atypical hand movements and microcephaly. He also proposed that the particular occurrence of this syndrome in girls could be linked to the X-linked genetic inheritance of this syndrome. However, of inspite of his great interest, the cause of Rett syndrome remained unknown (Hagberg et al., 1983). Dr Hagberg paper did manage to enhance the awareness of Rett syndrome in worldwide scientific community. Three years later in 1986, Suzuki et al found same clinical picture of RTT in their study of seven girls. They agreed with Rett's and Hagberg's description of signs and symptoms of the disorder but they could not found any abnormalities in blood chemistry of these young patients and found ammonia levels to be normal in these females (Suzuki et al., 1986).

From 1983 until late 1990s, many studies were conducted not only to discover the root cause of syndrome but also to define the clinical picture and different treatment options especially in scientific communities of countries like Spain, Germany, United Kingdom, Norway, Japan and Tunisia (Glaze et al., 1987; Campos-Castelló et al., 1988; Keret et al., 1988; Roberts and Conner, 1988; Loder et al., 1989; Holm and King, 1990; Yano et al., 1991; Witt Engerström, 1992; Budden, 1995; Plöchl et al., 1996; Haas et al., 1997; Glasson et al., 1998).

Nearly three decades after the first discovery of RTT, in 1999 the disorder was

shown to be caused primarily by mutations in the X-linked gene, *MECP2* (Amir et al., 1999). Amir et al used a systemic gene screening approach and identified mutations in the gene (*MECP2*) encoding X-linked methyl –CpG-binding protein 2 (*MeCP2*) as the primary cause of RTT. Their study also suggested aberrant epigenetic regulation as potential mechanism underlying the RTT pathology.

The discovery of the genetic cause of RTT enhanced the scientific research interest and number of groups had developed *Mecp2* knockout mouse models (Chen et al., 2001; Guy et al., 2001; Shahbazian et al., 2002b) in order to explore the underlying biology and pathophysiology of Rett syndrome.

In addition to neurological phenotypes, a number of overt 'peripheral' phenotypes are also common in RTT. For instance spinal deformity (principally scoliosis and excessive kyphosis) is a very common feature with approximately 50-90% of patients developing severe scoliosis, (Keret et al., 1988; Huang et al., 1994; Lidström et al., 1994; Percy et al., 2010) many of whom require corrective surgery. Other prominent skeletal anomalies include early osteoporosis, osteopenia, increased risk of low energy fracture and hip deformities (Keret et al., 1988; Roberts and Conner, 1988; Harrison and Webb, 1990; Leonard et al., 1999c; Cepollaro et al., 2001; Downs et al., 2008a; Hofstaetter et al., 2010; Leonard et al., 2010).

In my thesis I have used *Mecp2* knockout mice to analyse these skeletal anomalies. Various anatomical and biomechanical techniques have been employed to evaluate the bone structure and strength. Additionally, I have tested the reversibility of biomechanical phenotypes following un-silencing of the *Mecp2* gene. Evaluation of the outcomes of these experiments should provide information about challenges, benefits, drawback and prospects of gene-based therapies in targeting bone phenotypes in Rett syndrome.

1.1 Clinical picture of Rett syndrome

Rett syndrome (RTT) is a severe neurodevelopmental disorder which almost exclusively affects females, with prevalence between 1in 10,000 and 1 in 15,000 female births (Hagberg et al., 1983; Neul et al., 2010). Rett syndrome is an X-linked dominant disorder as more than 95% of RTT cases arise *de novo* (Webb

and Latif, 2001). RTT is lethal in hemizygous males, who die around birth, and if they do survive beyond birth then males present a different clinical picture from that shown in young females with Rett syndrome (Hagberg et al., 1983; Webb and Latif, 2001).

The uncertainty of diagnosis of Rett syndrome associated with the occasional presence of apparently affected males, is further complicated by the very wide clinical spectrum presented by females, which ranges from the severely affected 'classical' cases through a wide range of disability to a milder variant forms. This variability has been partly ascribed to the particular type of mutation (Neul et al., 2010) but also the degree to which skewing of X chromosome inactivation favours the expression of the normal *MECP2* allele (Webb and Latif, 2001).

The Rett syndrome not only affects the neurological system but also the respiratory, gastrointestinal and skeletal systems (figure 1-1).

RTT was sometimes co-classified with other autism spectrum disorders with features differentiating Rett syndrome from the former including an initial period of 6-18 month of apparently normal growth (low mean birth weight and head circumference were also observed in few cases) (Leonard and Bower, 1998; Huppke et al., 2003), followed by rapid destructive phase between 1-4 years during which patients display loss of hand skills, impaired mobility and speech, development of stereotypic hand movement (continuous repetitive wringing, twisting, clapping hand automatism during wakefulness) and difficulties in social interactions (figure 1-1).

This rapid deterioration phase is followed by plateau stage during which patients get no worse or their intensity lessens. Late motor deterioration starts between 5 and 25 years of age and can last for decades (Engerström, 1992; Neul et al., 2010).

Autistic features also form the frequent part of RTT clinical spectrum including hypersensitivity to sound, expressionless face, and indifference to the surrounding environment and un responsiveness to the social cues (Nomura, 2005) and mental retardation (Chahrour and Zoghbi, 2007).

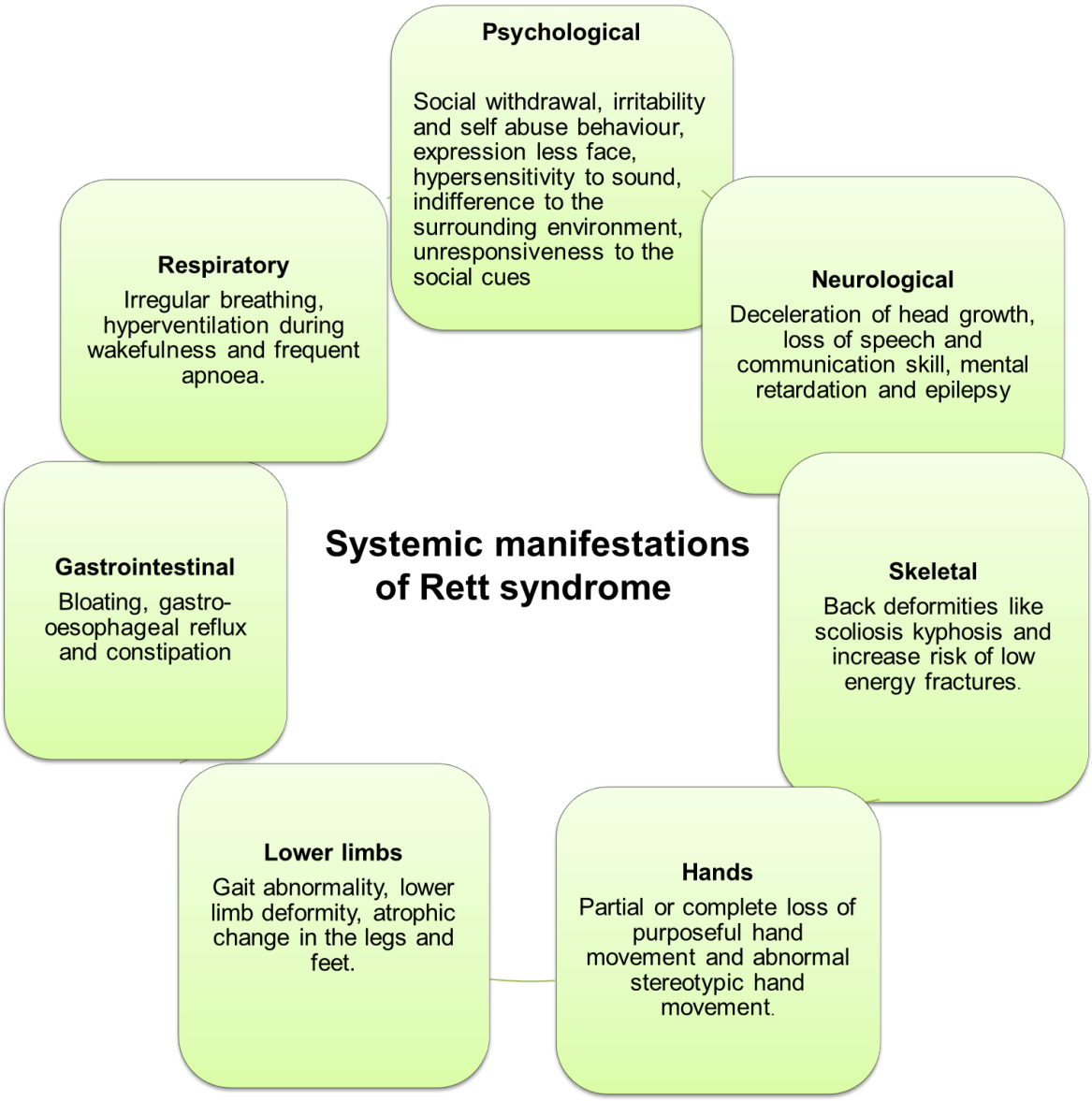

Figure1-1 Systemic manifestations of Rett syndrome

Musculoskeletal abnormalities of RTT includes scoliosis, which starts at an early school age, and distal lower limb abnormalities (Hagberg et al., 2002). In a recent study in an Australian cohort, investigators also showed the development of scoliosis in majority (85.5%) of cases (Anderson et al., 2014).Radiographic studies on RTT patients have demonstrated osteopenia (Leonard et al., 1995; Leonard et al., 1999c; Cepollaro et al., 2001).

Females with Rett syndrome are at increased risk of fracture as it is stated that about one third had sustained a fracture by the age of 15 years, compared with only 15% of control population of age 20 years (Leonard et al., 1999c). In another population based study the fracture risk in RTT patients was found to be nearly four times the population rate (Downs et al., 2008a). Decrease in bone volume has been reported in RTT patients, and it was concluded that the slow bone creation at a young age eventually causes low bone density, pointing towards the possible direct effect of *MECP2* mutations on bone development (Gonnelli et al., 2008; Leonard et al., 2010).

Rett syndrome patients also suffer from breathing difficulties including episodic hyperventilation and apnoea during wakefulness (Kerr et al., 1997; Julu et al., 2001). In a study on Australian cohort, abnormal breathing pattern were reported for two thirds of women (66.4%) including 74.2% who suffered from hyperventilation and 88.7% with apnoeic episodes (Anderson et al., 2014)

Epilepsy also occurs commonly during the plateau phase (Hagberg et al., 2002).Risk of epilepsy is also thought to be genotype related (Jian et al., 2006).

Gastrointestinal problems including swallowing dysfunction, gastro oesophageal reflux, constipation and distension are also observed in RTT patients (Reilly and Cass, 2001; Hagberg, 2002; Oddy et al., 2007; Motil et al., 2012; Anderson et al., 2014).

According to Neul *et al* RTT diagnostic criteria is as below:

Table1-1 Revised diagnostic criteria for RTT 2010

Main criteria	**Supportive criteria**
Partial or complete loss of acquired purposeful hand skills.	Breathing disturbances when awake.
Partial or complete loss of acquired spoken language.	Bruxism when awake.
Gait abnormalities: Impaired (dyspraxia) or absence of ability.	Impaired sleep pattern.
Stereotypic hand movements such as hand wringing/squeezing, clapping/tapping, mouthing and washing/rubbing automatisms.	Abnormal muscle tone.
	Peripheral vasomotor disturbances
	Scoliosis/ kyphosis
	Growth retardation
	Small cold hands and feet.
Exclusion Criteria	Inappropriate laughing/screaming spells.
Brain injury secondary to trauma, neurometabolic disease or severe infection.	Diminished response to pain.
Grossly abnormal psychomotor development in first 6 months.	Intense eye communication, eye pointing

Clinical presentation and severity of RTT display a wide variation and patients may exhibit all the essential features necessary for the RTT diagnosis or they may show differences leading to their assignment in atypical RTT diagnosis (Neul et al., 2010) See table below (table1-2).

Table1-2 Clinical criteria for diagnosis of "Classic and Atypical" RTT

Criteria for "Classic RTT"	Criteria for "Atypical RTT"
A period of regression followed by recovery or stabilization.	A period of regression followed by recovery or stabilization.
All main criteria and all exclusion criteria.	At least 2 out of the main criteria.
Supportive criteria are not required , although often present in typical RTT.	5 out of 11 supportive criteria.

1.2 Rett syndrome and the *MECP2* gene

The search for the genetic cause of Rett syndrome was seriously hampered by a lack of familial cases as majority of cases of the syndrome were found to be sporadic but with series of linkage analysis on the few familial cases the region of interest was found to be Xq28 in 1998 (Lewis et al., 1992; Sirianni et al., 1998; Webb et al., 1998; Xiang et al., 1998; Berg and Hagberg, 2001) (figure 1-2).

This discovery lead to intense screening of the Xq28 region for likely candidate genes until in 1999 Amir *et al* finally published first report, establishing mutations in *MECP2* gene in 5 out of 21 cases of Rett syndrome (Amir et al., 1999).

Rett syndrome is not a heritable disorder and most common mutations in *MECP2* arises *de novo* in germ cells, commonly on the paternal side (Trappe et al., 2001).

Since the original report by Amir et al, there have been a multiple confirmatory studies to detect mutations in the MECP2 gene in the young girls with Rett syndrome from worldwide and found that the more than 95% of RTT cases are usually the result of dominantly acting , *de novo* (Girard et al., 2001) mutations in the X-linked gene *MECP2*, which encodes methyl-CpG-binding protein 2 (MeCP2) (Wan et al., 1999; Bienvenu et al., 2000; Cheadle et al., 2000; Girard et al., 2001; Guy et al., 2011b; Zhang et al., 2012) other variant includes FOXG1,CDKL5 etc. More than 600 pathogenic *MECP2* mutations have been reported, including missense, nonsense, frameshift and large deletion mutations (RettBase: http://mecp2.chw.edu.au/mecp2/).

Studies have shown a genotype-phenotype relationship between phenotype and MECP2 mutation and it is fascinating because it gives the opportunity to explore mutations in a single gene (Amir et al., 2000; Ben-Ari and Spitzer, 2010). Truncation mutations within the MECP2 gene for example show relation with more severe RTT phenotypes (Weaving et al., 2003). Since MECP2 gene is an X-linked gene, the X-chromosome inactivation patterns (whether they are skewed or random or whether the mutant allele is of paternal or maternal origin) are linked to the severity of RTT phenotypes and this has been established by various groups (Ishii et al., 2001; Gibson et al., 2005; Xinhua Bao et al., 2008).

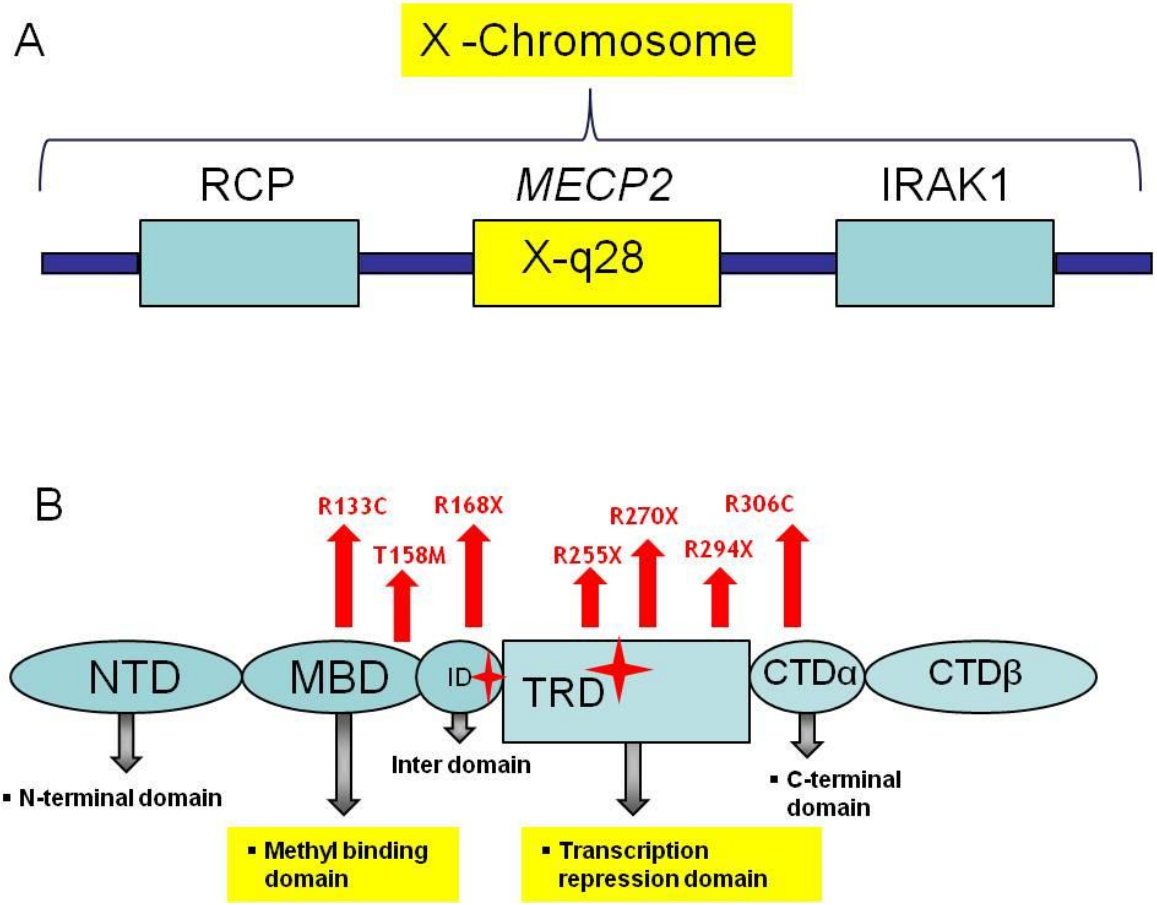

Figure1-2 The *MECP2* gene location and *MeCP2* protein structure with the most frequent sites of mutations

(A) *MECP2* gene is located in X-chromosome (Xq28), flanked by the *RCP* and *IRAK* genes. (B) The schematic figure showing the distinct functional domains of *MeCP2*. Apart from the N terminus, both *MeCP2* isoforms are identical and contain several functionally distinct domains: NTD, N-terminal domain; MBD, methyl binding domain; ID, inter domain; TRD, transcription repression domain; CTD, C-terminal domain; NLS; nuclear localisation signals. Most common point mutations are also shown (red arrows).

Males typically inherit a mutant *MECP2* allele, resulting in more severely affected phenotype, presenting with infantile encephalopathy and usually not surviving infancy. These differences between the heterozygous female and hemizygous male RTT phenotype are due to the proportion of cells in the nervous system expressing the mutant allele.

1.3 *MeCP2* Structure, Expression and Function

1.3.1 *MeCP2* Structure

MeCP2 is basically a nuclear protein with high affinity for DNA sequences containing methylated 5'-CpG-3' dinucleotides (Lewis et al., 1992). *MeCP2* belongs to Methyl-CpG binding protein family that binds to methylated DNA through their unique Methyl Binding Domain (MBD) (Singh et al., 2008).

In both human and mouse the *MECP2/Mecp2* gene is composed of four major exons (exon 1-4) and three introns (Intron 1-3). *MeCP2* protein structure is composed of five important domains, N-terminal Domain (NTD), Methyl Binding Domain (MBD), Inter Domain (ID), Transcription Repression Domain (TRD) and C-terminal Domain (CTD) and is approximately 53 kDa to 75 kDa in size (Nan et al., 1996; Jones et al., 1998; Zachariah and Rastegar, 2012; Olson et al., 2014). These domains combine to form a tertiary structure and this structural arrangement of MeCP2 provides a better understanding of *MeCP2* multifunctionality *in vitro* and *in vivo* (Adams et al., 2007) (Figure 1-2) *MeCP2* has two major splice isoforms, e1 and e2, that encode the proteins with different N-termini. *MECP2*_e2, which is the first discovered isoform uses a translational start site within exon 2, whereas the newer (and more abundant) isoform *MECP2*_e1 derives from mRNA in which exon 2 is found to be excluded (Mnatzakanian et al., 2004) (figure 1-3).

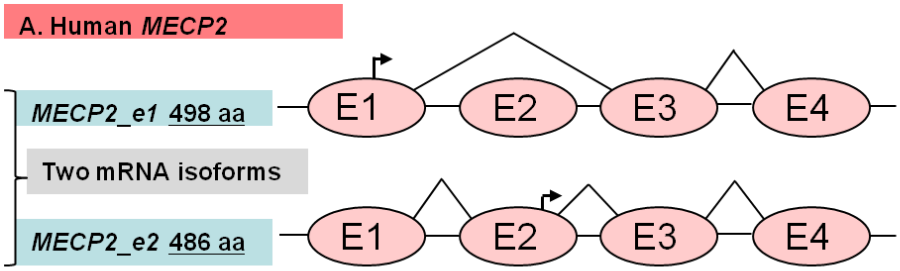

B. MeCP2 IS EXPRESSED AS TWO MAJOR ISOFORMS, e1 AND e2 WITH DIFFERENT N-TERMINI

```
MECP2_e1        MAAAAAAAPSGGGGGGEEERLEEKSEDQDLQGLKDKPLKFKKVKKDKKEEKEGKHEPVQP 60
MECP2_e2                MVAGMLGLREEKSEDQDLQGLKDKPLKFKKVKKDKKEEKEGKHEPVQP 48
                                ************************************

MECP2_e1        SAHHSAEPAEAGKAETSEGSGSAPAVPEASASPKQRRSIIRDRGPMYDDPTLPEGWTRKL 120
MECP2_e2        SAHHSAEPAEAGKAETSEGSGSAPAVPEASASPKQRRSIIRDRGPMYDDPTLPEGWTRKL 108
                ************************************************************

MECP2_e1        KQRKSGRSAGKYDVYLINPQGKAFRSKVELIAYFEKVGDTSLDPNDFDFTVTGRGSPSRR 180
MECP2_e2        KQRKSGRSAGKYDVYLINPQGKAFRSKVELIAYFEKVGDTSLDPNDFDFTVTGRGSPSRR 168
                ************************************************************

MECP2_e1        EQKPPKKPKSPKAPGTGRGRGRPKGSGTTRPKAATSEGVQVKRVLEKSPGKLLVKMPFQT 240
MECP2_e2        EQKPPKKPKSPKAPGTGRGRGRPKGSGTTRPKAATSEGVQVKRVLEKSPGKLLVKMPFQT 228
                ************************************************************

MECP2_e1        SPGGKAEGGGATTSTQVMVIKRPGRKRKAEADPQAIPKKRGRKPGSVVAAAAAEAKKKAV 300
MECP2_e2        SPGGKAEGGGATTSTQVMVIKRPGRKRKAEADPQAIPKKRGRKPGSVVAAAAAEAKKKAV 288
                ************************************************************

MECP2_e1        KESSIRSVQETVLPIKKRKTRETVSIEVKEVVKPLLVSTLGEKSGKGLKTCKSPGRKSKE 360
MECP2_e2        KESSIRSVQETVLPIKKRKTRETVSIEVKEVVKPLLVSTLGEKSGKGLKTCKSPGRKSKE 348
                ************************************************************

MECP2_e1        SSPKGRSSSASSPPKKEHHHHHHHSESPKAPVPLLPPLPPPPPEPESSEDPTSPPEPQDL 420
MECP2_e2        SSPKGRSSSASSPPKKEHHHHHHHSESPKAPVPLLPPLPPPPPEPESSEDPTSPPEPQDL 408
                ************************************************************

MECP2_e1        SSSVCKEEKMPRGGSLESDGCPKEPAKTQPAVATAATAAEKYKHRGEGERKDIVSSSMPR 480
MECP2_e2        SSSVCKEEKMPRGGSLESDGCPKEPAKTQPAVATAATAAEKYKHRGEGERKDIVSSSMPR 468
                ************************************************************

MECP2_e1        PNREEPVDSRTPVTERVS 498
MECP2_e2        PNREEPVDSRTPVTERVS 486
                ******************
```

Figure1-3 Splicing and composition pattern of *MECP2* gene

(A) Figure showing the splicing of Human *MECP2* gene. Two mRNA isoforms are generated; *MECP2*_e1 and *MECP2*_e2(B) The two isoforms generate two protein isoforms of MeCP2 with differing N-termini due to the use of alternative translation start sites (bent arrows). Yellow and green shadows refer to the amino acid differences in the N-terminal of both MeCP2_e1 (GenBank accession no. NM_001110792.1) and MeCP2_2 isoforms respectively (GenBank accession no. NM_004992.3).

1.3.2 *MeCP2* Expression

MeCP2 is widely expressed in many organs and its highest expression is found in brain, lung and spleen, compared to the expression levels in liver, heart, kidney and small intestines (Shahbazian et al., 2002b).

Mecp2 mRNA transcripts are highly expressed in skeletal muscle and heart, lung, moderate in brain and low in liver and spleen (D'Esposito et al., 1996; Reichwald et al., 2000; Adachi et al., 2005; Zhou et al., 2006).

The expression of *MeCP2* in brain has been extensively studied, as the majority of Rett syndrome phenotypes are neurological. However *MeCP2* mis-expression results in peripheral phenotypes as well for example the bone phenotype (scoliosis/ limb movements), breathing and respiratory abnormalities, cardiac problems, difficulty in feeding (Matarazzo et al., 2004; Smrt et al., 2007; Alvarez-Saavedra et al., 2010). Over expression of *MeCP2* in the mouse heart leads to cardiac septum hypertrophy and the mutated expression of MeCP2 in the skeletal tissue produces detrimental deformities (Alvarez-Saavedra et al., 2010).

In brain, both the distribution and levels of *MeCP2* show regional variation as recently demonstrated by studies in the adult murine brain regions, specifically in the cortex, striatum, olfactory bulb, hippocampus, thalamus, cerebellum, olfactory bulb and brain stem (Olson et al., 2014). The highest *MeCP2* expression was found in the cortex and cerebellum among the studied brain regions (Zachariah and Rastegar, 2012).

Among the *MeCP2* expressing cells, neurons show the highest MeCP2 expression, while lower amounts of *MeCP2* are found in glial cell types (Ballas et al., 2009; Zachariah and Rastegar, 2012). For normal maturation (Kishi and Macklis, 2004; Singleton et al., 2011) and proper function of neurons a normal *MeCP2* expression is required (Shahbazian et al., 2002b; Nguyen et al., 2012).

MeCP2 expression has also been demonstrated in astrocytes, oligodendrocytes and microglia (Ballas et al., 2009; Zachariah and Rastegar, 2012; Liyanage et al., 2013; Olson et al., 2014).

1.3.3 *MeCP2 molecular* mechanism and function

MeCP2 is found to be a multifunctional protein as different domains of *MeCP2* have been assigned to facilitate multiple functions either by direct DNA binding, or by interaction with protein partners or recruiting other factors (Guy et al., 2011b).

Cells undergo differentiation mostly without alternating the sequence of the DNA but rather the changes in their transcriptional activity. In mammals, the joint action of chromatin remodelling complexes and epigenetic modifications at the level of DNA and histones sets the different cell- and development-specific transcriptional programs. Also the mammalian DNA is found to be covalently modified by the supplementation of a methyl group to cytosines that occur predominantly in CpG dinucleotides (Bird, 2002). Over the years lots of evidence has been gathered that DNA Methylation plays a very important role in normal mammalian development and also for the survival of differentiated cells (Jackson-Grusby et al., 2001; Goll and Bestor, 2005). The methyl mark is interpreted by the family of methyl-CpG binding proteins via a methyl-CpG-binding domain (MBD) (Hendrich and Bird, 1998). *MeCP2* which is the founding member of the MBD family (Nan et al., 1998a) mediates its interaction with chromatin remodelling complexes including Swi-independent 3a (Sin3a) and Histone deacetylase inhibitor (HDAC1/2) ((Jones et al., 1998; Nan et al., 1998a), the histones methyltransferase, Suv39H (Fuks et al., 2003), the DNA methyltransferase I (Kimura and Shiota, 2003) and the silencing mediator for retinoid and thyroid hormone receptors (SMRT) (Stancheva et al., 2003) through transcriptional repressor domain (TRD).

Over twenty years ago MeCP2 was first identified as a transcriptional repressor that binds to methylated CpG dinucleotides (Lewis et al., 1992; Wakefield et al., 1999). *MeCP2* binds DNA directly through its N-terminal methyl-CpG binding domain (MBD), whereas its C-terminal transcriptional repression domain (TRD) allows it to interact with co repressors such as Sin3a, HDAC1, and HDAC2 (Nan et al., 1998b). Recent studies have shown that *MeCP2* is expressed at higher levels than expected for classical site-specific transcriptional repressors. MeCP2 binds as abundantly and widely throughout the genome as histone H1, which suggest that the protein might have additional functions in chromatin biology (Skene et al., 2010). Transcriptional studies in mouse brains as well as human embryonic stem cell-derived neurons, have shown that most genes are actually down regulated in

RTT models that lack *MeCP2* (Ben-Shachar et al., 2009; Li et al., 2013b). One possible explanation to this is that MeCP2 acts as a “transcriptional noise dampener”, such that loss of *MeCP2* function results in the diversion of basal transcriptional machinery to repetitive elements, indirectly leading to global transcriptional down regulation (Skene et al., 2010).

Previous research has shown that membrane depolarization induces *de novo* phophorylation of *MeCP2* at serine amino-acid residue 421 (S421) that may regulate Bdnf transcription (Chen et al., 2003; Zhou et al., 2006) although activity-dependent DNA Methylation involving dissociation of the MeCP2 repression complex may also regulate Bdnf transcription (Martinowich et al., 2003). Neuronal activity induces differing phosphorylation states of MeCP2 and may be an important mechanism through which MeCP2 regulates neuronal plasticity through activity-dependent gene transcription. Tao et al have suggested that MeCP2 phosphorylation may provide a regulatory switch such that at rest S80 phosphorylation binds MeCP2 to chromatin but during depolarization S421 phosphorylation allows MeCP2 to dissociate from chromatin thereby providing a transcriptionally permissive state (Tao et al., 2009).

MeCP2 is implicated as a key regulator of activity-dependent gene expression; there is still much work needed to do, to identify the target genes involved in these critical processes. Moreover there is a possibility of identification of other phosphorylation sites on MeCP2, impacting its activity and ultimately gene expression that mediates effects on short- and long term synaptic plasticity as well as behavioural processes (Tao et al., 2009).

Significant insight into the functional consequences of *MeCP2* in the brain has come from the study of transgenic mice. Studies of mice with various temporal and spatial deletions of Mecp2 have revealed numerous morphological changes and alterations in synaptic transmission and plasticity that likely underlie the observed cognitive and behavioural deficits reminiscent of human Rett syndrome (Moretti and Zoghbi, 2006; Calfa et al., 2011; Na and Monteggia, 2011).

Various studies have identified and explored a role of MeCP2 in specific brain areas. The anxiety and impaired motor coordination phenotypes observed in

Mecp2 mutant mice point to the amygdale and cerebellum as particular regions of interest (Gemelli et al., 2006; Pelka et al., 2006).

1.3.3.1 *MeCP2* as a Transcriptional Regulator

Although traditionally considered a global transcriptional repressor, the precise role of *MeCP2* as a transcriptional repressor (Nan et al., 1998a) or transcriptional activator (Chahrour et al., 2008) is paradoxical. Therefore recent studies have categorized *MeCP2* as a genome-wide epigenetic modulator rather than a transcriptional regulator (Della Ragione et al., 2012). As mentioned previously, MeCP2 is a methyl binding domain protein which binds to DNA following the addition of a methyl group to carbon-5 of the cytosine pryimidine ring (DNA Methylation); principally at CpG dinucleotides (cytosine and guanine separated by a phosphate). Once bound, the proteins are traditionally thought to involve a larger repressor complex and chromatin remodelling proteins such as HDAC proteins which suppresses gene transcription by chromatin compaction (Jones et al., 1998). However, it is suggested the transcriptional repression of MeCP2 could be chromatin independent too by means of inhibiting the basal transcriptional machinery through interaction with general transcription factors IIB (Kaludov & Wolffe 2000). Furthermore, repression is also thought to occur by MeCP2 mediated chromatin remodelling. This involves MeCP2 acting to form a loop of inactive, methylated chromatin which regulates gene expression by containing deacetylated histones which condense the DNA and restrict transcription (Horike et al. 2005). Either way, mutations in MECP2 could affect any area of this process resulting in a partially functioning protein or a complete breakdown of operation *MeCP2* involvement in chromatin structure.

In 2008 Chahrour et al decided to analyse the gene expression profiles in the hypothalami of mice that have no *Mecp2* present (*Mecp2* null) or those that over express *MECP2* under the control of its endogenous promoter (*MECP2*-Tg) in the hope of deciphering more information into the molecular mechanism of MeCP2 (Chahrour et al., 2008). Through the use of microarray analysis, a variety of genes expressions were found misregulated in both mouse models. Surprisingly around eighty five percent of these genes expressions were found upregulated in transgenic hypothalami and dowregulated in *Mecp2*-null hypothalami suggesting

that many of these genes expression are likely activated by increased MeCP2 activity.

ChIP work with the antibody for *Mecp2* confirmed that *Mecp2* bound to the promoter region of six of the activated genes (Sst, Oprk1, Mef2c, Gamt, Grpin1 and A2bp1). The same group also identified Mecp2 to bind to the promoter region of the transcriptional activator CREB1 and also associate with this protein at the promoters of activated target gene (Chahrour et al., 2008). This data collected suggested in favour of the idea that MeCP2 has a role in activating target genes and not just repressing them. One explanation for these results might be that *MeCP2* is repressing a transcriptional repressor therefore activation of the target of this repressor would occur. However there is a possibility that changes observed might be secondary to the physiological properties of the hypothalamus. Overall these results propose a more complex mechanism of transcriptional regulation by MeCP2 with a variety of genes being either positively or negatively regulated.

MeCP2 has also been found to be involved in controlling chromatin structure (Zlatanova, 2005; Chadwick and Wade, 2007). Significant differences have been found in the chromo centres in *Mecp2* –deficient and *Mecp2*-WT neurons, further supporting role of *MeCP2* in organisation of chromatin (Singleton et al., 2011). *MECP2* mutation causing Rett syndrome have been found to disrupt the functions of higher order chromatin structure (Nikitina et al., 2007).

Recent studies have demonstrated that the DNA Methylation-dependent binding of *MeCP2* to the exons sequences modulates alternative splicing (Miyake et al., 2013) . Altered RNA splicing of synaptic genes have been found in autism as well as Rett syndrome (Smith and Sadee, 2011). *MeCP2* plays a role to regulate the alternative splicing of NMDA receptors subunit NR1 (Young et al., 2005).

1.3.3.2 *MeCP2* role in other biological functions

Recent research has demonstrated now that the *MeCP2* plays a role in regulating protein synthesis and it is postulated that the reduced protein synthesis in *MeCP2*-deficient cells is contributing to the RTT phenotypes detected in these cells (Li et al., 2013b). This finding confirmed the involvement of *MeCP2* in Rett syndrome

pathogenesis, the aforesaid functions are deteriorated in RTT patients (Kim et al., 2011).

Recent biophysical studies have probed the binding specificity of MeCP2 and have reported the interaction (via hydration within the major groove) with methylated DNA and also the interaction with nucleosomes (Ho et al., 2008). Despite this knowledge, the precise biological function of MeCP2 remains unclear. As described previously proposed additional or alternative functions include selective enhancement/activation of gene expression (Chahrour et al., 2008), chromatin regulation (Nikitina et al., 2007), and RNA processing (Young et al., 2005).

In summary MeCP2 is distributed across the genome very much in parallel with Methylation density, and to the exclusion, in neurons, of histon H1 (Skene et al., 2010). This conclusion suggest that MeCP2 play a major role in the suppression of transcription throughout very large scale genome-wide actions; in this way it may be best to ascribe MeCP2's function in terms of global dampening of transcriptional noise.

1.4 Bone phenotypes in Rett syndrome

The frequent occurrence of bone anomalies like osteoporosis (Haas et al., 1997; Leonard et al., 1999c), scoliosis (Amir et al., 2000; Ager et al., 2006; Bebbington et al., 2012), increase risk of fracture (Downs et al., 2008a; Hofstaetter et al., 2010) and generalized growth failure (Schultz et al., 1993) has raised questions between the possible links of MECP2 gene mutations at chromosome Xq28 on bone growth and attainment of peak bone mass.

1.4.1 *MeCP2* expression and bone development`

Alternation of the normal pattern of expression of *MeCP2* in skeletal tissues can lead to detrimental effects on normal bone development and later on results into severe malformations (Alvarez-Saavedra et al., 2010).

Although accumulating evidence suggests that the most of the RTT-like phenotypes are caused specifically by dysfunction of mature neurons (Matarazzo et al., 2004; Smrt et al., 2007) resulting from mis-expression of *MeCP2* target genes in the brain, however a role *for MeCP2* in peripheral cells has not been

ruled out. For example in case of bone tissue, their usually observed decreases in bone mineral density have been ascribed to abnormal activity of osteoblasts. The commonly observed dysmorphic features (scoliosis/kyphosis) of *MeCP2* duplication patients (Van Esch et al., 2005; Friez et al., 2006; Smyk et al., 2008) could stem from *MeCP2* dysfunction in peripheral tissues.

The slow bone creation at a young age in Rett syndrome patients may eventually cause low bone density, showing that the influence of *MECP2* is not restricted to damaging brain tissues, but has a direct effect on bone development (Budden and Gunness, 2001).

1.4.2 Factors affecting bone remodelling and their relevance to Rett syndrome Patients

Most of the females with RTT suffer from growth retardation (early deceleration of head growth, followed by weight and height deceleration) (Schultz et al., 1993; Reilly and Cass, 2001; Oddy et al., 2007; Jefferson et al., 2011). Inspite of this description, other bone related symptoms such as fractures and bone mass are not included in clinical scales evaluating severity scores in Rett syndrome (Bebbington et al., 2008) .

In 1999, an Australian, population based study revealed that girls with Rett syndrome showed a 4 times higher rate (Downs et al., 2008a) of fracture as compare with a sample of control children (Leonard et al., 1999c). Moreover nearly one third had sustained a fracture by the age of 15 years as compared with only 15% of girls and women in the general population of 20 years age (Cooley and Jones, 2002).

Factors effecting the bone mineral density and increase fracture risk in the general population include genetic predisposition (subjects with p.R168 and p.R270 mutations in *MECP2* gene) (Downs et al., 2008a), hormonal factors (Huppke et al., 2001), previous fractures, lack of soft tissue padding, lack of bone strength (Zysman et al., 2006), weight bearing exercise, vitamin D levels (Motil et al., 2011) and use of antiepileptic drugs (AECs) (Downs et al., 2008a; Leonard et al., 2010; Jefferson et al., 2011).

Greater frequency of fractures of lower limb fractures have been reported within RTT (Leonard et al., 1999c; Jones et al., 2002; Cooper et al., 2004; Downs et al., 2008a; Roende et al., 2011b) and vertebral fractures were not found commonly (Roende et al., 2011b).

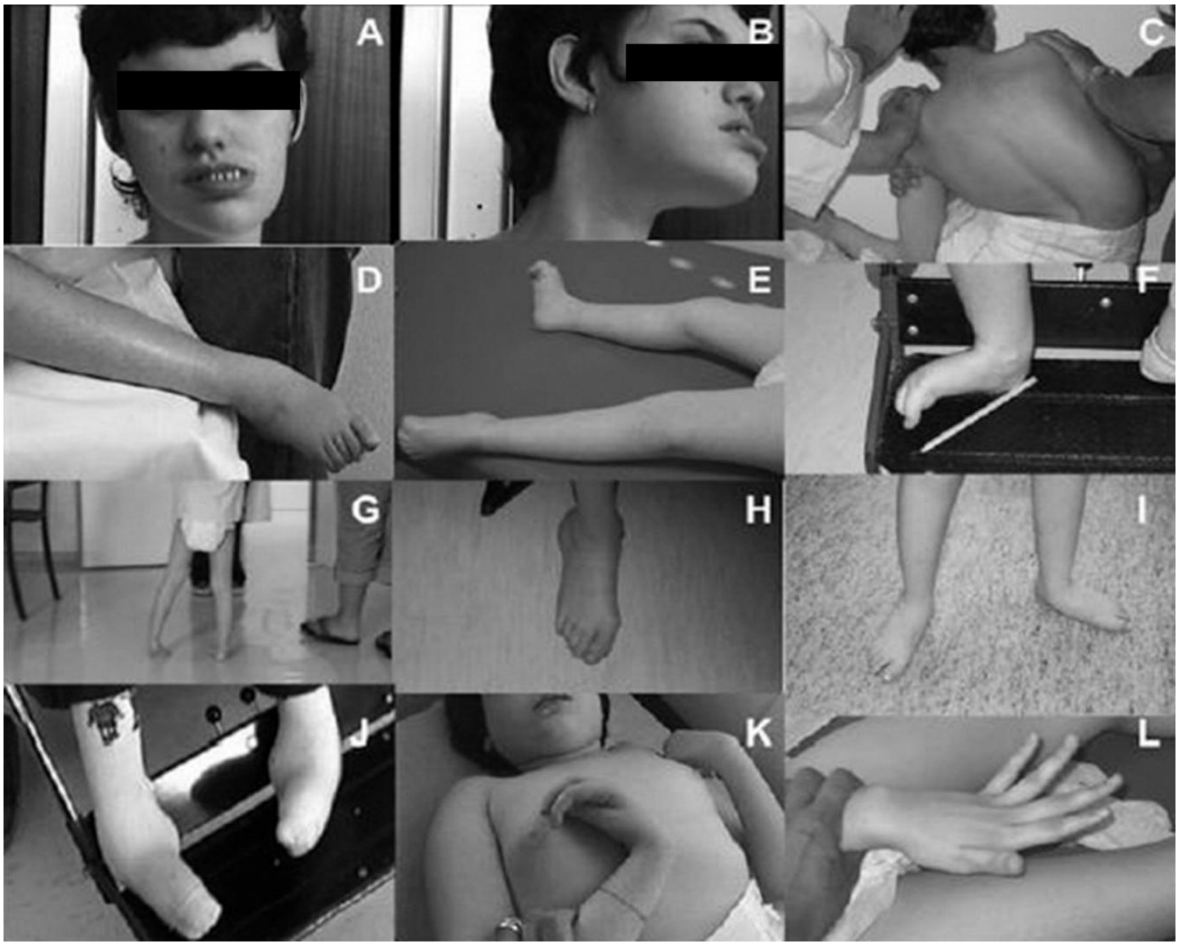

Figure 1-4 Several different dysmorphic skeletal features of Rett syndrome: (A, B) Bruxism and pragmatism in an adult patient; (C) severe scoliosis in a 14-year-old patient; (D) segmental dystonia; (E, F) the same peculiar dystonic feet posture in two different patients aged 2 and 16 years, respectively; (G) dystonia of the left inferior limb that interferes with gait; (H, I) two different patients with feet dystonia; (J) severe fixed feet in an adult patient; (K) dystonia of the hands in a 12-year-old patient (L); hand athetosis in a 14-year-old patient. (Temudo et al., 2008). Figure included with permission. Copyright © 2008, Movement Disorder Society. License Number obtained after permission: 3510771178758. Licensed publish content by John Wiley and Sons.

Individuals with RTT are at risk of developing osteoporosis (Haas et al., 1997; Leonard et al., 1999b; Motil et al., 2006) and mild hypercalciuria in Rett syndrome has been reported (Motil et al., 2006). This suggests that the RTT-pathogenesis might lie in bone resorption contributing to osteopenia.

Radiological studies on RTT patients (Carter et al., 1992; Cepollaro et al., 2001; Gonnelli et al., 2008; Motil et al., 2008; Nazarian et al., 2008; Shapiro et al., 2010; Jefferson et al., 2011; Roende et al., 2011a) have shown low bone mass from an early age, with fewer studies showing similar findings in patients over 30 years of age (Zysman et al., 2006; Motil et al., 2008; Shapiro et al., 2010).

Several different dysmorphic skeletal features have also been observed in individuals suffering from Rett syndrome including severe scoliosis (Percy et al., 2010; Riise et al., 2011), bruxism and pragmatism in an adult patient, (Temudo et al., 2007), facial features at infancy and childhood includes microcephaly, flat occiput/brachycephaly, broad face, hypertelorism, wide mouth and pointed chin (Allanson et al., 2011) (figure 1-4 A-L).

Scoliosis is exceedingly common in Rett syndrome developing 50-90% of individuals with the condition (Keret et al., 1988; Bassett and Tolo, 1990; Harrison and Webb, 1990; Holm and King, 1990; Guidera et al., 1991b; Huang et al., 1994; Lidström et al., 1994; Brunner and Gebhard, 2002; Ager et al., 2006; Downs et al., 2009; Koop, 2011; Gabos et al., 2012). Scoliosis becomes apparent at an early age and worsens rapidly during adolescence and continue to deteriorate further even after the skeletal maturation (figure 1-4C).

Risk of Scoliosis is appeared to be link to specific chromosomal changes and among the numerous mutations of *MECP2,* only two mutations (R294X and R306C) are found to have reduced risk of developing scoliosis (Ager et al., 2006; Percy et al., 2010). Rett syndrome patients tend to have long single curves in which the pelvis might act as an end vertebra, resulting in pelvic obliquity (Riise et al., 2011). Cases of milder skeletal phenotype found associated with balancing double curves, usually of smaller magnitude (Riise et al., 2011).

Skeletal deformities and increased likelihood of fractures may reflect abnormalities in adult bone structure or in the process of bone formation or in the cells and

mechanisms linked to bone turnover and remodelling. In next section I will briefly review the basic biology of bone and its formation.

1.5 Bone Structure and Composition

Bone is a highly specialized and dynamic connective tissue and its properties depend largely on the unique nature of its extracellular matrix. Throughout life, it is being continuously removed and replaced.

1.5.1 Bone tissue

Bone is composed of a hierarchical structure and can be divided as follow (Yuan et al., 2011):

Table1-3 Bone hierarchical structure

Level	Structure
Macroscopic	Cortical bone and trabecular bone
Microscopic	Osteon or haversian systems and trabeculae
Sub microscopic	Lamellae and mineralised collagen
nanostructure	Mineralised collagen fibrils
sub nanostructure	Molecular and atomic structure of major components

At the macroscopic level, bone is divided into cortical and cancellous bone Trabecular bone in comparison to cortical bone is more active metabolically, is remodelled more often than the cortical bone and on this basis considered younger on average than the cortical bone. Every year 25% of trabecular bone is replaced compared to only 2-3% of cortical bone (Swaminathan, 2001).

At the microscopic level, bone can be either described as lamellar or non-lamellar. All the mature bone is mostly lamellar. Non lamellar bone is rarely present in the normal human skeleton after the age of 4 or 5 years old (Buckwalter, 1995).

1.5.1.1 Cortical bone

The cortical bone forms the hard bone shell at the outer surface of each bone and composed of a thick and a dense layer of calcified tissue (compact bone tissue) (Fratzl, 2007). It is also known as compact bone tissue due to its minimal gaps and spaces. In humans and many other mammals, the porosity of normal cortical bone is below 3% at the optical microscopic level. Cortical bone is composed of haversian systems known as osteons. Osteons are circular or oval in cross section and contain central blood vessels in a cylindrical canal known as a Haversian canal. The blood vessels are surrounded by three to eight concentrically arranged lamellae. Osteons run parallel to the long axis of the bone (major loading direction). Along their way they give off branches, Volkmann canals, which join adjacent haversian canals. The most commonly suggested arrangement of collagen fibres in lamellae of an osteon is that they lie in parallel in each lamella to the next as a twisted helicoidally structure. Between the individual lamellae are small spaces called lacunae and each contains a cell called an osteocyte. Each central canal, with its surrounding lamellae, lacunae, osteocyte and a canaliculi, forms a Haversian system (Giraud-Guille, 1988) (figure 1-4).

1.5.1.2 Trabecular bone

In contrast to cortical bone, trabecular bone (also known as cancellous bone) does not contain osteons, although like cortical bone it is lamellar in structure. The microstructure of the trabecular bone is made of a series of interconnecting rods or occasionally plates of bone called trabeculae. As in cortical bone, the trabeculae contain osteocytes that lie in lacunae and again radiating from the lacunae are canaliculi containing osteocyte processes. Unlike osteocytes in the cortical bone, those in trabeculae normally receive their nourishment directly from the blood circulating through the marrow cavity. Haversian canals occur in very thick trabeculae (Fratzl, 2007).

1.5.2 Bone Matrix

Bone matrix is composed of organic (collagens and non-collagenous proteins) and inorganic (mineral crystals). The primary organic component of the bone matrix is type 1 collagen, although minor amounts of other collagen types such as types III and V have been reported as well (Niyibizi and Eyre, 1989, 1994). Type 1 collagen

comprises approximately 95% of the entire collagen content of bone and about 80% of the total proteins present in bone (Niyibizi and Eyre, 1994). The inorganic component of bone matrix is known to consist largely of hydroxyapatite [$Ca_{10}(PO_4)_6(OH)_2$] and small but significant amounts of substitution ions such as HPO_2^-, Na^+, Mg^{2+}, citrate, carbonate, K^+ and others whose positions and configurations are not completely known yet (Ziv and Weiner, 1994).

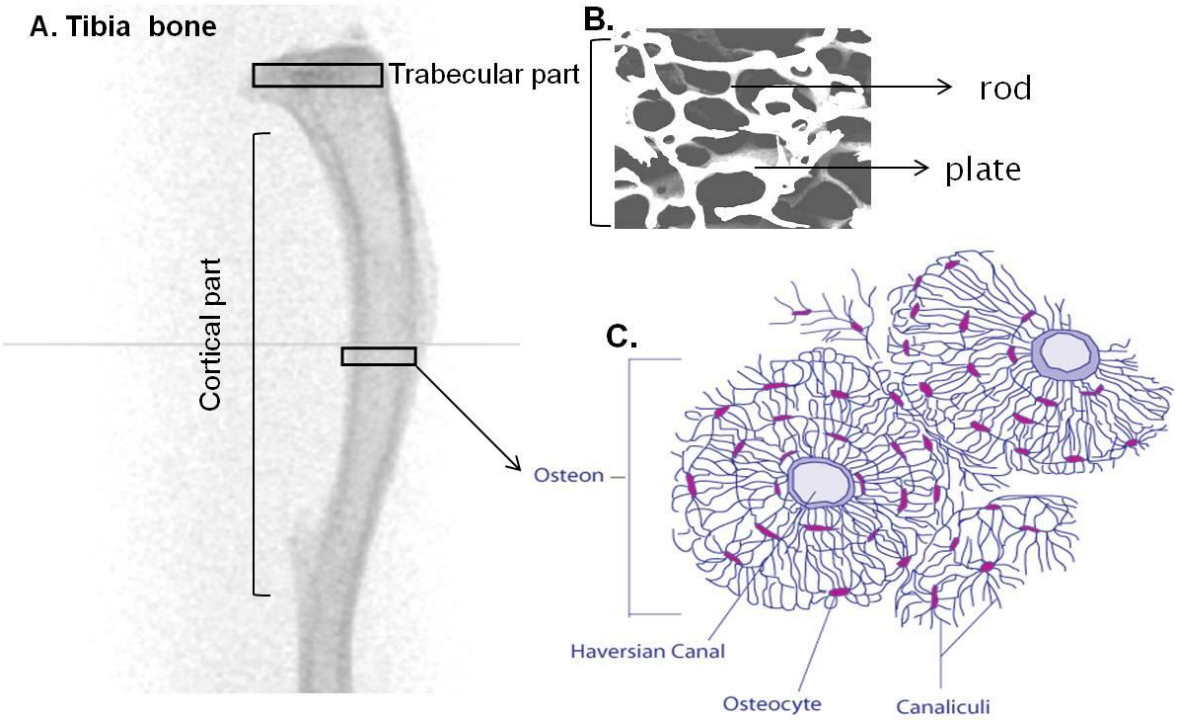

Figure1-5 Bone structure

(A) Mouse tibia bone showing cortical shaft and trabecular part towards the periphery. (B) Trabecular part of the bone composed of rods and plates. (C) Transverse section of a typical long bone's cortex. Modified and adopted Gray's anatomy 20th Edition.

1.5.3 Bone Cells

Bone cells are responsible for producing, modifying and maintaining a continuous cellular layer that covers all available extracellular matrix surfaces. The majority of these cells are in turn, connected in a network of cells which is dispersed thought out the matrix (figure1-5). Four types of cells are commonly recognised, three (osteoblast, osteoclast and bone lining cells) of which cover the surfaces of bone tissue while the fourth type of cells (osteocyte) are encased within the mineralised extracellular matrix (Miller and Jee, 1987; Burger and Klein-Nulend, 1999; Hadjidakis and Androulakis, 2006).

The processes of cellular differentiation that gives rise to the skeleton are regulated by genes, which first establish the pattern of skeletal structure in the form of cartilage and mesochyme and then replace them with bone through the differentiation of osteoblasts (Wellik and Capecchi, 2003).

1.5.4 Osteoblast and Osteocyte

Osteoblasts are a cuboidal, polar, basophilic cells covering (Lian and Stein, 1995) the bone matrix at sites of active matrix formation. Undifferentiated mesenchymal stem cells that have the potential to become osteoblasts usually reside in bone canals, endosteurm, periosteum and marrow. Osteoblasts remain in their undifferentiated form until they are stimulated to proliferate and differentiate into mature osteoblasts. Osteoblasts produce extracellular matrix proteins and are regulators of matrix mineralization during initial phase of bone formation and later bone remodelling. In addition to bone formation, osteoblasts regulate osteoclast differentiation and resorption activity by the secretion of cytokines or by direct cell contact (Lian and Stein, 1995).

Osteoblast derives from pluripotent mesenchymal stem cells (Caplan, 1991; Pittenger et al., 1999). Several specific transcription factors are responsible for the commitment of pluripotent mesenchymal cells into the osteoblast cell lineage. One of the most important of these is Cbfa1 (core-binding factor α1), a transcription factor belonging to the *runt*-domain gene family, which plays a critical role in osteoblast differentiation (Hoshi et al., 1999). Cbfa1-deficient mice are completely lacking in bone formation (Hoshi et al., 1999). Another runt-related gene that plays an important role in the commitment of multipotent mesenchymal cells to the

osteoblastic lineage and for osteoblast differentiation at an early stage is Runx-2. Runx-2 is involved in the production of bone matrix proteins (Otto et al., 1997), as it is able to up-regulate the expression of major bone matrix protein genes, such as type 1 collagen, osteopontin, bone sialoprotein and osteocalcin (Miyoshi et al., 1991; Ogawa et al., 1993). Runx-2 deficient mice are completely lacking in bone formation, because of an absence of osteoblasts.

The progressive development of the osteoblast phenotype from an immature cell to a mature osteoblastic cell synthesizing specific bone proteins is characterized by a definite sequential expression of tissue specific genes that identifies three periods of osteoblast development: proliferation, maturation and extra-cellular matrix synthesis, and matrix mineralization.

During active proliferation phase, pre-osteoblasts express genes that support proliferation and several genes encoding for extracellular matrix proteins such as type 1 collagen and fibronectin. During this phase bone morphogenic proteins (BMP), BMP-2 and BMP-5 play a significant role in increasing alkaline phosphatise activity, osteocalcin synthesis (Takuwa et al., 1991; Yamaguchi et al., 2000) and parathyroid hormone (PTH) responsiveness (Kodama et al., 1982; Takuwa et al., 1991).

During the post proliferative phase, which is characterized by the high synthesis of alkaline phosphatise, the extracellular matrix progresses into the mineralization phase in which osteoblasts synthesize several proteins that are associated with the mineralized matrix in vivo (Hauschka et al., 1989), including sialoprotein, osteocalcin and osteopontin (Gerstenfeld et al., 1987; Owen et al., 1990). Osteopontin is expressed during the active proliferation phase (Lian and Stein, 1995), and highest level of expression is achieved during mineralization. Osteopontin might be involved in the control of the relationship between the cells and extra-cellular matrix (Oldberg et al., 1986). Osteocalcin is maximally expressed during the phase of mineralization in (Hauschka et al., 1989) and it is involved in the regulation of mineral deposition and that it acts as a bone matrix signal that promotes osteoblast differentiation and activation (DeFranco et al., 1991; Chenu et al., 1994). Osteocalcin synthesis is regulated by various hormones, 1, 25 OH Vitamin D, and growth factors e.g (Tissue growth factor -β.) TGF-β.

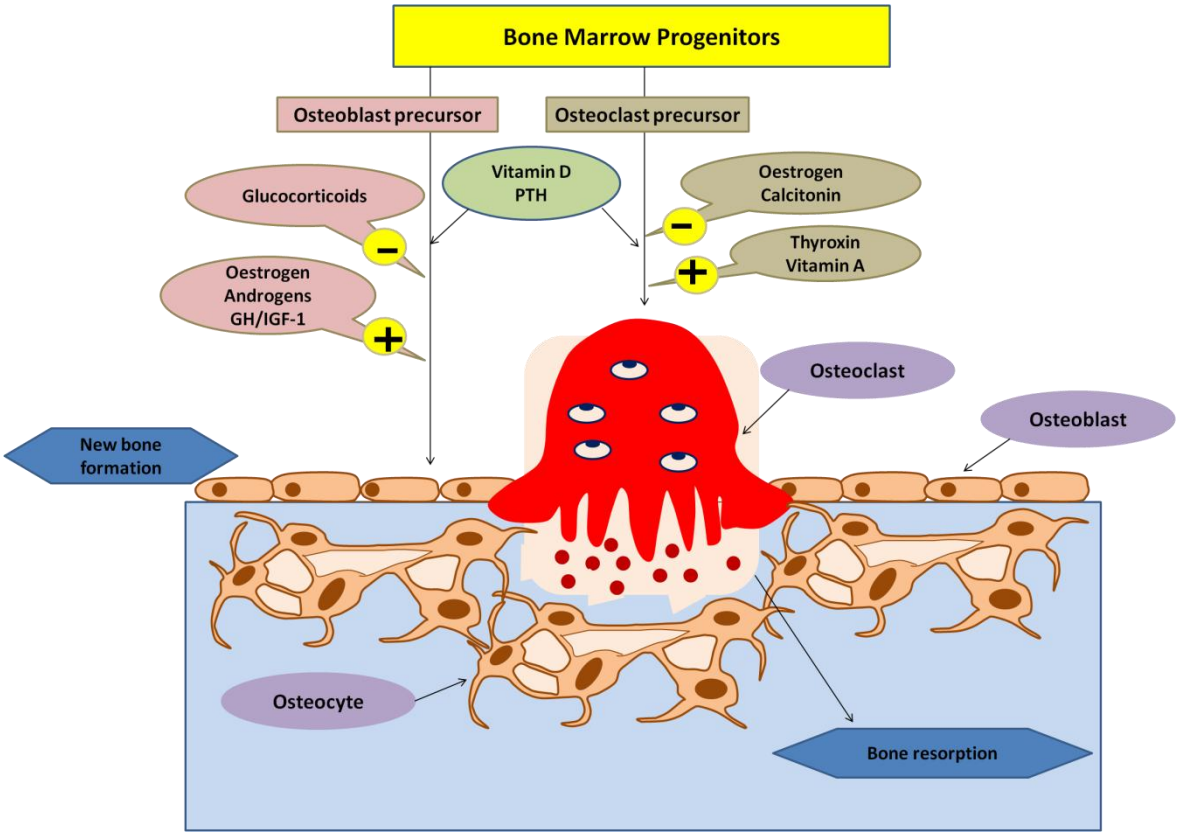

Figure1-6 Bone cells and contributing factors

Representative diagram showing different factors affecting bone cell's differentiation and regulation. Osteoblast derives from pluripotent mesenchymal stem cells. Osteoblasts express receptors for various hormones including PTH, 1, 25(OH) 2D3, oestrogens, and glucocorticoids which are involved in the regulation of osteoblast differentiation and activity. Vitamin D affects the metabolic activity of osteoblasts through a series of Vitamin-D-responsive genes that reflect a more mature osteoblast phenotype. Osteocytes are metabolically quiescent osteoblasts embedded in bone matrix; they communicate with other bone cells through cell processes and function as strain and stress sensors. Osteoclasts cells are terminally differentiated multinucleated cells that are the principal, resorptive cells. These multinucleated cells derived from hematopoietic stem cells. Factors including vitamin D, PTH, oestrogen, calcitonin, thyroxin, and vitamin A are involved in the regulation of Osteoclast differentiation and activity.

At the end of the synthesis and mineralization of the extracellular matrix, 50%-70% of mature osteoblasts undergo apoptosis, whereas the remainder can differentiate into lining cells or osteocytes or into the cells that deposit chondroid bone (Franz-Odendaal et al., 2006). Osteocytes are metabolically quiescent osteoblasts embedded in bone matrix; they communicate with other bone cells through cell processes and function as strain and stress sensors (Lozupone et al., 1996) (figure 1-6).

Osteoblast also synthesizes IGF-1, interleukin-1 (IL-1) and IL-6. IL-1 can affect proliferation, collagen and osteocalcin synthesis and alkaline phosphatise production (Kim et al., 2002).

Osteoblasts express receptors for various hormones including PTH (Demiralp et al., 2002), $1,25(OH)_2D_3$ (Lian et al., 1999), oestrogens (Boyce et al., 1999) and glucocorticoids (Ishida and Heersche, 1998) which are involved in the regulation of osteoblast differentiation and activity. Vitamin D affects the metabolic activity of osteoblasts through a series of Vitamin-D-responsive genes that reflect a more mature osteoblast phenotype (figure 1-6).

Activation and regulation of bone resorption requires an interaction between osteoblasts and osteoclasts (Grano et al., 1990). In order to obtain mature osteoclasts, the presence of osteoblasts was necessary and this phenomenon was explained with the identification of RANK (receptor activator of nuclear factor κB)/RANKL (RANK ligand)/OPG (osteoprotegerin) system (Yasuda et al., 1998). RANKL is an essential factor for the recruitment, differentiation, activation and survival of osteoclastic cells through binding to its specific receptor RANK, on the surface of osteoclast. OPG is a soluble receptor of RANK and is synthesized by osteoblasts. OPG inhibit osteoclast differentiation and activity (Lacey et al., 1998). OPG-deficient mice exhibit an osteoporotic phenotype and presents an increased number of osteoclasts (Bucay et al., 1998). Through the modulation of RANKL and OPG, osteoblasts can control osteoclast differentiation and activity and consequently bone remodelling.

Osteocytes are terminally differentiated cells of the osteogenic lineage that are derived from mesenchymal precursor cells. Important markers of osteocytes includes matrix extracellular phophoglycoprotein (Gowen et al., 2003), sclerostin

(Balemans et al., 2001), dentin matrix protein and phex protein (Feng et al., 2006). The osteocytes are the most abundant cells in adult bone and are constantly spaced throughout the mineralized matrix.

Mature osteocytes have a characteristic dendritic cell shape with processes radiating from the cell body through the canaliculi in different directions. These processes of osteocytes form an intercellular network through gap and adherent junctions with surrounding osteocytes, the cells lining the bone surface and bone marrow (figure 1-6). Osteocytes through this unique 3D network, are anatomically placed in a prime position not only to sense deformations driven by stresses place upon bone, but also to respond with passage of signal to the neighbouring osteocytes (Vatsa et al., 2007).

Although it has not been determined which of the osteocyte cell parts are most important for the function of the osteocyte as mechanosenor, it has been suggested that fluid flow over dendritic processes in the lacunar canalicular porosity can induce strains in the actin filament bundles of the cytoskeleton that are more than an order of magnitude larger than tissue level strains (Han et al., 2004). In single osteocytes mechanical stimulation of both cell body and cell process resulted in up-regulation of intracellular NO production (Vatsa et al., 2006). These results indicate that both cell body and cell process might play a role in mechanosensing and Mechanotransduction in bone (Vatsa et al., 2006).

Furthermore it was shown that a mechanically stimulated single osteocyte can pass on the information of local mechanical stimulus to the neighbouring cells in the vicinity independent of intercellular connections, suggesting that this communication happens through extracellular soluble factors (Vatsa et al., 2007). Other studies have suggested an alternative mechanosensing structure i.e., osteocytes project a single cilia from their cell surface (Xiao et al., 2006). Osteocyte cilia can translate fluid flow stimuli into a cellular response, indicating that primary cilia might act as a mechanosensitive structure within the osteocytes (Malone et al., 2007).

Osteocytes also play a pivotal role in bone remodeling. The final step of the mechanical signal transduction pathway towards bone remodeling is the transmission of molecules produced by osteocytes to the effector cells i.e.,

osteoblasts and osteoclasts. Due to the close physical proximity of osteocytes to local osteoblasts and periosteal fibroblasts, it is highly plausible that soluble factors produced by osteocytes act in a paracrine manner to affect these cells. Soluble mediators released by osteocytes may regulate the properties of neighbouring bone cell populations including their proliferation and differentiation. Studies have supported the hypothesis that the osteocyte is an orchestrator of different cell populations in bone in response to mechanical loading (Vezeridis et al., 2006).

1.5.5 Osteoclast

Osteoclasts are terminally differentiated multinucleated cells that are the principal, resorptive cells of bone, and play a critical role in the development of the skeleton and regulation of its mass. These multinucleated cells derived from hematopoietic stem cells (Suda et al., 1999; Teitelbaum, 2000; Nakamura et al., 2003) (figure 1-6). Thus a premyeloid precursor can differentiate into either an osteoclast a macrophage or a dendritic cell, depending on whether it is exposed to receptor activator of NF-kBB ligand (RANKL; also called tumor necorsis factor-related activation-induced cytokine (TRANCE), osteoprotegerin ligand (OPGL) or osteoclast differentiation factor (ODF) macrophage colony-stimulating factor (M-CSF) or granulocyte-macrophage colony-stimulating factor (GM-CSF), respectively (Kong et al., 1999; Nutt et al., 1999; Suda et al., 1999). Osteoclast lack many of the antigens that are characteristic of macrophages and inflammatory polykaryons, in particular Fc and C3 receptors and express very high levels of Tartrate-resistant acid phosphatase (TRAP) and vitronectin receptor (VNR). They also express calcitonin receptors (CTRs) that are absent from macrophages. Most uniquely osteoclasts *ex vivo* excavate bone within hours, but macrophages show no excavation whatsoever, even on extended incubation on bone surfaces.

Many of Osteoclast responses are dependent on cells of the osteoblastic lineage; osteoblastic cells, after diverse stimuli express osteoclast-resorption-stimulating activity (ORSA) as the common pathway for osteoclast stimulation. Although ORSA has been detected in culture supernatants from hormone stimulated osteoblastic cells it has also frequently been detectable only when osteoblasts are in contact with osteoclasts (Chambers, 1982; Chambers et al., 1984; Thomson et al., 1986; Wesolowski et al., 1995). Studies have shown that osteoclasts formed *in*

vitro similarly depend on osteoblastic cells for activation of bone resorption (Wesolowski et al., 1995; Jimi et al., 1996)

Several cytokines and hormones, including macrophage colony-stimulating factor (M-CSF)(Yoshida et al., 1990; Fuller et al., 1993), interleukin 1 (IL-1)(Jimi et al., 1995), RANKL (Lacey et al., 1998; Yasuda et al., 1998) and tumour necrosis factor (TNF-a)(Kobayashi et al., 2000), regulate the differentiation, activation and survival of osteoclast. They are essentially responsible for the mineralized matrix degradation during physiological and pathological bone turnover.

Osteoclast resorption consists of several complicated processes: (1) the proliferation of osteoclast progenitors; (2) differentiation of the progenitors into mononuclear perfusion osteoclast (pOCs); (3) fusion of pOCs into multinucleated osteoclasts; (4) adherement of osteoclasts to calcified tissue; (5) polarization; that is, the development of a ruffled border and clear zone (actin ring), followed by the secretion of acids and lysosomal enzymes into the space beneath the ruffled border ; (6) finally apoptosis (Grano et al., 1990).

Presence or absence of mechanical stimulation is known to affect formation, absorption, and maintenance of the bone, especially in association with multiplier effects such as the systemic or hormonal disorders (Bourrin et al., 1995; Xie et al., 1997). Animal studies have shown that the bone resorption is observed in the palate of rats after experimental loading device and that the osteoclast resorption is potentially a pressure threshold-regulated phenomenon (Mori et al., 1997; Sato et al., 1998).

Bone resorption under compressive strain is attributed to the accumulation of micro-damage that exceeds the bone’s capacity for repair and certain thresholds of strains induced in bone govern its response (Nicolella et al., 2005). Interestingly one of the recent studies has suggested that the osteoclastic resorption is location-dependent and is sensitive to the local strain intensity (Fujiki et al., 2013). Bone histomorphometric analysis from this study showed that osteoclasts were localized in the bone subsurface adjacent to the loading site and the in the periphery of the bone marrow space of the intracortical region. More than 90% of the osteoclasts were observed in the areas with strain intensity higher than 85.0 μ strain for the high stimulation group.

1.6 Bone homeostasis, remodelling and mechanobiology

Bone accumulates damage throughout life and is continuously removed and replaced. The ongoing replacement of old bone tissue by new bone tissue is called remodelling. The regulation of bone resorption serves two important functions firstly the maintenance of the skeleton as a structural support system which is constantly being remodelled and secondly a metabolic role in mineral homeostasis as bone provides a reservoir of calcium and phosphate for the body. Remodelling helps in removal of damaged and injured bone, replacing it with new tissue and freeing up reservoirs of calcium required by other tissues. The premise of mechanobiology, which includes the interaction of mechanical stimuli and biological responses, is that biological processes, including bone remodelling, are regulated by signals to cells generated by mechanical loading. Exactly how external and muscle loads are transferred to the tissue, how the cells sense these loads, via either through stress or strain levels, and how the signals are translated into the cascade of biochemical reactions to produce cell expression are still unknown.

Bone replacement is started with orthoclastic bone resorption followed soon after by osteoblastic bone formation. These are usually regarded as independent processes, but, in reality, resorption and formation are closely linked within discrete temporary anatomic structures (Rho et al., 1998). These structures were first named by Frost (Frost, 1969), who gave them the term ‘basic muticellular units’ usually abbreviated to BMU. A fully developed BMU consists of a team of osteoclasts in front forming the cutting cone, a team of osteoblasts behind forming the close cone, some form of blood supply and associated connective tissue (Parfitt, 1994). The lifespan of a single BMU is about 6-9 months during which several generations of osteoclasts (average life of about 2 weeks) and osteoblasts (average life of about 3 months) are formed.

The BMU basically moves in three directions, excavating and refilling a tunnel through cortical bone or trench across the surface of trabecular bone. A cortical bone BMU travels at about 20μm per day (Parfitt, 1994) while the cancellous BMU travels about half this distance at about half the speed, thus functioning similar timings as compact bone (Parfitt et al., 1996).

Two types of bone remodelling have been suggested: One that is not site dependent and second that is targeted towards the specific sites (Parfitt et al., 1996). The re-establishment of mineral content does not require that bone is removed or replaced in a specific area. However, the repair of both fractures and microfractures or any damage in bone by fatigue loading requires site dependent remodelling. Whether this remodelling occurs, and if indeed it does how much of bone turnover is targeted and how much is non-targeted is still unknown (Burr, 2002).

In adulthood the activities of osteoblasts and osteoclasts are balanced in adults and remodelling has no overall effect on the amount of bone. However during childhood there is more modelling than remodelling. Modelling helps in the maintenance of the normal shape of bones during growth and is responsible for the increase in bone circumference during growth. In late adulthood, bone loss occurs as in menopausal osteoporosis, when the amount of bone resorption is higher than the amount of bone formation. Trabecular bone is more active in remodelling than the cortical bone. Bone modelling and remodelling are influenced by parathyroid hormone (PTH), oestrogen, calcitonin, serotonin and leptin growth factors which primarily act on osteoblasts modifying RANKL and OPG expression but minimally affecting RANK expression. Other factors like cytokines, and prostaglandins, hereditary and nutritional factors and physical activity also affects bone remodelling (Seeman and Delmas, 2006; Shapiro, 2008).

Both PTH and 1,25 $(OH)_2D_3$ increase RANKL mRNA expression and decrease OPG mRNA expression but these changes vary with maturation of osteoblast cells (Thomas et al., 2001). Oestrogen acting directly on osteoblasts, has a dual effect; it increase bone formation and reduce bone resorption by enhancing osteoblast proliferation (Majeska et al., 1994), and further reduce osteoclast activity by increasing OPG production in osteoblasts (Hofbauer et al., 1999). Calcitonin, a known inhibitor of bone resorption, can act directly on osteoblasts by enhancing proliferation, increasing OPG mRNA expression and inhibiting RANKL mRNA (Tian et al., 2007). Leptin has also been reported to be expressed by osteoblasts (Reseland et al., 2001). Leptin is a cytokine like hormone also secreted by adiposities and controls food and energy expenditure. Leptin is a potent inhibitor of bone formation and possibly act through a central relay (Elefteriou, 2008). Destruction of Leptin receptors leads to an increased cancellous bone mass. This

finding confirms that leptin can control bone formation through the central nervous system (Takeda et al., 2002). Following these observations, a number of central nervous mediators which are able to modulate bone remodelling have been identified in animal studies. Among these researches, the Neuropeptide Y system (Baldock et al., 2002) supports the idea that the central nervous system is involved in the control of bone remodelling.

1.6.1 Mechanotransduction in bone tissue

Several researches with different loading mechanisms showed that mechanical stimuli have an influence at the cellular level of bone tissue. Prerequisite for this influence is the transduction of mechanical signals into the cell; this phenomenon is termed as Mechanotransduction. The mechanotransduction process is essential for the maintenance of skeletal homeostasis in adults. This phenomenon is considered to be regulated by hormones, osteoblastic cells and mechanical stimuli. Mechanotransduction involves mechanoreceptors, such as integrins, cadherins and stretch-activated Ca^{2+} channels, together with various signal transduction pathways and ultimately regulates gene expression in the nucleus.

1.6.1.1 Cellular mechanism of Mechanotransduction

Initially transfer mechanism of the mechanical signal, deformation of the cell membrane by stretch as well as shear stress mediated by the fluid flow in the canaliculi is detected by the osteoblasts and osteocytes respectively (Duncan and Turner, 1995; Pavalko et al., 2003). Osteoblasts are directly activated by loading, which leads to matrix synthesis and proliferation, as well as being indirectly activated by growth factors, and by the release of prostaglandins and NO by the osteocytes (Mikuni-Takagaki, 1999).

Glycocalix is a primary sensor of mechanical loading signals that can transmit force to plasma membrane or the submembrane cortex (actin cortical skeleton) (Tarbell et al., 2005). Mechanotransduction sites within the plasma membrane include lipid rafts, calveolae or at more remote regions of the membrane including intercellular junctions (adherens junctions) and cell matrix contacts (Pavalko et al., 2003). Mechanical strain also enhanced expression of cadherins, proteins of the adherens junctions which interlink the cytoskeleton between neighbouring cells (Rezzonico et al., 2003). Adhesion kinase interacts with the large conductance

calcium-activated hSlo K+ channel in the focal adhesion complexes of human osteoblasts (Rezzonico et al., 2003). Previous research has shown GTPases, such as RAS are activated by mechanical strain in osteoblast-like cells. Stretch-activated Cation channels (SA-CAT) are also thought to be responsible for Mechanotransduction in osteoblasts. It has also been studied that expression of connexion (Cx) 43, a major component of gap junctions, is increased by mechanical strain and regulated by prostaglandin E2 (PGE_2) in an autocrine manner (Cherian et al., 2005).

Signal transduction of mechanical stimuli is dependent on the structural integrity of the microfilament component of the cytoskeleton. Research has shown that cyclic forces induce an enhanced cytoskeleton anchorage of tyrosine-phosphorylated proteins and an increased activation of FAK and mitogen-activated protein (MAP) kinase. Attractive candidates for integrating mechanical signals includes, nuclear matrix proteins including nuclear matrix protein (NMP) 4/cas interacting zinc finger protein (CIZ). These transcription factors localize at adhesion plaques, transfer into the nucleus, bind to consensus DNA sequences, and can activate promoters of mechanosensitive genes. Mechanical stimulation leads to upregulation of growth factors, such as insulin-like growth factor (IGF) I and II, vascular endothelial growth factor (VEGF), transforming growth factor (TGF) β1 and bone morphogenetic protein (BMP) 2 and 4, which act via autocrine and paracrine mechanisms, through their tyrosine and serine/threonin receptors (Mikuni-Takagaki, 1999; Hughes-Fulford, 2004). Furthermore BMP-2 induced signalling pathway, leads to the expression of the three osteogenic master transcription factors including Osterix, Runx2, and Dlx5 (Lee et al., 2003). Previous studies have provided evidence of signal pathways interacting, such as for IGF-I with the estrogen receptor (ER) signaling pathway in the proliferative response to mechanical strain (Lau et al., 2006). A crosstalk among anabolic, intercellular pathways may enhance the upregulation of these pathways, eventually leading to the cellular response on mechanical loading.

Osteoblast differentiation is triggered by mechanical stimulation, which induces the secretion of hormones and growth factors, thus affecting the differentiation and proliferation potential of osteoblasts. Osteocytes are the mechanotransducer cells of bone. It is osteocytes that combine actions of hormones and growth factors and promote osteoblastogenic events in response to a range of mechanical stimuli,

including (oscillating) fluid flow, substrate strain membrane deformation, vibration, altered gravity and compressive loading.

Nitric oxide (NO) secretion is another key load-sensing event. Research has demonstrated secretion of NO by cyclically stretched primary osteoblasts. NO binds to a regulatory site on Ras and potentially stimulates proliferation and ECM production through the Ras-Raf-mitogen-activated protein kinase (MEK)-extracellular signal-regulated kinase (ERK) cascade. Cyclo-oxygenase (Cox) 1,2 activation downstream of NO and ERK1,2 activation is also necessary for induction of anabolic functional changes in osteoblast (Kapur et al., 2003).

Studies have shown that osteocytes are very sensitive to stress applied to intact bone tissue. Imaging research involving computer simulation models have shown that mechanosensors lying at the surface of bone, as osteoblasts and bone lining cells do, would be less sensitive to changes in the loading pattern than the osteocytes, lying within the calcified matrix (Skerry et al., 1989; el Haj et al., 1990; Dallas et al., 1993; Lean et al., 1995; Terai et al., 1999; Tatsumi et al., 2007). Furthermore targeted ablation of osteocytes in mice disturbs the adaptation of bone to mechanical loading (Tatsumi et al., 2007).

When bones are loaded, the resulting deformation will cause a thin layer of interstitial fluid surrounding the network of osteocytes to flow from regions under high pressure to regions under low pressure (fluid flow hypothesis). This flow of fluid is sensed by the osteocytes which in turn produce signalling molecules that can regulate bone resorption through the osteoclasts, and bone formation through osteoblasts leading to adequate bone remodeling (Cowin et al., 1995; You et al., 2000). Previous study has shown that the cell shape and distribution of actin and paxillin staining in osteocytes of mouse tibiae and calvariae were orientated accordingly to the respective mechanical loading patterns applied in these bones, suggesting that osteocytes might be able to directly sense matrix strains in bone (Vatsa et al., 2008).

The conversion of physical force into biochemical information is essential to overall development and physiology and goes beyond the skeletal system. Bone is naturally designed to respond to and adapt to changes in mechanical loads. The mechanisms by which overloading or underuse in mechanical stimuli cause bone

formation or resorption are the same, although the direction of changes is different. There are no absolute levels of activity that constitute overuse or underuse for example it is worth noting that overloading and underuse should be defined as the increase and decrease respectively, in activity relative to that in which skeleton is currently habituated (Skerry, 2008). One of important manifestations of aberrant mecahncotransduction “cross talk” between osteoblasts and osteoclasts is osteoporosis, in which an increased rate of bone resorption and reduced bone formation *per se* is observed. RTT bone phenotype has been frequently linked with osteoporosis. Osteoporosis can originate from disease, hormonal or dietary deficiency and show a clinical spectrum of loss of bone density, thinning of bone tissue and increased vulnerability to fractures. Similar bone loss can also result from decreases in mechanical loading owing to inactivity/ extended bed rest or exposure to microgravity (Bucaro et al., 2004).

1.7 Bone development and growth

Bone development (ossification) involves two types of processes; intramembranous ossification (flat bones) and endochondral ossification (long bones). The main difference between the two types of development is the presence of the cartilaginous phase in endochondral ossification (figue 1-7).

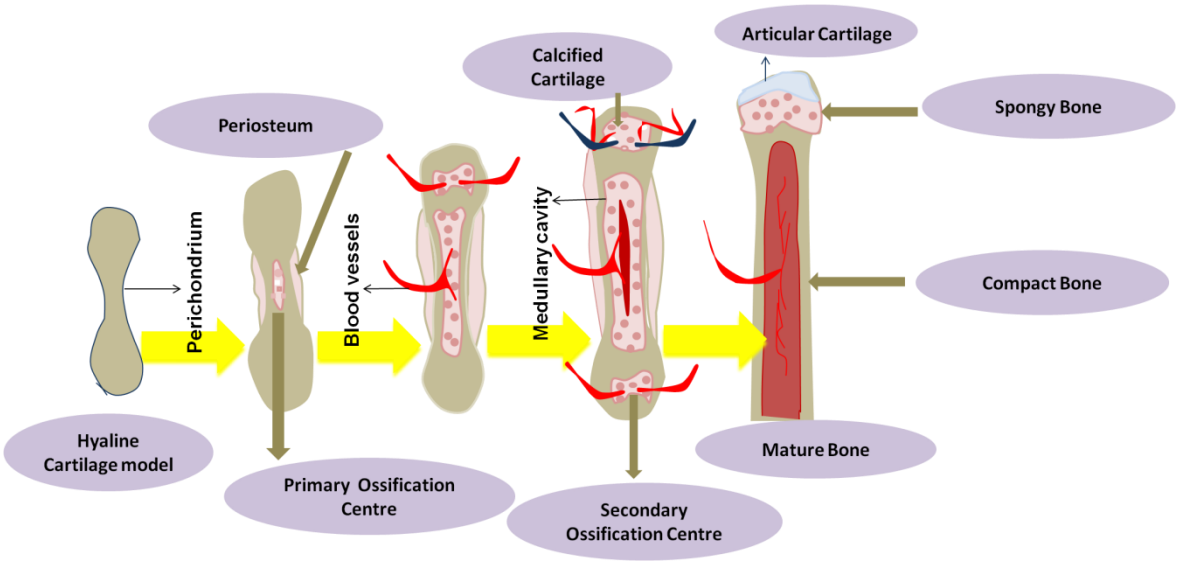

Figure1-7 The ossification process in long bone
Progression of ossification from the cartilage model of the embryo to young adult.

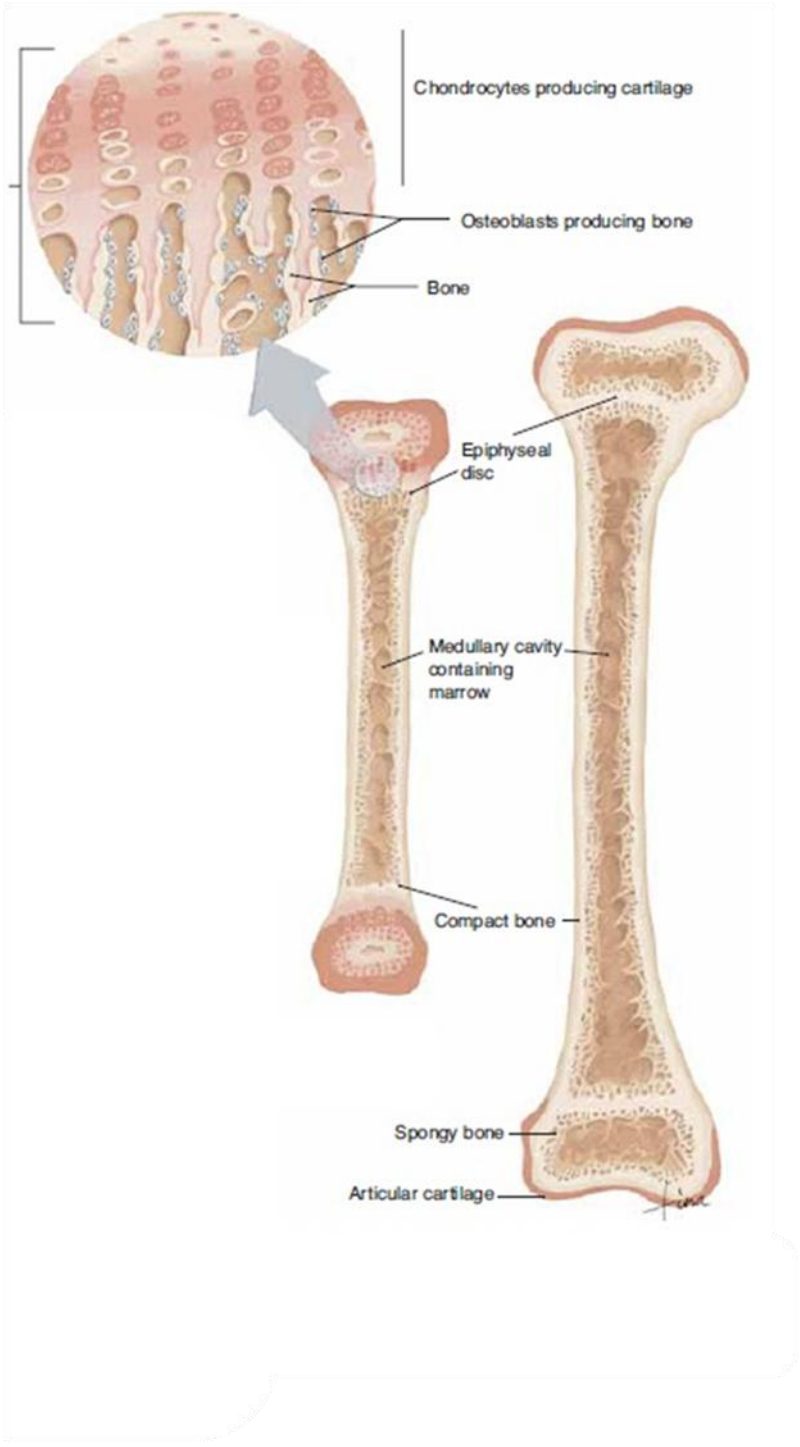

Figure 1-8 Microscopic view of an epiphyseal disc showing cartilage production and bone replacement

1.7.1 Intramembranous ossification

A group of mesenchymal cells, under the influence of the local growth factors, forms a condensation within the highly vascularised area of the embryonic connective tissue by proliferating and differentiating directly into pre-osteoblasts and then on osteoblasts(Shapiro, 2008). The osteoblasts then join together to form an ossification centre. Subsequent mineralisation of the osteoid matrix begins working outward from the ossification centre (figure 1-7). This leads to the early trabeculae formation and the periosteum develop resulting in the formation of woven bone.

1.7.2 Endochondral ossification

Most bones of the skeleton, including those of the limbs, vertebral column, pelvis and base of skull, develop by endochondral ossification. In this process of ossification the primitive mesenchymal cells differentiate into chondrocytes and produce crude cartilage models of the adult bone destined to form at that site. An avascular fibrous layer, the perichondrium, surrounds each cartilage model. Chondrocytes near the centre becomes hypertrophic and matrix undergoes mineralization (Boyce et al., 1999). Perichondrium then converts into periosteum by invasion of capillaries and osteoclast, which later on establish a vascular network. Pro osteoblasts also enter with the invading capillaries and differentiate into osteoblasts, which deposit osteoid on remnants of the mineralized cartilage, creating a primary ossification centre. Secondary ossification centres appear at one or both ends and expand by endochondral ossification to form the epiphyses of long bones (figure 1-7). As the epiphyses expand, they remain separated from the primary ossification centre, now occupying the diaphysis and metaphysic of the developing bone, by the physis or growth plate. Very limited growth in size of epiphysis continues by endochondral ossification beneath the articular cartilage at the articular-epiphyseal cartilage complex (Boyce et al., 1999). The epiphyseal side ofthe growth plate soon becomes capped by a layer of trabecular bone, which prevents further growth from that side but proliferation of chondrocytes in the growth plate and endochondral ossification on the metaphyseal side continues till maturity (Jubb, 1993) (figure 1-8).

1.8 Animal models of Rett Syndrome

Rett syndrome being a monogenic disorder has raised an interest in the scientific community to investigate further the pathogenesis, causative factors and therapeutic interventions (Neul and Zoghbi, 2004). Since Rett syndrome is caused by *MECP2* mutations, RTT can be modelled using *Mecp2* knockout mice. Several models of RTT have been created and many of them have shown RTT phenotype similar to the one found in Rett syndrome patients. Summary of animal models that have been used is as below:

1. One of the early mouse models was created by Chen *et al* by the deletion of exon 3. In this *Mecp2*$^{-/y}$ (null) male mice model *Mecp2* was knocked out either globally or specifically in central nervous system (CNS)(Chen et al., 2001). The mouse model showed nervousness, pila erection, body trembling, and occasional hard respiration around age of 5 weeks but showed a normal growth before that period. The heterozygous females, *Mecp2*$^{-/+}$ with mosaic network of cells expressing WT *Mecp2* allele and cells expressing mutant *Mecp2* allele (absent *Mecp2*) displayed many of the cardinal features that characterise RTT in humans, with initial period of approximately 4 months of normal growth followed by weight gain, reduced activity, ataxia and gait abnormalities during the later stage (Chen et al., 2001). The same group of researchers created another mouse model by knocking out *Mecp2* specifically in postnatal neurons and the mouse model displayed the similar milder phenotype as compared to the germ line *Mecp2* deletion. Both of these models showed that RTT phenotype is caused primarily by lack of functional copy of *Mecp2*.

2. Guy and colleagues (Guy et al., 2001) also have developed mouse models mimicking the human RTT phenotype. In 2001 they created a *Mecp2*$^{-/y}$ (null) mouse model in which *Mecp2*-exon3 and exon4 were deleted. This mouse, unlike the mice created by Chen et al (Chen et al., 2001), did display an apparent normal development in first 3-4 weeks after birth corresponding to the characteristic normal growth in first 6-18 months in RTT patients. After 4 weeks, the henizygous KO male mice developed gait

abnormalities, hypoactivity, and respiratory problems followed by premature death around 12-14 weeks. Heterozygous female mice, *Mecp2*$^{-/+}$ show normal developmental period of 3 months followed by inertia development and hind limb clasping. Some of the females remain symptomless as long as one year while majority developed RTT like phenotype between 6-9 months which grew more severe but then stabilised.

3. More mouse models have been developed as well including *Mecp2*^{308} mouse model (Shahbazian et al., 2002a). This mouse model was created with a truncated version of Mecp2 and recapitulated many features of RTT phenotype but display an extended survival of up to one year as compared to early morbidity and mortality shown in Stop mouse model.

4. In 2006, another group of researchers have generated a mouse line by insertion of missense mutation in Mecp2 to replace amino-acid threonin T158 with methionine to mimic one of the most common missense mutation in human (Bienvenu and Chelly, 2006). This mouse model displayed a milder RTT phenotype in comparison to Null mouse models and a slightly extended survival (Goffin et al., 2012). The analysis of this mouse model suggested that a single *MECP2* mutation could be almost as lethal as the absolute absence of the protein.

5. Guy et al in 2007 created a functional knockout mouse model through silencing the endogenous *Mecp2* gene by the insertion of a lox-stop cassette (Dragatsis and Zeitlin, 2001) into intron 2 of *Mecp2* gene (Guy et al., 2007). *Mecp2*$^{Stop/y}$ male mice displayed tremor, hypoactivity, breathing problems, gait problems, and general deterioration with death around 11 weeks of age. The same group of researchers used a modified approach of this model to create a mouse model in which Cre recombinase and modified oestrogen receptor (Cre-ER) were combined with the *Mecp2*$^{lox/stop}$ allele. This combination allowed conditional activation (un-silencing) of endogenous *Mecp2* under its own promoter and regulator elements (Guy et al., 2007). This Stop mouse model (Guy et al., 2007) mirrors the human disease in that the inactivation is lethal in males and leads to delayed but enduring phenotypes in females, making them a good model to test efficacy

of new therapeutic interventions. I have used this mouse model in my current project and will be described in more detail in next chapter.

6. Another mouse model was created by Samaco et al (Samaco et al., 2008)by silencing *Mecp2* in tyrosine hydroxylase containing neurons. These mice displayed motor abnormalities and respiratory problems with an increased rate of apnoea. The observations obtained from this mouse model points towards the possible link between dysfunction in aminergic systems may be responsible for the breathing problems of RTT.

7. More recently a subtle RTT phenotype including autistic like repetitive behaviours was observed in a mouse model created by Chao et al. In this mouse model a *Mecp2* was silenced specifically in inhibitory GABAergic cells (Chao et al., 2010).

1.9 Reversibility of RTT-like phenotype

It is generally accepted that the abnormalities in brain development lead to permanent neurological and psychiatric features due to the limited ability of brain to generate new neurons or radically repair itself. However during the past decade a number of animal models of such diseases including Down syndrome, fragile X syndrome and Angelman syndrome (Dolen et al., 2007; Fernandez et al., 2007) have started showing that some disease phenotypes can be rescued even in adult mice (Ehninger D, 2008). The similar trend has been reported in RTT (Guy et al., 2007; Derecki, 2012; Derecki NC, 2012).

Rett syndrome has been found to result from failure of neurons to mature or failure to maintain a mature phenotype (Kishi and Macklis, 2004; Palmer et al., 2008). Although *MeCP2* is also present in astrocytes (Schmid et al., 2008) a deletion and neuron specific expression of *Mecp2* studies in mice showed a dominant mutant phenotype is principally due to absence of *MeCP2* in neurons (Chen et al., 2001; Guy et al., 2001; Luikenhuis et al., 2004).

Whether RTT phenotype is reversible or even preventable needs much consideration. Since neurons seems to require *MeCP2* throughout their lives, there is possibility that the introduction of normal *MeCP2* or treatment strategies

targeting *MeCP2*-related signalling might restore function and thereby reverse RTT phenotype. Another possibility is based on the assumption that may be *MeCP2* is essential for neuronal development during a specific time frame and after which damage caused by its absence is permanent and are thus insensitive to simple restoration of *MeCP2* or other intervention beyond a critical period.

1.9.1 Rescue of RTT like phenotype in *Mecp2* knockout animal models

Several mouse model studies have been conducted in order to test the reversibility of RTT-like phenotype.

1.9.1.1 Global reintroduction of *Mecp2* in mouse model studies

In one study it was shown that modest over expression of *Mecp2* transgene under a generic neuron-specific (tau) promoter in the *Mecp2*-null mice could prevent RTT like phenotype on the other hand the severe overexpression of *Mecp2* transgene (2-4 fold of the WT level) in the same mouse model showed a profound motor dysfunction (Luikenhuis et al., 2004). This study highlighted the importance of maintain MeCP2 protein expression at an appropriate level. This is especially important when considering potential gene therapies.

Similarly another study using an early brain-specific activation of *Mecp2* under either nestin (drive *Mecp2* expression on pre-mitotic cells) or tau (drive *Mecp2* expression on post mitotic neurons) promoter, suggested that the introduction of *Mecp2* to the nervous system under artificial promoter is sufficient to enable a modest amelioration of RTT- like phenotype (Giacometti et al., 2007).

Guy and colleagues (Guy et al., 2007) have created a mouse model in which endogenous *Mecp2* gene is silenced by insertion of a lox-stop cassette but can be conditionally activated. These mouse models showed robust symptom reversal and dramatically enhanced survival if treated once symptoms had developed. Another study by the same authors has shown an improvement in wide range of respiratory and locomotors phenotypes along with the structural remodelling in the brain following *Mecp2* activation (Robinson et al., 2012a).

Another interesting study (McGraw et al., 2011) in which an adult mouse model of RTT was created (tamoxifen-induced excision of a floxed *Mecp2*) suggested that *MeCP2* is critical for maintenance of neurological function in the adult nervous system. Studies conducted by Robinson & colleagues and McGraw & colleagues suggested, that potential therapies for RTT are likely to be required throughout life.

1.9.1.2 Restricted re expression of *Mecp2* in mouse model studies

Studies, on more restricted expression of *Mecp2*, in which promoters other than the endogenous *Mecp2* promoter have been used, have shown a more modest effect. Study conducted by Alvarez Saavedra *et al* in which they have used Ca^2/calmodulin dependent protein kinases II (CamKII) or enolase promoter in the forebrain and cerebellum/striatum respectively, didn't rescue the RTT like phenotype in *Mecp2*$^{-/y}$ male mice (Alvarez-Saavedra et al., 2007). However *Mecp2*$^{-/+}$ female mice shown improvement in mobility and locomotors activity to WT levels (Jugloff et al., 2008). The sustained deficits found in these mouse models could be due to dysfunction of region or cell types in the brain still devoid of *Mecp2* or enhanced expression of exogenous promoters or other unknown mechanism.

1.10 Therapeutic interventions for RTT

Currently several treatment strategies are employed in order to combat the underlying pathology of Rett syndrome. *MECP2* target approaches broadly includes, activating a silent copy of MECP2, gene therapy, and pharmacological approaches.

Guy et al (Guy et al., 2007) demonstrated reversibility of the *Mecp2* knockout phenotype, as described in previous section and raised interest in exploring therapeutic approaches designed to reverse existing pathogenesis of RTT and to prevent its onset.

1.10.1 Reactivation of the normal allele

As described earlier, *MECP2* is located on the X chromosome and is subject to X chromosome inactivation (XCI). Each cell in a heterozygous female RTT patient expresses either the normal or mutant *MECP2* allele, never both. The process of X

chromosome inactivation is random and results in an approximately 50:50 mixture of cells, although there might be variations between individuals. Studies have shown a mosaic pattern of brain cells expressing normal and mutant *Mecp2* alleles (Guy et al., 2007). The likely strategy will involve re activation of the inactive X to allow expression of the normal allele in the same cells (Mohandas et al., 1981). However this approach is unlikely applicable, as the re activation of entire inactive X can lead to pathological levels of gene expression at many loci. Re-activation needs to be targeted only at the *MECP2* locus but currently no obvious resources are there to target re-activation.

1.10.2 Pharmacological approaches

Identifying factors that are downstream of *MeCP2* function and tackle those pharmacologically seems to be a sensible approach to develop therapeutic interventions in RTT. Nevertheless it is unlikely for drug molecules to replace the yet unknown, function of *MeCP2*. For example brain biopsies from RTT patients have reported decrease in monoamines (noradrenalin, serotonin and dopamine) levels (Lekman et al., 1989). This reduction was also observed in *Mecp2*-null mice (Roux et al., 2010). The *in* vitro application of noradrenalin to the brainstem in *Mecp2* null mice, which displayed irregular rhythms, stabilized the respiratory network rhythmogenesis (Van Esch et al., 2005) suggesting a potential role of monoamine in RTT therapy.

Similarly loss of *MeCP2* is associated with other neurotransmitters like glutamate (Maezawa and Jin, 2010), GABA (Chao et al., 2010) and various pharmacological approaches have been employed for therapeutic benefits in RTT patients.

Another pharmacological approach would be to target immediate consequences of the specific mutation responsible for the *MeCP2* abnormal functions in the particular patient. Many patients carry nonsense mutations in *MECP2* (e.g p.R168X, p.R255X, p.R270X) which are associated with premature stop codons (PSC_s). Antibiotics like aminoglycoside, which permit ribosomal read-through of PSC_s during translation, would enable production of full length functional protein (Martin et al., 1989). Forty percent of typical Rett syndrome patients with *MECP2* mutations have one of the nonsense mutations (Philippe et al., 2006), aminoglycosides seem a promising avenue to achieve a full length functional

MeCP2. However the low read through efficiency together with the known toxicity of these drugs indicates that currently available aminoglycoside drugs are unlikely to represent a new therapeutic approach at present.

1.10.3 Gene therapy

Gene therapy is a promising approach for treating multiple disorders including neurological, genetic and cancers (Blömer et al., 1996). Overall the gene therapy involves delivering of new genetic instructions into target tissues to compensate for missing or aberrant genes or to convey a new function. Gene therapy for genetic disorders provides treatment at the molecular level to fix the primary underlying cause of the disorder instead of tackling variable secondary effects.

As previously explained Rett syndrome is caused mainly by the *MECP2* gene mutations whose encoding sequences, isoforms and resultant protein products are well studied. The lack of effective conventional therapeutic approaches and a lack of understanding of the downstream effects of *MeCP2* highlight the importance of tackling RTT at the genetic level. Also the reported phenotype reversibility of RTT-like phenotypes in *Mecp2* knockout mice models makes it a very important candidate for gene therapy. In RTT the major objective of this therapy will be to deliver a working copy of *MECP2* to as many affected brain cells as possible to raise function (at both the molecular and cellular level) above a threshold required for improvement of the clinical picture. One study has demonstrated the potential for lentiviral transgene delivery to improve the phenotype of *Mecp2* null neurons derived from neuronal stem cells in culture (Rastegar et al., 2009).

Recently an improvement in survival and severity profile was reported in a *Mecp2* null male mice (Gadalla et al., 2013). The researchers have used a neonatal intracranial delivery approach of a single-stranded (ss) AAV9/chicken β-actin (CBA)-MECP2 vector resulting into a significant improvement in the phenotype severity score, in locomotor function and in exploratory activity. In another recent study using a female mouse models it was shown that self-complementary AAV9, bearing *MeCP2* cDNA under control of a fragment of its own promoter (scAAV9/*MeCP2*), is capable of reversing and stabilising RTT phenotype (Garg et al., 2013). However encouraging these results may be, there are many challenges to overcome for this approach to be successful. Some of these challenges include

finding an appropriate vector, transducing sufficient cells, avoidance of transgene repression and over expression of exogenous *MeCP2* in the mosaic female brain.

It will be important to assess how such novel therapies impact on non-CNS aspects of RTT and thus it is important to characterised and investigate inherent reversibility of bone phenotypes in animal models of Rett syndrome.

1.11 Summary and Aims

Rett syndrome (RTT), traditionally considered a neurodevelopmental disorder, mainly affects girls and is due principally to mutations in the X-linked gene methyl-CpG-binding protein 2 (*MECP2*). Whilst it is well established that the majority (>95%) of classical RTT cases are due to mutations in the *MECP2* gene, the underlying function and regulation of *MeCP2* protein remains unclear. *MeCP2* is a nuclear protein and is especially abundant in the brain. However, it is also expressed throughout the body and in addition to the neurological phenotypes, a number of overt peripheral phenotypes are also common in RTT. For instance, spinal deformity (principally scoliosis) is a very common feature with ~50-90% of patients developing severe scoliosis, many of whom require corrective surgery. Other prominent skeletal anomalies include early osteoporosis, osteopenia, bone fractures and hip deformities. Previous studies have found that Rett syndrome patients have reduced bone mass. As a result, RTT patients have an increased risk of fractures and commonly sustain low-energy fractures. Whilst *MeCP2* is known to be expressed in bone tissues and studies have suggested a role of the protein in osteoclastogenesis, the role of *MeCP2* in bone homeostasis is poorly defined.

The exact mechanism by which disrupted *MeCP2 function* affects bone tissue is not yet defined. Therefore the main aim of my PhD was to assess skeletal phenotypes in a mouse model of Rett syndrome and to explore whether aspects of bone-related pathologies were amenable to genetic recue of the *Mecp2* gene.

Specific goals were as follow:

- To establish whether silencing of the *Mecp2* gene results in biomechanical bone phenotypes in a *Mecp2*$^{stop/y}$ mouse model of Rett syndrome.

- To establish if postnatal reactivation (genetic rescue) of *MeCP2* gene results in any reversal or prevention of RTT-related biomechanical bone phenotypes.

- Explore the effects of *MECP2* protein mutation on bone structure, bone mineral, bone collagen or bone cells.

The overall objective of my thesis research is thus to analyse the biomechanical and anatomical properties of bone tissue in a mouse model of Rett syndrome and explore whether such features are potentially reversible using gene-based therapeutic approaches.

Chapter 2

General materials and methods

2.1 Experimental Animals Models

The Mecp2-stop mouse model [*Mecp2*$^{stop/y}$ (male) and *Mecp2*$^{+/stop}$ (female)] and Mecp2 genetic rescue mice [*Mecp2*$^{stop/y}$*, CreER* (male) and *Mecp2*$^{+/stop}$, *CreER* (female)] were created and supplied by Prof Adrian Bird's laboratory at the University of Edinburgh, Edinburgh, United Kingdom (UK) (Guy et al., 2007, Robinson et al., 2012). These mice together with wild-type littermates were used as part of a larger study to assess various neurological and brain morphological phenotypes (Robinson et al., 2012). After the completion of such behavioural phenotyping studies, adult male and female mice were killed by cervical dislocation and were transcardially perfused with 4% paraformaldehyde (0.1M phosphate buffered saline, pH 7.4) prior to shipping to the University of Glasgow, Glasgow, UK for use in my PhD studies. Another subset of mice was used to establish the expression of Mecp2 in bone cells (see section 2.5 for details)

2.2 Design of Mecp2 stop and rescue mouse mode

Guy and colleagues (Guy et al., 2007) created a mouse model in which the endogenous Mecp2 gene was silenced by insertion of a *lox-stop* cassette flanked by loxP sites. By crossing this line with mice expressing an inducible Cre recombinase fused to a modified oestrogen receptor (CreER) (Hayashi and McMahon, 2002), an additional cohort of mice enabled the conditional reactivation of MeCP2 under the control of its endogenous promoter and regulatory elements by Stop cassette deletion (figure 2-2) (Guy et at., 2007; Robinson et al., 2012).

2.2.1 *lox- stop* cassette and Mecp2 stop models

A strategy has been adopted in studies (Nagy, 2000) aiming to characterise the function of gene products by rescuing lineage or developmental stage specific

knockout phenotypes by conditional gene repair. This approach is based on the targeted insertion of a positive selection gene cassette (typically the neomycin phosphotransferase gene, *neo*) flanked by *loxP* sites into an intron. Positive selection cassettes have been known to have the potential to interfere with normal expression of the targeted allele by promoter interference, disruption of normal splicing patterns or by premature transcript termination (Meyers et al., 1998).Insertion of *neo* (neomycin phosphotransferase) within an intron has its potential drawbacks on the expression level of the target gene, including unaltered expression, a reduction in targeted gene expression (generating a hypomorphic allele), or complete inactivation (Meyers et al., 1998; Nagy et al., 1998; Dietrich et al., 2000; Wolpowitz et al., 2000).

Usually conditional gene inactivation employs the Cre/*loxP* site-specific recombination system, which provides a means to control the development and tissue specific gene disruption, thus circumventing the early lethality found in knockouts of developmentally critical genes (Sauer, 1998). The Cre/*loxP* system has also been employed to activate conditionally transgene expression by employing a floxed synthetic transcriptional/translational 'stop' cassette (STOP) (Lakso et al., 1992). The STOP cassette consists of the 3' portion of yeast His3 gene, an SV40 polyadenylation sequence and a false translation initiation codon followed by a 5' splice donor site. The floxed STOP cassette is inserted between the promoters and coding sequences of a transgene, ensuring that few, if any, transcripts containing the coding region are generated. In presence of Cre, recombination at the *loxP* sites, Tamoxifen excises the STOP cassette, and there by activating expression of the transgene (Lakso et al., 1992; Wakita et al., 1998) (figure 2-1).

In summary, the one powerful use of Cre/*loxP* technology is in the conditional removal or activation of gene function. In the former, Cre mediated recombination leads to the precise excision of an essential region within a gene so that a functional product is not produce and in the latter, Cre-mediated recombination removes a functional barrier to the production of an active gene product, thereby switching on gene activity.

Mecp2-stop mice [*Mecp2*$^{stop/y}$ (male) and *Mecp2*$^{+/stop}$ (female)] (Guy et al., 2007) were created using a *lox-stop* cassette (Dragatsis and Zeitlin, 2001) which was

inserted into intron 2 of *Mecp2* to generate an incomplete *Mecp2* mRNA that precludes translation of Mecp2 protein. Guy and colleagues performed the western blots and *in situ* immunofluorescence to confirm the absence of detectable MeCP2 protein in *Mecp2*$^{lox\text{-}Stop/y}$ (*Stop/y*) animals.

2.2.2 Rescue of Mecp2 stop models

Guy and colleagues (Guy et al., 2007) controlled the activation of *Mecp2* by combining a transgene expressing a fusion between Cre recombinase and a modified oestrogen receptor (cre-ER) with the *Mecp2*$^{lox/Stop}$ allele (Hayashi and McMahon, 2002).

2.2.2.1 Cre recombinase and modified oestrogen receptors

As described previously in section 2.3.1, Cre integrase from bacteriophage P1 to catalyze recombination between its *loxP* target sites has gained popularity as an essential tool for conditional gene activation or inactivation in mouse models (Rossant and Nagy, 1995; Rossant and McMahon, 1999; Nagy, 2000).

Scientific community thought about the way in which the utility of Cre/*loxP* system approach can be enhanced is by developing ways in which Cre activity can be controlled and a number of groups has described various approaches to control the spatial and temporal expression of the enzyme (Rossant and McMahon, 1999; Nagy, 2000).

A fusion gene is created between Cre and mutant form of the ligand-binding domain of the oestrogen receptor (ER^{TM}). This mutation prevents binding of its natural ligand (17b-estradiol) at normal physiological concentrations, but renders the ER^{TM} domain responsive to 4 hydroxyl (OH)-TM (Fawell et al., 1990; Littlewood et al., 1995). Fusion of Cre with ER^{TM} leads to the ER^{TM} dependent cytoplasmic sequestration of Cre by Hsp90 (Picard, 1994) and thus preventing Cre-mediated recombination, a nuclear event.

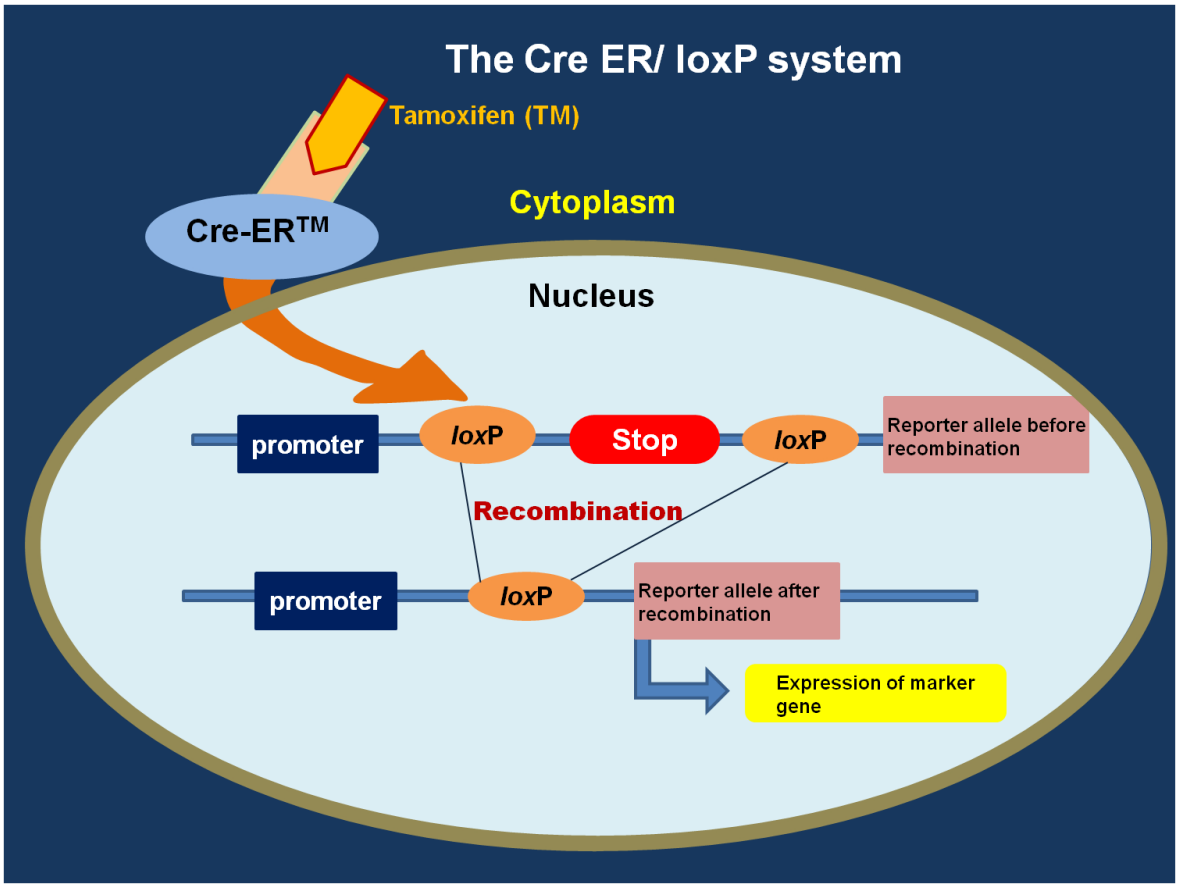

Figure2-1 Representative diagram showing, the Cre ER/*lox*P system.

CreER is tamoxifen inducible Cre recombinase. The Cre-ER protein in rescue models remained in the cytoplasm unless exposed to the oestrogen analog tamoxifen (TM), which causes it to translocate to the nucleus. Cre-mediated recombination removes a functional barrier (*lox*P-*Stop* cassette) to the production of an active gene product, thereby switching on gene activity.

Guy and colleagues rescue model was created by adopting the techniques used by Hayashi *et al* in which they had created a more broadly useful strain of mouse to generate a line in which Cre-ER^{TM} is ubiquitously expressed. Crossing these mice to an appropriate target strain permitted TM-dependent recombination in all tissues, with precise temporal control, at embryonic and adult stages (Hayashi and McMahon,2002).

2.2.2.2 Tamoxifen treatment

The Cre-ER protein in rescue models remained in the cytoplasm unless exposed to the oestrogen analog tamoxifen (TM), which causes it to translocate to the nucleus (figure 2-1). Guy and Colleagues verified this in their Stop mouse models by southern blotting that the Cre-ER molecule did not spuriously enter the nucleus in the absence of TM and cause unscheduled deletion of the *lox-Stop* cassette in Mecp2$^{lox\text{-}Stop/+}$, cre-ER (Stop/+, cre) females. Even after 10 months in the presence of cytoplasmic Cre-ER, there was no sign of deleted allele found (Guy et al., 2007).

The absence of spontaneous deletion of the *lox-Stop* cassette was evaluated independently confirmed by the finding that *Stop/y* males showed identical survival profiles in the presence or absence of Cre-ER. Therefore it was evaluated that in the absence of TM, the Cre-ER molecule does not cause detectable deletion of the *lox-Stop* cassette. The ability of Tamoxifen (TM) to delete the *lox-Stop* cassette in *Mecp2*$^{lox\text{-}Stop/y}$, cre-ER (Stop/y, cre) male mice rescue was also tested and showed high levels of recombination efficiency (Guy et al., 2007).

2.2.2.3 Tamoxifen injection regime

The unsilencing of the mice (removal of *Stop* cassette) was achieved by tamoxifen (100mg/kg; Sigma, UK) treatment, administered via intrapertoneal injection at an injection volume of 5ml/kg (dissolved in corn oil) body weight. A treatment regime of one injection of tamoxifen per week for 3 weeks followed by four daily injections on consecutive days in the fourth week was employed (Guy et al., 2007; Robinson et al., 2012a) (figure 2-3).

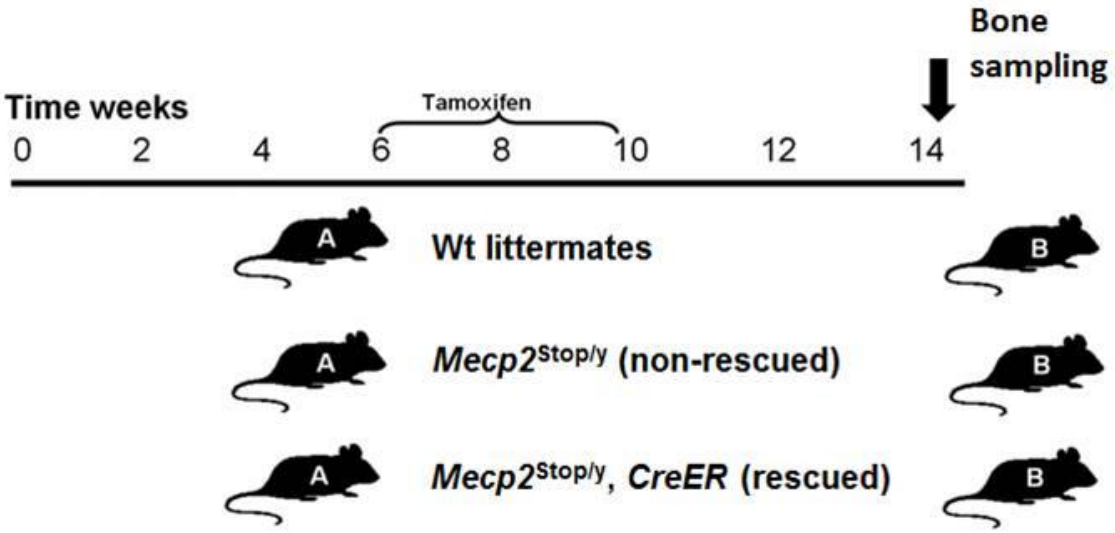

Figure2-2 Experimental design of Tamoxifen regime (rescuing) of *Mecp2*$^{stop/y}$ mice

Experimental design of the current study showing treatment (A) and sampling phases (B) in male mouse comparison cohorts. Wild-type (Wt) , *Mecp2*$^{stop/y}$ (non-rescue) and *Mecp2*$^{stop/y}$,*CreER* (rescue) were given one injection of tamoxifen (100mg/Kg) per week for 3 weeks (age 6-8 weeks) then followed by 4 daily injections in consecutive days in the 4th week (age 9 weeks). Mice were then culled at 14 weeks and bones were sampled for imaging, histology and biomechanical tests.

2.2.2.4 Behavioural testing after tamoxifen treatment

After the tamoxifen treatment, Guy and colleague (Guy et al., 2007) performed observational test to monitor the specific features of the RTT-like mouse phenotype. These tests include inertia, gait, hind-limb clasping, tremor, irregular breathing, and poor general condition. Each symptom was later on scored weekly as absent, present or severe (scores 0, 1, and 2 respectively). Wild type mice always showed the zero score, whereas *Stop/y* animals typically showed aggregated symptoms and hence the higher scores (3-10) during the last 4 weeks of life. On the other hand majority of symptomatic *Stop/y, cre* were rescued by TM treatment.

These mice did showed milder symptoms and score (1-2) and were thought to survive for up to 4 weeks from the date of first injection, instead they survived well beyond the maximum recorded life span of *Mecp2*$^{lox\text{-}Stop/y}$ (17 weeks).

Heterozygous females may be the most accurate model for human RTT (Kriaucionis and Bird, 2003) because both knockout Mecp2$^{+/-}$ and silenced *Mecp2*$^{Stop/+}$ females develop RTT like symptoms, including inertia, irregular breathing, abnormal gait, and hind-limb clasping at 4-12 months of age. Similar to the RTT patients, the phenotype stabilizes, and the mice have an apparently normal life span. The mice do become obese with time which is not seen in RTT patients.

Similar to the *Stop/y*, cre male mice, Guy et al, TM-treated Stop/+ females with clear neurological symptoms were also used for behavioural testing. These mice progressively reverted to a phenotype that scored at or very close to wild type. The report from this study (Guy et al., 2007) demonstrated that the late onset neurological symptoms in mature adult Stop/+,cre heterozygotes are reversible by *de novo* expression of MeCP2.

Behavioural studies performed by Robinson and colleagues on these *Stop/y, cre* and *Stop/+, cre* showed an improvement in structural deficits in cortical neurons, rescue of respiratory phenotype and improvement in sensory motor tasks (Robinson et al., 2012a). In my PhD project I have used these cohorts of these mice to explore putative RTT-related bone phenotypes (see next chapters 3, 4 and 5).

2.3 Breeding strategy of *Mecp2*- Stop mice

Local *Mecp2*-Stop colonies at University of Aberdeen were established by breeding heterozygous *Mecp2*$^{Stop/+}$ mice in which the endogenous *Mecp2* allele is silenced by a targeted stop cassette (*Mecp2*^{tm2Bird}, Jackson Laboratories Stock No. 006849) were crossed with hemizygous Cre ESR transgenic mice (CAG-Cre/ESR1*, Jackson Laboratories Stock No. 004453) to create experimental cohorts (Guy et al., 2007) (table 2-1)

A breeding strategy of crossing C57BL6/J/CBA F1 animals and using the F2 offspring (Robinson et al., 2012a) was used. The genotype of the mice was determined by polymerase chain reaction (Guy et al., 2007). Mice were housed in groups with littermates, maintained on a 12-h light/dark cycle and provided with food and water *ad* libitum. Experiments were carried out in accordance with the European Communities Council Directive (86/609/EEC) and a project licence with local ethical approval under the UK Animals (Scientific Procedures0 Act (1986).

2.4 Age of experimental animals

Age matched male mice cohort (Wild-type, *Stop/y, Stop/y*,cre) of mean age14 weeks ± 4 days and female mice cohort (Wild-type, Stop/+, Stop/+,cre) of mean age of 20 months ± 5days were used in my PhD project experiments.

All mice were treated were treated by a single injection of tamoxifen (see section 2.3.2.3) at 6 week postnatal age followed by 2 further weekly does at 7 week age and 8 week age with subsequent 4 consecutive daily doses in 9 week (figure 2-1) . The mice were culled after 4 weeks of tamoxifen treatment.

Female (*Stop*/+, cre) mouse models were rescued with injection of tamoxifen at 18 months of age followed by 3 weekly injection and 4 consecutive daily doses. The mice were culled 2 months after the tamoxifen treatment. Wild type control mice were treated with tamoxifen in parallel with their *Mecp2*$^{stop/y}$ and *Mecp2*$^{stop/y,\ Cre\ ER}$ littermates.

2.5 Establishment of expression of MeCP2 on bone cells

To establish MeCP2 expression in bone tissues, we have used an MeCP2-GFP reporter line (McLeod et al., 2013). The heterozygous female mice aged 10-13 weeks were engineered to express a *Mecp2*-EGFP fusion by a targeted gene knock-in in mouse ES cells (generated in Adrian Bird's laboratory at the University of Edinburgh; *Mecp2*$^{tm3.1Bird}$, Jackson Laboratories stock no. 014610). Mecp2 status was detected in cells by the presence or absence of fluorescence in living or fixed cells. Further on the experimental cohort was produced by breeding *Mecp2*$^{+/-}$ females with Mecp2 $^{GFP/Y}$ males (supplied by Adrian Bird's laboratory) on a C57BL6/j background).

2.5.1 Methodology

In these mice, MeCP2 has a GFP tag cloned into the 3' end of exon 4 to create a C terminal GFP fusion product which enables the straightforward localisation of endogenous MeCP2 protein via epifluorescence or laser scanning confocal microscopy (figure 2-3).

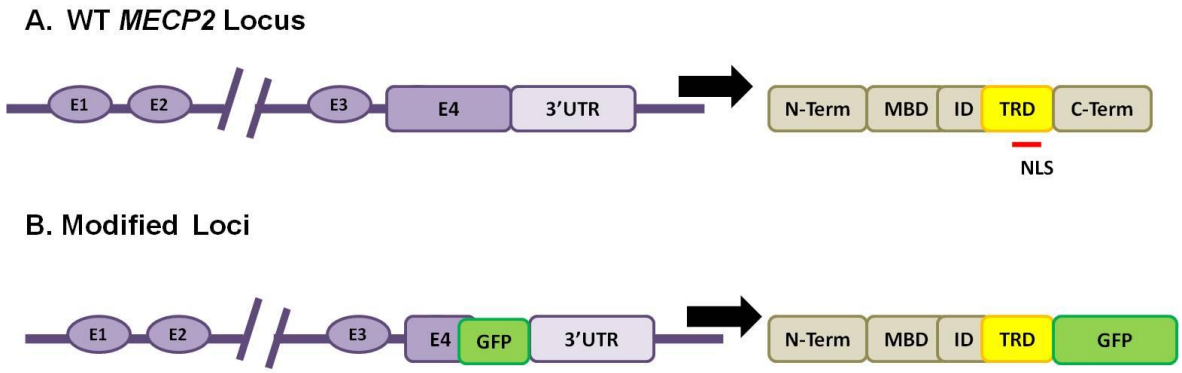

Figure 2-3 *MECP2*-GFP mouse model GENOTYPE CONSTRUCT
Schematic diagram showing GFP tagged *MECP2* mouse model design. A GFP tag is cloned into the 3'end of exon 4 to create a C terminal GFP fusion product. NTD, N-terminal domain; MBD, methyl binding domain; ID, inter domain; TRD, transcription repression domain; CTD, C-terminal domain; NLS; nuclear localisation signals (red line).

Femur bone from male and female mice were dissected out and decalcified in 10% EDTA Solution (7.4 pH) (280g EDTA, 1.5 L of distilled water, 180ml of ammonium hydroxide), for two weeks in a refrigerator at 4°C. The fresh 10% EDTA solution was changed every other day, until the bones are properly decalcified. Midshaft transverse section of 20µm thickness were carefully cut by using a Leica VT1000 microtome (Leica Milton Keynes, UK) which is maintained by Robert Kerr, West Medical Building, University of Glasgow, Glasgow, UK. Images were taken by using laser scanning confocal microscopy (Zeiss LSM710, Bio-Rad Radiance 2100, UK) using 20x and 40x objectives. Laser scanning confocal microscopy is maintained by Andrew Todd, west medical building, University of Glasgow, Glasgow, UK.

After the laser scanning confocal microscopy, we observed that all bone cells express nuclear GFP fluorescence in wild type male (figure 2-4 Ai-iV) and female mice. In contrast, GFP fluorescence is found absent in hemizygous Stop

(*Mecp2*$^{stop/y}$) mice (figure 2-4 Bi-iv), in which *Mecp2* is silenced by a stop cassette, and is observed only in ~50% of bone cells nuclei in female heterozygous Stop (*Mecp2*$^{+/stop}$) mice in which one *Mecp2* allele is silenced to mimic the mosaic expression pattern seen in human Rett syndrome (Guy et al., 2007; Robinson et al., 2012a).

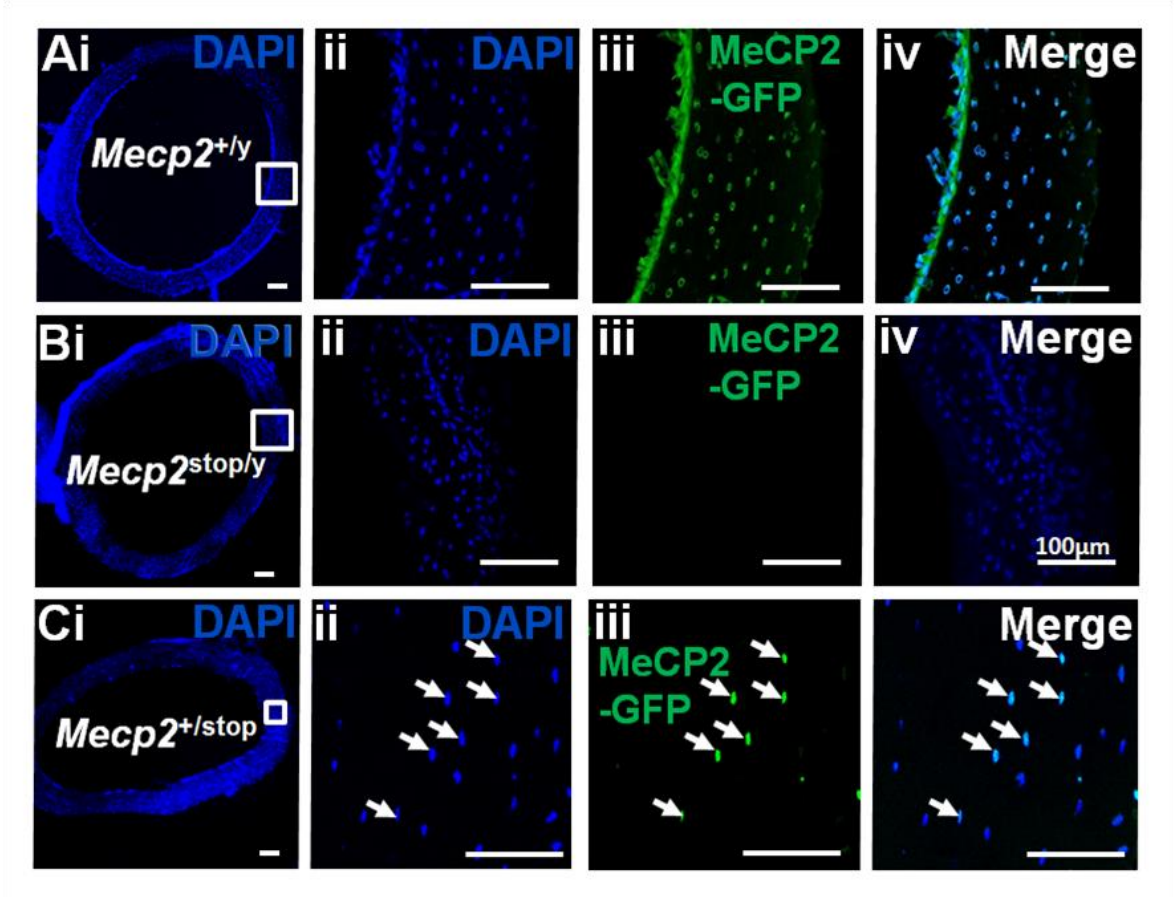

Figure 2-4 MeCP2 is expressed widely in bone tissues

(Ai) Low power and (ii-iv) high power micrographs of transverse sections taken from mid shaft mouse femur showing GFP expression in all DAPI-labelled nuclei in a male wild type (*Mecp2*$^{+/y}$) mouse in which the native MeCP2 is tagged with a C-terminal GFP. Note that MeCP2 is restricted to the nucleus of osteocytes as indicated by the complete overlap with DAPI staining but present in all nuclei. (B) GFP expression is not observed in stop mice in which MeCP2 expression is functionally silenced by a neo-stop cassette. (C) Low power (i) and (ii-iv) high power micrographs showing mosaic expression of GFP-tagged MeCP2 protein in ~ 50% of DAPI positive nuclei in a female heterozygous stop (*Mecp2*$^{+/stop}$) mouse in which one *Mecp2* allele is functionally silenced. All scale bars: 100µm.

2.6 General solutions

All chemicals below without specified origins were supplied from Merck Ltd. (BDH Laboratories, UK) or Sigma-Aldrich Company Ltd, (Sigma, UK).

2.6.1 0.2 M PB

Materials

- Solution A: 37.44 g of NaH_2PO ($2H_2O$) in 1200 ml ultrapure H_2O
- Solution B: 84.90 g of NaH_2PO_4 in 3000 ml ultrapure H_2O

Methods

Add 1120 ml of solution A to 2880 ml of Solution B and mix well. Adjust PH to 7.4 with either HCL or NaOH. Add 3000 ml distilled water to the final solution.

2.6.2 0.1 M PB

0.1 PB was made by 50/50 (v/v) dilution with distilled water.

2.7 Dissection

2.7.1 Material

Dissection of mice was carried out to obtain, right and left femur, tibia, humerus and lumbar 5 vertebrae from each mouse (n=6 per genotype).

- 50 mL Falcon tube containing 70% ethanol (EtOH) for sterilizing surgical equipment.
- Dissection board
- Pins
- Scissors
- Plain and tooth forceps

2.7.2 Method

2.7.2.1 Tibia and Femur dissection

Each Mouse was pinned to the dissection board, lying on the dorsal back with ventral surface of the body facing up. Hind limbs were sprayed down with 70% ethanol / 30% H_20. For each right and left leg, first nails were trimmed off with small dissecting scissors. Then a cut is made in the skin around the full circumference of the ankle. A second cut down the inside of the leg is made, starting at the ankle cut and ending at the tip of the 3rd metatarsal. With the help of small teethed forceps skin was peeled from the ankle towards the phalanges. Another cut is made inside the leg, starting at the original ankle cut and continuing along the tibia and femur. Skin was peeled off to the level of the hip. The medial thigh muscles are dissected 2mm proximal to and along the course of the deep femoral branch.

Dissection is continued laterally in 2 mm distance to and along the bundle of the femoral nerve, artery and vein. The tendinous insertion sites of the medial thigh muscles are clipped and the entire medial thigh muscle package excised. Excision of calf muscle composed of gastrocnemicus, soleus and plantaris from the fascia. To keep the bones in natural environment freshly dissected bones were transferred in labelled tubes filled with 0.1 M Phosphate buffer solution (figure 2-5).

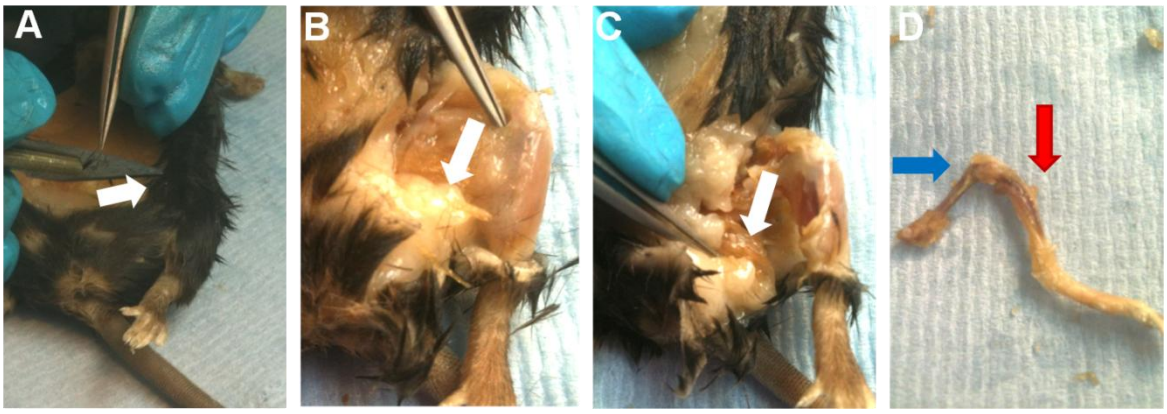

Figure2-5 Dissection of femur and tibia

Images showing stepwise dissection of lower limb long bones (femur and tibia). (A-D) dissection of mouse femur and tibia. (A); white arrow point towards the start of incision area for dissection on left lower limb. (B); Skin and subcutaneous tissue removed around femur and tibia (C); Skin, subcutaneous fat and muscle removed around femur and tibia to expose the underlying bones; white arrow points toward the skin, subcutaneous fat and medial thigh muscles (D); Image showing dissected femur (blue arrow) and tibia (red arrow).

2.7.2.2 Lumbar vertebrae 5 dissection

Each Mouse was pinned to dissection board, with ventral surface of the body facing up. Ventral body surface was sprayed down with 70% ethanol / 30% H_20. After the fur, skin and soft tissue removal, vertebrae were identified. With the help of forceps, scissors and scalpel, Lumbar 5 vertebrae were carefully dissected out from the rest of vertebrae. Excision of vertebral surrounding structure consists of Para spinal ligaments and muscles (figure 2-6).

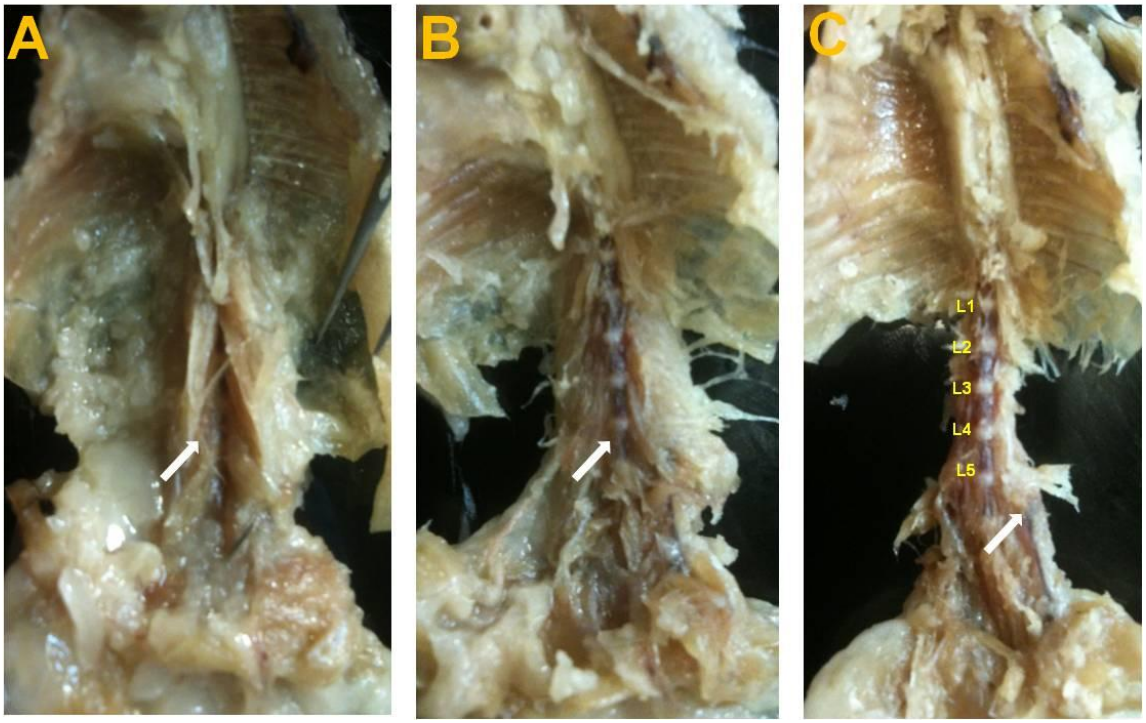

Figure2-6 Dissection of 5th Lumbar vertebrae

Images showing stepwise dissection of 5th lumbar vertebrae (A-C). (A) image taken after the dissection and removal of skin, subcutaneous tissue and organs. (B);Image taken after removal of muscles and ligaments around the vertebral column. (C); Image showing lumbar vertebrae. White arrow points towards the hip bone as the identifying anatomical point for the lumbar vertebral dissection.

2.8 Morphometric measurements

After the dissection both right and left femur and tibia along with the 5th lumbar vertebrae from each experimental genotype group were subjected to morphometric measurement (see below) before further biomechanical, radiological and histological analysis.

2.8.1 Whole body weights

Whole body weight measurements were taken using analytical balance (APX60, Denver Instruments, UK) and accuracy was taken to be 0.0001g. These measurements were required for the normalisation of individual bone weight measurement. For results, see chapter 3 result section.

2.8.2 Individual bone weights

Femur, tibia and lumbar vertebrae wet weight measurements were obtained using analytical balance (APX60, Denver Instruments, and UK) and accuracy was taken to be 0.0001g. These measurements were taken to analyse if there are any gross differences in individual weights of the bones of three comparison genotypes. For results see chapter 3 and 4 result section.

2.8.3 Individual bone lengths

In order to obtain the individual bone lengths, femur and tibia were imaged in an anteroposterior position and posteoranterior position, using a WolfVision VZ9.4F (WolfVision Ltd, Maidenhead, UK).

Images were analysed for subsequent measurements using Axiovision 4.8 Software (Carl Zeiss Ltd, Cambridge, UK). Femur gross length measurement was taken from the proximal anatomical point of the greater trochanter to the distal anatomical point of medial condyle (Di Masso et al., 1998). Tibial gross length measurements were taken from proximal anatomical point of centre of the condyles to the distal anatomical point of medial malleolus (Di Masso et al., 2004) (figure 2-7).

Right femurs were used for mechanical testing (the proximal part for the femoral neck test and the midshaft part of femur bone was used for microindentation), see details in chapter 3.

Left femurs were used for the bone histology (the proximal femur for Sirius red and TRAP staining, the distal femur for scanning electron microscopy), see details in chapter 4 and 5.

Right tibias were used for µCT, see chapter 4 and three-point bending tests, see details in chapter 3 and left tibias used for the ash weight density measures, see full text in chapter 3.

The 5^{th} lumbar vertebrae were used for trabecular bone structure measures, see chapter 4 for full detail.

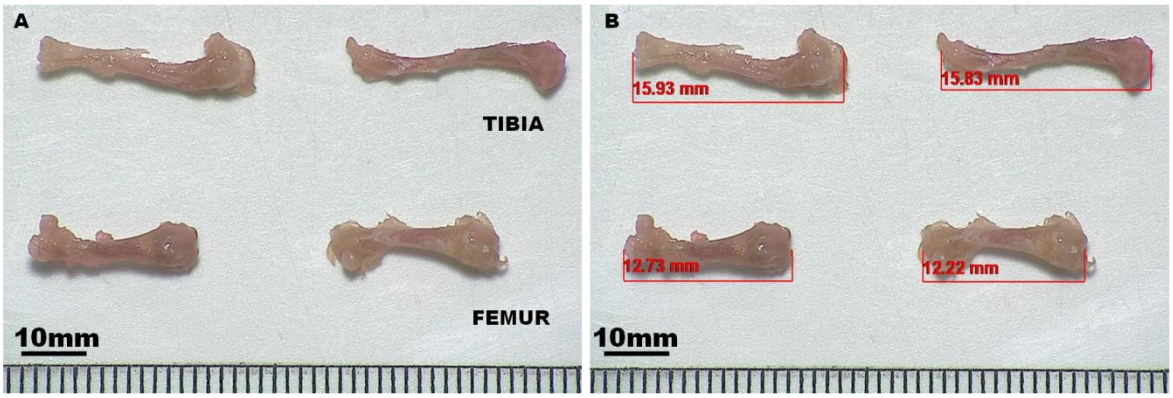

Figure2-7 Morphometric length measurements of femur and tibia
(A) Image of femur and tibia obtained using a WolfVision VZ9.4F Visualizer to obtained length measurements (WolfVision Ltd, Maidenhead, UK). (B) Images were analysed for subsequent length measurements using Axiovision 4.8 Software (Carl Zeiss Ltd, Cambridge, UK). Femur gross length measurement was taken from the proximal anatomical point of the greater trochanter to the distal anatomical point of medial condyle. Tibial gross length measurements were taken from proximal anatomical point of centre of the condyles to the distal anatomical point of medial malleolus.

2.9 Data handling and analysis

For each biomechanical, structural and histological analysis data results have been summarized using descriptive statistics. These were presented as mean ± standard deviation (SD) values and compared by using one way ANOVA followed by Tukey's *post hoc* test. All statistical analyses were performed with the aid of Prism 5.0 (Graph pad) software.

I have performed a series of biomechanical, morphological and histological on the above mentioned dissected bones which will be described in detail in the next three result chapters.

Chapter 3

Biomechanical tests revealed genotype differences in bone properties

3.1 Introduction

The majority of females with Rett syndrome are growth retarded (Schultz et al., 1993; Neul et al., 2010; Roende et al., 2011b) and this postnatal pattern of altered growth is one of RTT's earliest clinical expressions. Head growth typically decelerates during the first year of age and this further followed by a decline in somatic (height and weight) growth (Armstrong et al., 1999; Neul et al., 2010). Although not included in the clinical scales for diagnosis of Rett syndrome, patients nevertheless do suffer from bone related symptoms such as increased risk of fractures, spinal deformity (eg. scoliosis) (Roberts and Conner, 1988; Guidera et al., 1991a; Cepollaro et al., 2001; Neul et al., 2010) and bone mass anomalies (Leonard et al., 1999c; Budden and Gunness, 2001, 2003; Bebbington et al., 2008; Shapiro et al., 2010; Jefferson et al., 2011; Roende et al., 2011a). The effects of this high fracture incidence on the quality of life, care needs, and outcome for RTT patients, are likely to be of importance. Children having fracture episodes was reported to be one of the most strongly negative associations with mother's mental health status (Laurvick et al., 2006).

In my current study, I have looked at the bone biomechanical properties in an accurate genetic mouse model of Rett Syndrome in order to establish the possible impact of MeCP2 insufficiency on bone strength and propensity of fractures.

3.1.1 Fracture risk epidemiology in RTT patients

As described in the introductory chapter, multiple clinical studies suggest that patients with Rett syndrome suffer from an increased risk of fracture (Leonard et al., 1999c; Bebbington et al., 2008; Downs et al., 2008a).

It was found in one study that nearly one third of RTT patients had sustained a fracture by the age of 15 years(Leonard et al., 1999c), compared with only 15% of girls and women in the general population by the age of 20 year (Cooley and Jones, 2002). Similar finding were found by Downs and Colleagues, who reported 38% of RTT patients in their study suffered from fracture episodes.

The incidence of any facture episode was 43.3 episodes per 1000 patient per years and thus the fracture rate was found to be around 4 times higher in RTT patients as compared to the girls of similar age (Downs et al., 2008a). Recently in a case control study of a Danish RTT patient cohort, the investigators reported an approximately 36% fracture events occurrence among cases as compared to the 27% in controls of same age. The first fracture event typically occurred (77.3% of cases) below 15 years of age (Roende et al., 2011b).

Studies have been conducted in past to establish the site, cause (Leonard et al., 1999c; Jones et al., 2002; Cooper et al., 2004; Downs et al., 2008a) and mechanism (Roende et al., 2011b) of fractures within Rett syndrome patients but exactly how and why RTT patients suffer from bone symptoms remains poorly defined.

3.1.2 Fracture site in RTT patients

Greater frequency of fractures was found in lower limb long bones (Leonard et al., 1999c; Jones et al., 2002; Cooper et al., 2004; Downs et al., 2008a; Roende et al., 2011b) within RTT patients as compared to the controls, although fractures have been reported in all regions (spine, ribs, sternum, clavicle, humerus, radius, ulna, wrist bones, fingers, femur, tibia, fibula, patella, ankle bones, foot), including face. The bone found most commonly to be fractured was femur followed by tibia, humerus, ankle and wrist bones respectively (Downs et al., 2008a). Vertebral fractures were not found to be common in Rett syndrome young population and mostly found in elderly patients aged ~60 years (Roende et al., 2011b).

3.1.3 Determinants of Fracture risk in RTT patients

Genetic predispositions as the cause of RTT bone symptoms have been observed by Downs and colleagues. In their study they categorized the cases according to mutation types, including p.R106W, p.R133C, p.T158, p.R168X, p.R255X,

p.R270X, p.R294X, p.R306C, C-terminal deletion, early truncating and large deletion mutations. The study found a threefold increased risk of fracture in patients with p.R270X mutation and nearly twofold increase in patients with p.R168X mutations. Individuals with p.R270X were found to be particularly susceptible (Downs et al., 2008a). Interestingly this mutation in the nuclear localization signal region of the transcription repression domain is the one that was found to be most severe in a number of studies (Huppke et al., 2003; Colvin et al., 2004). However no association between the mutation types and fracture distribution was found by Roende and colleagues and they attributed this due to the lack of actual number of different *MECP2* mutations in their study cohort (Roende et al., 2011b) as compared to Downs and colleagues. The issue regarding genotype and fracture occurrence within RTT are in dire need of further studies.

Low bone mass is seen in RTT (Haas et al., 1997; Leonard et al., 1999c; Cepollaro et al., 2001; Motil et al., 2006; Zysman et al., 2006; Gonnelli et al., 2008; Shapiro et al., 2010) and an association between low bone mass and fractures in RTT has been found.

In Rett syndrome 80% of patients suffer from seizures (Jian et al., 2006), prompting widespread use of antiepileptic drugs (AEDs). In a recent study it was observed that 64% of the Rett syndrome patients are taking anti-epileptic drugs (Anderson et al., 2014). Interestingly it has been observed that the risk of fracture increases with antiepileptic drugs and was found elevated for valporate (anti-epileptic drug) in particular, prescribed on its own or in combination with other AEDs after one or more years (Leonard et al., 2010). In another case control study RTT subjects with a diagnosis of epilepsy were found to have nearly 3 times the risk of fracture and those receiving more than two AEDs had nearly twice the risk of those who were receiving no medication (Downs et al., 2008a).

Risk of epilepsy in itself and development of scoliosis(Ager et al., 2006), in RTT patients is also thought to be genotype related (Jian et al., 2006), pointing towards the potential relationship between genotypes and bone strength acquisition.

Physical activity is often limited in RTT with patients have difficulty in standing and walking, which declines further with age (Downs et al., 2008b). Association of risk

of fracture with mobility is less clear in RTT population (Leonard et al., 1999c; Downs et al., 2008a). It was also found that years without anticonvulsant medication and learning to walk were both separately protective against fractures, but when both variables were combined, only the absence of medication remained significant (Leonard et al., 1999c). Maintaining mobility, particularly in those RTT patients with high-risk mutations, has potential as an environmental modification to optimize bone health(Roende et al., 2011b).

Reduced serum 25 hydroxyvitamin D levels [25-(OH) D] <50nmol/L, have been found in Rett syndrome patients. This reduction in vitamin D levels could be, associated with less exposure to sunlight, inherently dark skin, an indoor life style, the latitude at which they live. Among all these above stated factors, only race and ethnicity influenced 25-(OH)D levels in the RTT. Ambulatory status of girls and women with RTT did not show an association with 25-(OH)D concentration (Motil et al., 2011). On the other hand biochemical analysis of serum calcium, phosphate, alkaline phosphate, and Parathyroid hormone levels in RTT were not shown to differ from controls (Jefferson et al., 2011). The normal biochemical findings suggest that vitamin D deficiency, if present is not severe and other factors responsible for decrease in bone strength and fractures should be taken into consideration.

Individual with severe physical and intellectual morbidities like RTT patients often live in protected environments and usually are not subject to fractures by falls, trauma, childhood games and other sports activities (Cass et al., 2003). Hence the high fracture rate in young Rett syndrome population may represent the effects of other risk factors, such as genotype and the presence of epilepsy.

3.1.4 Low energy fractures in RTT patients

Recently Roende and colleagues (Roende et al., 2011b) found in their study that “low energy fractures” (Spontaneous fractures of bones that occur without any external trauma or falls) to be the common characteristic of fractures in Rett syndrome patients.

In their case control study, the majority of Rett cases suffered from low-energy fractures as compared to the controls that experienced significantly high-energy

fractures (fractures due to falls from one level to another or because of activities involving speed). Cases tended to fracture mostly the lower limb by low energy mechanisms, whereas controls tended to fracture mostly the upper limb by high energy mechanisms.

In order to understand the mechanisms underlying the bone fractures an enhanced knowledge of biomechanical properties is required. In the next section of this chapter I am going to discuss a brief review of bone biomechanics.

3.2 Biomechanical properties of bone

As described in chapter 1, the organic and inorganic constituents together give bone its unique properties. In general the mineral phase provides the “stiffness”. The viscoelastic properties and resistance to fracture are attributed to the collagen phase (Currey, 1979).

There is clinical and laboratory evidence that, in addition to bone mineral density, the mechanical properties of bone tissue may play a critical role in bone strength (Currey, 1979; Chavassieux et al., 2007). Alterations in these mechanical properties would be expected to play a significant factor in bone fracture risk, even though it has not been clear what mechanical properties are most important (Currey, 2004).

Bone is a composite hierarchical material, therefore investigation of the relationship between the materials properties and the geometry and mechanical behaviour of whole bone is challenging and very complicated.

A thorough understanding of this relationship is of importance as it helps to understand the normal behaviour of whole bones during physiological loading as well as identifying areas of peak stresses which are more likely to fracture during intense activity, and allows the prediction of effects of various pathological processes and drug treatments (Sharir et al., 2008).

The hierarchical structure of bone material changes at different length scales. It is also a graded material, as its composition, structure and mechanical properties may vary continuously or in discrete steps from one location to another (Suresh, 2001).The mechanical behaviour of bone is determined by its geometry and the properties of the material of which it is made.

There are a number of biomechanical parameters that can be used to characterize the integrity of bone. One of the key relationships is between applied load to bone and displacement in response to the load-displacement curve (figure 3-1). The extrinsic stiffness or rigidity of the bone (*S*) is represented by slope of the elastic region of the load-displacement curve. Other biomechanical properties of the bone can be derived from the same graph including ultimate force (F_u), work to failure (area under the load-displacement curve *, U*) and ultimate displacement (d_u). Each of these biomechanical parameters reflects a different property of bone. Ultimate force also called ultimate load reflects the general integrity of the bone structure; stiffness measure is closely related to the mineralization of the bone (figure 3-1).

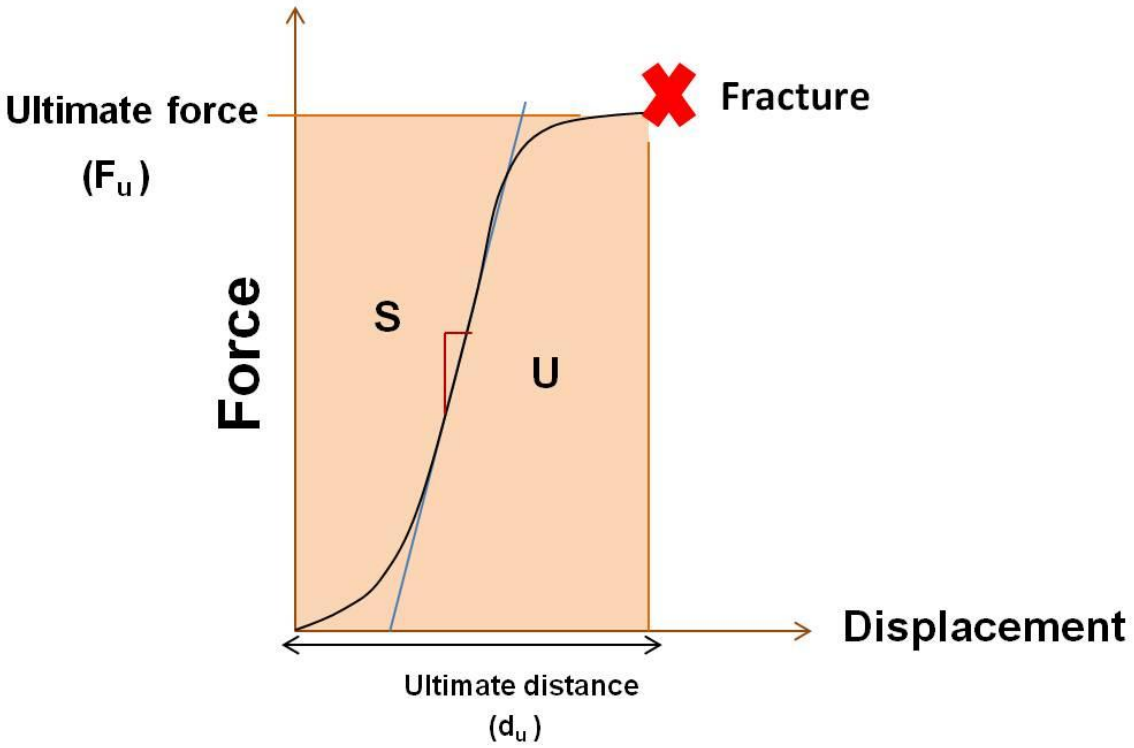

Figure3-1 Load-displacement curve for bone

The Load displacement curve displaying stiffness (*S*) or rigidity (slope of the curve); Ultimate force (F_u) (the height of the curve); area under the curve is work to failure (*U*); and Ultimate displacement (d_u) (total displacement to fracture). Red Cross represents the fracture (breaking point). Figure modified and adopted from (Turner, 2006).

Work to failure is the amount of energy necessary to break the bone; and ultimate displacement is inversely related to the brittleness of the bone. Biomechanical status of bone cannot be described by just one of these properties; in order to understand the biomechanical status of a bone fully, the range of these properties need to be considered. For example in young children bone tends to be poorly mineralized and weak, but very ductile (increased ultimate distance), resulting in increased work to failure. On the other hand bones can be very stiff as in osteopetrotic patient but also very brittle, resulting in increased risk of fracture and reduced work to failure (Turner, 2006)(figure 3-2).

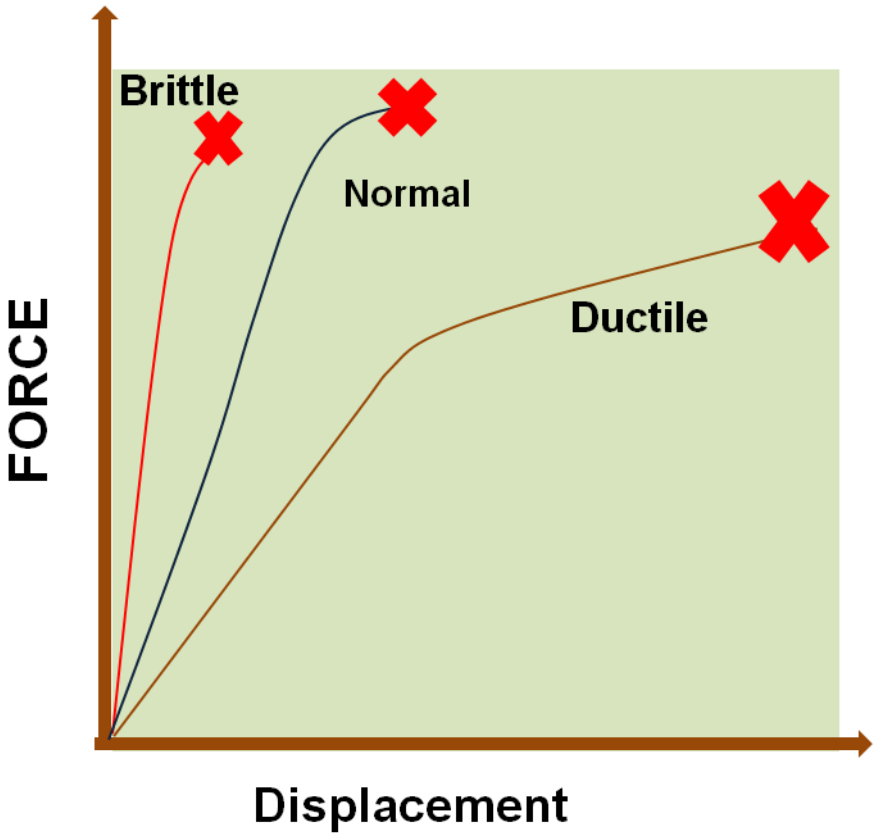

Figure3-2 Load displacement curve showing various bone pathologies

Brittle bones displayed a reduced work to failure and inversely proportion to the displacement. Young children bones are usually ductile, showing increased work to failure and large ultimate displacement. Red Cross represents the fracture event (breaking point). Figure modified and adopted from (Turner, 2006).

When load is converted into stress and deformation converts into strain, by the relationship between stress and strain in bone follows a curve called the stress-strain curve. The slope of the stress-strain curve within the elastic region is called the elastic or Young's modulus (*E*). Young's modulus is a measure of the intrinsic stiffness of the material (Turner, 2006)(figure 3-3).

Strength and stiffness are commonly used to define the bone health. Strength and stiffness are not directly proportional to risk of fracture but the amount of energy required to cause fracture is directly related to risk of fracture (Currey, 1979).

As described earlier, the bone tissue is a two-phase porous composite material composed primarily of collagen and mineral, with mechanical properties determined primarily by the amounts, arrangement, and molecular structure of both of these constituents. The mineral part provides strength and stiffness to the tissue (Turner, 2006). The collagen phase is tough and improves bone's work to failure or toughness. The ratio of mineral to collagen in bone does affect bone's strength and brittleness (Wang et al., 2002) (figure 3-3).

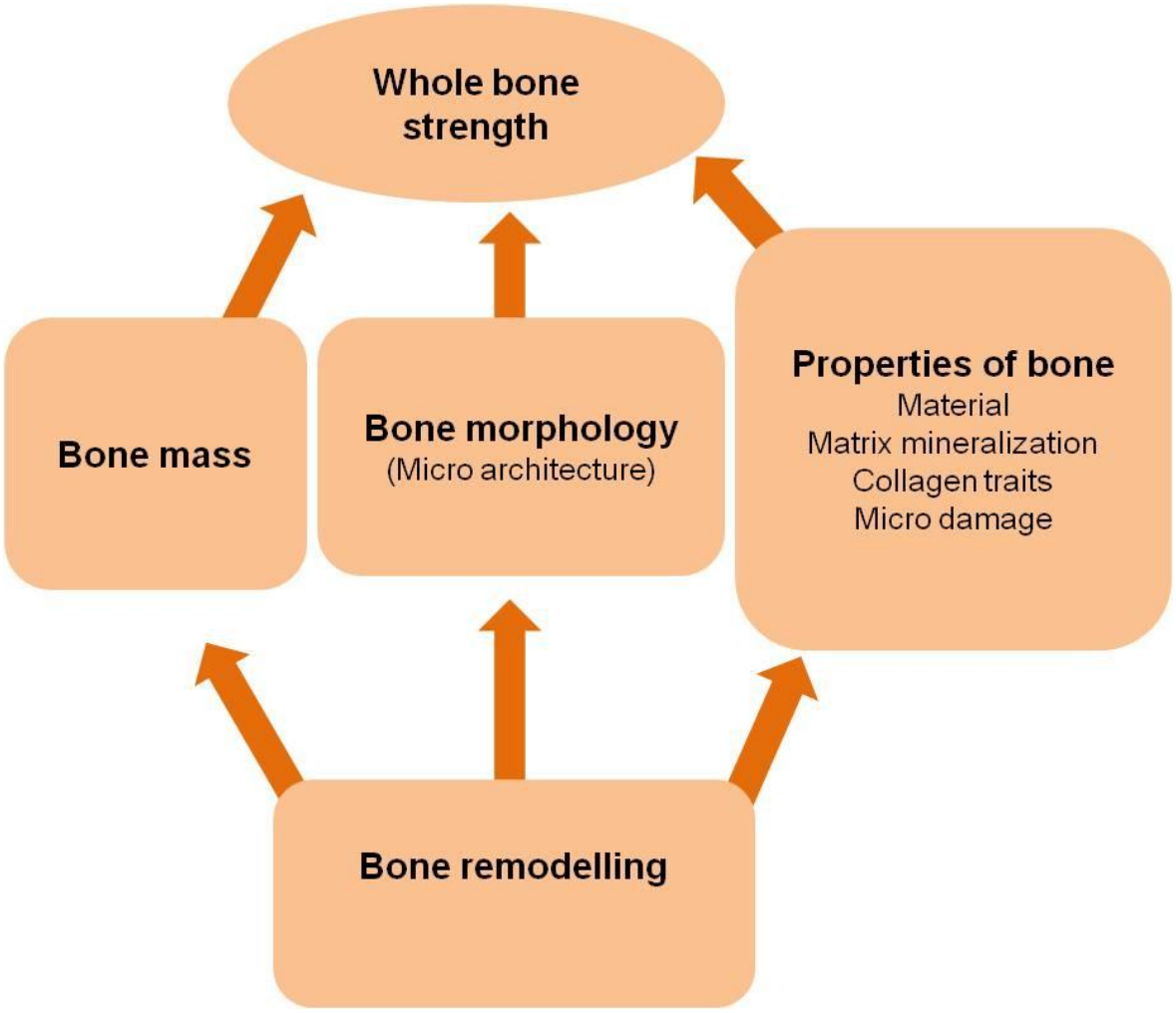

Figure3-3 Summary of contributing factors towards the bone strength

Bone hardness is represented by the resistance of the material to the load as the structure is deformed. This response occurs in many material including bone, tendons and ligaments (Choi and Goldstein, 1992). A hard material will respond with a minimum deformation to the load increase. When the material fails in the end of the elastic phase, it is considered a fragile material. The higher the load imposed to the bone, the higher the deformation. In addition, if the load exceeds the elastic limits of the material, there will be a permanent deformation and failure of material (Choi and Goldstein, 1992) (figure 3-4).

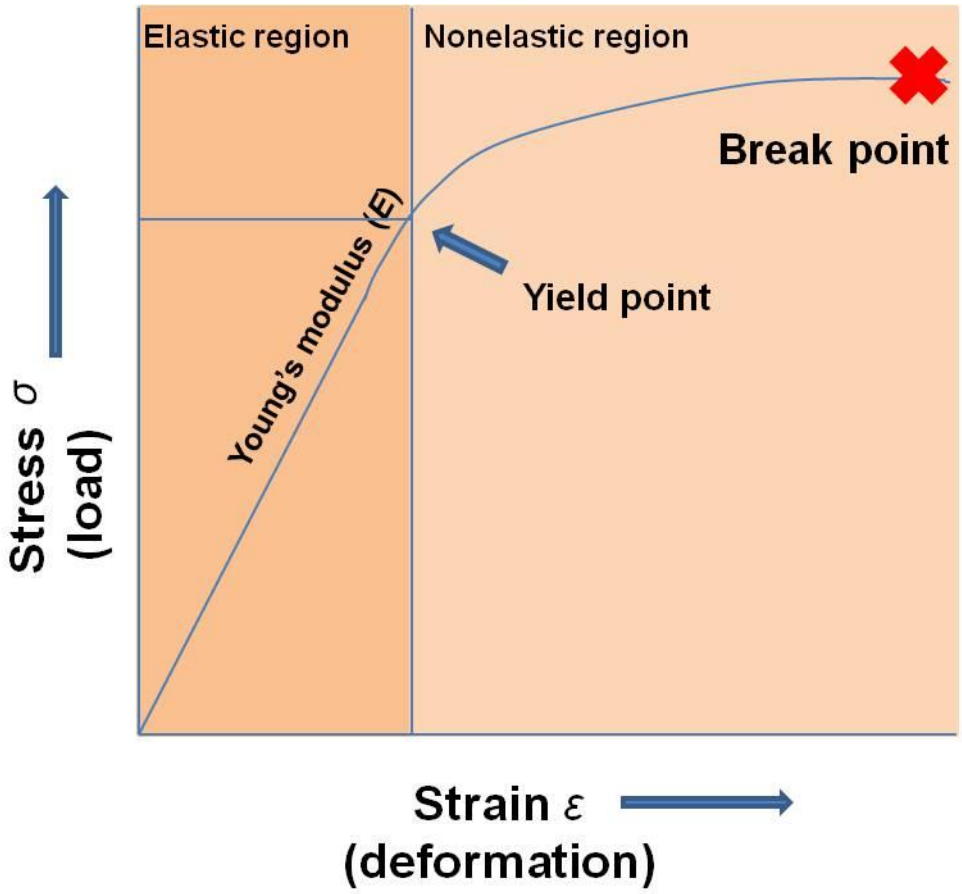

Figure3-4 The Stress-strain curve for bone

The slope of the curve is called Young's modulus (E). The yield point represents a transition, above which strains begin to cause permanent damage to the bone structure. Red Cross represents the fracture event (breaking point). Figure modified and adopted from (Turner, 2006).

3.3 Animals models and bone biomechanics

Animal models, in particular mice, offer the possibility of naturally achieving or genetically engineering a skeletal phenotype and determining the resulting change in bone's mechanical properties. In contrary to traditional strength tests on small animal bones, fracture mechanics tests display smaller variation and therefore offer the possibility of reducing sample size (Vashishth, 2008).

Many types of mechanical tests have been proposed for mouse bones. As mouse bones have the well-defined organizational hierarchy, mechanical tests scale the natural length scale from mineral and protein levels to whole bone tests. Nano and microindentation tests have been conducted on inbred or genetic knockout mouse bones to determine the local elastic and viscoelastic properties associated with bone protein and bone mineral modifications (Akhter et al., 2004a; Kavukcuoglu et al., 2007; Ng et al., 2007; Tang et al., 2007).

At the whole bone level, three and four-point bending tests have been popular due to the inherent simplicity of such tests in determining the mechanical properties associated with changes in the structure and material due to exercise (Maloul et al., 2006; Wergedal et al., 2006; Wallace et al., 2007), variations among different inbred mouse strains (Wergedal et al., 2006) accelerated senescence and ovariectomy and growth factor (Maloul et al., 2006). Less common biomechanics tests for mouse bone includes femoral neck test which have been used in past to determine genetic influence on bone and whole bone fracture studies (Hessle et al., 2013).

In Three-point bending test, the tested bone is positioned onto two supports, and a single-prolonged loading device is applied to the opposite surface at a point precisely in the middle between the two supports. The alternative 4-point bending method is similar except for the fact that the load is applied by two loading, located equi-distance from the midpoint (Brodt et al., 1999)The main advantage of this test is that the whole section of bone between two load-applying prongs is subjected to a uniform moment. Nevertheless, bones are mostly tested in 3-point bending, since their irregular surface geometry creates difficulty in having both prongs contact the bone simultaneously.

Along with bending tests, indention technique has been used in order to determine the mechanical properties in mouse bones (Hessle et al., 2013). The indentation technique allows determining the hardness of a material. The hardness is the resistance to the penetration of a hard indenter.

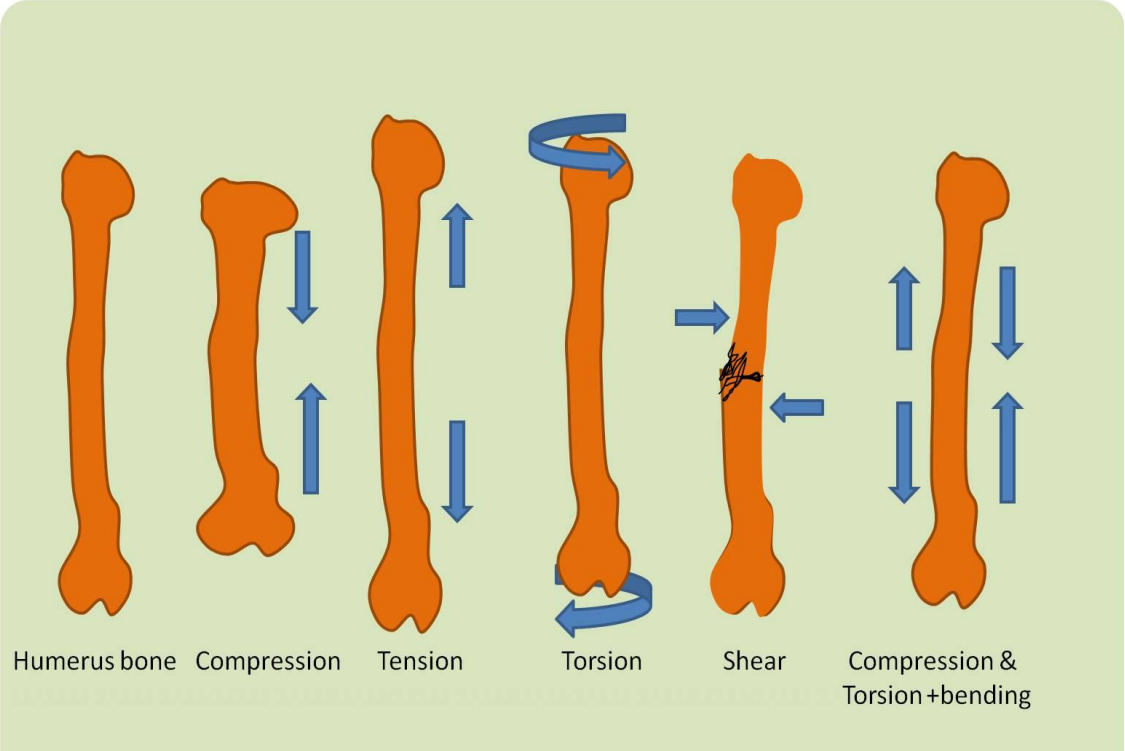

Figure 3-5 Load Types (Compression, Tension, Torsion, Shear, Bending)

Bone as a structure may be loaded in tension, compression, bending, shear, torsion, or a combination of these modes (figure 3-5). If the magnitude of applied load does not exceed the bone' elastic limits, fracture does not occur and the bone, elastically deformed, returns to its prestrained state. The failure mode of bone under circumstances of catastrophic overload is directly related to the loading mode of the bone. That is, from an evaluation of the fracture characteristics, it is possible to speculate what loading modes produced the fracture.

3.3.1 Load Types

The skeletal system is subjected to a variety of different types of forces on such a way that the bone receives loads in different directions. There are loads produced by the weight sustentation, by the gravity, by muscle forces and by external forces.

The loads are applied in different directions producing forces that may vary from five different types: compression, tension, shear, curvature or torsion.

TENSION

Because bone as a structural component of the musculoskeletal system must withstand large axial loads (both compressive and tensile) to sustain weight bearing and locomotion, it by adaptation, exhibits greater strength when subjected to tension directed longitudinally versus tension directed transversely. This observation is essentially a restatement of Wolff's law and helps to explain bone's anisotropic mechanical behaviour (i.e., varying strength as a function of load direction) (figure 3-5).

COMPRESSION

Compressive forces on a structure tend to shorten and widen it. As in pure tension, maximal stresses occur on a plane perpendicular to the applied load; however, the stress distribution and resultant fracture mechanics in compressive failure are often very complicated. Unlike failure in tension, compressive failure in bone does not always proceed along the theoretic perpendicular plane of maximum stress, but rather once a crack is initiated it may propagate obliquely across the osteons following the line of maximum shear stress.

SHEAR

Tensile and compressive forces act perpendicular or normal to a structure's surface. In contrast, shear forces act parallel to the surface and tend to deform a structure in an angular manner.

BENDING

Bending is a loading mode that results in the generation of maximum tensile forces on the convex surface of the bent member and maximum compressive forces on the concave side. Between the two surfaces, that is, through the cross section of the member, there is a continuous gradient of stress distribution from tension to compression. Because mature healthy bone is stronger in compression than in tension, failures usually begins on the tension surface. In very young animals or

severely osteoporotic bone, however folding or buckle fractures are sometimes noted on the concave or compression side of the bone, indicating in a compressive mode subsequent to bending.

TORSION

Torsion loading is a geometric variation of shear and acts to twist a structure about an axis (the neutral axis). The amount of deformation is measured in terms of shear angle, alpha. As in bending, in which maximum tensile and compressive stresses occur on the surface and distant from the neutral axis, torsional loading produces maximum shear stresses over the entire surface, and these stresses are proportional to the distance from the neutral axis.

The skeletal system injury can be produced by applying a high-magnitude single strength of one these types of load or by repeated application of low-magnitude single strength of one these types of load or by repeated application of low-magnitude loads over a long period. The second type of injury in the bone is called stress fracture; fatigue fracture or bone distension. These fractures occur because of cumulative microtrauma imposed on the skeletal system, when the placement of loads on the system is so frequent that the process of bone repair cannot be equal to the breakdown of the bone tissue(Egan, 1987).

3.3.2 Aim of the study

Given that Rett syndrome patients have a demonstrated increased risk of fracture and reduced bone strength, the aim of this study was to analyse the biomechanical properties of bones in *Mecp2*-Stop mice modelling Rett Syndrome compared to wild-type and genetically rescued mice. We aimed to explore potential genotype-related deficiencies in mechanical properties of bone and hypothesize reduced bone strength in *Mecp2*-Stop mice with improved functional integrity following genetic rescue.

3.4 Material and Methods

Right tibial and femoral shafts from each comparison genotypes of male and female cohorts were subjected to mechanical testing (three point bending and

microindentation tests) after they are scanned by Sky scan 1172/A X-ray computed microtomgraphy (μCT). The mechanical tests were selected to test the cortical and cancellous parts of the bone. The tests were performed using a Zwick/Roell z2.0 testing machine (Leominster, UK) with a 100N load cell.

3.4.1 Three-point bending test

For three-point bending test (Hessle et al., 2013), tibias were placed on the lower supports, at 8 mm separation, with the posterior surface of the tibia facing down. Load was applied on the shaft of the tibia using the Zwick/Roell testing machine until the fracture occurred (figure 3-5)

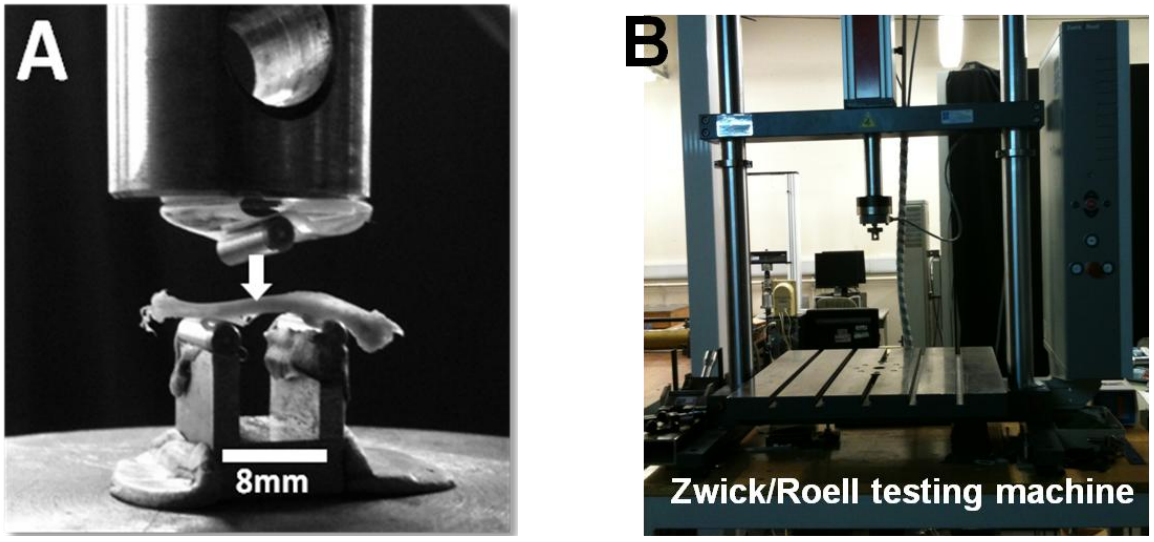

Figure3-6 Three point bending test on right tibias
(A)Tibia was placed on the lower supports, with posterior surface facing down. Load was applied until the fracture occurred. Supports were separated 8mm. (B) Test was performed using the Zwick/Roell testing machine with a 100N load cell until fracture occurred. These tests were performed in Mechanical Engineering Lab, Rankine Building, Department of Engineering University of Glasgow.

From each bone tested, a load-displacement graph was obtained using the testXpert® II software installed in computer linked to the Zwick/Roell z2.0 testing machine. The stiffness was calculated by measuring the slope in the graph of force-displacement and the ultimate load by measuring the maximum force that

the bone was able to resist. The second moment of area was calculated using the equation that considers the bone as a hollow cylinder:

$$I = \frac{\pi}{64}({D_0}^4 - Di^4) \qquad \text{(eq.1)}$$

Where **I** is the second moment of area, the D_0 is outside diameter and the Di is the internal diameter; both of these measurements were taken from the µCT

Young's modulus measure was also estimated from the geometry of the loading device and the measured stiffness of the bone. Such an estimate is based on beam theory and the approximation of the shaft of the tested bone as a uniform hollow tube.

For Young's modulus following equation was used:

$$\text{Young's modulus} = \mathrm{E} = \frac{\mathrm{Stiff}\tau.\mathrm{Ls}^3}{48.\mathrm{I}} \qquad \text{..... (eq.2)}$$

Where $stiff\tau$ is the stiffness, determine from the load-displacement curve. Ls is the separation of the supports and I is the second moment of area of the tibias. This is a commonly used method to estimate the mechanical properties of the material bone within the whole bone (Sharir et al., 2008).

3.4.2 Micro indentation hardness test

Right femur diaphysis from male and female mice cohort were cut transversely at midpoint of each bone shaft, using a diamond saw (IsoMet Plus Precision Saw; Buehler Ltd.). The midpoint of each bone was measured using venire calliper. Distal mid-shaft sections were used for the micro indentation test in each mouse bone. Proximal part of each right femur per mouse per genotype was used in femur neck test (see below).

Bone sections were air dried and embedded in metallurgical mounting resin prepared by using, VARI-SET Acrylic powder/liquid system (VARI-SET 10/20 liquid, Meta Prep, UK). The moulds were then allowed to solidify at room temperature for 24 hours. The bone cross-section surface was subsequently hand polished using silicon carbide papers with decreasing grain size (240, 400, 600,

800, and 1200) impregnated with diamond pastes (15, 6 and 1µm) to produce a smooth polished surface.

Vickers test method (Dall'Ara et al., 2007; Hessle et al., 2013) was employed while using the microindentation hardness test. Seven indentations with an applied load of 25gf were done, along the transverse section of each specimen, using a Wilson Wolport Micro-Vickers 401MVA machine UK (figure 3-6). The indenter of the machine is held in place for each indentation for 10 or 15 seconds according to the average value found in the literature. Furthermore, to avoid overlapping of deformation from one indentation to another a minimum distance of 2 diagonals between indentations was established (ASTM E384).The Vickers pyramid number (HV) was calculated with an equation where the load (L) is in grams force and the average of the two diagonals (d) is in millimetres:

$HV=1.854\ \frac{L}{D^2}$ ..... (eq.3) (figure 3-7)

3.4.3 Femoral neck fracture test

The femoral neck fracture test was used to test the mechanical properties (stiffness and ultimate load) at the proximal part of femur. The shaft of the femur was fixed in a mechanical chuck and placed in the Zwick/Roell z2.0 mechanical testing machine (Akhter et al., 2004b). The bone sample was clamped at a 9˚ angle lateral to the vertical axis of the bone (Hessle et al., 2013). Load was applied to the femoral head until fracture occurred. After each bone being tested the load-displacement graph is obtained by using the testXpert® II software installed in computer linked to the Zwick/Roell z2.0 testing machine Stiffness and ultimate load measurement were calculated in a similar method as described earlier (see section3.4.2 above) (figure 3-7).

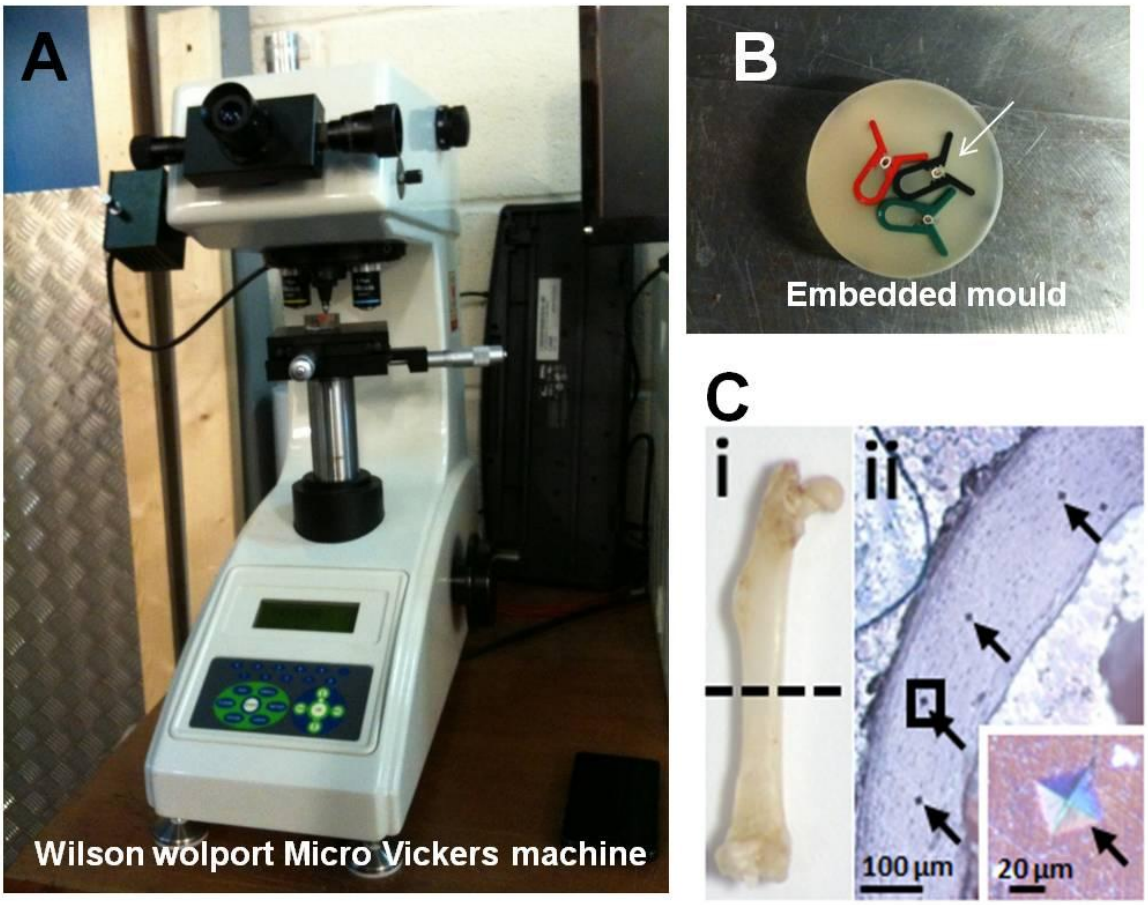

Figure3-7 Microindentation Test for hardness

(A) Image showing Wilson Wolport Micro-Vickers 401MVA machine used for the micro indentation test. (B) Resin mould, with embedded bone tissue, white arrow pointing towards the bone sample held in clippers. (Ci) mouse femur, dotted line black line showed the midpoint of femur, distal half was used for the microindentation test. (Cii) transverse section of the bone sample showing the diamond shape indentation marks on the bone samples (arrows). (Ciii) Insert shows higher power image of region indicated by box in Cii. Scales bars as shown.

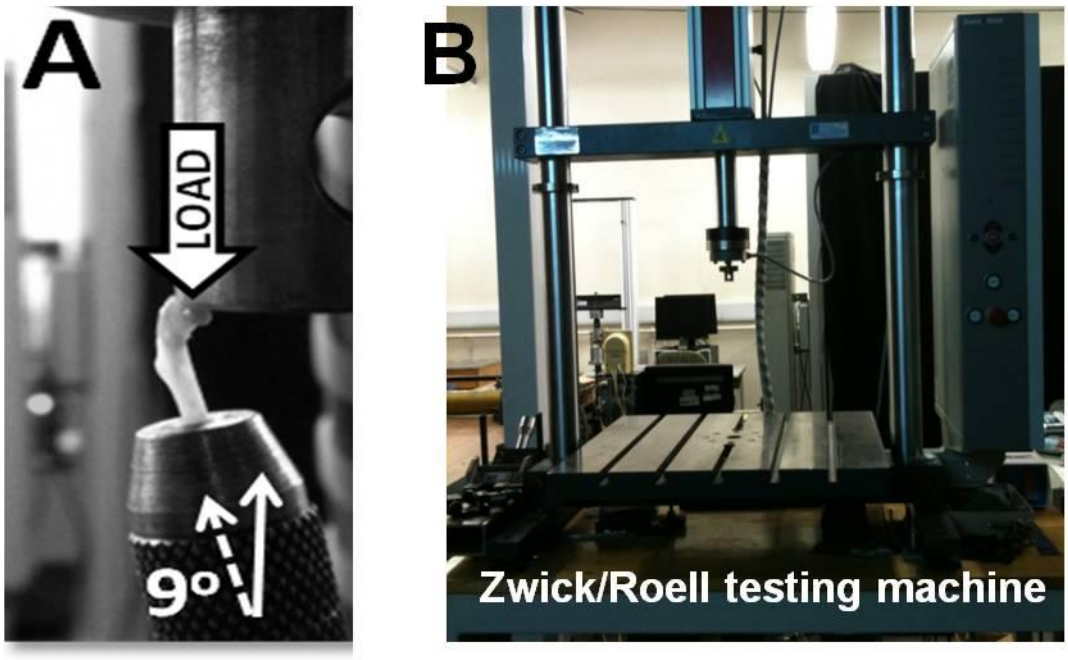

Figure3-8 Femur neck test
(A) Image showing proximal femur mounted at 9° to the horizontal plane in the mechanical chuck. Load was applied on the head of the femur until the fracture is produced. (B) Image showing Zwick Roell testing machine used for the femur neck test.Results

3.5 RESULTS

In order to determine any gross skeletal abnormalities caused by MeCP2 deficiency, the tibia and femur of male *Mecp2*$^{stop/y}$ mice together with wild-type littermates were examined for gross morphometric analyses; measurements are summarized below (table 3-1).

Morphometric measurements revealed no significant difference in average body weights of male and female genotypes. Weight measures of femur and tibia showed a significant reduction in Stop mice and Rescue mice showed a significant treatment effect and improvement in weight of femur bone. No difference in femur length was observed. All data given as mean ± SD for each group of samples (n=5

per genotype). Significance was assessed by one way ANOVA with Tukey's post hoc test. Abbreviations: * p<0.05, ** p<0.01. Symbol¶ (a comparison is made between Wild-type control and Stop).Symbol ϕ (a comparison is made between Stop and Rescue). Symbol ψ (a comparison is made between Wild-type control and Rescue). For ease of understanding, the male mice comparison genotypes will be addressed as Wt (control); Stop (*Mecp2*$^{stop/y}$); and Rescue (*Mecp2*$^{stop/y}$, *CreER*) mice and female genotypes cohort as Wt (control); Stop (*Mecp2*$^{+/stop}$); and Rescue (*Mecp2*$^{+/stop}$, *CreER*) mice in subsequent chapters.

3.5.1 No difference in whole body weights of male and female cohorts

No difference in whole body weights was observed genotypes in male mice (figure 3-9).

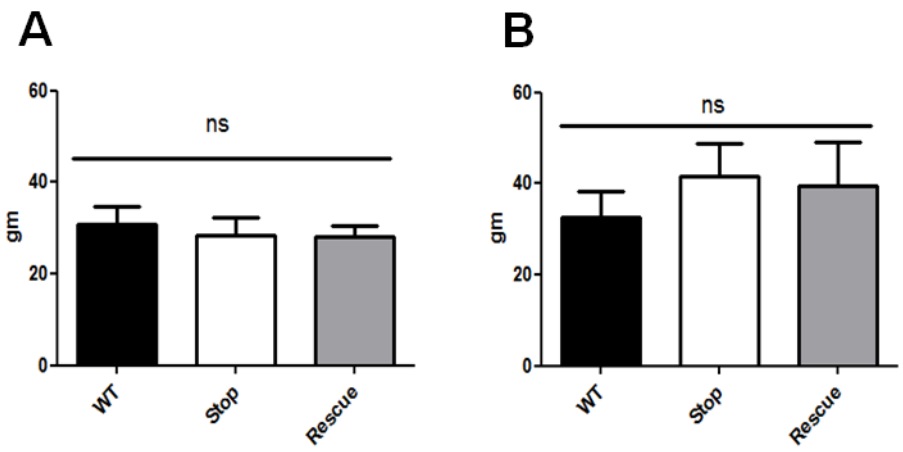

Figure3-9 Bodyweight measurements in male and female mice cohort.

Bar graphs showing, male (A) and female (B) mice cohort analysis results for whole body weight measurements (A) In male mice whole body weight comparison among genotypes showed no significant difference (WT= 30.73 ± 3.75 g; Stop = 28.50 ± 3.75g; Rescue= 28.21 ± 2.37g; n=6 per genotype; p<0.05, ANOVA with Tukey's *post hoc* test) (p<0.05). (B) Similar trend was seen in female mice cohort (p<0.05) (WT= 32.72 ± 5.59g; Stop= 41.70± 7.15g; Rescue= 39.47 ± 9.77g; n=6 per genotype; p<0.05, ANOVA with Tukey's *post hoc* test). Abbreviation: ns = not significant, Plots show mean ± SD.

3.5.2 Reduced weight of femur and tibia in *Mecp2*-Stop male mice

Mecp2$^{stop/y}$ mouse femurs showed a significantly (*p<0.05*) reduced weight in comparison with wild-type (Wt) littermate controls and *Mecp2*$^{stop/y}$*, CreER*. A similar trend of reduction in whole bone weight was observed in *Mecp2* Stop mice tibias, weight measures (table 3-1).

Table 3-1 Morphometric measurements of stop male and female mice

	Male Mouse			Female Mouse		
	Wild-type	Stop	Rescue	Wild-type	Stop	Rescue
Femur Weight (mg)	51.90±3.77	44.80±3.41*¶	51.80±5.87*ϕ	84.66±9.47	79.50±8.64	87.40±6.99
Femur Length (mm)	13.78±0.23	13.62±0.22	13.70±0.20	14.15±0.57	13.45±0.87	14.02±0.02
Tibia Weight (mg)	55.50±2.11	49.20±1.21**¶	52.12±2.96	68.84±4.08	66.60±2.	68.80±10.40
Tibia Length (mm)	17.66±0.84	15.94±0.48**¶	16.88±1.13	16.33.0±0.66	15.90±1.52	15.31±0.59
Average body weights (g)	30.73±3.75	28.501±3.75	28.21±2.37	32.72±5.59	41.70±7.15	39.47±9.77

3.5.3 No significant difference in long bone (femur and tibia) weights in *Mecp2*-Stop female mice

In contrast of the measurements made in male tissues, the female comparison cohort did not show any significant *p*>0.05 difference in femur weight measures between genotypes and similarly no reduction in female tibia weight was found (table 3-1).

3.5.4 Significant reduction in tibial length of Stop male mice

There was an accompanying reduction *p<0.05* in tibial length in male *Mecp2* Stop mice but no significant difference in femoral length between comparison groups (table 3-1).

3.5.5 No significant difference in long bone (femur and tibia) length measures in Mecp2-Stop female mice

Female *Mecp2* Stop mice showed no significant difference in tibial and femur length among the comparing genotypes (table 3-1).

3.5.6 Significant reduction in biomechanical properties in Stop male mice and improvement in bone integrity of Rescue male mice.

Following the morphometric analysis, mechanical tests were applied in order to explore possible differences in the biomechanical properties of MeCP2-deficient mice bones. Results from this test revealed a reduced structural stiffness (p<0.01), ultimate load (p<0.01) and Young's modulus (p<0.05) measures in male *Mecp2*$^{stop/y}$ mice. Samples from Rescue *mice* revealed that stiffness, ultimate load and Young's modulus measures were not different from wild-type values (figure 3-10).

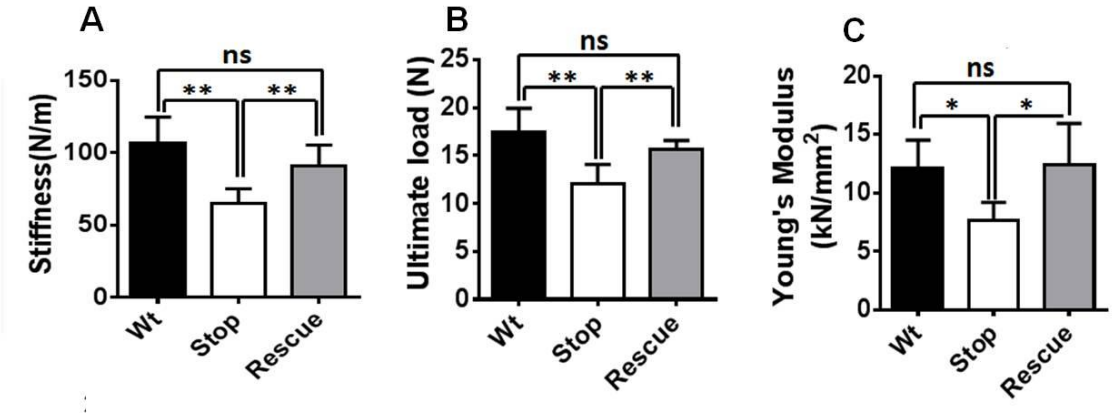

Figure3-10 Three point bending test results in male mice cohort
Male mice measures of (A) cortical bone stiffness (WT= 106.8 ± 17.88 N/mm; Stop = 64.7 ± 10.50 N/mm; Rescue= 90.7 ± 14.83 N/mm , n=5 per genotype; p<0.01, ANOVA with Tukey's *post hoc* test) (B) Ultimate load (WT= 17.50 ± 2.45 N; Stop= 12.09 ± 1.94 N; Rescue=15.7 ± 0.08 N; n=5 per genotype; p<0.01, ANOVA with Tukey's *post hoc* test) and (C) Young's modulus (WT= 12.1 ± 2.37 kN/mm²; Stop= 7.6 ± 1.60 kN/mm²; Rescue = 12.4 ± 3.49 kN/mm^2; n=5 per genotype; p<0.05, one way ANOVA with Tukey's *post hoc* test) were significantly reduced in *Mecp2*$^{stop/y}$ (Stop) mice as compared to wild-type (WT), and genetically rescued *Mecp2*$^{stop/y;}$ *CreER* (rescue) mice. Abbreviation: ns = not significant; * p<0.05, ** p<0.01. Plots show mean ± SD.

3.5.7 Female mice tibia showed no difference in biomechanical properties of bones

The same tests when conducted on tibia from female *Mecp2* Stop mice showed no significant difference in stiffness, ultimate load and Young's modulus (measure of stress-strain relationship) measures (figure3-11).

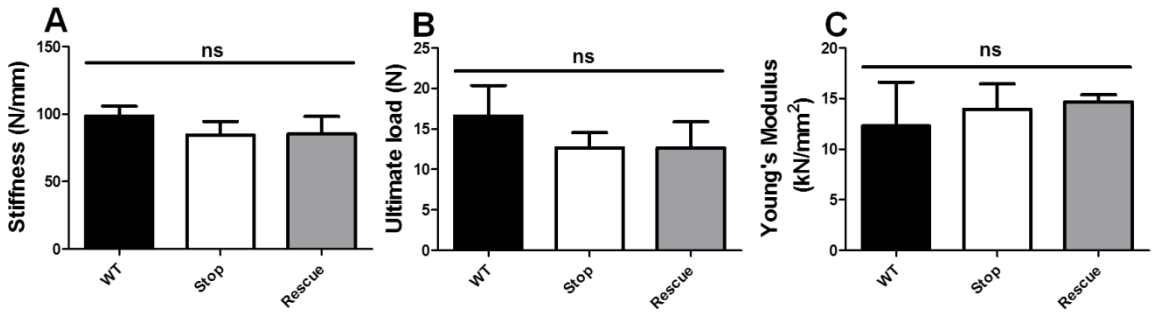

Figure3-11 Three point bending test measures in female cohorts
Bar plot showing measures of (A) cortical bone stiffness, (WT= 98.62 ± 7.24 N/mm; Stop = 84.48 ± 10.07 N/mm; Rescue= 85.17 ± 13.00 N/mm , n=5 per genotype;, ANOVA with Tukey's *post hoc* test) (B) ultimate load (WT= 16.60 ± 3.77 N; Stop= 12.68 ± 1.86 N; Rescue=12.63 ± 3.25 N; n≤5 per genotype; *p*0>0.05, ANOVA with Tukey's *post hoc* test) and (C) Young's modulus (WT= 12.29 ± 4.33 kN/mm²; Stop= 13.94 ± 2.50 kN/mm²; Rescue = 14.67 ± 0.70 kN/mm^2; n=3-5 per genotype; *p*0>0.05, one way ANOVA with Tukey's *post hoc* test) in female wild-type (Wt), *Mecp2*$^{Stop/+}$ (Stop) and *Mecp2*$^{stop/+}$ (Rescue) mice. Abbreviation: ns = not significant; Plots show mean ± SD.

3.5.8 Male and Female Rescue mice showed a significant improvement in bone hardness

Results from male mice showed significantly reduced bone hardness in male Stop mice as compared to wild-type littermates. Moreover, tamoxifen-treated Rescue mice did not differ significantly from wild-type and showed a significant treatment effect when compared with the *Mecp2*$^{Stop/y}$ cohort (WT= 73.7 ± 1.3 HV, Stop = 65.4 ± 1.2 HV, Rescue = 72.1 ± 4.7 HV, n = 5 per genotype, *p*<0.01, ANOVA with Tukey's *post hoc* test). A significant deficit in bone hardness was also observed in female *Mecp2* Stop mice femurs (WT= 72.8 ± 6.3 HV, Stop = 63.2 ± 3.0 HV,

Rescue = 75.7 ± 2.2 HV, n=3-5 per genotype; p<0.01, ANOVA with Tukey's *post hoc* test). Again, rescue mice showed a significant treatment effect and measures were not found significantly different, from wild-type (figure 3.12).

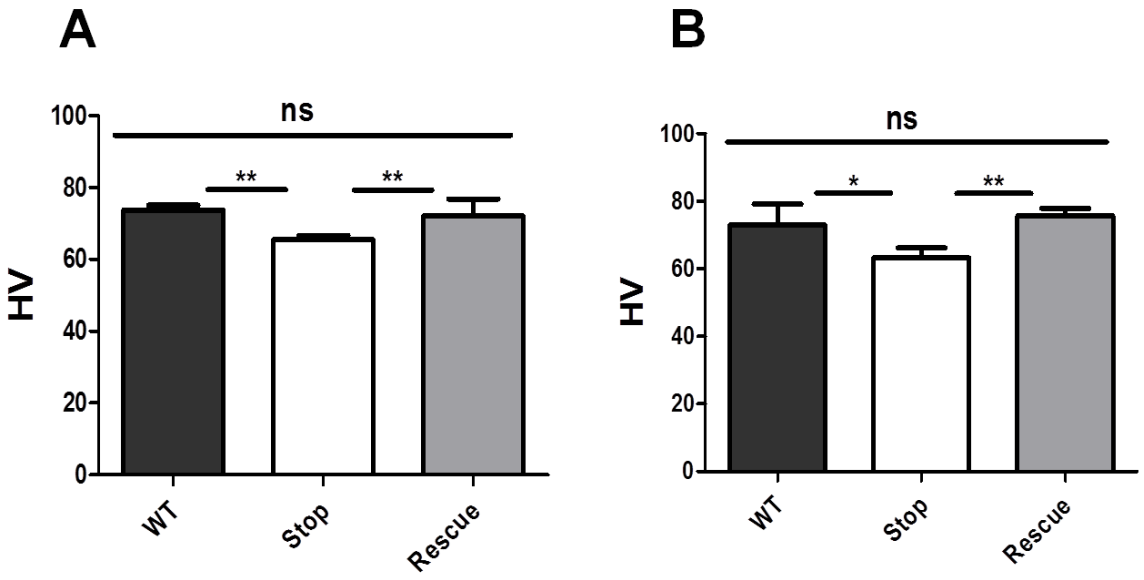

Figure3-12 Microindentation results in male and female cohorts
(A) Bar chart showing a significant reduced cortical bone hardness in *Mecp2*$^{stop/y}$ (Stop) mice when compared with the wild-type (Wt) controls (p<0.05, one way ANOVA with Tukey's *post hoc* test, n = 5 femurs per genotype). In contrast, micro hardness measures in rescued *Mecp2*$^{stop/y,}$ CreER (rescue) mice were not different from controls (p>0.05; n=5 femurs). (B) Microindentation hardness test results in female mice showed a similar pattern with reduced cortical bone hardness in *Mecp2*$^{+/stop}$ (Stop) mice when compared with wild-type(Wt) controls and rescued mice (n= 3-5 femurs per genotype, one way ANOVA with Tukey's *post hoc* test). Abbreviations: ns = not significant, * = p<0.05, **= p<0.01, ***=p<0.001). Plots show mean ± SD.

3.5.9 Male and Female Stop mice showed no significant difference in femur biomechanical properties

This test was conducted to assess possible group differences in the mechanical properties of the femoral neck. Femurs were mounted and force applied as shown in figure 3-7. In male mice, no significant differences were observed in stiffness and ultimate load measures of biomechanical properties.

Similar findings were obtained in the female mice cohorts (Figure 3-13).

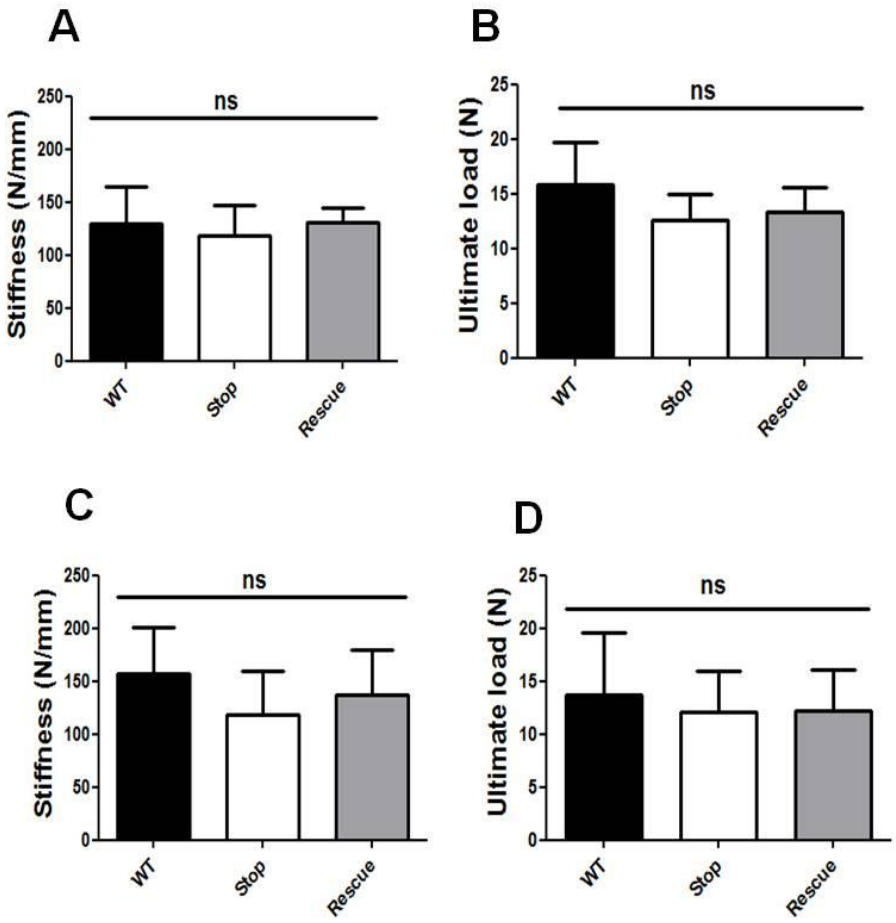

Figure3-13 Fracture neck test results of male and female cohort

Bar Plot of male stop (A-B) mice femur neck test results, showing; (A) stiffness, (WT = 130 ± 35.1 N/mm; Stop= 119 ± 28.2 N/mm; Rescue = 131 ± 13.9 N/mm, n=5 per genotype; p>0.05, ANOVA with Tukey's *post hoc* test) (B) ultimate load (WT = 15.9 ± 3.9 N; Stop = 12.6 ± 2.4 N; Stop = 13.4 ± 2.2 N, n = 5 per genotype, p>0.05, ANOVA with Tukey's *post hoc* test) (C-D) Female mice femur displayed the similar pattern; (C) cortical bone stiffness WT = 157± 43.23 N/mm; Stop= 118 ± 41.73 N/mm; Rescue = 137± 42.33 N/mm, n=5 per genotype; p>0.05, ANOVA with Tukey's *post hoc* test) (D) ultimate load (WT = 13.77 ± 5.77 N; Stop = 12.05 ± 3.93 N; Stop = 12.6 ± 3.90 N, n=3-5 per genotype, p>0.05, ANOVA with Tukey's *post hoc* test). Abbreviation: ns = not significant; Plots show mean ± SD.

3.6 Discussion

As describe earlier, *MeCP2* is a nuclear protein, abundant in post mitotic cells of the brain but also widely expressed throughout the body (Shahbazian et al., 2002b; Braunschweig et al., 2004; Zhou et al., 2006). The results of my fluorescence confocal microscope images confirmed this nuclear expression of *Mecp2* in all bone cells nuclei stained with DAPI (4',6-Diamindino-2 Phenylindole Dilactate, a blue fluorescent nucleic acid stain) of male wild type GFP tagged mice(figure 2-4Ai-iv) .

Further on, confocal images from hemizygous stop male mice (figure 2-4 Bi-iv) in which *Mecp2* is silenced by a stop cassette, GFP tagged *Mecp2* nuclear expression was found absent in all bone cells. On the other hand heterozygous *Mecp2*$^{+/stop}$ (Stop) female (figure 2-4 Ci-iv) showed only ~50% of nuclear bone cells expression of *Mecp2* in mice in which one *Mecp2* allele is silenced to mimic the mosaic expression pattern seen in human Rett syndrome (Guy et al., 2007; Robinson et al., 2012a).

For the morphometric and biomechanical analysis I have used the lower limb long bones (femur and tibia) as these were found to be the most commonly effected bones in RTT patients in terms of increase rate of fracture was found in these bones (Downs et al., 2008a; Roende et al., 2011b).

The results of morphometric analysis of long bones revealed that Mecp2 stop male have an abnormal skeletal phenotype that shares components of the clinical skeletal features of RTT patients (Neul et al., 2010). Long bone morphometric analysis showed that Mecp2 stop male mice have lighter (a significant reduction of 14% in femur weight and 13% in tibial weight) and shorter bones (a significant reduction of 10% in tibial lengths) as compared to age matched wild type controls (table 3-1). These findings were consistent with the growth retardation found in RTT patients (Schultz et al., 1993; Neul et al., 2010).

Although there was no significant difference found in whole body weight measures of three comparison groups in male stop mice cohorts. The basis for this apparent discrepancy was the observation that male stop mouse model often had more subcutaneous fat than their wild type matched littermates detected during the

dissection. These findings of my study were also found consistent with the findings of O'Connor and colleagues study on RTT bone phenotype using the Mecp2 null mouse model.

In Robinson and colleagues study of morphological and phenotype reversal in *Mecp2* stop male mice, an observation of reduced skeletal size along with the presence of a kyphotic curvature of the spine had been made (Robinson et al., 2012a). In my project I have used the same stop mice. Kyphotic posturing frequently observed in the stop mice is comparable to the '*S'* type scoliotic curvature of the spine that is more common among RTT patients (Koop, 2011; Riise et al., 2011). These skeletal dysmorphic findings in stop mouse model were also found consistent with the bone phenotype of Mecp2 null mouse model by O'Connor *et al*. One of the unique features of my study was the use of Rescue mice. Morphometric analysis of rescue mice in which Mecp2 gene has been reactivated showed a significant improvement in femur bone weight (15%) as compared to stop mice. A similar trend of increase in tibial weight (10%) as compared to wild type was also observed but it does not reach statistical significance owing to the power of my study. Tibial and femur length measurements remained reduced.

In contrast to male stop mice, adult female heterozygous *Mecp2*$^{+/stop}$ mice did not showed any significant differences in gross tibia and femur length/weight measures. However an interesting similar trend as found in male stop was also noted in female stop mice cohort displaying lighter bones (7% reduction in femur weight and 5% reduction in tibial weight) and in case of tibia shorter bones (5%) as compared to age match wild type but the values did not reached the statistical significance (table 3-1).

My study is the first study in which female mice have been used to explore the bone phenotype of RTT. Female *Mecp2*$^{+/stop}$ are a gender appropriate and accurate genetic model of RTT yet display a more subtle and delayed onset (4-12 months) of neurological features (Guy et al., 2007) compared to hemizygous male mice who become symptomatic by the age of 6-8 weeks.

A major finding of the current study was the demonstrated robust deficits in mechanical properties and micro-hardness of bone seen in the male *Mecp2* Stop

mice. This is the first time that biomechanical tests have been performed on stop mice modelling RTT bone phenotype. Such deficiencies in mechanical and material properties were profound (39.5% reduction in stiffness in the three point bending test; 37% decrease in Young's modulus, 31% in load and 12.3% reduction in micro hardness) (figure 3-10) and could explain the occurrence of low energy fractures reported in Rett syndrome patient (Leonard et al. 1999; Zysman et al. 2006; Downs et al. 2008; Leonard et al. 2010). Whilst I have not observed overt signs of spontaneous fractures in experimental colonies of mice, such a magnitude of reduced bone stiffness and load properties could mirror the 4 times increased risk of fracture in Rett patients compared to the population rate (Downs et al. 2008). Given that the mice are housed under standard laboratory conditions and there is not opportunity for traumatic bone insult, it is perhaps not surprising that spontaneous fractures are not apparent.

Male rescue mice interestingly showed a significant improvement in bone stiffness (40%), ultimate load (10%),Young's modulus (61%) and microindentation (12%) when the gene is reactivated as compared to male stop mice. These findings were quite encouraging and potentiated our hypothesis of genetic basis of RTT bone phenotype (figure 3-10).

Mechanical properties and micro hardness test was also performed in female heterozygous cohort. This is the first time that female mice modelling RTT bone phenotype has been used.

Biomechanical analysis of heterozygous stop female showed similar trend (15% reduction in stiffness and 24% reduction in ultimate load as compared to age matched wild-type control) as the results of their morphometric analysis results but like morphometric findings, these values does not reach the statistical significance (figure 3-11).

The finding that a similar significant reduction as male stop mice values, in micro hardness (14%) measure was seen in female mice that are heterozygous and mosaic for the mutant allele is important and demonstrates that the bone deficits are not restricted to the more severe male RTT-like phenotype but are seen in a gender and MeCP2 expression pattern appropriate model of RTT.

A very interesting finding in female heterozygous rescue mice was found to be a significant improvement in microhardness (19%) when the gene is reactivated as compared to the stop female. These findings were quite encouraging and displayed that the bone deficits rescue is not restricted to the more severe male RTT-like phenotype but rescue effects can be seen in a gender and MeCP2 expression pattern appropriate model of RTT (figure 3-12).

Analysis of femoral neck fracture showed no difference between genotypes. Male stop mice showed a decrease of 9% in stiffness and 21% decrease in load measures but the values did not reach the statistical significance. Male rescue mice displayed a 10% improvement in stiffness and 6% improvement in ultimate load measures but these values were also not found statistically different (figure 3-13).

Female stop mice showed a similar trend of decrease in stiffness values of 15% and load value of 13% as compared to age matched wild type control, while female rescue mice showed a 16% improvement in stiffness as compared to stop mice and no improvement are seen in ultimate load values. Similar to male stop and rescue mice measures of femur neck test all these measures did not reached the statistical significance (figure 3-14).

It is possible that the complex microstructure of bone in the femoral neck (cf. the simple cortical shaft geometry) is a confounding factor and limits the sensitivity of this test. Indeed, we also noted greater variance in this test than in the other biomechanical tests which may limit our ability to resolve subtle changes in this parameter. Nevertheless, this test has been used in other rodent models to show deficits in femoral neck integrity (Hessle et al., 2013).

An important finding of the current study and one with therapeutic implications is that the observed deficits in cortical bone material and biomechanical properties were rescued by delayed postnatal activation of the *Mecp2* gene. This finding mirrors the improvements seen in multiple non-bone phenotypes seen in the *Mecp2*$^{Stop/y}$ mice after delayed activation of the *Mecp2* gene including survival, normalized bodyweight, locomotor and behavioural activities and well as morphological features within the brain (Guy et al., 2007; Robinson et al., 2012a).

These results suggest that the bone abnormalities present in RTT patients may be at least partially reversible using gene-based therapies that are currently being developed (Gadalla et al., 2013; Garg et al., 2013) should the animal studies translate to clinical studies. However, it is also possible that significant amelioration of bone phenotypes may also be achieved using pharmacological strategies. Pharmacological approaches are being investigated in RTT, both in pre-clinical studies as well as clinical trials (Gadalla et al., 2011; Gadalla et al., 2013; Garg et al., 2013). Of particular importance for this approach with respect to bone phenotypes is to identify the mechanisms by which MeCP2 deficiency results in altered bone properties. Whilst we show that MeCP2 is expressed in osteocytes (figure 3.8), the protein is widely expressed throughout the body and it is possible that metabolic and endocrine perturbations elsewhere in the body (Motil et al., 2006; Motil et al., 2011; Roende et al., 2014) may also impact on bone homeostasis.

However the results obtained from our biomechanical tests study were quite encouraging, the decrease in bone strength in *Mecp2* deficient mouse and the subsequent improvement of bone integrity when the gene is switch back lead us to explore further into the mechanism by which *Mecp2* is causing this deficiency in bone strength. The experiments performed in this regard will be discussed in detail in the next chapters.

Chapter 4

Radiology based structural studies to assess trabecular and cortical bone parameters in a mouse model of Rett Syndrome

4.1 Introduction

Radiographic and ultrasound studies have been conducted in Rett syndrome patients to better understand the underlying pathology that may account for the reduced bone strength and increased risk of fractures in RTT patients (Leonard et al., 1995; Leonard et al., 1999b; Cepollaro et al., 2001). The majority of these imaging studies have been conducted to investigate the bone mineral density and bone mineral content in RTT patients. However there remains to be a detailed study exploring the effect of *MECP2* mutations on bone structural geometry in humans. One reason for this may be the lack of appreciation of bone phenotypes in what is considered a largely neurological disorder. Another difficulty might be the application of radiological test in patients with many other confounding impairments. For instance, patients with scoliosis who require spinal rod placements have implanted metal, which interferes with the ability of Dual-energy X-ray absorptiometry (DXA) in provision of accurate assessment of bone parameters.

Bone mass has been investigated in detail in RTT patients (Haas et al., 1997; Leonard et al., 1999c; Cepollaro et al., 2001; Motil et al., 2006; Zysman et al., 2006; Gonnelli et al., 2008; Shapiro et al., 2010) as it is shown to be a strong predictor of fracture risk in adults (Hui et al., 1988) and children (Hui et al., 1988; Flynn et al., 2007). Although prospective measures of BMD in the lumbar spine of children with cerebral palsy did not predict subsequent fracture risk (Henderson, 1997).

Neurological disabilities found in RTT patients evolves over several years with potential co-morbidities such as poor nutrition due to problems with swallowing (Oddy et al., 2007), surgical procedures (Kerr et al., 2003) for the correction of bone deformities (scoliosis) and certain anticonvulsant medications usage (Leonard et al., 2010), that together may limit the development of normal bone mass. The availability of murine RTT models now permits an assessment of the effects of *MECP2* mutation on bone mass independent of theses contributing factors. The ultra structure and density of bone in mice with and without the *Mecp2* protein have been investigated in a study by O'Connor and colleagues (O'Connor et al., 2009b). This study showed, growth retardation, abnormal growth plates (irregular shape chondrocytes) and decreased cortical and trabecular bone parameters. Another study conducted on the same *Mecp2* null mouse model by Shapiro and colleagues found differences in cortical thickness, mineralization of the medullary cavity in long bones and spinal bone density (Shapiro et al., 2010). O'Connor and colleague in their *Mecp2* knockout mouse model also found modestly lower values of bone mineral density (BMD) and bone mineral content (BMC) but this decrease did not achieve statistical significance and hence bone mineral density changes as a cause of bone anomalies seen in RTT murine model is still not fully understood.

Rett syndrome bone phenotypes have been frequently compared to osteoporosis which has been defined as '*a systemic skeletal disease characterized by low bone mass and micro-architectural deterioration of bone tissue with a resulting increase in fragility and risk of fractures'* (Zysman et al., 2006). Hence, a comprehensive approach to investigate bone material and structural properties is required to better understand the bone phenotype in RTT.

Previous studies investigating various osteoporotic processes in murine model have used femur, tibia and lumbar 5 and 6 vertebrae (Sheng et al., 2002; Rubin et al., 2004) as sample biopsies to better understand underlying structural pathologies in a range of conditions. The work presented in the current chapter was an analysis of long bones and vertebrae in order to explore aspects of cortical and trabecular bone structure of *Mecp2* stop mice.

4.1.1 Bone structure and Bone strength

Predicting fracture propensity for fracture requires a proper understanding of the relationship between bone structure and the mechanical properties of bone. The material composition and structural design of bone determines its strength.

In recent years the concept of bone strength has moved beyond density alone and has expanded to include an amalgamation of all the factors that determine how well the skeleton can resist fracturing, such as micro architecture, accumulated microscopic damage, the quality of collagen, the size of mineral crystals and the rate of bone turn over (Chavassieux et al., 2007).

In particularly, the supremacy of bone structure has been found over tissue-level material properties. The net response of osteoblasts for bone formation and osteoclasts for bone resorption are reflected by changes in the trabecular structure and bone volume fraction (Nazarian et al., 2008).

Studies in the past have concluded that a unified consideration of the relationship of bone tissue mineralization and trabecular structure can predict the mechanical properties of normal and pathologic bones (Cody et al., 1991; Kim et al., 2007).

4.1.2 µCT use in skeletal phenotypes

Histological and radiological studies are usually employed to understand the bone micro architecture. Micro computerised tomography (µCT) has now become the gold standard for the evaluation of bone morphology and micro architecture in mice and other small animals (Martín-Badosa et al., 2003). The accuracy of µCT morphology measurements has been evaluated both in animals (Waarsing et al., 2004; Bonnet et al., 2009) and in humans (Kuhn et al., 1990; Müller et al., 1998) specimens. These studies have shown that 2D and 3D morphologic measurements by µCT generally are correlated highly than these from 2D histomorphometry.

4.1.3 Aim of the study

The results obtained from the analyses of biomechanical properties described in the previous chapter were encouraging in that they demonstrated a reduction in bone strength in Mecp2 mice and also an amelioration of this phenotype in stop mice genetic rescue. This suggested that at the functional level in stop mice, bone deficits were overt but reversible. The aim of the experiments described in the current chapter was to explore further the potential structural alterations in bone of *Mecp2* deficient mice that might account for some of the observed biomechanical deficits. I hypothesised that the reduction in bone strength, seen in *Mecp2* stop mice is due to alternations in bone structure and bone mineral density (BMD) levels. In order to analyse these features I have used the µCT scanning technology to analyse the ultra structure of bones from wild-type, Mecp2 stop and genetically rescued mice of male and female cohorts.

4.2 Material and Methods

The structural properties of bone samples from wild-type, Mecp2-stop and genetically recued mice were assessed using scanning electron microscopy and were also visualised using a µCT scanner (see below). The result analysis obtained were then used to investigate cortical and trabecular bone structure.

4.2.1 Micro-computed tomography (µCT)

After the gross morphometric measurements (chapter 3) a subset of bone samples was scanned using µCT. The samples were scanned prior to any biomechanical tests being performed. All scans were conducted using the micro computed tomography facility at the Orthopaedic Research group, University of Edinburgh, Edinburgh, UK. We have used the Sky Scan 1172/A X-ray Computed Microtomgraphy system (µCT) maintained by Robert Wallace, Chancellors Building, Orthopaedic Research Group, Edinburgh, UK.

The micro CT scanner is composed of a sealed micro focus X-ray tube, air cooled with a spot size lens and a camera. The maximum length of object that is capable of fitting into this device is 40mm. Bone specimens were scanned in wet form by placing them first in a vial containing water to maintain hydration (figure 4.1).

The sample vial was subsequently fixed to the machine stub (mounting plate) with masking tape, which in turn was securely fastened to the holder in the µCT x-ray chamber. This must be secured correctly as any movement of the sample could render the scan unusable.

Multiple projection images were obtained with a rotation of 0.45°- 0.1° between each image. Given a series of projection images a stack of 2D sections was reconstructed for each specimen. CT-Analyser v1.8.1.3 (Skyscan, Kontich, Belgium) and NRecon v1.6.6.0 (Skyscan, Kontich, Belgium) were used for the task of reconstruction and whole data processing as described in user's manual and according to protocols followed by local technical faculty. Image slices obtained and stored in the .bmp format with indexed grey levels ranging from 0 (black) to 255 (white). Understandably, this is a resource intensive computer task and as such a dedicated computer was used for this process (2x 3GHz Quad core CPUs, 8Gb Ram, NVIDIA Quadro FX 570).

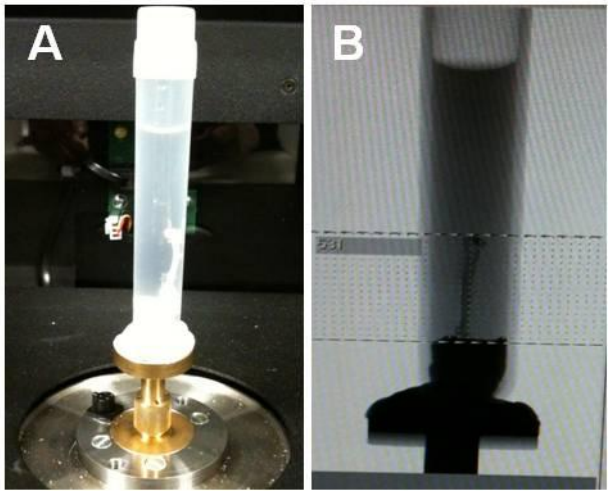

Figure4-1 Micro CT scanning of Tibia

(A) Mouse tibia in the test tube filled with water to maintain hydration during the CT scanning (B) Scanned image of tibia placed in test tube taken during the µCT scan. Images were scanned at a voxel resolution of 34µm for male and female stop tibia, using a sky scan micro CT machine. The X-ray tube was operated at 54KV and 185µA. The Sky scan 1172 micro CT scanner at Chancellor's building, Orthopaedic Research Group facility at the University of Edinburgh, Edinburgh UK was used for the trabecular and cortical bone parameters analysis.

4.2.2 Micro-computed tomography (µCT) for cortical bone measures

In order to obtain accurate internal and external diameter measures for calculating second moment of area and for cortical bone structural parameter evaluation, right tibias from male (n=5) and female cohorts (n3-5) were scanned at a voxel resolution of 34µm using a sky scan micro CT machine. The X-ray tube was operated at 54KV and 185µA. For cortical bone parameter analyses, 2mm midshaft region of interest (ROIs) were selected from tibial diaphysis, starting from the anatomical point of tibiofibular junction in each bone specimen.

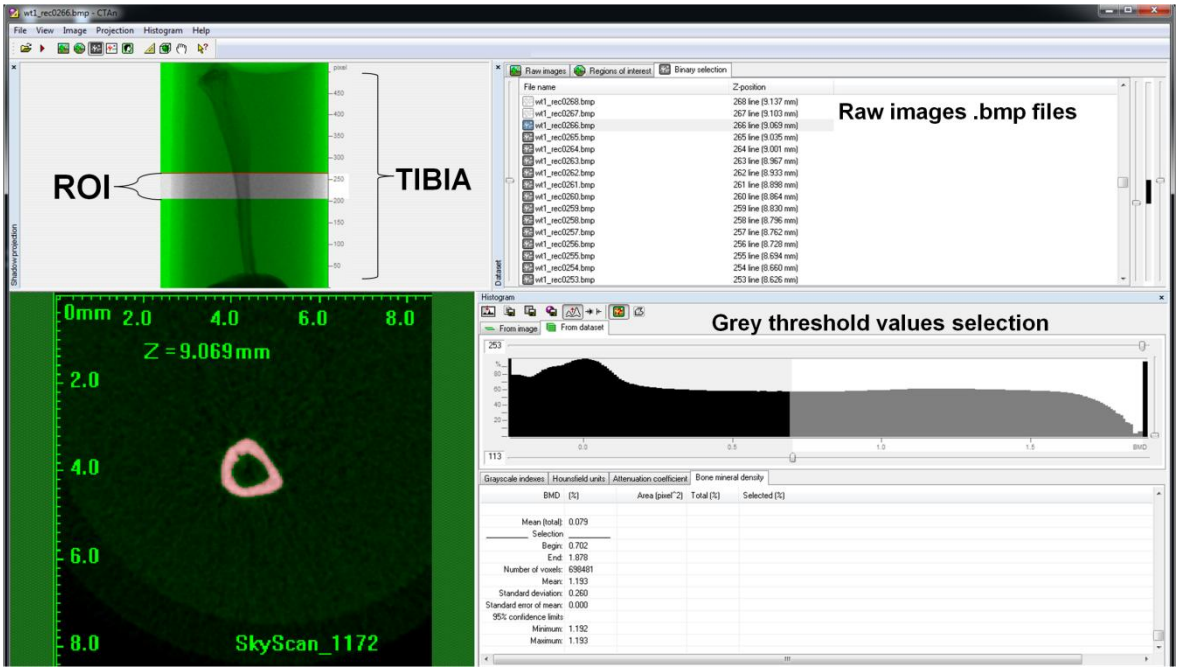

Figure4-2 Screen shot of image analysis while using the CT analyser software, displaying region of interest at mid diaphysis of tibia

Representative screen shot showing mouse tibia with a region of interest at the mid-diaphysis, while CT scan images of tibia were analysed using the CT analyser software v 1.8.1.3. A region of interest (2mm) was selected from tibial shaft per bone specimen per genotype. A lower grey threshold value of 113 and upper grey threshold value of 255 was used as thresholding values. Care was taken that all the reconstruction parameters selected were applied identically to all bone scans.

Images obtained were reconstructed and analysed using the NRecon software v 1.6.6.0 and CT analyser software v 1.8.1.3. The data from each scan was then split by region of interest. A lower grey threshold value of 113 and upper grey threshold value of 255 was used as thresholding values in each cortical bone sample. All the reconstruction parameters selected were applied identically to all bone scans (figure 4-2).

Individual two dimensional object analyses were performed on six sections per bone specimen within each comparison genotype group to calculate the inner and outer perimeters of bone. An average of six values per specimen then used as the final measure for the inner and outer perimeter and subsequently cortical thickness measurement was derived from these values. Three dimensional analyses further used to calculate marrow area, cortical area, total area and bone volume.

4.2.3 Scanning Electron Microscopy (SEM)

The Undecalcified, left distal femur metaphyseal region from both male mice (n=5) and female (n=3-5) mice were selected to observe any trabecular structural differences using scanning electron microscope (SEM) Stereoscan 250 MK3, Cambridge, UK) at the Anatomy Department, University of Glasgow, Glasgow, UK.

4.2.3.1 Sample preparation for SEM

Distal parts of left femur per bone per genotype from both male and female mice were cut with diamond saw (IsoMet plus Precision Saw; Buehler Ltd.) transversely, 3mm above the condyles. The 3mm distance from the medial condyle was measured with vernier calliper before cutting. Bones were then stored in 2.5% paraformaldehyde in 0.1M sodium phosphate buffer (water, pH7.4) at 4°C for 48h. Adherent soft tissue was removed by immersion in 3% hydrogen peroxide solution for 48h. After rinsing with distilled water, specimens were defatted in 50:50 methanol/chloroform for 24h at room temperature and transferred to a 5% trypsin solution (0.1M PB, pH 7.4) at room temperature for 48h. After cleaning with

distilled water, specimens were desiccated. Samples were gold coated by using a sputter coater (Polaron E5000, East Sussex, UK). An extra coating with silver paint was done to have the proper imaging. Images were obtained using a scanning electron microscope (Stereoscan 250 MK3, Cambridge, UK).

4.2.4 5th Lumbar vertebrae, µCT scan for trabecular parameters

5th Lumbar vertebrae from the mice from each genotype were scanned at a resolution of 5µm.

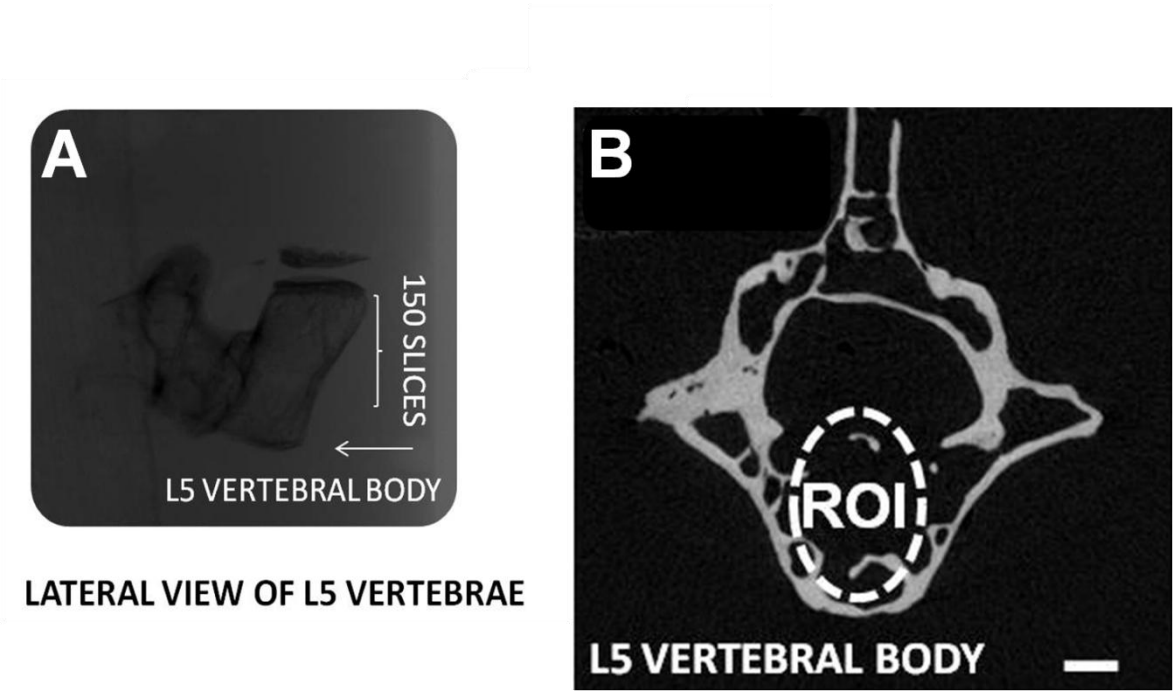

Figure4-3 Micro CT scan of 5th Lumbar vertebrae

The L5 vertebrae (n=6) from each genotype of male mice cohort (WT, Stop, and Rescue) were dissected out. The micro CT scans of each vertebra were taken using the sky scanner µCT facility. (A) Lateral view of L5 vertebrae scanned at 5um resolution. A cylindrical shape region of interest (ROI), comprising of 150 slices was taken from the body of the vertebrae. The shell properties of cortical bone were not included. (B) Reconstructed image of 5th Lumbar vertebrae, showing the selection region of interest (ROI) within the body of vertebrae. A lower grey threshold value of 81 and upper grey threshold value of 252 was used as thresholding values in each trabecular bone sample. Scale bar=200µm.

A higher resolution was needed to scan the trabecular bone and hence 5 µm selected for the mouse trabecular bone parameters as compared to the cortical bone parameters(Ito, 2005). The X-ray tube was operated at 41kV and 240µA.

Table 4-1: Trabecular bone parameters

Abbreviation	Description	Definition	Standard Unit
TV	**Total volume**	**Volume of the entire region of interest**	**mm^{-3}**
BV	**Bone volume**	**Volume of the region segmented as bone**	**mm^{-3}**
BS	**Bone surface**	**Surface of the region segmented as bone**	**mm^{-3}**
BV/TV	**Bone volume fraction**	**Ratio of the segmented bone volume to the total volume of the region of interest.**	**%**
BS/TV	**Bone surface density**	**Ratio of the segmented bone surface to the volume of the region of interest.**	**mm^{-2}/ mm^{-3}**
BS/BV	**Specific bone surface**	**Ratio of the segmented bone surface to the segmented bone volume.**	**mm^{-2}/ mm^{-3}**
Conn.D	**Connectivity density**	**A measure of the degree of connectivity of the trabeculae normalised by TV.**	**1/ mm^{-3}**
SMI	**Structure model index**	**An indicator of the structure of trabeculae, 0=parallel plates, 3= cylindrical rods**	
Tb.N	**Trabecular number**	**Average number of trabeculae per unit length**	**1/mm**
Tb.Th	**Trabecular thickness**	**Mean thickness of trabeculae assessed using Direct 3D methods.**	**mm**
Tb.Sp	**Trabecular separation**	**Mean distance between trabeculae**	**mm**
DA	**Degree of anisotropy**	**Length of longest divided by shortest mean Intercept length vector.**	**a**

Note: Modified and adopted from (Bouxsein et al. 2010)**.**

A lower grey threshold value of 81 and upper grey threshold value of 252 was used as thresholding values in each trabecular bone sample. A cylindrical region of interest (150 slices or 0.774mm) was selected from the centre of each vertebral body excluding the cortical shell area, in order to analyse only the trabecular parameter specifically (figure 4.3). Images reconstructed and analysed using the NRecon 1.6.6.0 and CT-Analyser 1.8.1.3 software. Vertebral body lengths were determined by measuring a line drawn at a 90° angle from the proximal part of the

vertebral body to the distal part. Three dimensional analysis was performed for the following parameters: trabecular thickness, trabecular separation, trabecular bone volume, trabecular porosity, as well as degree of anisotropy (DA) and structure model index (SMI); for details of these parameter see (table 4-1

4.2.4.1 Density calibration of 5th lumbar vertebrae in µCT scanner

Bone mineral density (BMD) was standardized to the volumetric density of calcium hydroxyapatite (CaHA) in terms of g.cm^{-3}. For bone mineral density (BMD) calibration, the Skyscan CT- analyser, was calibrated by means of phantom rods, with known BMD values of 0.25 and 0.75 g.$^{cm-3}$ CaHA respectively.

Trabecular (medullary) density can refer to the density of a defined volume of bone plus soft tissue.

Hounsfield units (HU) are a standard unit of x-ray CT density, in which air and water are ascribed values of -1000 and 0 respectively. The Skyscan CT-analyser software provides for an integrated calibration of datasets into these two density scales (HU and BMD). Both require the appropriate calibration phantom scans and measurements.

For density calibration, a scan of free standing tibia, within a tube of water was performed. Then the two BMD rods (under the same conditions as the bone scan) with BMD values of values of 0.25 and 0.75 g.cm-3 CaHA were scanned as well.

Reconstruction of the scan of the bone in the water tube was done by using the NRecon 1.6.6.0 and CT-Analyser 1.8.1.3 softwares. Reconstruction parameter were selected and same parameter were applied throughout the scans of each sample bone per genotype. Also care was taken with the selection of the lower and upper contrast limits.

With the scans and reconstruction of the bones and the calibrating phantoms complete, the HU and BMD calibration was implemented in CT-analyser.Following density range calibration was selected (Table 3-2).

Table 4-2: Density range calibration

Calibration unit	Min Value	Max Value
Index	**0**	**255**
HU	**-1000**	**7292**

4.3 Results

µCT analysis was used to examine the three dimensional structure of wild-type and *Mecp2* stop male and female tibias. Micro CT analysis of male Mecp2-Stop mice tibia revealed considerable differences in cortical bone parameters while several trends were noteworthy in the trabecular bone.

4.3.1 Micro CT revealed male *Mecp2*-Stop mice to display altered cortical bone properties.

One of the major structural findings of my current study was the reduction found in cortical bone parameters results obtained from the µCT analysis of male *Mecp2* mice cortical bone. These results were consistent with the reduced biomechanical strength findings and also correlate with the reduced cortical bone parameters seen in RTT patients.

A significant difference in male stop mice cortical bone parameters was found in cortical bone thickness (54%), outer perimeter (20%), inner perimeter (12%), marrow area (38%), total area (20%) and bone volume (30%) values as compared to wild type control mice However no significant difference was seen in cortical area values of *Mecp2* stop mice (figure 4-4 i-vii). Rescue mice didn’t show any improvement in bone cortical parameters and values obtained, remain reduced when a comparison is made with WT control values.

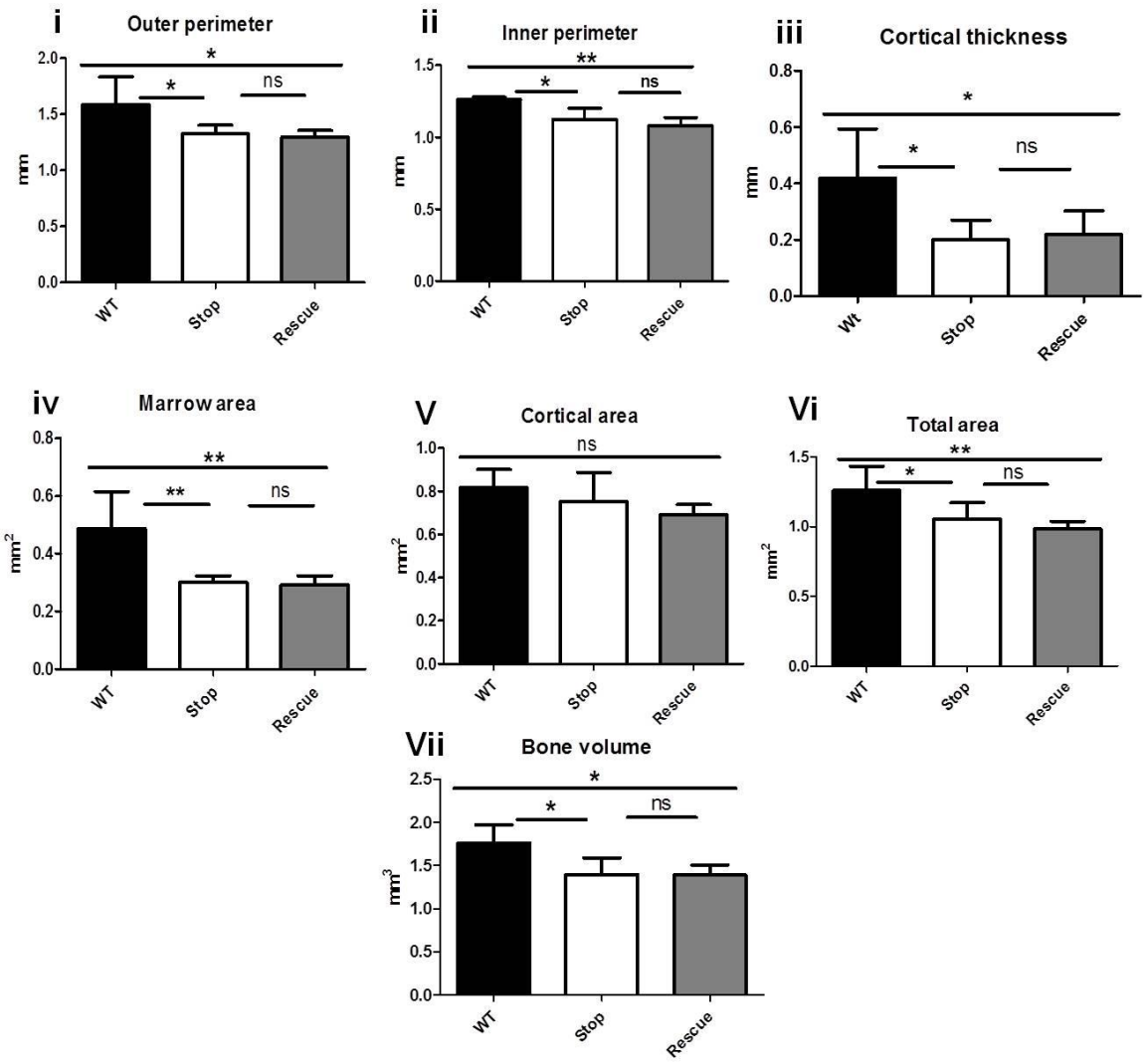

Figure4-4 Cortical bone parameter in Mecp2 Stop and Rescue male mice

Bar graphs **(**i-vii**)** showing a significant decrease in cortical thickness, (WT= 0.41±0.17mm, Stop= 0.19±0.07mm, Rescue= 0.21±0.08mm; n=5 per genotype; *p*<0.05, ANOVA with Tukey's post hoc test outer perimeter (WT= 1.65±0.22mm, Stop= 1.32±0.07mm, Rescue= 1.38±0.05mm; n=5 per genotype; *p*<0.05, ANOVA with Tukey's post hoc test), inner perimeter (WT= 1.26±0.24mm, Stop= 1.12±0.07mm, Rescue= 1.08±0.05mm; n=5 per genotype; p<0.05, ANOVA with Tukey's post hoc test), marrow area (WT=0.48±0.14mm², Stop=0.30±0.02mm², Rescue=0.29±0.03mm²; n=5 per genotype; p<0.05, ANOVA with Tukey's post hoc test),total area (WT=1.26±0.17mm², Stop=1.05±0.11mm², Rescue=0.98±0.05mm²; n=5 per genotype; p<0.05, ANOVA with Tukey's post hoc test), and bone volume (WT= 1.75±0.21 mm³, Stop=1.39±0.19 mm³, Rescue= 1.39±0.11 mm³; n=5 per genotype; p<0.05, ANOVA with Tukey's post hoc test). No significant difference was seen in cortical area (WT=0.81±0.08 mm², Stop=0.75±0.13 mm², Rescue= 0.69±0.045 mm²; n=5 per genotype; p>0.05, ANOVA with Tukey's post hoc test) values of Mecp2 stop mice as compared to wild-type controls. Abbreviation: ns = not significant; * p<0.05, ** p<0.01. Plots show mean ± SD.

4.3.2 Micro CT scans of heterozygous female *Mecp2*-Stop and Rescue mice showed no significant differences in cortical structure parameters

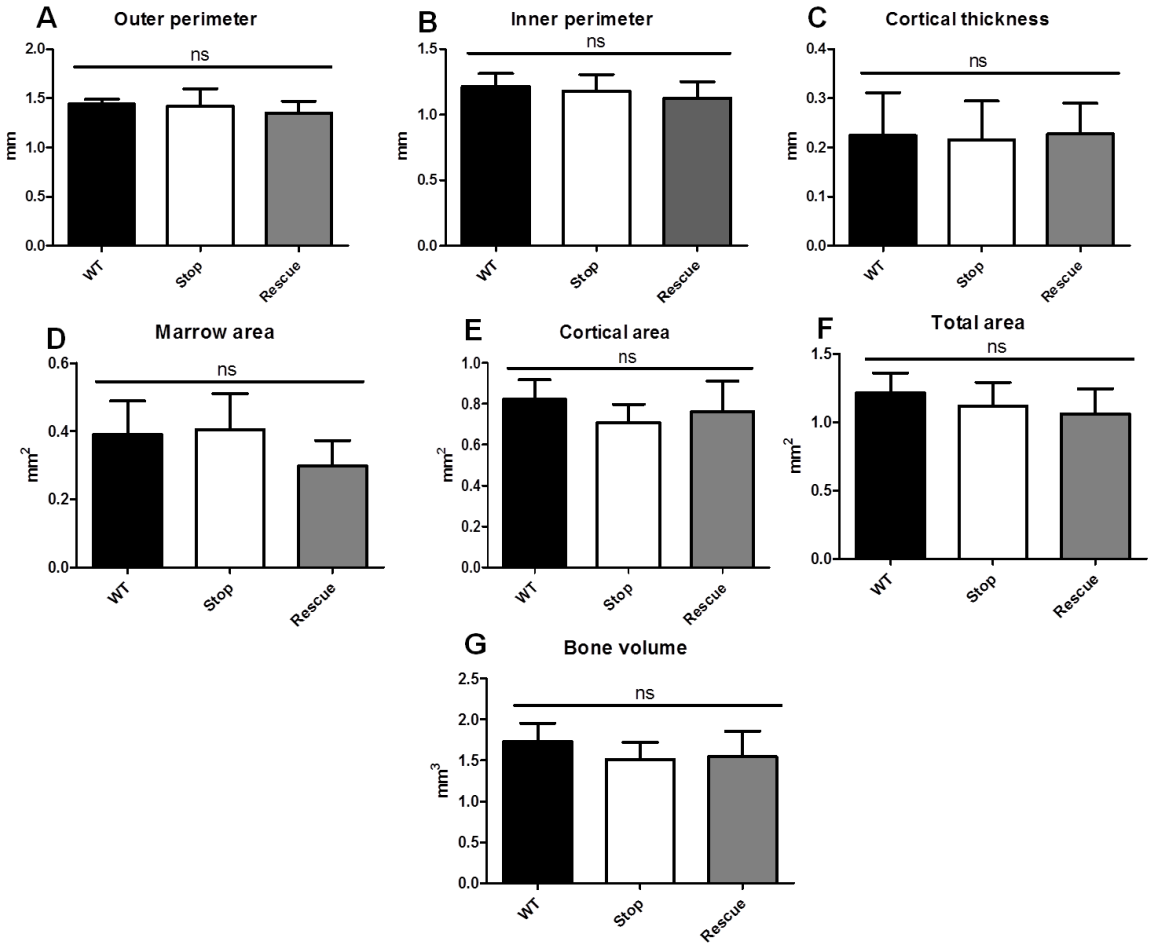

Figure4-5 Cortical bone parameters in *Mecp2* Stop and Rescue Female mice.

Bar graphs (A-G) showing no significant difference (p>0.05) in results of outer perimeter (WT= 1.44±0.05mm, Stop= 1.42±0.17mm, Rescue= 1.35±0.05mm; n=3-5 per genotype; p0>.05, ANOVA with Tukey's post hoc test), inner perimeter (WT= 1.21±0.09mm, Stop= 1.18±0.12mm, Rescue= 1.12±0.12mm; n=3-5 per genotype; p>0.05, ANOVA with Tukey's post hoc test) cortical thickness (WT= 0.22±0.08mm, Stop= 0.21±0.07mm, Rescue= 0.22±0.06mm; n=3-5 per genotype; p>0.05, ANOVA with Tukey's post hoc test), cortical area (WT=0.82±0.09 mm², Stop=0.71±0.08 mm², Rescue= 0.76±0.14 mm²; n=3-5 per genotype; p>0.05, ANOVA with Tukey's post hoc test), marrow area (WT=0.39±0.09mm², Stop=0.40±0.10mm², Rescue=0.29±0.07mm²; n=3-5 per genotype; p>0.05, ANOVA with Tukey's post hoc test), total area (WT=1.21±0.14mm², Stop=1.11±0.17mm², Rescue=1.06±0.18mm²; n=3-5 per genotype; p>0.05, ANOVA with Tukey's post hoc test), and bone volume (WT= 1.73±0.22 mm³, Stop=1.51±0.21mm³, Rescue= 1.54±0.31 mm³; n=3-5 per genotype; p>0.05, ANOVA with Tukey's post hoc test) as compared to wild-type controls

4.3.3 Scanning electron microscopy revealed altered trabecular structure in Stop male mice

Qualitative analysis using scanning electron microscopy (SEM) of the distal femur (n=5 per genotype) revealed porous structure in cortical bone (3 of 5 mice) as well as alterations in the architecture of trabecular bone in Mecp2$^{stop/y}$ mice (figure 4-6). The central metaphyseal region in Mecp2$^{stop/y}$ mice showed a sparse trabecular mass consisting of short, thin trabecular rod and plate structures. In contrast, a more robust trabecular structure, with a network of shorter and thicker rods and plates was found in wild-type control tissue (figure 4-6). The porosity and altered trabecular structure was less evident in rescued Mecp2$^{stop/y}$, CreER mice.

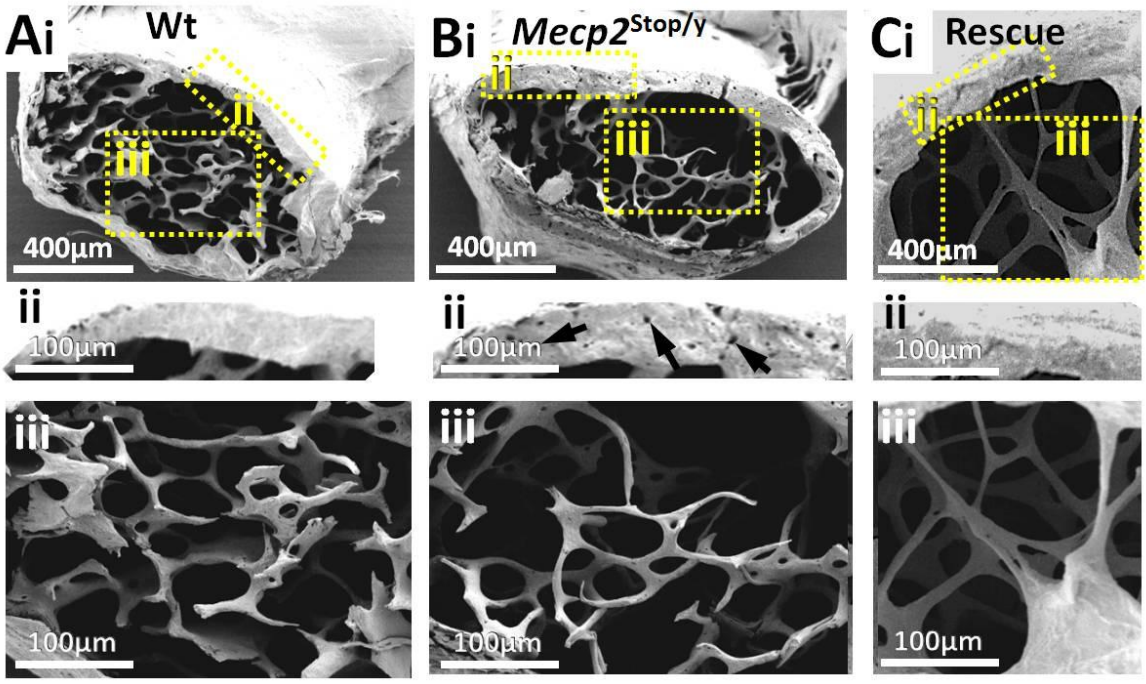

Figure 4-6 Scanning electron microscopy reveals pitted cortical bone and altered trabecular structure in distal femur of male MeCP2-deficient mice.

Scanning electron micrographs of distal femur in (Ai) wild-type (Wt) and (Bi) Mecp2$^{stop/y}$ (stop).Higher powered images of cortical (ii) and metaphyseal (iii) regions (areas indicated in A) reveal a more porous structure in cortical bone (arrows in Bi indicate pores) and a sparse trabecular structure in Mecp2$^{stop/y}$ mice when compared with representative with Wt controls. (Ci-iii) Representative micrograph from a Mecp2$^{stop/y}$, CreER (rescue) mouse.

4.3.4 Micro CT scans showed improvement in trabecular bone thickness in Rescue male mice

Three dimensional µCT scan analyses were performed to obtain a quantitative measure of trabecular architecture in wild-type, Stop and Rescue mouse 5th lumbar vertebrae. A significant reduction of 5th lumbar, trabecular thickness (~30%) was observed in Stop male mouse tissues compared to the wild-type controls. Interestingly rescue male mice 5th lumbar µCT scan results, showed a significant increase (+80%, p<0.01) in trabecular rod and plates thickness compared to *Mecp2*$^{stop/y}$ mice (Wt=0.073 ± 0.01mm; Stop = 0.051 ± 0.02mm; Rescue= 0.09 ± 0.02 mm; n=6 per genotype; p<0.01, ANOVA with Tukey's *post hoc* test) suggesting a significant treatment effect (figure 4.6).

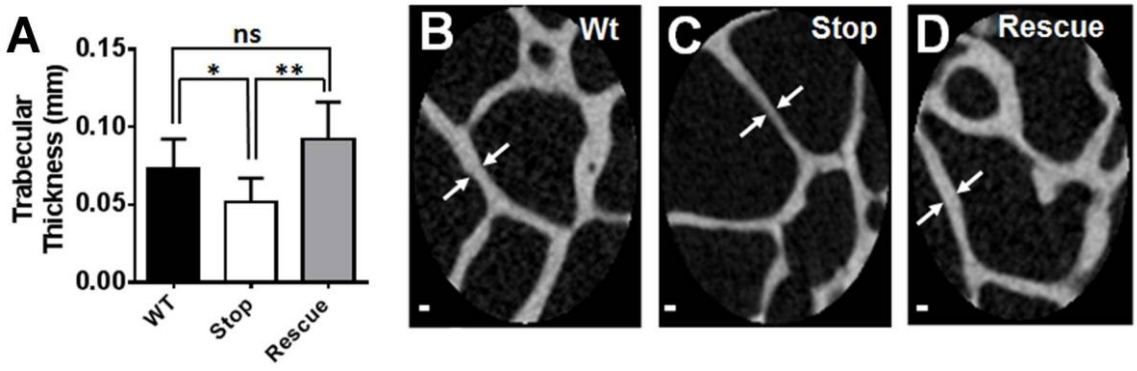

Figure4-7 MicroCT scans of L5 vertebrae revealed thinner trabecular mass in *MeCP2*-deficient mice

(A) Bar plot showing quantitative analysis of trabecular thickness (arrows in B-D). Note the reduced thickness in *Mecp2*$^{stop/y}$ samples (p<0.05; n=6 per genotype). (B-D) Micrographs showing representative trabecular samples from wild-type (Wt), *Mecp2*$^{stop/y}$ (Stop) and *Mecp2*$^{stop/y}$, *CreER* (rescue) mice. (E) Scale bar: B-D, 50µm. Abbreviations: ns = not significant, * = p<0.05, ** = p<0.01; one way ANOVA with Tukey's *post hoc* test). Plots show mean ± SD.

Length of the vertebral bodies revealed a significant difference (WT= 4.157 ± 0.52mm, Stop= 3.48 ± 0.39mm, Rescue= 3.14 ± 0.37mm; n=6 per genotype; p<0.05, ANOVA with Tukey's post hoc test) in Mecp2 stop and rescue mice vertebral body length measurements as compared to age matched wild-typecontrol. No significant difference was observed in trabecular separation, trabecular bone volume, trabecular porosity, bone mineral density (BMD), degree of anisotropy (DA) and structure model index (SMI) between comparison genotypes of male mice cohort. All findings are summarized in figure 4.6 and table 4.3.

Trabecular bone parameters	Wild-type	*Mecp2*$^{stop/y}$	*Mecp2*$^{stop/y}$, *CreER*
Bone Volume fraction%	12.350±5.750	11.130±4.667	16.990±8.921
Bone mineral density g/cm³	0.962±0.069	0.926±0.067	0.949±0.600
Bone surface density mm²/mm³	8.147±3.047	8.934±3.109	11.29±5.999
Specific bone surface mm²/mm³	70.250±12.730	78.1000±17.920	66.140±9.904
Connectivity density 1/mm³	215.900±93.797	180.900±47.803	271.600±111.258
Structure model index	1.033±0.556	0.720±0.667	1.002±0.486
Trabecular number 1/mm	1.648±0.0.522	2.124±0.633	1.815±0.723
Trabecular thickness mm	0.073±0.018	0.051±0.015*¶	0.091±0.024**ϕ
Trabecular separation mm	0.624±0.356	0.479±0.257	0.144±0.315
Degree of anisotropy	2.633±1.311	2.946±0.875	2.467±0.596
Mean Intercept length	0.151±0.037	0.107±0.033	0.323±0.359

Table 4-3 Lumbar vertebrae trabecular bone parameters

Body of 5th Lumbar vertebrae was selected as region of interest (ROI) and was analysed to assess the trabecular part of the bone. All data given as mean ± SD for each group of samples (n=6 per genotype). Significance was assessed by one way ANOVA with Tukey's post hoc test. Abbreviations: * p<0.05, ** p<0.01. Symbol¶ (a comparison is made between Wild-type control and Stop male mice). Symbol ϕ (a comparison is made between Stop and Rescue male mice).

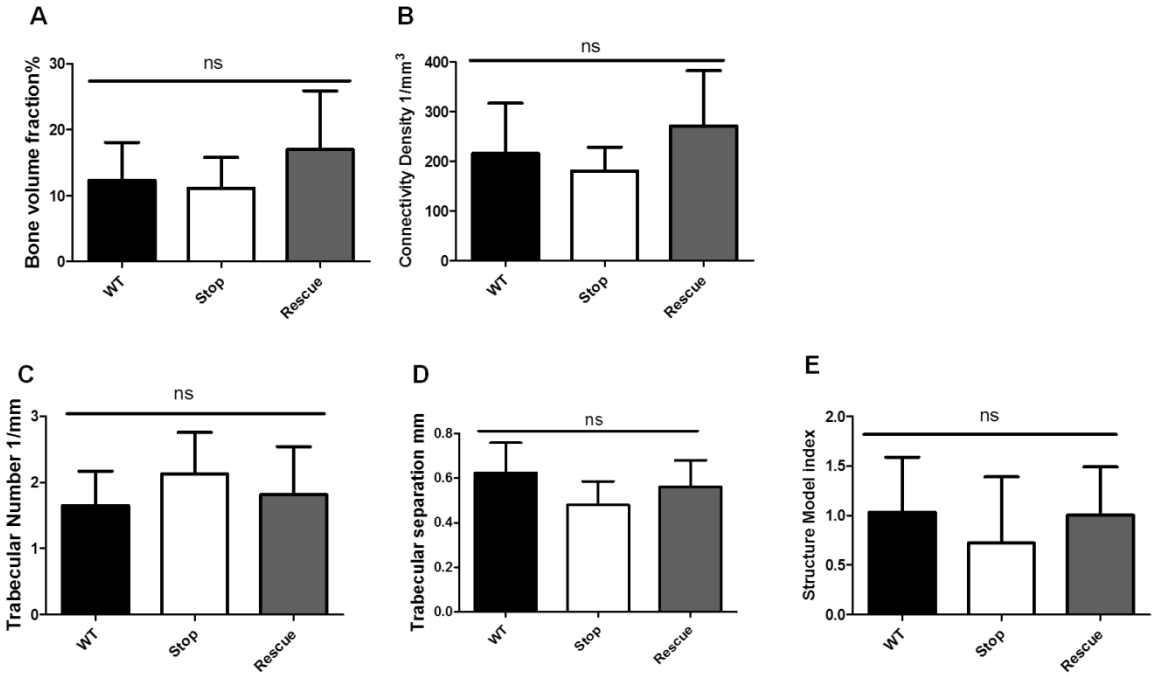

Figure4-8 Trabecular bone parameters bar graphs of *Mecp2* stop mice

Bar graphs (A-E); displaying trabecular bone parameters, showed an apparent trend of decrease in bone volume fraction (%), connectivity density (1/mm^3), trabecular separation and structure model index measurements but these values does not reach any statistical significant (p>0.05) difference; n=6; Abbreviations: ns = not significant ; one way ANOVA with Tukey's *post hoc* test). Plots show mean ± SD.

4.3.5 Bone density measurements from µCT did not revealed any significant difference in *Mecp2* stop mice.

In order to analyse bone density measurements, 5th Lumbar vertebrae were scanned, and no significant difference was not observed in male stop mice genotypes (WT= 0.96±0.06; Stop= 0.92±0.07; Rescue=0.94±0.06 n≤7 per genotype; p>0.05, ANOVA with Tukey's *post hoc* test). All data given as, mean ± SD (figure 4-9). To further confirm these finding we have performed and experiment to calculate the ash content. See chapter 5 for full details.

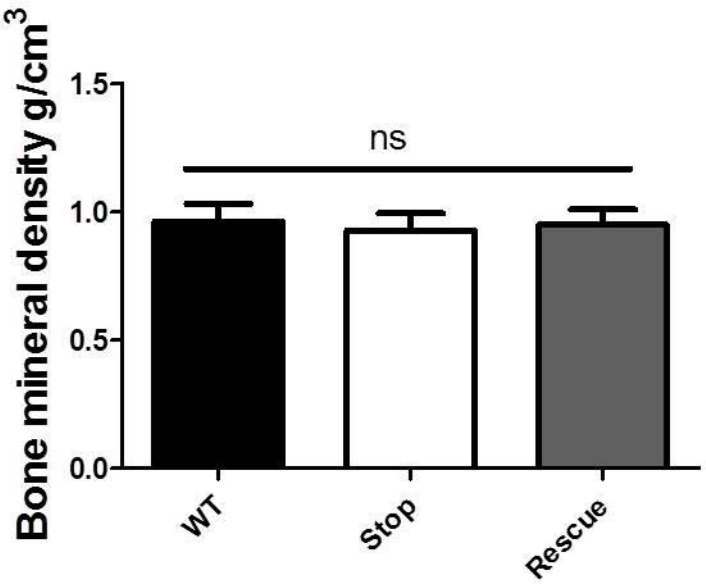

Figure4-9 Micro CT derived bone mineral density in *Mecp2* stop mice 5th lumbar vertebrae

Bone mineral density (BMD) values in Stop and rescue mice cohorts. (A) BMD values derived from the CT scan after density calibration showed no significant difference $p>0.05$ among the comparison genotypes; n=6, one way ANOVA with Tukey's *post hoc* test. Abbreviations: ns = not significant; one way ANOVA with Tukey's *post hoc* test). Plots show mean ± SD.

4.4 Discussion

The main finding of the current chapter was the demonstration that *MeCP2* deficient in bone results in significant changes in bone both at macro and microstructure levels. The alternation in cortical and trabecular bone parameters in the structure found could account for the biomechanical defects reported in the previous results. Radiological study using µCT revealed some interesting finding in *Mecp2* stop and rescue hemizygous male and heterozygous female mice.

The cortical bone parameters analysis of male *Mecp2* stop mice revealed a 54% decrease in cortical thickness, 20% reduction in total area and outer perimeter values, 12% reduction in inner perimeter along with the 38% reduction in marrow and 30% reduction in bone volume measures in a bone (tibia) that is 90% the length of the age-matched wild-type group (figure 4-4). This cortical bone thinning found in *Mecp2* stop mice was consistent with what is expected in an osteoporotic model and it is known that reductions in bone strength and increases in cortical

micro damage affect the fragility of bone (Seeman, 2008a). Interestingly, RTT bone phenotype has been frequently related to osteoporosis because of the reduced level of bone strength, increase in fracture risk and reduced bone mineral density reported in RTT patients (Zysman et al., 2006; Roende et al., 2011b). My findings of cortical bone parameters were also found consistent with the one reported in RTT patients by Leonard and colleagues. They reported a decrease in total area of 20%, medullary area of 47%, cortical thickness of 30% and cortical area of 20% in patients suffering from Rett syndrome (Leonard et al., 1999b). However in my study *Mecp2* stop showed a modest reduction of only 8% in cortical area which did not reached statistical significance owing to the high variance found in stop mice.

These values of reduction in cortical bone parameters were also consistent with my earlier biomechanical test results analysis and pointed towards the potential underlying alternation in ultra-structural arrangement as the possible mechanism of reduced bone strength values seen in Mecp2 stop mice. My findings of cortical bone parameters were also found consistent with the O'Conner's micro CT analysis of cortical bone of Mecp2 null mouse model, in which they showed a similar reduction of 20% in total area and a similar significant but modest reduction of 17% reduction in cortical thickness, 7% reduction in outer perimeter and 14% reduction in marrow area (O'Connor et al., 2009b) as compared to *Mecp2* male stop mouse model. The slight variations in results of my study and O'Conner's RTT bone analysis could be because of the high variance found in *Mecp2* stop mice statistical analysis, or difference of age, strain or type of mutation among the mouse models (O'Connor et al., 2009b). There was a difference of age between the two mouse models, *Mecp2* null mouse model was much younger 8 weeks as compared to stop mouse model which was of 14 weeks. Hence the enhanced reduction of cortical bone parameter in my stop mouse models could be the result of worsening of bone phenotype with age. This point is also further supported by the fact that bone phenotype (reduction in cortical thickness, cortical area of bone, total area and bone mineral density values) in RTT patients have also been reported to deteriorates with age (Leonard et al., 1999c; Motil et al., 2008).

Finding of 30% reduction in bone volume by µCT in current study in particular is very interesting as it is consistent with the bone histomorphometric analysis of iliac crest biopsies of 5 RTT children. This histological analysis in RTT patients showed

decreased bone volume, decreased osteoclast surface and number, and a reduced rate of bone formation suggesting decreased osteoblast function in RTT patients (Budden and Gunness, 2003).

One of the unique features of the current study was the use of rescue male mice for the structural analysis of bone. Rescue mice did showed a significant improvement in biomechanical properties but failed to show improvement in cortical bone structural parameters (figure 4-4). These findings surfaced the need to explore further the possible causes of improvement in bone strength identified in rescue male mice, outside the realms of structural entity of bones and hence we carried out the extracellular matrix analysis (see chapter 5).

In this study we also explored the cortical parameters in heterozygous stop female mice. This is the first time that female mouse model has been used to explore the structural properties of *Mecp2* deficient mice. Unlike male mouse, female mouse displayed a modest decrease in cortical thickness (5%), total area (7%), cortical area (13%) and bone volume (14%). This decrease in values didn't reach statistical significance because of the high variance and with the number of animals that I had available for this study. This subtle decrease in cortical bone parameters was found consistent with my biomechanical tests results of stop female mice. Female stop rescue mice similar to the male stop mice did not showed any significant improvement in cortical structural parameter.

After the cortical bone analyses, I also wanted to explore the trabecular structure of the bone. For this reason distal femoral metaphyseal region was scanned and imaged using the scanning electron microscopy. Qualitative analysis by scanning electron microscopy did reveal altered trabecular architecture (thin trabeculae) in *Mecp2* stop mice, consistent with the overall osteoporotic picture and suggesting clear structural differences between genotypes which would be consistent with reduce bone integrity results obtained after the biomechanical analysis. The cortical area surrounding the central rod and plate mass showed characteristic pits in *Mecp2*$^{stop/y}$ which were much less numerous in wild-type controls. These could result from increased nutrient foramina or poorly laden osteoporotic bone due to osteoblast dysfunction. This is further supported by the known fact that the increasing porosity of cortical bone effectively trabecularizes the cortex and hence leads to osteoporotic bone phenotype (Brown et al., 1987; Foldes et al., 1991).

The quantitative μCT on the trabecular portion of L5 vertebrae were carried out and the results were found consistent with the SEM osteoporotic findings in that the trabecular thickness was significantly reduced in *Mecp2* stop mice (figure 4-6). The trabeculae in vertebral bodies of Mecp2 stop mouse were found significantly thinner and but displayed a trend of increase in number and hence reduced trabecular separation, although the enhance in trabecular number and trabecular separation was not found statistically significant due to the high statistical variance shown in *Mecp2* stop mice. This discrepancy could also be because of the overall, decrease in length of vertebral body in Mecp2 stop mice as compared to the age matched wild type group and hence the apparent increase in number and reduced trabecular separation. Nonetheless, the significant thinner trabecular finding in vertebral bodies and thinning of cortical thickness along with decrease in total area and bone volume found in cortical bone supported the overall osteoporotic picture seen commonly in RTT patients (Zysman et al., 2006; Roende et al., 2011a; Roende et al., 2011b).

An interesting finding consistent with the functional tests results on long bones was seen, and trabecular thickness was normalized to wild type levels upon unsilencing *Mecp2* in the Rescue cohort. This is indicative of a pronounced phenotypic rescue and evidence of structural remodelling upon activation of MeCP2 analogous to structural rescuing demonstrated in the brain by Robinson and colleagues (Robinson et al., 2012b).

Other parameters of the trabecular bone showed loss of bone volume fraction percentage (10%), connectivity density (17%) and structural model index (30% reduction, indicating more plate like trabecular structure rather than rod like) (Hildebrand and Rüegsegger, 1997) in male stop mice but these values didn't reached the statistical significance owing to the high variance among the comparison groups (figure 4-7). The number, thickness, spacing, distribution and connectivity (i.e., connection) of trabeculae reflect the trabecular network and determine bone strength (Chavassieux et al., 2007). It is also known that for the same defect in trabecular density, loss of connectivity has more deleterious effects on bone strength than thinned but well-connected trabeculae (Weinstein and Hutson, 1987; van der Linden et al., 2001). In my trabecular bone analysis I found significant reduction in trabecular thickness and loss of connectivity in Mecp2 stop 5^{th} lumbar vertebrae, though the latter does not reach statistical significance. As

stated earlier, overall the decrease in trabecular thickness, bone volume fraction % in vertebral bodies points towards an osteopenic phenotype frequently reported in RTT patients and seen in RTT bone phenotype animal models as these results were also found consistent with µCT and histomorphometric analysis reported by O'Connor and colleague using the Mecp2 null mouse model (O'Connor et al., 2009b).

Surprisingly, bone mineral density (µCT) values didn't show any difference in comparison genotypes in male stop mice 5th lumbar vertebrae (figure 4-8). Reduced bone mass is commonly associated with osteoporotic phenotypes (Hui et al., 1988; Leonard et al., 1999c; Cummings et al., 2002; Ager et al., 2006; Flynn et al., 2007) and bone mineral density, differences have been reported in *Mecp2*-null mice (Shapiro et al., 2010). The lack of observed differences (density) in the current study could be due to differences between mouse models (strain, mutation type, age). However my findings of bone mineral density were consistent with the ones reported in *Mecp2* null of bone mineral density and bone mineral content. They did found a modest difference in BMD and BMC, but this decrease did not reach statistical significance due to the small number of animal they used in the study (O'Connor et al., 2009a).

Interestingly among the indicators of cortical bone loss, the percentage cortical area is considered to be the most directly related to bone mass (Leonard et al., 1999c). In my current study no significant difference was observed both in cortical area and bone mineral density suggesting that the primary cause of reduced bone strength might be the result of cellular, osteoblast decrease activity as seen by reduction in bone volume or because of the increase osteoclast number/activity or probable defect in organic part of the bone. Based on these findings I had performed histological experiments. See Chapter 5 for further details.

Chapter 5

An analysis of the material composition of bone in an mouse model of Rett Syndrome

5.1 Introduction

A number of clinical studies have investigated potential properties of bones that might underlie reduced bone strength seen in RTT patients. Such studies have adopted both static and dynamic histomorphometric approaches (Budden and Gunness, 2001, 2003; Zysman et al., 2006; Motil et al., 2008). Overall, these studies have so far revealed consistent decreases in bone volume, accompanied by reduction in bone formation rates (Budden and Gunness, 2003; O'Connor et al., 2009b).However significant changes in osteoid thickness and number per bone surface as well as absolute osteoclast number has remained inconclusive (Budden and Gunness, 2003; O'Connor et al., 2009b; Rastegar et al., 2009). And hence the exact cellular mechanism leading to bone phenotypes in RTT remains poorly defined.

5.1.1 The material composition of bone: collagen and mineral

Bone is a specialized connective tissue and is composed of an organic matrix of type 1 collagen. The unique feature of collagen component is its mineralization with an inorganic phase comprising of calcium hydroxyapatite-like crystals. The organic matrix of bone tissue provides flexibility, whereas increasing amount of mineral contributes towards material stiffness (Cooper et al., 2004).

Collagen molecules are structural macromolecules present in the extracellular matrix. They include as a part of their structure one or several domains that have a characteristic triple helical conformation. Most common types includes I II, III,V, and XI with less common subtypes including types IV and VIII (van der Rest and Garrone, 1991). Type 1 collagen is the most ubiquitously distributed and most abundant of the collagen family of protein.

Structure wise, collagen is a heterotrimer which is composed of two alpha1 chains and one alpha 2 chain (Dalgleish, 1997). The type 1 collagen is encoded by COL1A1 and COL1A2 respectively. Collagen abnormalities can result from mutations in these genes with over 200 of such mutations having been reported (Chavassieux et al., 2007). Mutations at these loci can lead to pathologies such as osteogenesis imperfect (OI) and Ehlers-Danlos syndrome. Mutations at these loci have also been reported to be linked with osteoporosis and Marfan's syndrome (Dalgleish, 1997; Chavassieux et al., 2007). Bone phenotype in OI, has been particularly linked with RTT bone phenotype.

As described in the introductory chapter, the basic structural units (BSUs) in bone matrix are not uniformly mineralized. More recently completed BSUs are less densely mineralized than older BSUs that have had more time to undergo secondary mineralization (crystal enlargement) (Boskey, 2003). Even within a BSU, the organisation is formed as a composite. The higher and lower density lamellae with collagen fibers oriented in different directions creates a structure that serves to prevent the occurrence of cracks and limits crack progression in skeletal tissue. Loss of the lamellar organization as seen in woven bone in Paget's disease and loss of heterogeneity in tissue mineral density as frequently seen in prolong use of bisphosphonate may affect bone's ability to prevent crack occurrence and progression (Boivin and Meunier, 2002). Keeping this in mind, the mechanism of low energy fractures seen in RTT patients can be explained however research in terms of collagen component of bone pathologies seen in RTT patients is still poorly define.

Recently a case control study (Roende et al., 2014) has been conducted by Roende and colleagues, which revealed a decrease in the bone formation marker N-terminal propeptides of collagen type 1 (PINP), pointing towards the potential role of collagen along with mineral component as the contributing factors to altered bone integrity seen in Rett Syndrome. However, analogous and controlled studies assessing collagen content and composition have so far not been conducted in animal mouse models of RTT.

5.1.2 The Cellular Machinery for bone homeostasis and turnover

As mentioned earlier the cellular activities of bone modelling and remodelling determine the material composition and structure of bone. Bone modelling represents the formation of new bone phase whereas bone remodelling encompasses both a resorptive phase and a bone formation phase. The whole process of bone modelling and remodelling contributes to the bone strength (Chavassieux et al., 2007). Bone cells (see section 1.5.3) plays a vitol role in this regards, osteoclast in particular starts the remodelling by first differentiation under the stimulation by osteoblast cells (Nakashima, 2014).

Receptor activator of nuclear factor-kB (RANK) LIGAND (RANKL) is expressed and secreted by osteoblast precursor cell and binds RANK expressed by osteoclasts, thus promoting the differentiation and activity of osteoclasts. Osteoblasts secrete osteoprotegerin (OPG), which binds to RANKL and inhibit the RANK-RANKL interaction (Nakashima, 2014). RANKL knockout mice have display severe osteoporosis and an analysis of cell types reveal that they lack osteoclasts despite the presence of osteoprogenitors (OPG). In contrast to the consequences of reduced RANKL expression, increased expression of RANKL may explain disorders associated with increased / excessive resorption such as multiple myeloma. Interestingly OPG-deficient mice showed a sever osteoporosis as well resulting from increase in osteoclastic activity and formation (Horowitz et al., 2001; Kon et al., 2001; Chavassieux et al., 2007).

5.1.3 Aim of the study

Results from the previous chapters showing altered biomechanical as well as material (microhardess) properties of MeCP2-deficient bone suggest that there are likely to be alteration in bone composition. In the current set of experiments I hypothesised that alterations in the protein or mineralisation of MeCP2 deficient bone may explain the earlier biomechanical and material bone phenotypes observed in the mouse model of Rett Syndrome. Thus, the specific aim of the experiments in this chapter was to determine whether deletion and restoration of MeCP2 is accompanied by detectable changes in bone mineralisation, collagen content and osteoclast number / activity.

5.2 Methods and Material

5.2.1 Preparation of histological sections of bone

Whilst the distal parts of male MeCP2 stop/y, wild-type and rescued mouse left femurs were used for scanning electron microscopy imaging described in chapter 4, the proximal aspects of left femurs (n=5 per genotype) were used for histological analysis. Because of the limited availability of tissue samples in my study I have selected two important experiments as the initial histological analysis. Firstly, I have looked at the collagen content as this parameter has never been analysed in both RTT patients or animal studies before. Also since I did not find any difference in inorganic part (mineral content) I wanted to explore the organic part of the bone. Furthermore since collagen forms the primary organic component of bone matrix it was appropriate to start an initial analysis by measuring the collagen content first. Osteoblast is involved in the synthesis of collagen hence the results obtained could also be the indirect measure of osteoblast function. Secondly the results of previous experiments of trabecular thinning seen in *Mecp2* stop mice and significant improvement seen in rescue mice raised questions as to whether increased/decreased osteoclast activity in the bone tissue is the primary cause of under lying pathology. Alternate sections were stained with either Sirius red staining for collagen content (see section 5.2.2.1) or tartrate-resistant acid phosphatase (TRAP) staining for osteoclasts (see section 5.2.3.1).

5.2.1.1 Decalcification of proximal parts of stop femur

The bone samples were first decalcified in 12% EDTA, (pH 8.0, 5N NaOH) for 14 days. The fresh solution was added every second day over the 14 day period. The specimens were then kept in the decalcifying solution in a refrigerator at 4°C prior to tissue sectioning.

5.2.1.2 Processing of tissues for histology

Following fixation by 10% neutral buffered formalin, tissues were placed in plastic cassettes and processed using a Leica TP1020 tissue processor (Leica Milton Keynes, UK) maintained by David Russell, Laboratory of Human Anatomy, University of Glasgow. The overnight processing programme took tissues through

graded alcohols (70%, 90%, 100%; 1hr, 1hr, 1.5hrs), amyl acetate and molten paraffin wax. Tissues were then transferred for embedding

5.2.1.3 Embedding tissues in paraffin

Embedding was performed on a Tissue Tek embedding centre maintained by David Russell, Laboratory of human anatomy, University of Glasgow. Molten wax was poured into moulds and bone samples were carefully oriented to provide a longitudinal (LS) sections on cutting. Wax hardens around the plastic embedding cassettes and makes up the finished block, allowing blocks to be easily cut.

5.2.1.4 Cutting of histological sections

Longitudinal sections of 5 μm thickness (150 slices in total) were cut using a microtome (Leica RM2035, Milton Keynes, UK) maintained by David Russell, Laboratory of human anatomy, University of Glasgow.

5.2.2 Quantitative measurement of collagen in bone

A variety of stains are available to stain collagen including, Masson's trichrome which is one of the commonly used staining methods employed for collagen and collagen related pathologies (O'Brien et al., 2000; Lazzarini et al., 2005). Other studies have used sirius red staining because of its specific binding to collagen (Puchtler et al., 1973; Junqueira et al., 1979; Malkusch et al., 1995; Wright et al., 2003; Hui et al., 2004; Goodman et al., 2007; Kliment et al., 2011; Huang et al., 2013).

However trichrome stain has limitation as it is not specific to collagen, in contrast, the sirius red stain is based on the application of a single dye that has been shown to specifically stain collagen types I, II and III and is highly sensitive in detecting small amounts of collagen (Junqueira et al., 1979).

Moreover in a recent study (Huang et al., 2013) a collagen proportional area (CPA) images, stained with trichrome staining was compared with sirius red stain and it was found that the reproducibility of collagen proportional area image analysis stained with sirius red stain was superior to that achieved with trichrome. Moreover the mean CPA stained with sirius red was found to be significantly greater than CPA stained with trichrome and this was found to be consistent with

their morphological findings that sirius red staining detected more collagen then did trichrome staining.

In my current study I have used Picro-sirius red method of staining (after (Puchtler et al., 1973; Junqueira et al., 1979) to detect the percentage of Picro-sirius red stained collagen content in each bone specimen per genotype as sirius red staining for collagen is one of the best understood techniques of collagen staining (for methodology see section 5.2.2.1).

After staining, percentage collagen content was calculated by pixel counting technology (see section 5.2.2.2 for details). Pixel counting technology is potentially a highly accurate technology that calculates collagen area however the reliability could be influenced by threshold settings, magnification and image resolution (Huang et al., 2013). In order to obtain reliable analysis, both during the staining and image analysis I and technical staff were blinded to the identification of the sample.

5.2.2.1 Sirius Red staining for collagen

After cutting, the bone sections were de-waxed with *Histoclear (Fisher)*, for 15 mins and hydrated through 100%, 90% and 70% alcohols. Nuclei were stained with Mayer's haematoxylin for 8 minutes, and then slides were washed for 10 minutes.

Specimens were then stained in Picro-sirius red solution [prepared by adding 0.5g of Sirius red F3B (Sigma-Aldrich, C.1.35782) in 500 ml of saturated aqueous solute ion of picric acid]. This gives near optimal staining, which does not increase with longer incubation. Tissue samples were washed in two changes of acidified water [prepared by adding 5 ml of acetic acid (glacial) in 1 litre of water (tap or distilled)]. Specimens were then dehydrated in increasing ethanol concentrations, cleared in *Histoclear* and mounted in DPX (consists of distyrene, a plasticizer, and Xylene) (Sigma Aldrich). To standardize staining, care was taken that all sections were stained in a single batch (figure 5-6).

5.2.2.2 Region of interest and image analyses of bone sections for collagen content

To assess total collagen content, bright field images were sampled using a 40X objective lens on an Axioskop50 microscope (Zeiss, Cambridge, UK) with Carl Zeiss AxioCam MRc camera (Zeiss, Cambridge, UK) and images were further analysed using Zeiss Axiovision v.4.8.3.0 software and colour segmentation plugin.

Care was taken to obtain all images with same magnification, thresholding and image resolution. A demarcation, line was drawn across each specimen image, at the beginning of third trochanter across the whole bone section to standardise and specify the exact area from which region of interests (219.31µm x 164.56µm) were selected each, from both medial (femoral head side) and lateral side (trochanter side) per bone per genotype (figure 5-6).

The Regions of interests were further analysed and quantified by using the Image J 1.47v, colour segmentation plugin. This plugin helps to segment (different colours) within the examining bone image. The Positive sirius red stained pixels were selected and quantified by using Imagej (colour segmentation plugin) with pixel area count and reported as a percentage of the total tissue area (219.31µm x164.56µm) specified in each bone per genotype (Malkusch et al., 1995; Kiernan, 2008) (figure 5-6, Bi-Biii). The detailed steps of methodology are as below:

Steps

1. To calculate the area of red pixels corresponding to the Sirius red stained collagen fibres, images were opened in image j 1.47v (figure 5-1).

2. Under the Colour segmentation, POINTCROSS tool was selected, in the toolbar section of image j software.

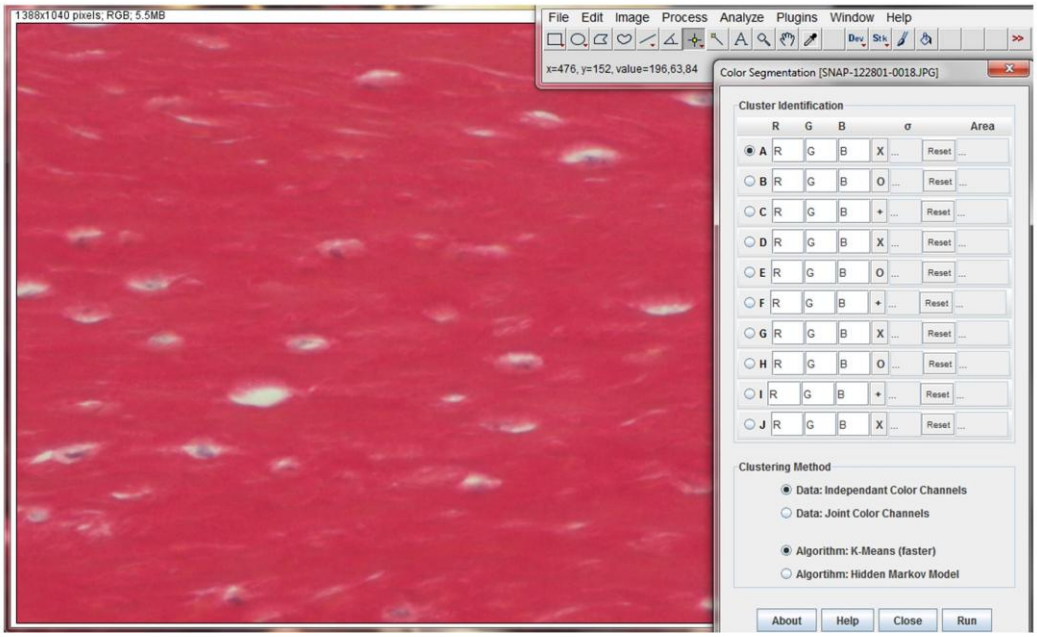

Figure 5-1 Selection of image through image j Colour-Segmentation plugin

3. First cluster of high intensity red pixels was defined by clicking on the image.

4. Subsequent clusters of white, blue (nuclei) pixels of osteocyte cells and remaining faint red pixels were selected by clicking on the image (figure 5-2).

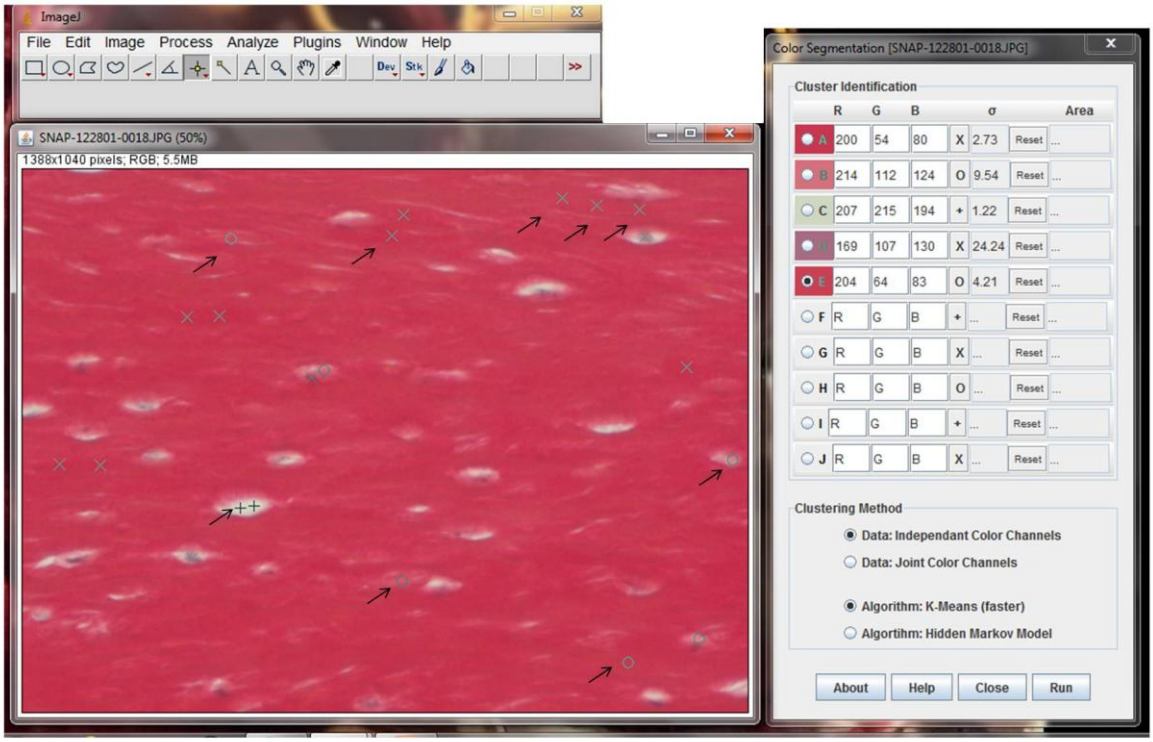

Figure 5-2 Selection of different pixel colour clusters

5. Under the data organization section dependant channels option was selected.

6. Further on algorithm of K-Means clustering was carried out. After this selection, Run option was clicked and an output image was obtained per sample.

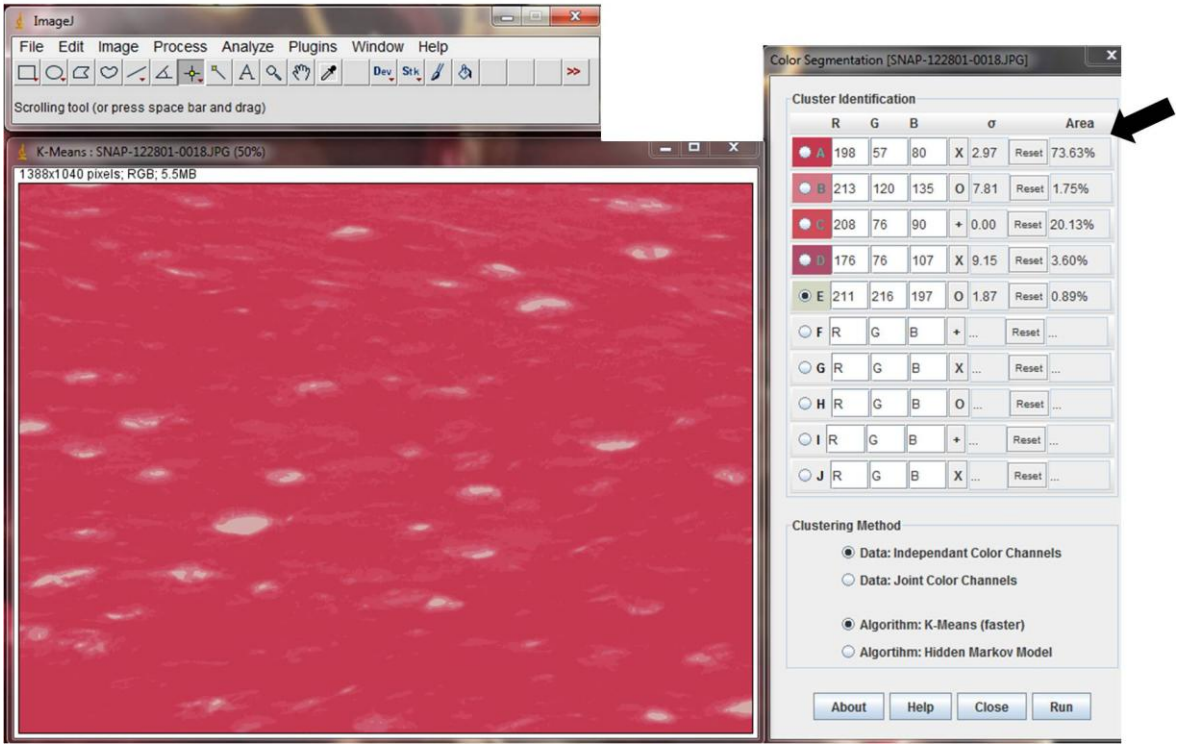

Figure 5-3 Percentage area measurement by Colour segmentation plugin

7. The subsequent output images gave the percentage area measurements of each defined colour cluster.

8. The % area of red pixels corresponding to collagen fibres, relative to total tissue area, was estimated using a colour segmentation plugin in Image J (Biomedical imaging Group, EPFL, Switzerland :http://bigwww.epfl.ch/sage/soft/colorsegmentation/) using independent colour channels and the K-means algorithm (figure 3-3).

5.2.3 TRAP staining for osteoclast

Alternate sections from the proximal femur longitudinal sections were stained with Tartrate-resistant acid phosphatase (TRAP) staining to assess resorption activity (osteoclast number per bone surface).

5.2.3.1 Tartrate-resistant acid phosphatase (TRAP) staining for osteoclasts

After cutting, the bone sections were de-waxed with *Histoclear*, for 15 mins and hydrated through 100%, 90% and 70% alcohols. TRAP solution was prepared by adding in 100 ml of distilled water, 1.15 g of sodium Tartrate, 1.22 g of sodium acetate. Solution was adjusted to pH5 by using 1M HCl before 5 mg Fast Red TR 10 mg Naphol AS-MX *(Sigma Aldrich,* N-4875) was added. Specimens were then stained in TRAP solution for 1 hour at 37°C. Tissue samples were washed in two changes of tap water. Nuclei were stained with Mayer's haematoxylin for 8 minutes, and then slides were washed for 10 minutes for blueing of nuclei. To standardize staining, care was taken that all sections were stained in a single batch. A slide was treated with the same solution minus the substrate, as a negative control. Method of staining adopted from O'Connor *et* al (O'Connor et al., 2009b).

5.2.3.2 Region of interest and image analyses of bone sections for osteoclast number

To quantify osteoclast number in histological sections, images were sampled by bright field microscopy using a 40X objective lens on an Axioskop50 microscope (Zeiss, Cambridge, UK). A rectangle area of 1.47 mm^2 was selected as the region of interest below the anatomical point of femoral trochanter in each bone specimen per genotype. The TRAP stained cells were independently counted by at least two blinded reviewers, and each multinucleated and TRAP stained cell was counted as one osteoclast. Total numbers of osteoclasts were counted within the region of interest both on the medial and lateral side per bone specimen per genotype. For each sample an average number of osteoclasts were counted using the method

described by Sawyer and colleagues (Sawyer et al., 2003) and adopted by O'Connor and colleagues (O'Connor et al., 2009b). Osteoclast were defined as TRAP stained, multinucleated, light blue stained cells containing foaming cytoplasm lying close to an eroded lacuna or on the bone surface (figure 5-4). TRAP-positive osteoclasts adjacent to bone showing one nucleus or no nuclei at all in the plane of section were also included in the count as the osteoclasts. The number of TRAP stained cells was independently counted by two blind reviewers, assuming each TRAP stained cell was one osteoclast. Average number of osteoclast counts was calculated for each bone per genotype and total mean values for all three genotypes were compared.

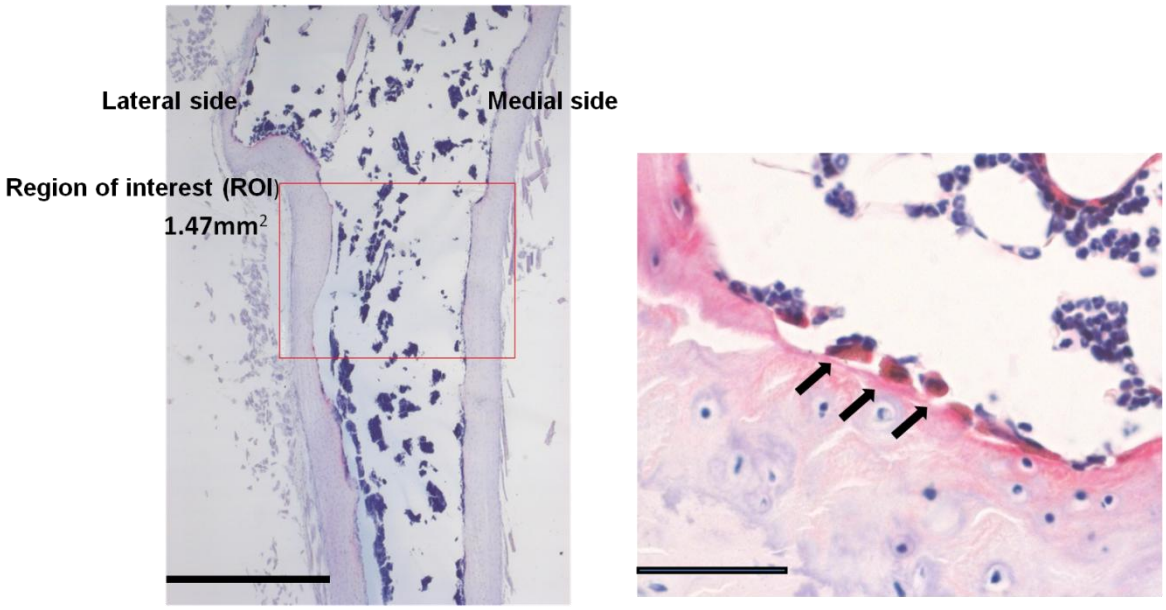

Figure5-4 Region of interest selection for osteoclast count in male stop mice

(A) Low power bright field micrograph showing, the method for selection of regions of interest (ROI) for the quantification of osteoclast number. A rectangular region of interest (1.47 mm^2) was selected below the anatomical point of beginning of trochanter. (B) High power (40x) image of region of interest) showing osteoclasts (black arrows) (A) Scale bar= 1000μm (B) Scale bar= 50μm

5.2.4 Ash weight density

In order to confirm the density findings obtained from CT scan measures, I performed an ash weight density experiment. For this experiment, Left tibias from both male and female mice cohorts were place in Pyrex crucibles and dried at 100°C for 24h in a muffled furnace at the Organic Chemistry Department, University of Glasgow, Glasgow, UK. Weight measurement of the crucibles was taken separately at the beginning of experiment by using the analytical balance (APX60 Analytical Balance, Denver Instruments). Weight measures were taken after the bones have been dried and ashed in muffled furnace.

Dry weight measures were obtained (APX60 Analytical Balance, Denver Instruments) while the tibias were still in the crucibles to avoid any tissue loss as the mouse bones are understandably very small and fragile to handle, especially after being heated at high temperature . The specimens were then reduced to ash at 650°C for 24h and the ash weight measurement were taken in a same manner as dry weight measures. The ratio of ash weight and dry weight was used to obtain the final ash content (Kriewall et al., 1981; Keene et al., 2004). The ash content can be expressed on either a *dry* or *wet* basis:

$$\%\ Ash\ (dry\ basis) = \frac{M\ ash}{M\ dry}\ \text{X } 100$$

$$\%\ Ash\ (wet\ basis) = \frac{M\ ash}{M\ wet}\ \text{X } 100$$

Where $M\ ash$ refers to the mass (weight) of the ashed sample and $M\ dry$ and $M\ wet$ refer to the original masses (weights) of the dried and wet bone samples.

5.3 Results

5.3.1 *Mecp2* stop mice showed decrease in collagen content

Sirius red staining was conducted as an initial experiment to assess any gross defects in overall collagen content of the bone samples from *Mecp2*$^{stop/y}$ mice and wilt-type and genetic rescue controls. The percentage college content values were derived by quantifying pixel area count of positive sirius red stain, localization in each region of interest per bone per genotype. Final values were reported as a percentage of the total tissue area (1.47mm^2) specified in all genotypes. Stop male mice showed a significant decrease in collagen content compared to Wt mice (WT = 65.1 ± 8.6%; Stop= 48.8 ± 9.1 %; Rescue = 55.63 ± 11.4 %; n = 5 specimens per bone per genotype, p<0.01, one way ANOVA with Tukey's *post hoc* test). An interesting finding of reduced collagen content and increased pale stained extracellular are in tissue sample of *Mecp2* stop was also made as compared to the age matched wild type and rescue mice (figure 5-5).

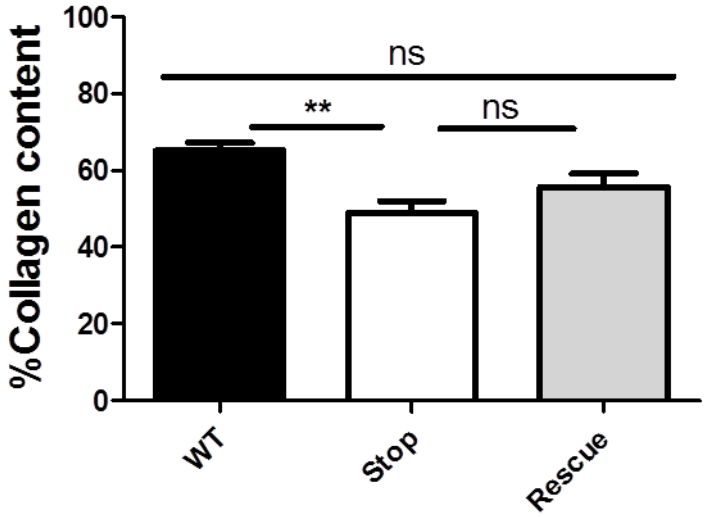

Figure5-5 Collagen content analysis in Mecp2 stop mice
Bar chart showing percentage Collagen content in *Mecp2*$^{Stop/y}$ (Stop) mice is reduced as compared to wild-type (Wt; p<0.01); n = 5 specimens (5 sections from each medial and lateral side) per bone per genotype. No significant treatment effect was seen in rescue mice. Abbreviations: ns = not significant; one way ANOVA with Tukey's *post hoc* test). Plots show mean ± S.D.

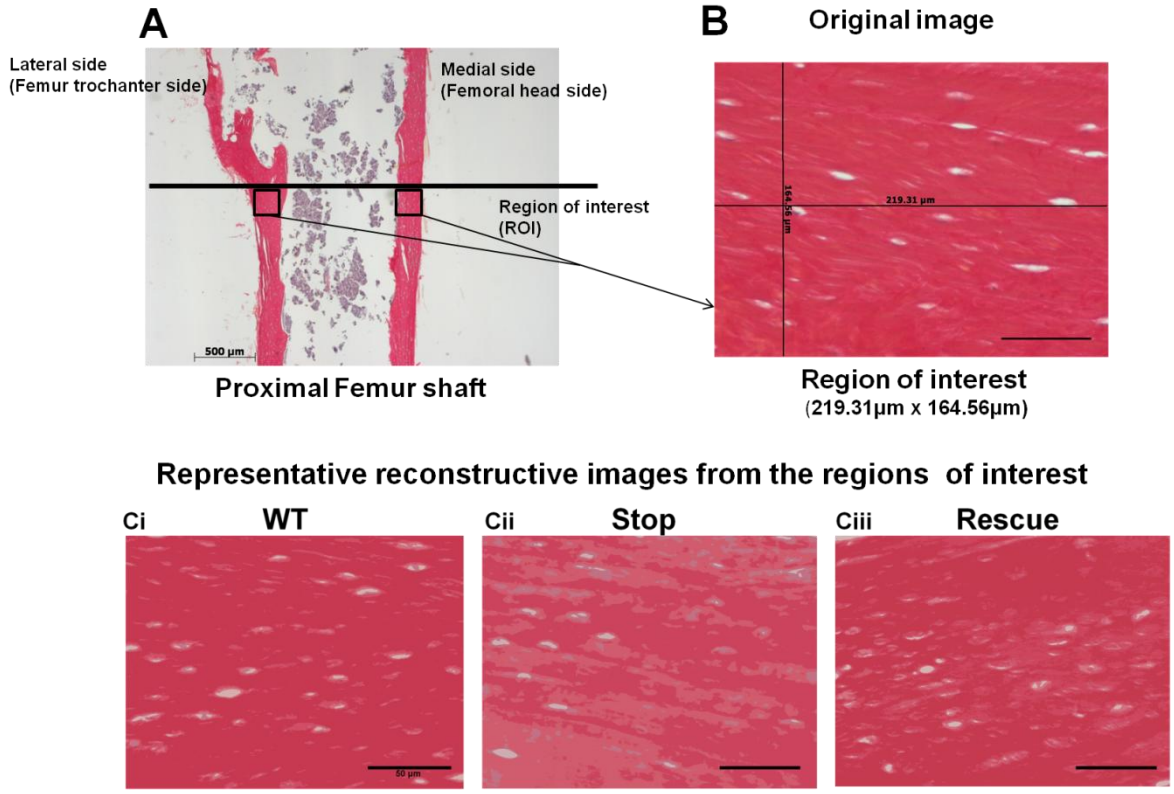

Figure 5-6 Comparison of %collagen content

(A) Low power micrograph showing position of (boxes) region of interest (ROI) selected for the quantification of collagen. Regions of interest are selected from both the medial and lateral side of each proximal femur at a site demarcated by the beginning of trochanter. A line was drawn across the section so that both the sections are selected at the same level. (B) Higher power bright field micrograph showing sirius red stained region of interest. (Ci-iii) Representative, high power (40 x objective) micrographs showing representative regions of interest from each experimental cohort/genotype. Images of region of interest were reconstructed for the quantification of percentage college content by using image j (colour segmentation plugin). (A) Scale bar= 500µm (B) Scale bar= 50µm

5.3.2 Osteoclast number did not showed any significant difference in *Mecp2* stop mice

TRAP staining was conducted to assess resorption activity (osteoclast number per bone surface within region of interest) but showed no difference between genotypes (WT=12.61±8.51 (n); Stop =17.48±6.13 (n); Rescue =18.90±4.61 (n); n=5 per genotype, $p>0.05$, one way ANOVA with Tukey's *post* hoc test) (figure 5-7).

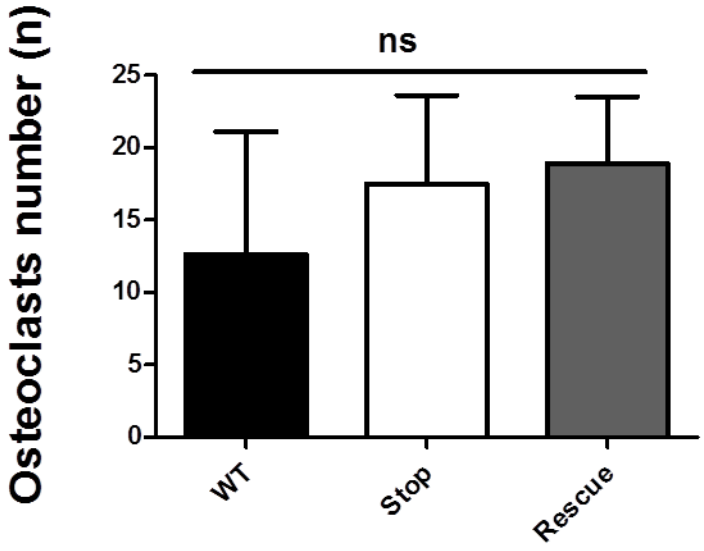

Figure5-7 Osteoclast number quantification analysis in *Mecp2* Stop mice

Bar chart showing no significant difference in osteoclast number between the three comparison genotypes (WT=12.61±8.51; Stop =17.48±6.13; Rescue =18.90±4.61; n=5 per genotype, $p<0.05$, one way ANOVA with Tukey's *post* hoc test). Values refer to absolute number (n) count of osteoclast within the specified tissue region) Abbreviations: ns = not significant. Plots show mean ± S.D.

5.3.3 Ash density analysis of bone tissues in *Mecp2* stop mice

The analysis of mechanical (reduced bone strength), material (reduced bone hardness measure), structural (thinning of cortical and trabecular bone) experiments revealed an osteoporotic picture of the bone tissue similar to the one frequently reported in RTT patients.

A surprising result was the finding of no significant difference in bone mineral density measures obtained after the μCT (see chapter 4). Decrease in bone mineral density has been frequently reported in RTT patients (Budden and Gunness, 2001; Cepollaro et al., 2001; Budden and Gunness, 2003; Shapiro et al., 2010; Jefferson et al., 2011; Roende et al., 2013b). In order to re confirm the bone mineral density values derived from μCT, I performed ash weight density test. Ash weight density is frequently used to asses' ash content. Studies have been done to compare the results from bone mineral density and ash weight tests. I also performed this experiment to confirm the findings of my earlier experiment.

Left tibia was used to analyse the percentage mineralization (ash content) see above section 4.2.5 for methodology. Results showed no significant difference in percentage ash content measured on the basis of dry weight measures and in percentage ash content values measured on the basis of wet weight measures between genotypes of male mice (figure 5-8).

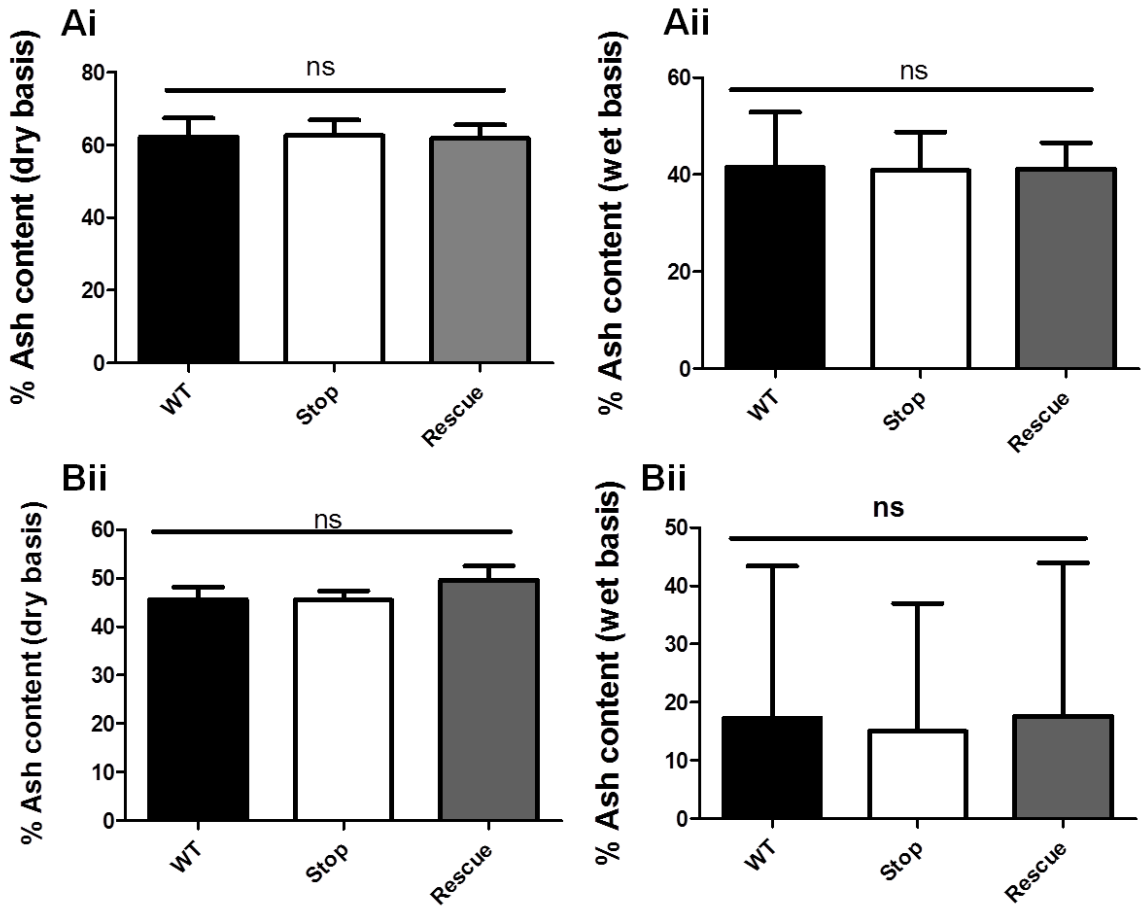

Figure5-8 Ash Content analysis in male and female stop mice

(Ai-Aii) Bar charts showed no difference in percentage ash content in male mice cohort (dry basis) (WT= 62.15± 5.22%; Stop =62.57± 4.25%; Rescue =61.75 ± 3.72%; n =6 per genotype, $p>0.05$, ANOVA with Tukey's post hoc test) and (wet basis) (WT=41.54 ± 11.35%; Stop =40.88 ± 7.92%; Rescue =41.23 ± 5.36%; n=6 per genotype, $p>0.05$, ANOVA with Tukey's post hoc test). (Bi-Bii) Percentage ash content values in Stop female mice showed similar pattern of no significant difference, in % ash content (dry basis) (WT= 45.58± 6.37%; Stop =45.49± 3.78%; Rescue =49.55 ± 5.128%; n=3-5 per genotype, $p>0.05$, ANOVA with Tukey's post hoc test) and % ash content (wet basis) (WT= 17.27 ± 26.27%; Stop=15.00 ± 21.99%; Rescue =17.59 ± 26.36%; n=3-5 per genotype, $p>0.05$, ANOVA with Tukey's post hoc test). Abbreviations: ns = not significant, Plots show mean ± S.D.

A similar trend of percentage ash content results was observed in female cohort tibias. No significant difference was found in heterozygous Stop female cohort of values of percentage ash content calculated on either dry weight basis or wet weight basis All data given as, mean ± SD (figure 5-8).

5.4 Discussion

The major finding of the current set of experiments was the observation that the collagen content is appreciably reduced in bone sections stained with sirius red from MeCP2-defience mice as compared to wild-type littermate mice. Sirius red stain was first described by Junqueira et al. in 1979 (Junqueira et al., 1979) and is a dye that binds to the [Gly-x-y] triple-helix structure found in all collagen fibers. This property of sirius red stain can be utilized to assess collagen in various tissue sections under bright field and polarized light microscope (Junqueira et al., 1979; Whittaker et al., 1994) and in cell culture (Walsh et al., 1992).

In my initial analysis, to observe any gross changes in collagen content, I have used bright field microscope to assess the overall content of collagen in a specified region of interest per bone per genotype. The Sirius red stained images were further analysed by using the colour segmentation plugin of Imagej. The colour segmentation is an Imagej plugin that allows to segment an colour image or a stack of colour by pixels clustering. I have used the colour segmentation plugin to segment the bone cells from the extracellular content. The high intensity sirius red stained collagen content area was identified in each image per slide per bone by using Imagej software and the collagen content was calculated as a percentage of the specified area of each image (expressed in pixels).

The results obtained showed mean colour area percentage of collagen in *Mecp2* stop mice to be 48.8% which was significantly decreased compared with the control group ($p<0.01$). This reduction in % collagen content was found consistent with the mean colour area percentage of collagen of 47.7% seen in histological sections of female albino rat (ovariectomy induced) models of osteoporosis (Naim, 2011). The overall picture of reduced collagen content and increase pale stained space within the extracellular bone matrix found in my study adds to the osteoporotic picture of RTT bone phenotype. However bone histomorphometric analysis of collagen content in children and adolescents with RTT is unknown.

The magnitude of the reduction in my study was in the range of ~25% and thus it can be predicted to have a profound effect on overall material and mechanical properties of bones in these mice. Interestingly, there was a trend towards a reversal of collagen level deficits in genetically rescued mice (~15% increase compared to knockout mice) but this change did not achieve statistical significance. Hence, this study did not provide direct evidence that restoration of MeCP2 can results in improvement of organic part of extracellular matrix. In RTT patients bone anomalies have always being considered and investigated in terms of decrease in bone mineral density, while little attention has been paid to the organic part of extracellular matrix.

As described earlier the organic (collagenous and non-collagenous proteins) and inorganic phase (minerals) both contributes towards the bone strength (Marotti et al., 1994). Collagen fibrils are stiffened by integration of the mineral phase. The presence of mineral phase increases bone strength; but in woven bone, which is constituted by unorganized collagen fibrils, the mechanical properties are decreased despite a high mineral content (Marotti et al., 1994). As majority of collagen content consists of type 1 form of collagen, my finding of decrease in collagen content are also consistent with the results of a recent analysis of biochemical bone marker, in which all the bone markers including N-terminal , propeptides of collagen type 1(PNIP), the C-terminal telopeptide cross links (CTX); and osteocalcin (see section 1.5.4) were found decreased in blood samples taken from Rett patients (Roende et al., 2014).

Osteoblast plays a major role in collagen homeostasis as it synthesizes and secretes the C-terminal propeptides of the alpha 1 and alpha 2 chains of type 1 collagen (Johansen et al., 1992). Hence the reduction in collagen content from the current study can be interpreted as the decreased osteoblast function in *Mecp2* stop mice.

Interestingly, MeCP2 has been found to regulate the expression of RANKL gene (Kitazawa and Kitazawa, 2007) expressed by osteoblasts (Alvarez-Saavedra et al., 2010)(see section 1.5.4 and 5.1.2 for details of RANKL and its role in bone homeostasis) further supporting the potential involvement of MeCP2 in skeletogenesis. Also MeCP2 overexpression, duplication and triplication has been found to result in diminished ossification resulting in severe kyphosis, a distorted

sternum, spina bifida and dysmorphic feature in male TTM20dTg mice (kyphosis, scoliosis).

Interestingly, RTT bone phenotype, other than osteoporosis has also been linked to share features with a disorder known as Osteogenesis imperfecta (OI). OI is an inherited disorder characterized by increased bone fragility with recurrent fractures mainly caused by the defects in collagen synthesis (Smith et al., 1975; Camacho et al., 1999). Nonetheless the possible role of collagen defects, in RTT bone phenotype needs more attention. This current study has limitation as I have calculated the gross values of collagen content by using the bright field microscopy. In future studies a polarized light microscopic (Lillian and Whittaker, 2005) examination to identify the collagen structure in detail can give further details.

Histological experiment to count osteoclast number was also performed to analyse the resorptive activity of the bone (O'Connor et al., 2009b). Connor and colleague also looked at the absolute osteoclast number in their *Mecp2* null mouse model and did not find any difference. They relate the non-significance of their findings to the small number of animals they have used in their study. I wanted to look at the osteoclast number to see if there is any significant difference in the resorption activity in bone that is causing all the apparent increase in bone fragility in *Mecp2* stop mice. The multinucleated osteoclast-like cells form pits on bone or dentine slice express high concentrations of 5 isozyme of tartrate-resistant acid phosphatase (TRAP) (Alatalo et al., 2000).

TRAP is a histochemical marker of the osteoclast. It is also characteristic of macrophages and other cells of mononhitiocytic lineage (Alatalo et al., 2000; Hayman et al., 2000). This enzyme partially dephosphorlylates the bone matrix phophoproteins osteopontin and bone sialoprotein, which have been implicated in cell attachment (Ek-Rylander et al., 1994). The TRAP “knockout” mouse has shown that the enzyme is essential for normal mineralization of cartilage in developing bones and for maintaining the integrity and turnover of the adult skeleton (Hayman et al., 1996).

As an initial experiment to analyse the bone resorption activity I have calculated the number of TRAP stained osteoclast within the specified region of interest

selected per bone per genotype. TRAP is confirmed as a valid marker for identification of osteoclasts on the other hand TRAP activity is an osteoclastic marker of weak sensitivity. This may be due to known fact that synthesis of enzyme is not being unique to osteoclasts (Ballanti et al., 1997). Osteoclasts are heterogeneous with respect to cellular size and shape. They used to be recognised mainly on the basis of multinuclearity and cell width but since these criteria do not recognize mononucleated osteoclasts, this methodology has been questioned (Palle et al., 1989).

Tartrate-resistant acid phosphatase (TRAP) is detectable in large amounts in the lysosomes of osteoclasts and its activity is now considered an established cytochemical marker useful for recognizing polynucleated as well as mononucleated osteoclasts in bone sections (Baron et al., 1986). At present, the number of osteoclasts is determined by counting the number of TRAP-positive multinucleated osteoclast-like cells (Takahashi et al., 1988).

The results obtained displayed no significant difference of osteoclast number among the three comparison genotypes of male stop mice. However if we look at the analysis bar graph an interesting trend of 30% increased osteoclast number in stop mice and 50% increase in rescue mice as compared to wild type control mice was found indicating towards the slight increase in bone resorptive activity as compared to the age matched wild type control. The non-significance of this experiment results could be the result of high biological variance seen in tissue samples analysis (figure 5-4).

Our results of no significant difference in osteoclast number were inacordance to the finding obtained by O'Connor *et al*. Similar to our finding they did not find any significant difference in osteoclast number per bone surface (WT= 6.34±2.43, Mecp2 null= 6.60±2.30) in their TRAP stained tibial section of *Mecp2* null mouse mode. In another study conducted on five RTT girls revealed a decrease in osteoclast number and surface (Budden and Gunness, 2003). However this study had the limitations that patients and controls were not age matched and hence conclusion about resorption activity or rates cannot be inferred from these surface estimates. On the other hand Motil and colleagues study has displayed increase in bone turnover (increased resorption to formation) by age (Motil et al., 2008). Resorptive activity measures in RTT bone phenotype are still unclear and future

bone histomorphometric studies need to be done to fully understand the cellular mechanism of bone resorption in RTT patients.

After the histological experiments in organic part of bone I also looked at the inorganic (mineral) content of the bone of male and female stop mice by conducting the ash weight density measurements. Although I already had obtained the bone mineral density measurement from µCT scans analysis, I performed this experiment to confirm and validate the finding of µCT mineralisation calculations as various report in RTT patients have reported decrease in bone mineral density (Haas et al., 1997; Leonard et al., 1999b; Leonard et al., 1999c; Cepollaro et al., 2001; Motil et al., 2006; Zysman et al., 2006; Gonnelli et al., 2008; Alvarez-Saavedra et al., 2010; Shapiro et al., 2010).

No significant difference was seen in wet and dry ash weight density values of male and female stop mice and the results from the experiment confirmed the findings of µCT. In adults mammals 20% of bone weight is water, 45% is ash and 35% is organic matrix (Carter and Spengler, 1978). On a dry weight bases, mineral content is 65 to 70% and organic matrix is 30 to 35%. In this current study *Mecp2* stop male mice showed a 62% of ash content on dry basis which was comparable to wild type and rescue values and 41% ash content based on wet basis and consistent with the normal range. Compare to male mice, female stop mice displayed 45% ash content analysis on dry weight basis and 15% on wet weight basis, this apparent decrease in density measures obtained from male and female stop cohorts was gender and age appropriate (Henry and Eastell, 2000).

Overall similar to male stop mice cohort, female mice cohort showed no significant difference among the three comparison genotypes. O' Connor and colleagues in their *Mecp2* null mouse model, had displayed a modest reduction of bone mineral density and bone mineral content values (O'Connor et al., 2009b) but results does not reach the statistical significance. Also a recent study (Roende et al., 2014) on bone metabolism of patients with RTT has revealed some interesting insights. Bone metabolism can be characterized by biochemical markers of bone formation, resorption, mineralization and turnover (Szulc et al., 2000; Jürimäe, 2010). Roende and colleagues characterise bone metabolism in RTT patients, by comparing biochemical bone markers levels in RTT patients with healthy controls. They found that both markers of bone formation the N-terminal propeptides of

collagen type 1 (PINP); markers of bone resorption, the C-terminal telopeptide cross links (CTX); of bone turnover, osteocalcin (OC); and of bone mineralization, bone specific alkaline phosphatase (B-ALP) were significantly reduced. Interestingly they also found no significant association between bone markers levels and volumetric bone mineral density calculations obtained from DXA scans of lumbar spine and femur neck of the patients. The difference of bone mineral density value obtained from this study and previous studies (Cepollaro et al., 2001; Motil et al., 2006; Gonnelli et al., 2008) could be because the Roende *et al* adjusted their analysis of biochemical bone markers for age and puberty while previous studies have only analysed biochemical markers of bone formation in RTT children and young adults less than of 25 years of age. Studies (Rauchenzauner et al., 2007; Tuchman et al., 2008; Jürimäe, 2010) on biochemical bone markers in healthy persons have reported high levels in early childhood, peaking in puberty and decreasing to stable levels in the mid-20s.

Children with disabilities and limited mobility are at increased risk of osteoporosis (Aronson and Stevenson, 2012). RTT patients display osteoporotic bone phenotype (Zysman et al., 2006) and have been compared with cerebral palsy (CP) patients in past to analyse the bone mineral density values (Haas et al., 1997). Interestingly biochemical markers (OC, B-ALP, and N- telopeptides) in cerebral palsy (CP) patients with motor deficiencies have shown a wide variety in serum levels (Henderson et al., 1995; Henderson et al., 2002) and no significant association with measures of bone mass as BMD z scores of the lumbar spine and distal femur region have been found (Henderson et al., 2002).

Moreover another study comparing CP and healthy children reported no significant difference in both formation and resorption markers (Chen et al., 2011). Thus the reduced level of bone turnover seen in children and adolescents with RTT could be a direct effect of *MECP*2 gene mutation, although levels of bone markers did not differ between different mutation groups in patients with RTT (Roende et al., 2014). This could be due to an overall general effect of *MECP2* on regulation of growth and bone turnover. This is corroborated by my findings of decrease cortical bone volume, alteration in trabecular structure, reduced bone strength in *Mecp2* stop mouse model along with the growth plate abnormalities, decreased femoral trabecular and cortical bone volume and decreased bone mineral apposition rates seen in other *Mecp2* mouse models (O'Connor et al., 2009a; Shapiro et al., 2010).

The results obtained from this study are quite interesting. As described earlier, in my initial experiments I did find a difference in bone strength and structural parameters in *Mecp2* stop mice. In this current study, I found a possible defect (reduced collagen content) in organic part and not the traditionally considered inorganic part (ash weight density) of extracellular matrix to be responsible for bone fragility.

Future experiments need to be more focused on the organic part of extracellular matrix in order to determine the possible mechanisms of bone fragility commonly seen in RTT patients.

Chapter 6

General discussion

The overall aim of the experiments described in this thesis was to explore the effects of MeCP2 protein on bone tissue using various biomechanical, radiological and anatomical techniques applied to mice in which the *Mecp2* gene was functionally silenced. A secondary theme was to assess whether such features are potentially reversible by genetic rescue of the *Mecp2* gene. This has important therapeutic implications as it would predict whether future gene-based therapeutic interventions are likely to impact on bone phenotypes. In this chapter I will integrate the major findings of this thesis, the significance of these findings and finally, I will discuss possible future experiments to extend this work and derive the maximum benefits from the results I have obtained to date.

6.1 Major findings of the study

My first aim was to see whether inactivating the *Mecp2* gene in male and female mice will result in overt bone phenotypes. My study is only the second study to explore RTT-like bone phenotype in mice and the first study to investigate such phenotypes in female mice as well as to investigate biomechanical properties of bone. Female *Mecp2*$^{+/stop}$ mice are a gender appropriate and accurate genetic model of RTT yet they display a more subtle and delayed onset (4-12 months) of neurological features (Guy et al., 2007; Robinson et al., 2012a) compared to hemizygous male mice. Male Mecp2-null mice typically become symptomatic by the age of 5-8 weeks (Guy et al., 2007) and because of this rapid and severe disease trajectory are more commonly used in preclinical studies (Gadalla et al., 2011). In keeping with this pattern, the results of my work revealed a more pronounced bone phenotype in male stop mice and subtle or undetectable bone phenotypes in heterozygous female mice.

At the outset of the project there was no published literature on the expression of MeCP2 in bone. Therefore, an important initial experiment was to assess this in a

MeCP2-GFP reporter mouse line in which MeCP2 protein with an C-terminal GFP tag (McLeod et al., 2013) is expressed under its endogenous promoter and regulation. In male mice the MeCP2-GFP was observed to co-localise with DAPI in the nucleus but was absent elsewhere. This is consistent with MeCP2 displaying a similar nuclear-specific expression pattern as reported in brain neurons as well as other tissues. These experiments also showed heterozygous *Mecp2*$^{+/stop}$ mice to display punctate nuclear GFP fluorescence in ~50% of nuclei and no detectable MeCP2-GFP in the other cells. The heterozygous *Mecp2* stop female mice in which one *Mecp2* allele is inactivated mimic the mosaic expression seen in human Rett syndrome (figure 3-8).

Having established the presence of MeCP2 in bone and the efficient silencing of the gene in the Mecp2-stop mouse line the results of my subsequent anatomical and biomechanical phenotyping revealed that *Mecp2* stop male mice display a range of abnormal skeletal phenotypes that shares many of the features seen in clinical cased of RTT. Morphometric analysis revealed that the long bones of *Mecp2* stop male mice are lighter and shorter as compared to the age matched wild type group. This finding correlates with the growth retardation pattern seen commonly in RTT patients (Neul et al., 2010). Male stop mice are also known to display skeletal dysmorphic feature of kyphosis, which is comparable to pathogenomic '*S'* type of curvature seen in RTT patients (Ager et al., 2006; Koop, 2011; Riise et al., 2011).

One of the major finding of the current study came after the biomechanical analysis of male and female stop mice. The robust deficits were seen in mechanical properties were profound (39.5% reduction in stiffness in the three point bending test; 31% in load and 12.3% reduction in micro hardness) and could explain the weakness in MeCP2 deficient bone that accounts for the increasing occurrence of low energy fractures reported in Rett syndrome patients (Roende et al., 2011b). Frequent findings of reduction in bone strength (brittle bones) and hence increase incidence of fracture has given human RTT bone phenotype an overall osteoporotic bone phenotype picture (Haas et al., 1997; Zysman et al., 2006). However, the current studies do not discriminate whether the observed

defects arise from absence of MeCP2 protein or MeCP2 *per se* (ie. a primary pathology) or whether global silencing of Mecp2 throughout the body results in endocrine or systems defects elsewhere in the body that results a secondary pathology within the skeletal system. This question could potentially be address by using bone-linage specific cre lines. In terms of the potential secondary pathology, it is important to consider that the male mouse tissues used in the study were harvested at a time point at which the Mecp2-stop mice where showing fairly severe and advanced clinical signs (tremor, abnormal breathing, reduced locomotor activity and general poor condition) and these non-bone-related phenotypes may be an important factor. In contrast, the female heterozygous mice, despite being tested at a much later (many months rather than weeks) display similar non-bone phenotypes, albeit with much reduced severity (Guy et al., 2007).

Another important finding of my work came after the structural analysis of cortical and trabecular bone. Robust significant differences were seen in *Mecp2* stop mouse cortical and trabecular bone including a pronounced 54% reduction in cortical thickness, 30% in bone volume, 20% in total area, 38% in marrow area and 30% in trabecular thickness. Such findings are consistent with what is expected in an osteoporotic model (Seeman, 2008b).

Female stop mice bone phenotype results remained consistent with their overall subtle bone phenotypes and didn’t show an overt difference in morphometric measurements of long bone length and weight measurements. Within the nervous system there is evidence for both cell autonomous and non-cell autonomous effects of MeCP2-deficiency including morphological changes in dendritic architecture (Ballas et al., 2009). Whilst it is clear from the results of the current experiments that various bone phenotypes are more subtle, absent or below the level of detection in hemizygous females compared to equivalent measures in males, it is unclear whether this is indeed due to the fact that only ~50% of bone cells are expressing MeCP2 or whether dysfunction in other systems are contributing to the subtle phenotypes. Nonetheless, a similar significant reduction (14%) in micro hardness and a trend towards reduced biomechanical properties

seen in female mice that are heterozygous and mosaic for the mutant allele, demonstrate that the bone deficits are not restricted to the more severe male RTT-like phenotype but are also seen in a gender and *MeCP2* expression pattern appropriate model of RTT.

An important finding of the current study and one with therapeutic significance is that the bone anomalies observed in terms of cortical bone material and biomechanical properties were rescued by delayed postnatal activation of the *Mecp2* gene. Male rescue mice displayed a robust improvement in mechanical (stiffness 40%, ultimate load 10%, young's modulus 61% and micro hardness 12%) and structural bone parameters (trabecular thickness 80%) as compared to *Mecp2* stop male mice. Similarly another major finding was the rescue of female bone phenotype in female stop mice. Female rescue mice displayed a significant improvement in bone material properties (micro hardness 19%) and a trend of improvement in mechanical properties (stiffness, load) as compared to stop mice. These finding of rescue of bone phenotype in stop mice were consistent with the improvements seen in multiple non-bone phenotypes seen in the *Mecp2*$^{Stop/y}$ mice after delayed activation of the *Mecp2* gene including survival, normalized bodyweight, locomotor and behavioural activities (Guy et al., 2007; Robinson et al., 2012a).

These results were quite significant as they suggest that the bone anomalies seen in RTT patients may be at least partially reversible using gene-based approaches currently under development (Gadalla et al., 2013; Garg et al., 2013). However, it is also possible that significant amelioration of bone phenotypes may also be achieved by using pharmacological strategies (Gadalla et al., 2011; Garg et al., 2013). In order to apply all these therapeutic intervention most important aspect is to identify the mechanisms by which MeCP2 deficiency results in altered bone mechanical, material and structural properties. In my study I have found that *MeCP2* is expressed in osteocytes (figure 3-8), but the protein is widely expressed throughout the body and it is possible that metabolic and endocrine factors can influence the bone homeostasis (Motil et al., 2006; Motil et al., 2011; Motil et al., 2012).

A surprising finding of the current study was the absence of any significant difference in ash weight density or bone mineral density (µCT) in stop male and female cohorts. Our findings of no significant difference in bone mineral density (BMD) in Mecp2 mice were similar to the one reported in a *Mecp2* null mouse model (O'Connor et al., 2009a) while differs with other animal study in which bone mineral density were found reduced in *Mecp2* null mouse model (Shapiro et al., 2010). These are the only two animal model studies conducted in past to explore the RTT bone phenotype using the *Mecp2* null mouse model. The relationship between RTT bone phenotype and bone mineral density values in animal studies is still unclear.

Reduced bone mass is commonly associated with osteoporotic phenotypes and indeed these have been reported in RTT patients (Hui et al., 1988; Leonard et al., 1999c; Cummings et al., 2002; Ager et al., 2006; Flynn et al., 2007). Several clinical, density x-ray absorptiometry (DXA) studies (Haas et al., 1997; Leonard et al., 1999a; Cepollaro et al., 2001; Motil et al., 2008; Shapiro et al., 2010) in RTT patients have shown low absolute values of BMC (g) and or BMD (g/cm^2) compared to age-matched controls. The problem with use of DXA scan for assessment of bone mineral values is that the size adjusted absolute DXA values of aBMD (g/cm^2) may lead to interpretation of a relatively lower bone density among RTT patients than is actually the case (Roende et al., 2011a). Nonetheless these findings of bone mineral density from both µCT and ash content analysis are very interesting. They points towards the further need and importance of exploration of other possible factors (e.g. cellular dysfunction and alterations in the extracellular protein matrix) involved in the robust reduction of bone strength and structural parameters seen in *Mecp2* stop mice. Furthermore reversal of bone integrity (bone stiffness, hardness, trabecular thickness) seen in rescue mice after the gene reactivation leads to assess the mechanisms by which bone structure and properties are dynamically regulated by MeCP2 levels. As stated, it is also necessary to assess whether the influence of MeCP2 on bone homeostasis is a primary or secondary mechanism.

A number of studies have been conducted to investigate the role of specific genes, gene pathways and biochemical networks involved in the regulation of bone

homeostasis (Elefteriou et al., 2014; Quiros-Gonzalez and Yadav, 2014).

Studies involving leptin and neuropeptide Y2 have disclosed unrecognized interactions between the central nervous system, peripheral neurotransmitters and osteoblast function (Allison et al., 2007; Abdala et al., 2013; Elefteriou et al., 2014; Quiros-Gonzalez and Yadav, 2014). Several reports suggest that MeCP2 is an important regulator of neuronal gene expression (Skene et al., 2010; Guy et al., 2011b)). Neurological studies suggest that MeCP2 can affect osteoblast function by altering osteoblast chromatin structure as already seen in brain tissue or by altering cell maturation as observed in RTT neuronal tissues (Budden and Gunness, 2003; Chadwick and Wade, 2007). However, the precise role played by MeCP2 in the nucleus remains unclear (Chahrour et al., 2008; Skene et al., 2010; Guy et al., 2011a; Li et al., 2013a), but it is generally considered to regulate gene expression.

Another important finding of my studies and one which may relate to aberrant gene expression is the effect of MeCP2 deficiency on collagen content. As collagen is the most abundant gene product and structural determinant in bone, I conducted an initial analysis of collagen content and distribution using sirius red staining. The decreased levels (25% as compared to age matched wild type genotype) of intense sirius red stain observed in the MeCP2-deficient mice is consistent with reduced PINP (bone formation markers) levels in human RTT (Roende et al., 2013a) and the patches of reduced staining resemble those features characteristic of early osteoporosis (Leonard et al., 1999a). Whilst my work suggests that deregulation of collagen may be a significant potential mechanism underlying RTT-related bone phenotypes, further studies would be required to assess whether altered collagen level or altered balance of different collagen subtypes may result as a direct consequence of *MeCP2* deficiency.

In addition to structural protein, we also investigated the resorptive properties of the bone in terms of TRAP staining. The lack of any difference in osteoclast number between genotypes is consistent with a previous report (O'Connor et al., 2009a) and suggests the possible absence of any primary defect in bone remodelling.

My findings of osteoclasts were also consistent with the bone histomorphometric analysis performed by Budden and colleagues (Budden and Gunness, 2003). Although no difference in resorptive parameter (osteoclast number) was found, conclusions about the resorption activity or rates cannot be inferred from these surface estimates.

Overall, based on all these major findings of my study it could be said that Mecp2 stop mice display, osteopathic features of RTT (reduced bone strength, decrease in cortical and trabecular thickness, decrease in collagen content and tendency towards spinal curvature) which are also similar to those reported in collagen type 1 genetic disorder (osteogenesis imperfecta; brittle bone disease) (Dogba et al., 2013) pointing towards the possible importance of collagen defects in RTT. The RTT bone phenotype has previously been linked with osteogenesis imperfecta (OI) in past (Loder et al., 1989). Indeed, one patient in this study who suffered from increased rate of fractures had originally been given a primary diagnosis of osteogenesis imperfecta before the Rett syndrome was diagnosed.

Animal's studies and studies in human subjects suggest that skeletal fragility in osteogenesis (OI) is due to the defect in collagen synthesis, whereas the abnormalities in bone turnover and mineral are inconsistent. These findings of reduced collagen and no significant difference in bone mineral density were similar to the one I have observed in my analysis of skeletal phenotype of RTT. The collagen abnormalities seen in OI are the result of the two type 1 collagen genes, mutation COLIA1 and COLIA2. Over 200 mutation types have been reported. Two main classes of type 1 collagen mutations have been described (Seeman and Delmas, 2006). The first "null allele" mutation affects the pro-alpha1 or pro-alpha2 allele that impairs transcription and mRNA stability and produce low amounts of the secreted heterodimer. The abnormal heterodimers are incorporated into matrix, resulting in a quantitative and qualitative abnormal bone matrix (Seeman and Delmas, 2006). These results of quantitative abnormality of bone matrix were consistent with my finding of quantitative analysis of *Mecp2* stop mice showing reduction of 30% in collagen content and a recent study on bone biochemical markers (Roende et al., 2013a).

Whatever the mutation in OI, there is less bone synthesized (Seeman and Delmas, 2006), a feature that may parallel the bone phenotypes seen in RTT (Budden and Gunness, 2003; O'Connor et al., 2009a). Moreover abnormal collagen fibrils may be unable to provide nucleating and scaffolding sites for mineral propagation. Such mechanism point towards a hypothesis that low mineral density seen in RTT patients could result from a direct alteration in collagen homeosynthesis.

As mentioned earlier, although RTT-like bone phenotypes are frequently linked to an osteoporosis bone picture (Zysman et al., 2006), the biomechanical, structural and histological finding from my study has features consistent with both osteoporosis as well as those of OI bone phenotypes.

A mouse model having well-defined genetic mutations on the COLIA2 gene produces aplpha1 collagen homotrimers and non-functional pro alpha2 chains. These oim/oim mouse modelling human OI, displayed a bone phenotype characterized by spontaneous fractures and limb deformities (Camacho et al., 1999), both of these features are commonly reported in RTT(Guidera et al., 1991a; Roende et al., 2011b). OI, oim/oim mouse model (Camacho et al., 1999) also had displayed mechanical defects (30% decrease in stiffness, 20% decrease in collagen content, reduced trabecular thickness and an unchanged mineral content, but with a decreased mineral crystallinity). Other than mineral crystalline results, all the features of RTT bone phenotype in my *Mecp2* stop mouse study were qualitatively and indeed quantitatively similar (39.5% reduced stiffness, ~30% decrease in trabecular thickness, 25% decrease in collagen content and no difference in bone mineral deficits) suggesting that RTT bone phenotype shares common features with OI bone phenotype and that specific material properties such as mineral crytallinity and collagen content commonly seen in oim mice, could also be indicative and possibly predictive of bone fragility seen in RTT patients. Leonard and colleagues (Leonard et al., 1999a) did mentioned these similarities between OI bone phenotype and RTT bone phenotype but since then not much attention has been given both by human and animal based trials to explore further qualitative and quantitative dysfunction in organic part of extracellular matrix as a possible causes of bone fragility. To investigate the mineral crystalline structure directly, I have already initiated synchrotron X-ray nanomechanical (SAXS) imaging of mineralized fibre composites on *Mecp2* stop

mice humerus. I have performed this research experiment at MAX Lab at Lund University (Sweden). Results and analysis are in the process. *In situ* synchrotron X-ray scattering and diffraction, in combination with micromechanical testing can provide quantitative information on the nanoscale mechanics of bio mineralized composites of bone. In bone carbonated apatite forms a composite fibril with type 1 collagen of diameter ~ 50-200nm, which forms plywood-like lamellae in the bone with widths ~5-10μm that in turn form cylindrical osteons at the scale of ~100-200μm. Due to this well known hierarchical organization the structural and mechanical properties of the mineral/protein composite at small (submicron) scales are crucial to the mechanical function of the entire organ (Reznikov et al., 2014).

6.2 Significance of the study

Given the very limited previous attempts to explore the effects of *Mecp2* on skeletal tissue, my current studies brings significant advance understandings that *Mecp2* has a role in skeletal tissue regulation since inactivation of *Mecp2* resulted in RTT like bone phenotype in stop mouse and reactivation of *Mecp2* resulted in improvement of some of these defects identified in stop mice. My study is the first study to use female stop mice which is a genetically accurate mouse model of RTT, and the results obtained from stop mice bone phenotype analysis will contribute towards the pre clinical trials of gene therapy intervention.

Fractures due to osteoporosis are a major cause of long term dysfunction and even death (Heaney, 2003) in individuals with physical and mental disabilities (Gray et al., 1992; Lingam and Joester, 1994). Lack of soft tissue padding, inappropriate postural reactions, and lack of bone strength as major contributors to fractures and these factors are common among individual with RTT. For these reasons a thorough knowledge of mechanisms by which Mecp2 regulates and participates in bone homeostasis is required. Biomechanical and structural findings from my study will contribute towards the better understanding of these parameters and their link with MeCP2.

My study results along with other recent studies (Roende et al., 2013a) have found a defect most probably linked to bone formative factors (decrease in collagen content and no difference in osteoclast number) rather than bone resorptive

measures. In this scenario, use of pharmacological antiresorptive measures seems less useful by further decreasing the activity of osteoclasts and the osteoblast. In contrast anabolic bone treatment stimulating bone formation may be more relevant, but caution should be taken due to possible medical side effects regarding risk of inducing uncontrolled bone formation in childhood (Tashjian and Goltzman, 2008).

Also my study is the first study to provide initial quantitative analysis of collagen protein in RTT bone phenotype. Majority of the clinical trials in past have been focused to explore the inorganic part of the bone and not much research has been done to explore the organic part of the bone. My study highlights the importance of more insights into the collagen as underlying mechanism for the RTT bone phenotype

And lastly the most important significance of this study is the use of adult male and female rescue mice. Reversal studies (Guy et al., 2007; Robinson et al., 2012a; Gadalla et al., 2013; Garg et al., 2013) in stop mice have shown potential reversibility of RTT-like phenotypes. In this study I have shown the first evidence that RTT bone phenotype can be prevented/ improved by genetic manipulation. These data in rescue mice however at the proof of concept level should have an impact on the future therapeutic approaches not only just for RTT bone phenotype but for better bone health in other related bone pathologies (osteoporosis, osteogenesis imperfecta etc) for which gene based therapies might eventually have therapeutic potential.

6.3 Future studies

The nature of this project has been to explore the consequence of inactivation of *MeCP2* on bone tissue using an animal model of RTT. This represents a logical trajectory in reaching the ultimate goal of exact mechanism by which *MECP2* is linked with the skeletal tissue:

- In my current study I have used a functional knockout mouse model in which Mecp2 is silenced throughout the body including the nervous system. In order to discriminate where the bone phenotypes I have identified result primarily from local intrinsic bone dysfunction or whether central (nervous

system) dysfunction result in secondary bone phenotypes, experiments with different mouse cre lines may be informative. For instance mouse lines have been developed in which *Mecp2* is activated or inactivated only in the nervous system or only in peripheral tissues or other organ systems (Alvarez-Saavedra et al., 2007; Alvarez-Saavedra et al., 2010; Chao et al., 2010; Nguyen et al., 2012). An analysis of bone measures in these models would be highly informative.

- The role of collagen in the pathogenesis of RTT bone phenotype has not been explored yet. Basic validation of altered collagen level by techniques like immunoblotting would strengthen this conclusion whereas a better understanding of collagen (matrix) structure in bone from RTT model using approaches such as Small energy X-Ray (SAXS), a nanomechanical imaging of mineralized fibre composites can provide useful insights about the exact structural changes that might result from MeCP2 insufficiency

- In my current study I have used an adult mouse model, in future, animal studies need to be done to explore the possible effects of *MECP2* on the bone mass formation and later on ossification of bone, using the embryonic and early postnatal murine models. These experiments will give a better understanding of the exact time points over which the deleterious effects of *MeCP2* deficiency start impacting bone health/properties. This will also help in the development of future therapeutic strategies and time point at which they should be implemented.

Based on the findings of this study, the reduced bone size reduced mechanical properties of bone, altered structural parameters and extracellular organic deficits in an adult stop mouse model points towards the fact that MeCP2 has a general role in regulating bone growth. Improved knowledge of how it involved in bone metabolism is important to assist directions for prevention and treatment in order to improve bone health in RTT.

References

Abdala AP, Lioy DT, Garg SK, Knopp SJ, Paton JF, Bissonnette JM (2013) Effect of Sarizotan, a 5-HT1a and D2-Like Receptor Agonist, on Respiration in Three Mouse Models of Rett Syndrome. Am J Respir Cell Mol Biol.

Adachi M, Keefer EW, Jones FS (2005) A segment of the Mecp2 promoter is sufficient to drive expression in neurons. Hum Mol Genet 14:3709-3722.

Adams VH, McBryant SJ, Wade PA, Woodcock CL, Hansen JC (2007) Intrinsic disorder and autonomous domain function in the multifunctional nuclear protein, MeCP2. J Biol Chem 282:15057-15064.

Ager S, Fyfe S, Christodoulou J, Jacoby P, Schmitt L, Leonard H (2006) Predictors of scoliosis in Rett syndrome. J Child Neurol 21:809-813.

Akhter MP, Fan Z, Rho JY (2004a) Bone intrinsic material properties in three inbred mouse strains. Calcif Tissue Int 75:416-420.

Akhter MP, Wells DJ, Short SJ, Cullen DM, Johnson ML, Haynatzki GR, Babij P, Allen KM, Yaworsky PJ, Bex F, Recker RR (2004b) Bone biomechanical properties in LRP5 mutant mice. Bone 35:162-169.

Alatalo SL, Halleen JM, Hentunen TA, Mönkkönen J, Väänänen HK (2000) Rapid screening method for osteoclast differentiation in vitro that measures tartrate-resistant acid phosphatase 5b activity secreted into the culture medium. Clin Chem 46:1751-1754.

Allanson JE, Hennekam RC, Moog U, Smeets EE (2011) Rett syndrome: a study of the face. Am J Med Genet A 155A:1563-1567.

Allison SJ, Baldock PA, Herzog H (2007) The control of bone remodeling by neuropeptide Y receptors. Peptides 28:320-325.

Alvarez-Saavedra M, Sáez MA, Kang D, Zoghbi HY, Young JI (2007) Cell-specific expression of wild-type MeCP2 in mouse models of Rett syndrome yields insight about pathogenesis. Hum Mol Genet 16:2315-2325.

Alvarez-Saavedra M, Carrasco L, Sura-Trueba S, Demarchi Aiello V, Walz K, Neto JX, Young JI (2010) Elevated expression of MeCP2 in cardiac and skeletal tissues is detrimental for normal development. Hum Mol Genet 19:2177-2190.

Amir RE, Van den Veyver IB, Wan M, Tran CQ, Francke U, Zoghbi HY (1999) Rett syndrome is caused by mutations in X-linked MECP2, encoding methyl-CpG-binding protein 2. Nat Genet 23:185-188.

Amir RE, Van den Veyver IB, Schultz R, Malicki DM, Tran CQ, Dahle EJ, Philippi A, Timar L, Percy AK, Motil KJ, Lichtarge O, Smith EO, Glaze DG, Zoghbi

HY (2000) Influence of mutation type and X chromosome inactivation on Rett syndrome phenotypes. Ann Neurol 47:670-679.

Anderson A, Wong K, Jacoby P, Downs J, Leonard H (2014) Twenty years of surveillance in Rett syndrome: what does this tell us? Orphanet J Rare Dis 9:87.

Armstrong DD, Dunn JK, Schultz RJ, Herbert DA, Glaze DG, Motil KJ (1999) Organ growth in Rett syndrome: a postmortem examination analysis. Pediatr Neurol 20:125-129.

Aronson E, Stevenson SB (2012) Bone health in children with cerebral palsy and epilepsy. J Pediatr Health Care 26:193-199.

Baldock PA, Sainsbury A, Couzens M, Enriquez RF, Thomas GP, Gardiner EM, Herzog H (2002) Hypothalamic Y2 receptors regulate bone formation. J Clin Invest 109:915-921.

Balemans W et al. (2001) Increased bone density in sclerosteosis is due to the deficiency of a novel secreted protein (SOST). Hum Mol Genet 10:537-543.

Ballanti P, Minisola S, Pacitti MT, Scarnecchia L, Rosso R, Mazzuoli GF, Bonucci E (1997) Tartrate-resistant acid phosphate activity as osteoclastic marker: sensitivity of cytochemical assessment and serum assay in comparison with standardized osteoclast histomorphometry. Osteoporos Int 7:39-43.

Ballas N, Lioy DT, Grunseich C, Mandel G (2009) Non-cell autonomous influence of MeCP2-deficient glia on neuronal dendritic morphology. Nat Neurosci 12:311-317.

Baron R, Neff L, Tran Van P, Nefussi JR, Vignery A (1986) Kinetic and cytochemical identification of osteoclast precursors and their differentiation into multinucleated osteoclasts. Am J Pathol 122:363-378.

Bassett GS, Tolo VT (1990) The incidence and natural history of scoliosis in Rett syndrome. Dev Med Child Neurol 32:963-966.

Bebbington A, Downs J, Percy A, Pineda M, Zeev BB, Bahi-Buisson N, Leonard H (2012) The phenotype associated with a large deletion on MECP2. Eur J Hum Genet.

Bebbington A, Anderson A, Ravine D, Fyfe S, Pineda M, de Klerk N, Ben-Zeev B, Yatawara N, Percy A, Kaufmann WE, Leonard H (2008) Investigating genotype-phenotype relationships in Rett syndrome using an international data set. Neurology 70:868-875.

Ben-Ari Y, Spitzer NC (2010) Phenotypic checkpoints regulate neuronal development. Trends Neurosci 33:485-492.

Ben-Shachar S, Chahrour M, Thaller C, Shaw CA, Zoghbi HY (2009) Mouse models of MeCP2 disorders share gene expression changes in the cerebellum and hypothalamus. Hum Mol Genet 18:2431-2442.

Berg M, Hagberg B (2001) Rett syndrome: update of a 25 year follow-up investigation in Western Sweden--sociomedical aspects. Brain Dev 23 Suppl 1:S224-226.

Bienvenu T, Chelly J (2006) Molecular genetics of Rett syndrome: when DNA methylation goes unrecognized. Nat Rev Genet 7:415-426.

Bienvenu T, Carrie A, de Roux N, Vinet MC, Jonveaux P, Couvert P, Villard L, Arzimanoglou A, Beldjord C, Fontes M, Tardieu M, Chelly J (2000) MECP2 mutations account for most cases of typical forms of Rett syndrome. Hum Mol Genet 9:1377-1384.

Bird A (2002) DNA methylation patterns and epigenetic memory. Genes Dev 16:6-21.

Blömer U, Naldini L, Verma IM, Trono D, Gage FH (1996) Applications of gene therapy to the CNS. Hum Mol Genet 5 Spec No:1397-1404.

Boivin G, Meunier PJ (2002) The degree of mineralization of bone tissue measured by computerized quantitative contact microradiography. Calcif Tissue Int 70:503-511.

Bonnet N, Laroche N, Vico L, Dolleans E, Courteix D, Benhamou CL (2009) Assessment of trabecular bone microarchitecture by two different x-ray microcomputed tomographs: a comparative study of the rat distal tibia using Skyscan and Scanco devices. Med Phys 36:1286-1297.

Boskey A (2003) Mineral changes in osteopetrosis. Crit Rev Eukaryot Gene Expr 13:109-116.

Bourrin S, Palle S, Genty C, Alexandre C (1995) Physical exercise during remobilization restores a normal bone trabecular network after tail suspension-induced osteopenia in young rats. J Bone Miner Res 10:820-828.

Boyce BF, Hughes DE, Wright KR, Xing L, Dai A (1999) Recent advances in bone biology provide insight into the pathogenesis of bone diseases. Lab Invest 79:83-94.

Braunschweig D, Simcox T, Samaco RC, LaSalle JM (2004) X-Chromosome inactivation ratios affect wild-type MeCP2 expression within mosaic Rett syndrome and Mecp2-/+ mouse brain. Hum Mol Genet 13:1275-1286.

Brodt MD, Ellis CB, Silva MJ (1999) Growing C57Bl/6 mice increase whole bone mechanical properties by increasing geometric and material properties. J Bone Miner Res 14:2159-2166.

Brown JP, Delmas PD, Arlot M, Meunier PJ (1987) Active bone turnover of the cortico-endosteal envelope in postmenopausal osteoporosis. J Clin Endocrinol Metab 64:954-959.

Brunner R, Gebhard F (2002) [Neurogenic spinal deformities. I. Conservative and surgical treatment of spinal deformities]. Orthopade 31:51-57.

Bucaro MA, Fertala J, Adams CS, Steinbeck M, Ayyaswamy P, Mukundakrishnan K, Shapiro IM, Risbud MV (2004) Bone cell survival in microgravity: evidence that modeled microgravity increases osteoblast sensitivity to apoptogens. Ann N Y Acad Sci 1027:64-73.

Bucay N, Sarosi I, Dunstan CR, Morony S, Tarpley J, Capparelli C, Scully S, Tan HL, Xu W, Lacey DL, Boyle WJ, Simonet WS (1998) osteoprotegerin-deficient mice develop early onset osteoporosis and arterial calcification. Genes Dev 12:1260-1268.

Buckwalter JA, Glimcher, M.J, Cooper,R.R and Recker,R. (1995) Bone biology. *JBone Joint SurgAm* 8:1276-1289.

Budden SS (1995) Management of Rett syndrome: a ten year experience. Neuropediatrics 26:75-77.

Budden SS, Gunness ME (2001) Bone histomorphometry in three females with Rett syndrome. Brain Dev 23 Suppl 1:S133-137.

Budden SS, Gunness ME (2003) Possible mechanisms of osteopenia in Rett syndrome: bone histomorphometric studies. J Child Neurol 18:698-702.

Burger EH, Klein-Nulend J (1999) Mechanotransduction in bone--role of the lacuno-canalicular network. FASEB J 13 Suppl:S101-112.

Burr DB (2002) Targeted and nontargeted remodeling. Bone 30:2-4.

Calfa G, Percy AK, Pozzo-Miller L (2011) Experimental models of Rett syndrome based on Mecp2 dysfunction. Exp Biol Med (Maywood) 236:3-19.

Camacho NP, Hou L, Toledano TR, Ilg WA, Brayton CF, Raggio CL, Root L, Boskey AL (1999) The material basis for reduced mechanical properties in oim mice bones. J Bone Miner Res 14:264-272.

Campos-Castelló J, Peral Guerra M, Riviere Gómez A, Oliete García F, Herranz Tanarro J, Toledano Barrero M, Espinar Sierra J, Cristobal Sassot S, Lautre Ecenarro MJ, Franco Carcedo C (1988) [Rett's syndrome: study of 15 cases]. An Esp Pediatr 28:286-292.

Caplan AI (1991) Mesenchymal stem cells. J Orthop Res 9:641-650.

Carter DR, Spengler DM (1978) Mechanical properties and composition of cortical bone. Clin Orthop Relat Res:192-217.

Carter DR, Bouxsein ML, Marcus R (1992) New approaches for interpreting projected bone densitometry data. J Bone Miner Res 7:137-145.

Cass H, Reilly S, Owen L, Wisbeach A, Weekes L, Slonims V, Wigram T, Charman T (2003) Findings from a multidisciplinary clinical case series of females with Rett syndrome. Dev Med Child Neurol 45:325-337.

Cepollaro C, Gonnelli S, Bruni D, Pacini S, Martini S, Franci MB, Gennari L, Rossi S, Hayek G, Zappella M, Gennari C (2001) Dual X-ray absorptiometry and

bone ultrasonography in patients with Rett syndrome. Calcif Tissue Int 69:259-262.

Chadwick LH, Wade PA (2007) MeCP2 in Rett syndrome: transcriptional repressor or chromatin architectural protein? Curr Opin Genet Dev 17:121-125.

Chahrour M, Zoghbi HY (2007) The story of Rett syndrome: from clinic to neurobiology. Neuron 56:422-437.

Chahrour M, Jung SY, Shaw C, Zhou X, Wong ST, Qin J, Zoghbi HY (2008) MeCP2, a key contributor to neurological disease, activates and represses transcription. Science 320:1224-1229.

Chambers TJ (1982) Osteoblasts release osteoclasts from calcitonin-induced quiescence. J Cell Sci 57:247-260.

Chambers TJ, Athanasou NA, Fuller K (1984) Effect of parathyroid hormone and calcitonin on the cytoplasmic spreading of isolated osteoclasts. J Endocrinol 102:281-286.

Chao HT, Chen H, Samaco RC, Xue M, Chahrour M, Yoo J, Neul JL, Gong S, Lu HC, Heintz N, Ekker M, Rubenstein JL, Noebels JL, Rosenmund C, Zoghbi HY (2010) Dysfunction in GABA signalling mediates autism-like stereotypies and Rett syndrome phenotypes. Nature 468:263-269.

Chavassieux P, Seeman E, Delmas PD (2007) Insights into material and structural basis of bone fragility from diseases associated with fractures: how determinants of the biomechanical properties of bone are compromised by disease. Endocr Rev 28:151-164.

Cheadle JP, Gill H, Fleming N, Maynard J, Kerr A, Leonard H, Krawczak M, Cooper DN, Lynch S, Thomas N, Hughes H, Hulten M, Ravine D, Sampson JR, Clarke A (2000) Long-read sequence analysis of the MECP2 gene in Rett syndrome patients: correlation of disease severity with mutation type and location. Hum Mol Genet 9:1119-1129.

Chen CL, Ke JY, Wang CJ, Wu KP, Wu CY, Wong AM (2011) Factors associated with bone density in different skeletal regions in children with cerebral palsy of various motor severities. Dev Med Child Neurol 53:131-136.

Chen RZ, Akbarian S, Tudor M, Jaenisch R (2001) Deficiency of methyl-CpG binding protein-2 in CNS neurons results in a Rett-like phenotype in mice. Nat Genet 27:327-331.

Chen WG, Chang Q, Lin Y, Meissner A, West AE, Griffith EC, Jaenisch R, Greenberg ME (2003) Derepression of BDNF transcription involves calcium-dependent phosphorylation of MeCP2. Science 302:885-889.

Chenu C, Colucci S, Grano M, Zigrino P, Barattolo R, Zambonin G, Baldini N, Vergnaud P, Delmas PD, Zallone AZ (1994) Osteocalcin induces chemotaxis, secretion of matrix proteins, and calcium-mediated intracellular signaling in human osteoclast-like cells. J Cell Biol 127:1149-1158.

Cherian PP, Siller-Jackson AJ, Gu S, Wang X, Bonewald LF, Sprague E, Jiang JX (2005) Mechanical strain opens connexin 43 hemichannels in osteocytes: a novel mechanism for the release of prostaglandin. Mol Biol Cell 16:3100-3106.

Choi K, Goldstein SA (1992) A comparison of the fatigue behavior of human trabecular and cortical bone tissue. J Biomech 25:1371-1381.

Cody DD, Goldstein SA, Flynn MJ, Brown EB (1991) Correlations between vertebral regional bone mineral density (rBMD) and whole bone fracture load. Spine (Phila Pa 1976) 16:146-154.

Colvin L, Leonard H, de Klerk N, Davis M, Weaving L, Williamson S, Christodoulou J (2004) Refining the phenotype of common mutations in Rett syndrome. J Med Genet 41:25-30.

Cooley HM, Jones G (2002) Symptomatic fracture incidence in southern Tasmania: does living in the country reduce your fracture risk? Osteoporos Int 13:317-322.

Cooper C, Dennison EM, Leufkens HG, Bishop N, van Staa TP (2004) Epidemiology of childhood fractures in Britain: a study using the general practice research database. J Bone Miner Res 19:1976-1981.

Cowin SC, Weinbaum S, Zeng Y (1995) A case for bone canaliculi as the anatomical site of strain generated potentials. J Biomech 28:1281-1297.

Cummings SR, Bates D, Black DM (2002) Clinical use of bone densitometry: scientific review. JAMA 288:1889-1897.

Currey J (2004) Incompatible mechanical properties in compact bone. J Theor Biol 231:569-580.

Currey JD (1979) Changes in the impact energy absorption of bone with age. J Biomech 12:459-469.

D'Esposito M, Quaderi NA, Ciccodicola A, Bruni P, Esposito T, D'Urso M, Brown SD (1996) Isolation, physical mapping, and northern analysis of the X-linked human gene encoding methyl CpG-binding protein, MECP2. Mamm Genome 7:533-535.

Dalgleish R (1997) The human type I collagen mutation database. Nucleic Acids Res 25:181-187.

Dallas SL, Zaman G, Pead MJ, Lanyon LE (1993) Early strain-related changes in cultured embryonic chick tibiotarsi parallel those associated with adaptive modeling in vivo. J Bone Miner Res 8:251-259.

Dall'Ara E, Öhman C, Baleani M, Viceconti M (2007) The effect of tissue condition and applied load on Vickers hardness of human trabecular bone. Journal of Biomechanics 40:3267-3270.

DeFranco DJ, Glowacki J, Cox KA, Lian JB (1991) Normal bone particles are preferentially resorbed in the presence of osteocalcin-deficient bone particles in vivo. Calcif Tissue Int 49:43-50.

Della Ragione F, Filosa S, Scalabrì F, D'Esposito M (2012) MeCP2 as a genome-wide modulator: the renewal of an old story. Front Genet 3:181.

Demiralp B, Chen HL, Koh AJ, Keller ET, McCauley LK (2002) Anabolic actions of parathyroid hormone during bone growth are dependent on c-fos. Endocrinology 143:4038-4047.

Derecki CJ, Lu Z, Xu E, Abbott SB, Guyenet PG, Kipnis J (2012) Wild-type microglia arrest pathology in a mouse model of Rett syndrome. Nature 484:105-109.

Derecki NC CJ, Lu Z, Xu E, Abbott SB, Guyenet PG, Kipnis J (2012) Wild-type microglia arrest pathology in a mouse model of Rett syndrome. Nature 484:105-109.

Di Masso RJ, Celoria GC, Font MT (1998) Morphometric skeletal traits, femoral measurements, and bone mineral deposition in mice with agonistic selection for body conformation. Bone 22:539-543.

Di Masso RJ, Silva PS, Font MT (2004) Muscle-bone relationships in mice selected for different body conformations. J Musculoskelet Neuronal Interact 4:41-47.

Dietrich P, Dragatsis I, Xuan S, Zeitlin S, Efstratiadis A (2000) Conditional mutagenesis in mice with heat shock promoter-driven cre transgenes. Mamm Genome 11:196-205.

Dogba MJ, Bedos C, Durigova M, Montpetit K, Wong T, Glorieux FH, Rauch F (2013) The impact of severe osteogenesis imperfecta on the lives of young patients and their parents - a qualitative analysis. BMC pediatrics 13:153.

Dolen G, Osterweil E, Rao BS, Smith GB, Auerbach BD, Chattarji S, Bear MF (2007) Correction of fragile X syndrome in mice. Neuron 56:955-962.

Downs J, Young D, de Klerk N, Bebbington A, Baikie G, Leonard H (2009) Impact of scoliosis surgery on activities of daily living in females with Rett syndrome. J Pediatr Orthop 29:369-374.

Downs J, Bebbington A, Woodhead H, Jacoby P, Jian L, Jefferson A, Leonard H (2008a) Early determinants of fractures in Rett syndrome. Pediatrics 121:540-546.

Downs JA, Bebbington A, Jacoby P, Msall ME, McIlroy O, Fyfe S, Bahi-Buisson N, Kaufmann WE, Leonard H (2008b) Gross motor profile in rett syndrome as determined by video analysis. Neuropediatrics 39:205-210.

Dragatsis I, Zeitlin S (2001) A method for the generation of conditional gene repair mutations in mice. Nucleic Acids Res 29:E10.

Duncan RL, Turner CH (1995) Mechanotransduction and the functional response of bone to mechanical strain. Calcif Tissue Int 57:344-358.

Egan JM (1987) A constitutive model for the mechanical behaviour of soft connective tissues. J Biomech 20:681-692.

Ehninger D LW, Fox K, Stryker MP, Silva AJ (2008) Reversing nerodevelopmental disorders in adults. Neuron 60:950-960.

Ek-Rylander B, Flores M, Wendel M, Heinegård D, Andersson G (1994) Dephosphorylation of osteopontin and bone sialoprotein by osteoclastic tartrate-resistant acid phosphatase. Modulation of osteoclast adhesion in vitro. J Biol Chem 269:14853-14856.

El Haj AJ, Minter SL, Rawlinson SC, Suswillo R, Lanyon LE (1990) Cellular responses to mechanical loading in vitro. J Bone Miner Res 5:923-932.

Elefteriou F (2008) Regulation of bone remodeling by the central and peripheral nervous system. Arch Biochem Biophys 473:231-236.

Elefteriou F, Campbell P, Ma Y (2014) Control of bone remodeling by the peripheral sympathetic nervous system. Calcif Tissue Int 94:140-151.

Engerström IW (1992) Rett syndrome: the late infantile regression period--a retrospective analysis of 91 cases. Acta Paediatr 81:167-172.

Fawell SE, Lees JA, White R, Parker MG (1990) Characterization and colocalization of steroid binding and dimerization activities in the mouse estrogen receptor. Cell 60:953-962.

Feng JQ, Ward LM, Liu S, Lu Y, Xie Y, Yuan B, Yu X, Rauch F, Davis SI, Zhang S, Rios H, Drezner MK, Quarles LD, Bonewald LF, White KE (2006) Loss of DMP1 causes rickets and osteomalacia and identifies a role for osteocytes in mineral metabolism. Nat Genet 38:1310-1315.

Fernandez F, Morishita W, Zuniga E, Nguyen J, Blank M, Malenka RC, Garner CC (2007) Pharmacotherapy for cognitive impairment in a mouse model of Down syndrome. Nat Neurosci 10:411-413.

Flynn J, Foley S, Jones G (2007) Can BMD assessed by DXA at age 8 predict fracture risk in boys and girls during puberty?: an eight-year prospective study. J Bone Miner Res 22:1463-1467.

Foldes J, Parfitt AM, Shih MS, Rao DS, Kleerekoper M (1991) Structural and geometric changes in iliac bone: relationship to normal aging and osteoporosis. J Bone Miner Res 6:759-766.

Franz-Odendaal TA, Hall BK, Witten PE (2006) Buried alive: how osteoblasts become osteocytes. Dev Dyn 235:176-190.

Fratzl P (2007) Biomimetic materials research: what can we really learn from nature's structural materials? J R Soc Interface 4:637-642.

Friez MJ, Jones JR, Clarkson K, Lubs H, Abuelo D, Bier JA, Pai S, Simensen R, Williams C, Giampietro PF, Schwartz CE, Stevenson RE (2006) Recurrent infections, hypotonia, and mental retardation caused by duplication of MECP2 and adjacent region in Xq28. Pediatrics 118:e1687-1695.

Frost HM (1969) Tetracycline-based histological analysis of bone remodeling. Calcif Tissue Res 3:211-237.

Fujiki K, Aoki K, Marcián P, Borák L, Hudieb M, Ohya K, Igarashi Y, Wakabayashi N (2013) The influence of mechanical stimulation on osteoclast localization in the mouse maxilla: bone histomorphometry and finite element analysis. Biomech Model Mechanobiol 12:325-333.

Fuks F, Hurd PJ, Wolf D, Nan X, Bird AP, Kouzarides T (2003) The methyl-CpG-binding protein MeCP2 links DNA methylation to histone methylation. J Biol Chem 278:4035-4040.

Fuller K, Owens JM, Jagger CJ, Wilson A, Moss R, Chambers TJ (1993) Macrophage colony-stimulating factor stimulates survival and chemotactic behavior in isolated osteoclasts. J Exp Med 178:1733-1744.

Gabos PG, Inan M, Thacker M, Borkhu B (2012) Spinal fusion for scoliosis in Rett syndrome with an emphasis on early postoperative complications. Spine (Phila Pa 1976) 37:E90-94.

Gadalla KK, Bailey ME, Cobb SR (2011) MeCP2 and Rett syndrome: reversibility and potential avenues for therapy. Biochem J 439:1-14.

Gadalla KK, Bailey ME, Spike RC, Ross PD, Woodard KT, Kalburgi SN, Bachaboina L, Deng JV, West AE, Samulski RJ, Gray SJ, Cobb SR (2013) Improved survival and reduced phenotypic severity following AAV9/MECP2 gene transfer to neonatal and juvenile male Mecp2 knockout mice. Mol Ther 21:18-30.

Garg SK, Lioy DT, Cheval H, McGann JC, Bissonnette JM, Murtha MJ, Foust KD, Kaspar BK, Bird A, Mandel G (2013) Systemic delivery of MeCP2 rescues behavioral and cellular deficits in female mouse models of Rett syndrome. J Neurosci 33:13612-13620.

Gemelli T, Berton O, Nelson ED, Perrotti LI, Jaenisch R, Monteggia LM (2006) Postnatal loss of methyl-CpG binding protein 2 in the forebrain is sufficient to mediate behavioral aspects of Rett syndrome in mice. Biol Psychiatry 59:468-476.

Gerstenfeld LC, Chipman SD, Glowacki J, Lian JB (1987) Expression of differentiated function by mineralizing cultures of chicken osteoblasts. Dev Biol 122:49-60.

Giacometti E, Luikenhuis S, Beard C, Jaenisch R (2007) Partial rescue of MeCP2 deficiency by postnatal activation of MeCP2. Proc Natl Acad Sci U S A 104:1931-1936.

Gibson JH, Williamson SL, Arbuckle S, Christodoulou J (2005) X chromosome inactivation patterns in brain in Rett syndrome: implications for the disease phenotype. Brain Dev 27:266-270.

Girard M, Couvert P, Carrié A, Tardieu M, Chelly J, Beldjord C, Bienvenu T (2001) Parental origin of de novo MECP2 mutations in Rett syndrome. Eur J Hum Genet 9:231-236.

Giraud-Guille MM (1988) Twisted plywood architecture of collagen fibrils in human compact bone osteons. Calcif Tissue Int 42:167-180.

Glasson EJ, Bower C, Thomson MR, Fyfe S, Leonard S, Rousham E, Christodoulou J, Ellaway C, Leonard H (1998) Diagnosis of Rett syndrome: can a radiograph help? Dev Med Child Neurol 40:737-742.

Glaze DG, Frost JD, Zoghbi HY, Percy AK (1987) Rett's syndrome. Correlation of electroencephalographic characteristics with clinical staging. Arch Neurol 44:1053-1056.

Goffin D, Allen M, Zhang L, Amorim M, Wang IT, Reyes AR, Mercado-Berton A, Ong C, Cohen S, Hu L, Blendy JA, Carlson GC, Siegel SJ, Greenberg ME, Zhou Z (2012) Rett syndrome mutation MeCP2 T158A disrupts DNA binding, protein stability and ERP responses. Nat Neurosci 15:274-283.

Goll MG, Bestor TH (2005) Eukaryotic cytosine methyltransferases. Annu Rev Biochem 74:481-514.

Gonnelli S, Caffarelli C, Hayek J, Montagnani A, Cadirni A, Franci B, Lucani B, Rossi S, Nuti R (2008) Bone ultrasonography at phalanxes in patients with Rett syndrome: a 3-year longitudinal study. Bone 42:737-742.

Goodman ZD, Becker RL, Pockros PJ, Afdhal NH (2007) Progression of fibrosis in advanced chronic hepatitis C: evaluation by morphometric image analysis. Hepatology 45:886-894.

Gowen LC, Petersen DN, Mansolf AL, Qi H, Stock JL, Tkalcevic GT, Simmons HA, Crawford DT, Chidsey-Frink KL, Ke HZ, McNeish JD, Brown TA (2003) Targeted disruption of the osteoblast/osteocyte factor 45 gene (OF45) results in increased bone formation and bone mass. J Biol Chem 278:1998-2007.

Grano M, Colucci S, Cantatore FP, Teti A, Zambonin Zallone A (1990) Osteoclast bone resorption is enhanced in the presence of osteoblasts. Boll Soc Ital Biol Sper 66:1051-1057.

Gray B, Hsu JD, Furumasu J (1992) Fractures caused by falling from a wheelchair in patients with neuromuscular disease. Dev Med Child Neurol 34:589-592.

Guidera KJ, Borrelli J, Raney E, Thompson-Rangel T, Ogden JA (1991a) Orthopaedic manifestations of Rett syndrome. J Pediatr Orthop 11:204-208.

Guidera KJ, Borrelli J, Raney E, Thompson-Rangel T, Ogden JA (1991b) Orthopaedic manifestations of Rett syndrome. J Pediatr Orthop 11:204-208.

Guy J, Cheval H, Selfridge J, Bird A (2011a) The role of MeCP2 in the brain. Annu Rev Cell Dev Biol 27:631-652.

Guy J, Cheval H, Selfridge J, Bird A (2011b) The role of MeCP2 in the brain. Annu Rev Cell Dev Biol 27:631-652.

Guy J, Hendrich B, Holmes M, Martin JE, Bird A (2001) A mouse Mecp2-null mutation causes neurological symptoms that mimic Rett syndrome. Nat Genet 27:322-326.

Guy J, Gan J, Selfridge J, Cobb S, Bird A (2007) Reversal of neurological defects in a mouse model of Rett syndrome. Science 315:1143-1147.

Haas RH, Dixon SD, Sartoris DJ, Hennessy MJ (1997) Osteopenia in Rett syndrome. J Pediatr 131:771-774.

Hadjidakis DJ, Androulakis II (2006) Bone remodeling. Ann N Y Acad Sci 1092:385-396.

Hagberg B (2002) Clinical manifestations and stages of Rett syndrome. Ment Retard Dev Disabil Res Rev 8:61-65.

Hagberg B, Aicardi J, Dias K, Ramos O (1983) A progressive syndrome of autism, dementia, ataxia, and loss of purposeful hand use in girls: Rett's syndrome: report of 35 cases. Ann Neurol 14:471-479.

Hagberg B, Hanefeld F, Percy A, Skjeldal O (2002) An update on clinically applicable diagnostic criteria in Rett syndrome. Comments to Rett Syndrome Clinical Criteria Consensus Panel Satellite to European Paediatric Neurology Society Meeting, Baden Baden, Germany, 11 September 2001. Eur J Paediatr Neurol 6:293-297.

Han Y, Cowin SC, Schaffler MB, Weinbaum S (2004) Mechanotransduction and strain amplification in osteocyte cell processes. Proc Natl Acad Sci U S A 101:16689-16694.

Harrison DJ, Webb PJ (1990) Scoliosis in the Rett syndrome: natural history and treatment. Brain Dev 12:154-156.

Hauschka PV, Lian JB, Cole DE, Gundberg CM (1989) Osteocalcin and matrix Gla protein: vitamin K-dependent proteins in bone. Physiol Rev 69:990-1047.

Hayashi S, McMahon AP (2002) Efficient recombination in diverse tissues by a tamoxifen-inducible form of Cre: a tool for temporally regulated gene activation/inactivation in the mouse. Dev Biol 244:305-318.

Hayman AR, Bune AJ, Bradley JR, Rashbass J, Cox TM (2000) Osteoclastic tartrate-resistant acid phosphatase (Acp 5): its localization to dendritic cells and diverse murine tissues. J Histochem Cytochem 48:219-228.

Hayman AR, Jones SJ, Boyde A, Foster D, Colledge WH, Carlton MB, Evans MJ, Cox TM (1996) Mice lacking tartrate-resistant acid phosphatase (Acp 5)

have disrupted endochondral ossification and mild osteopetrosis. Development 122:3151-3162.

Heaney RP (2003) Advances in therapy for osteoporosis. Clin Med Res 1:93-99.

Henderson RC (1997) Bone density and other possible predictors of fracture risk in children and adolescents with spastic quadriplegia. Dev Med Child Neurol 39:224-227.

Henderson RC, Lin PP, Greene WB (1995) Bone-mineral density in children and adolescents who have spastic cerebral palsy. J Bone Joint Surg Am 77:1671-1681.

Henderson RC, Lark RK, Gurka MJ, Worley G, Fung EB, Conaway M, Stallings VA, Stevenson RD (2002) Bone density and metabolism in children and adolescents with moderate to severe cerebral palsy. Pediatrics 110:e5.

Hendrich B, Bird A (1998) Identification and characterization of a family of mammalian methyl-CpG binding proteins. Mol Cell Biol 18:6538-6547.

Henry YM, Eastell R (2000) Ethnic and gender differences in bone mineral density and bone turnover in young adults: effect of bone size. Osteoporos Int 11:512-517.

Hessle L, Stordalen GA, Wenglén C, Petzold C, Tanner EK, Brorson SH, Baekkevold ES, Önnerfjord P, Reinholt FP, Heinegård D (2013) The skeletal phenotype of chondroadherin deficient mice. PLoS One 8:e63080.

Hildebrand T, Rüegsegger P (1997) Quantification of Bone Microarchitecture with the Structure Model Index. Comput Methods Biomech Biomed Engin 1:15-23.

Ho KL, McNae IW, Schmiedeberg L, Klose RJ, Bird AP, Walkinshaw MD (2008) MeCP2 binding to DNA depends upon hydration at methyl-CpG. Mol Cell 29:525-531.

Hofbauer LC, Khosla S, Dunstan CR, Lacey DL, Spelsberg TC, Riggs BL (1999) Estrogen stimulates gene expression and protein production of osteoprotegerin in human osteoblastic cells. Endocrinology 140:4367-4370.

Hofstaetter JG, Roetzer KM, Krepler P, Nawrot-Wawrzyniak K, Schwarzbraun T, Klaushofer K, Roschger P (2010) Altered bone matrix mineralization in a patient with Rett syndrome. Bone 47:701-705.

Holm VA, King HA (1990) Scoliosis in the Rett syndrome. Brain Dev 12:151-153.

Horowitz MC, Xi Y, Wilson K, Kacena MA (2001) Control of osteoclastogenesis and bone resorption by members of the TNF family of receptors and ligands. Cytokine Growth Factor Rev 12:9-18.

Hoshi K, Komori T, Ozawa H (1999) Morphological characterization of skeletal cells in Cbfa1-deficient mice. Bone 25:639-651.

Huang TJ, Lubicky JP, Hammerberg KW (1994) Scoliosis in Rett syndrome. Orthop Rev 23:931-937.

Huang Y, de Boer WB, Adams LA, MacQuillan G, Rossi E, Rigby P, Raftopoulos SC, Bulsara M, Jeffrey GP (2013) Image analysis of liver collagen using sirius red is more accurate and correlates better with serum fibrosis markers than trichrome. Liver Int 33:1249-1256.

Hughes-Fulford M (2004) Signal transduction and mechanical stress. Sci STKE 2004:RE12.

Hui AY, Liew CT, Go MY, Chim AM, Chan HL, Leung NW, Sung JJ (2004) Quantitative assessment of fibrosis in liver biopsies from patients with chronic hepatitis B. Liver Int 24:611-618.

Hui SL, Slemenda CW, Johnston CC (1988) Age and bone mass as predictors of fracture in a prospective study. J Clin Invest 81:1804-1809.

Huppke P, Held M, Laccone F, Hanefeld F (2003) The spectrum of phenotypes in females with Rett Syndrome. Brain Dev 25:346-351.

Huppke P, Roth C, Christen HJ, Brockmann K, Hanefeld F (2001) Endocrinological study on growth retardation in Rett syndrome. Acta Paediatr 90:1257-1261.

Ishida Y, Heersche JN (1998) Glucocorticoid-induced osteoporosis: both in vivo and in vitro concentrations of glucocorticoids higher than physiological levels attenuate osteoblast differentiation. J Bone Miner Res 13:1822-1826.

Ishii T, Makita Y, Ogawa A, Amamiya S, Yamamoto M, Miyamoto A, Oki J (2001) The role of different X-inactivation pattern on the variable clinical phenotype with Rett syndrome. Brain Dev 23 Suppl 1:S161-164.

Ito M (2005) Assessment of bone quality using micro-computed tomography (micro-CT) and synchrotron micro-CT. J Bone Miner Metab 23 Suppl:115-121.

Jackson-Grusby L, Beard C, Possemato R, Tudor M, Fambrough D, Csankovszki G, Dausman J, Lee P, Wilson C, Lander E, Jaenisch R (2001) Loss of genomic methylation causes p53-dependent apoptosis and epigenetic deregulation. Nat Genet 27:31-39.

Jefferson AL, Woodhead HJ, Fyfe S, Briody J, Bebbington A, Strauss BJ, Jacoby P, Leonard H (2011) Bone mineral content and density in Rett syndrome and their contributing factors. Pediatr Res 69:293-298.

Jian L, Nagarajan L, de Klerk N, Ravine D, Bower C, Anderson A, Williamson S, Christodoulou J, Leonard H (2006) Predictors of seizure onset in Rett syndrome. J Pediatr 149:542-547.

Jimi E, Shuto T, Koga T (1995) Macrophage colony-stimulating factor and interleukin-1 alpha maintain the survival of osteoclast-like cells. Endocrinology 136:808-811.

Jimi E, Nakamura I, Amano H, Taguchi Y, Tsurukai T, Tamura M, Takahashi N, Suda T (1996) Osteoclast function is activated by osteoblastic cells through a mechanism involving cell-to-cell contact. Endocrinology 137:2187-2190.

Johansen JS, Williamson MK, Rice JS, Price PA (1992) Identification of proteins secreted by human osteoblastic cells in culture. J Bone Miner Res 7:501-512.

Jones IE, Williams SM, Dow N, Goulding A (2002) How many children remain fracture-free during growth? a longitudinal study of children and adolescents participating in the Dunedin Multidisciplinary Health and Development Study. Osteoporos Int 13:990-995.

Jones PL, Veenstra GJ, Wade PA, Vermaak D, Kass SU, Landsberger N, Strouboulis J, Wolffe AP (1998) Methylated DNA and MeCP2 recruit histone deacetylase to repress transcription. Nat Genet 19:187-191.

Jubb KVF, Peter C. Kennedy, Nigel Palmer (1993) Pathology of domestic animals, 5 Edition. Edinburgh: Elsevier saunders.

Jugloff DG, Vandamme K, Logan R, Visanji NP, Brotchie JM, Eubanks JH (2008) Targeted delivery of an Mecp2 transgene to forebrain neurons improves the behavior of female Mecp2-deficient mice. Hum Mol Genet 17:1386-1396.

Julu PO, Kerr AM, Apartopoulos F, Al-Rawas S, Engerström IW, Engerström L, Jamal GA, Hansen S (2001) Characterisation of breathing and associated central autonomic dysfunction in the Rett disorder. Arch Dis Child 85:29-37.

Junqueira LC, Bignolas G, Brentani RR (1979) Picrosirius staining plus polarization microscopy, a specific method for collagen detection in tissue sections. Histochem J 11:447-455.

Jürimäe J (2010) Interpretation and application of bone turnover markers in children and adolescents. Curr Opin Pediatr 22:494-500.

Kapur S, Baylink DJ, Lau KH (2003) Fluid flow shear stress stimulates human osteoblast proliferation and differentiation through multiple interacting and competing signal transduction pathways. Bone 32:241-251.

Kavukcuoglu NB, Denhardt DT, Guzelsu N, Mann AB (2007) Osteopontin deficiency and aging on nanomechanics of mouse bone. J Biomed Mater Res A 83:136-144.

Keene BE, Knowlton KF, McGilliard ML, Lawrence LA, Nickols-Richardson SM, Wilson JH, Rutledge AM, McDowell LR, Van Amburgh ME (2004) Measures of bone mineral content in mature dairy cows. J Dairy Sci 87:3816-3825.

Keret D, Bassett GS, Bunnell WP, Marks HG (1988) Scoliosis in Rett syndrome. J Pediatr Orthop 8:138-142.

Kerr AM, Webb P, Prescott RJ, Milne Y (2003) Results of surgery for scoliosis in Rett syndrome. J Child Neurol 18:703-708.

Kerr AM, Armstrong DD, Prescott RJ, Doyle D, Kearney DL (1997) Rett syndrome: analysis of deaths in the British survey. Eur Child Adolesc Psychiatry 6 Suppl 1:71-74.

Kiernan JA (2008) Histological and Histochemical Methods. Therory and Practice. Oxfordshire, UK: Scion.

Kim CH, Kang BS, Lee TK, Park WH, Kim JK, Park YG, Kim HM, Lee YC (2002) IL-1beta regulates cellular proliferation, prostaglandin E2 synthesis, plasminogen activator activity, osteocalcin production, and bone resorptive activity of the mouse calvarial bone cells. Immunopharmacol Immunotoxicol 24:395-407.

Kim DG, Hunt CA, Zauel R, Fyhrie DP, Yeni YN (2007) The effect of regional variations of the trabecular bone properties on the compressive strength of human vertebral bodies. Ann Biomed Eng 35:1907-1913.

Kim KY, Hysolli E, Park IH (2011) Neuronal maturation defect in induced pluripotent stem cells from patients with Rett syndrome. Proc Natl Acad Sci U S A 108:14169-14174.

Kimura H, Shiota K (2003) Methyl-CpG-binding protein, MeCP2, is a target molecule for maintenance DNA methyltransferase, Dnmt1. J Biol Chem 278:4806-4812.

Kishi N, Macklis JD (2004) MECP2 is progressively expressed in post-migratory neurons and is involved in neuronal maturation rather than cell fate decisions. Mol Cell Neurosci 27:306-321.

Kitazawa R, Kitazawa S (2007) Methylation status of a single CpG locus 3 bases upstream of TATA-box of receptor activator of nuclear factor-kappaB ligand (RANKL) gene promoter modulates cell- and tissue-specific RANKL expression and osteoclastogenesis. Mol Endocrinol 21:148-158.

Kliment CR, Englert JM, Crum LP, Oury TD (2011) A novel method for accurate collagen and biochemical assessment of pulmonary tissue utilizing one animal. Int J Clin Exp Pathol 4:349-355.

Kobayashi K, Takahashi N, Jimi E, Udagawa N, Takami M, Kotake S, Nakagawa N, Kinosaki M, Yamaguchi K, Shima N, Yasuda H, Morinaga T, Higashio K, Martin TJ, Suda T (2000) Tumor necrosis factor alpha stimulates osteoclast differentiation by a mechanism independent of the ODF/RANKL-RANK interaction. J Exp Med 191:275-286.

Kodama HA, Amagai Y, Koyama H, Kasai S (1982) A new preadipose cell line derived from newborn mouse calvaria can promote the proliferation of pluripotent hemopoietic stem cells in vitro. J Cell Physiol 112:89-95.

Kon T, Cho TJ, Aizawa T, Yamazaki M, Nooh N, Graves D, Gerstenfeld LC, Einhorn TA (2001) Expression of osteoprotegerin, receptor activator of NF-kappaB ligand (osteoprotegerin ligand) and related proinflammatory cytokines during fracture healing. J Bone Miner Res 16:1004-1014.

Kong YY, Yoshida H, Sarosi I, Tan HL, Timms E, Capparelli C, Morony S, Oliveira-dos-Santos AJ, Van G, Itie A, Khoo W, Wakeham A, Dunstan CR, Lacey DL, Mak TW, Boyle WJ, Penninger JM (1999) OPGL is a key regulator of osteoclastogenesis, lymphocyte development and lymph-node organogenesis. Nature 397:315-323.

Koop SE (2011) Scoliosis and Rett syndrome. Dev Med Child Neurol 53:582-583.

Kriaucionis S, Bird A (2003) DNA methylation and Rett syndrome. Hum Mol Genet 12 Spec No 2:R221-227.

Kriewall TJ, McPherson GK, Tsai AC (1981) Bending properties and ash content of fetal cranial bone. J Biomech 14:73-79.

Kuhn JL, Goldstein SA, Feldkamp LA, Goulet RW, Jesion G (1990) Evaluation of a microcomputed tomography system to study trabecular bone structure. J Orthop Res 8:833-842.

Lacey DL et al. (1998) Osteoprotegerin ligand is a cytokine that regulates osteoclast differentiation and activation. Cell 93:165-176.

Lakso M, Sauer B, Mosinger B, Lee EJ, Manning RW, Yu SH, Mulder KL, Westphal H (1992) Targeted oncogene activation by site-specific recombination in transgenic mice. Proc Natl Acad Sci U S A 89:6232-6236.

Lau KH, Kapur S, Kesavan C, Baylink DJ (2006) Up-regulation of the Wnt, estrogen receptor, insulin-like growth factor-I, and bone morphogenetic protein pathways in C57BL/6J osteoblasts as opposed to C3H/HeJ osteoblasts in part contributes to the differential anabolic response to fluid shear. J Biol Chem 281:9576-9588.

Laurvick CL, Msall ME, Silburn S, Bower C, de Klerk N, Leonard H (2006) Physical and mental health of mothers caring for a child with Rett syndrome. Pediatrics 118:e1152-1164.

Lazzarini AL, Levine RA, Ploutz-Snyder RJ, Sanderson SO (2005) Advances in digital quantification technique enhance discrimination between mild and advanced liver fibrosis in chronic hepatitis C. Liver Int 25:1142-1149.

Lean JM, Jagger CJ, Chambers TJ, Chow JW (1995) Increased insulin-like growth factor I mRNA expression in rat osteocytes in response to mechanical stimulation. Am J Physiol 268:E318-327.

Lee MH, Kwon TG, Park HS, Wozney JM, Ryoo HM (2003) BMP-2-induced Osterix expression is mediated by Dlx5 but is independent of Runx2. Biochem Biophys Res Commun 309:689-694.

Lekman A, Witt-Engerström I, Gottfries J, Hagberg BA, Percy AK, Svennerholm L (1989) Rett syndrome: biogenic amines and metabolites in postmortem brain. Pediatr Neurol 5:357-362.

Leonard H, Bower C (1998) Is the girl with Rett syndrome normal at birth? Dev Med Child Neurol 40:115-121.

Leonard H, Thomson M, Bower C, Fyfe S, Constantinou J (1995) Skeletal abnormalities in Rett syndrome: increasing evidence for dysmorphogenetic defects. Am J Med Genet 58:282-285.

Leonard H, Thomson MR, Glasson EJ, Fyfe S, Leonard S, Bower C, Christodoulou J, Ellaway C (1999a) A population-based approach to the investigation of osteopenia in Rett syndrome. Dev Med Child Neurol 41:323-328.

Leonard H, Thomson M, Glasson E, Fyfe S, Leonard S, Ellaway C, Christodoulou J, Bower C (1999b) Metacarpophalangeal pattern profile and bone age in Rett syndrome: further radiological clues to the diagnosis. Am J Med Genet 83:88-95.

Leonard H, Thomson MR, Glasson EJ, Fyfe S, Leonard S, Bower C, Christodoulou J, Ellaway C (1999c) A population-based approach to the investigation of osteopenia in Rett syndrome. Dev Med Child Neurol 41:323-328.

Leonard H, Downs J, Jian L, Bebbington A, Jacoby P, Nagarajan L, Ravine D, Woodhead H (2010) Valproate and risk of fracture in Rett syndrome. Arch Dis Child 95:444-448.

Lewis JD, Meehan RR, Henzel WJ, Maurer-Fogy I, Jeppesen P, Klein F, Bird A (1992) Purification, sequence, and cellular localization of a novel chromosomal protein that binds to methylated DNA. Cell 69:905-914.

Li Y, Wang H, Muffat J, Cheng AW, Orlando DA, Loven J, Kwok SM, Feldman DA, Bateup HS, Gao Q, Hockemeyer D, Mitalipova M, Lewis CA, Vander Heiden MG, Sur M, Young RA, Jaenisch R (2013a) Global transcriptional and translational repression in human-embryonic-stem-cell-derived Rett syndrome neurons. Cell Stem Cell 13:446-458.

Li Y, Wang H, Muffat J, Cheng AW, Orlando DA, Lovén J, Kwok SM, Feldman DA, Bateup HS, Gao Q, Hockemeyer D, Mitalipova M, Lewis CA, Vander Heiden MG, Sur M, Young RA, Jaenisch R (2013b) Global transcriptional and translational repression in human-embryonic-stem-cell-derived Rett syndrome neurons. Cell Stem Cell 13:446-458.

Lian JB, Stein GS (1995) Development of the osteoblast phenotype: molecular mechanisms mediating osteoblast growth and differentiation. Iowa Orthop J 15:118-140.

Lian JB, Stein GS, Stein JL, van Wijnen AJ (1999) Regulated expression of the bone-specific osteocalcin gene by vitamins and hormones. Vitam Horm 55:443-509.

Lidström J, Stokland E, Hagberg B (1994) Scoliosis in Rett syndrome. Clinical and biological aspects. Spine (Phila Pa 1976) 19:1632-1635.

Lillian R, Whittaker P (2005) Collagen and piecrosirius red staining: A polarized light assessment of fibrillar hue and spatial distribution. BrazilJmorpholSci 22:97-1c04.

Lingam S, Joester J (1994) Spontaneous fractures in children and adolescents with cerebral palsy. BMJ 309:265.

Littlewood TD, Hancock DC, Danielian PS, Parker MG, Evan GI (1995) A modified oestrogen receptor ligand-binding domain as an improved switch for the regulation of heterologous proteins. Nucleic Acids Res 23:1686-1690.

Liyanage VR, Zachariah RM, Rastegar M (2013) Decitabine alters the expression of Mecp2 isoforms via dynamic DNA methylation at the Mecp2 regulatory elements in neural stem cells. Mol Autism 4:46.

Loder RT, Lee CL, Richards BS (1989) Orthopedic aspects of Rett syndrome: a multicenter review. J Pediatr Orthop 9:557-562.

Lozupone E, Palumbo C, Favia A, Ferretti M, Palazzini S, Cantatore FP (1996) Intermittent compressive load stimulates osteogenesis and improves osteocyte viability in bones cultured "in vitro". Clin Rheumatol 15:563-572.

Luikenhuis S, Giacometti E, Beard CF, Jaenisch R (2004) Expression of MeCP2 in postmitotic neurons rescues Rett syndrome in mice. Proc Natl Acad Sci U S A 101:6033-6038.

Maezawa I, Jin LW (2010) Rett syndrome microglia damage dendrites and synapses by the elevated release of glutamate. J Neurosci 30:5346-5356.

Majeska RJ, Ryaby JT, Einhorn TA (1994) Direct modulation of osteoblastic activity with estrogen. J Bone Joint Surg Am 76:713-721.

Malkusch W, Rehn B, Bruch J (1995) Advantages of Sirius Red staining for quantitative morphometric collagen measurements in lungs. Experimental lung research 21:67-77.

Malone AM, Anderson CT, Tummala P, Kwon RY, Johnston TR, Stearns T, Jacobs CR (2007) Primary cilia mediate mechanosensing in bone cells by a calcium-independent mechanism. Proc Natl Acad Sci U S A 104:13325-13330.

Maloul A, Rossmeier K, Mikic B, Pogue V, Battaglia T (2006) Geometric and material contributions to whole bone structural behavior in GDF-7-deficient mice. Connect Tissue Res 47:157-162.

Marotti G, Muglia MA, Palumbo C (1994) Structure and function of lamellar bone. Clin Rheumatol 13 Suppl 1:63-68.

Martin R, Mogg AE, Heywood LA, Nitschke L, Burke JF (1989) Aminoglycoside suppression at UAG, UAA and UGA codons in Escherichia coli and human tissue culture cells. Mol Gen Genet 217:411-418.

Martinowich K, Hattori D, Wu H, Fouse S, He F, Hu Y, Fan G, Sun YE (2003) DNA methylation-related chromatin remodeling in activity-dependent BDNF gene regulation. Science 302:890-893.

Martín-Badosa E, Amblard D, Nuzzo S, Elmoutaouakkil A, Vico L, Peyrin F (2003) Excised bone structures in mice: imaging at three-dimensional synchrotron radiation micro CT. Radiology 229:921-928.

Matarazzo V, Cohen D, Palmer AM, Simpson PJ, Khokhar B, Pan SJ, Ronnett GV (2004) The transcriptional repressor Mecp2 regulates terminal neuronal differentiation. Mol Cell Neurosci 27:44-58.

McGraw CM, Samaco RC, Zoghbi HY (2011) Adult neural function requires MeCP2. Science 333:186.

McLeod F, Ganley R, Williams L, Selfridge J, Bird A, Cobb SR (2013) Reduced seizure threshold and altered network oscillatory properties in a mouse model of Rett syndrome. Neuroscience 231:195-205.

Meyers EN, Lewandoski M, Martin GR (1998) An Fgf8 mutant allelic series generated by Cre- and Flp-mediated recombination. Nat Genet 18:136-141.

Mikuni-Takagaki Y (1999) Mechanical responses and signal transduction pathways in stretched osteocytes. J Bone Miner Metab 17:57-60.

Miller SC, Jee WS (1987) The bone lining cell: a distinct phenotype? Calcif Tissue Int 41:1-5.

Miyake K, Yang C, Minakuchi Y, Ohori K, Soutome M, Hirasawa T, Kazuki Y, Adachi N, Suzuki S, Itoh M, Goto YI, Andoh T, Kurosawa H, Oshimura M, Sasaki M, Toyoda A, Kubota T (2013) Comparison of Genomic and Epigenomic Expression in Monozygotic Twins Discordant for Rett Syndrome. PLoS One 8:e66729.

Miyoshi H, Shimizu K, Kozu T, Maseki N, Kaneko Y, Ohki M (1991) t(8;21) breakpoints on chromosome 21 in acute myeloid leukemia are clustered within a limited region of a single gene, AML1. Proc Natl Acad Sci U S A 88:10431-10434.

Mnatzakanian GN, Lohi H, Munteanu I, Alfred SE, Yamada T, MacLeod PJ, Jones JR, Scherer SW, Schanen NC, Friez MJ, Vincent JB, Minassian BA (2004) A previously unidentified MECP2 open reading frame defines a new protein isoform relevant to Rett syndrome. Nat Genet 36:339-341.

Mohandas T, Sparkes RS, Shapiro LJ (1981) Reactivation of an inactive human X chromosome: evidence for X inactivation by DNA methylation. Science 211:393-396.

Moretti P, Zoghbi HY (2006) MeCP2 dysfunction in Rett syndrome and related disorders. Curr Opin Genet Dev 16:276-281.

Mori S, Sato T, Hara T, Nakashima K, Minagi S (1997) Effect of continuous pressure on histopathological changes in denture-supporting tissues. J Oral Rehabil 24:37-46.

Motil KJ, Schultz RJ, Abrams S, Ellis KJ, Glaze DG (2006) Fractional calcium absorption is increased in girls with Rett syndrome. J Pediatr Gastroenterol Nutr 42:419-426.

Motil KJ, Ellis KJ, Barrish JO, Caeg E, Glaze DG (2008) Bone mineral content and bone mineral density are lower in older than in younger females with Rett syndrome. Pediatr Res 64:435-439.

Motil KJ, Barrish JO, Lane J, Geerts SP, Annese F, McNair L, Percy AK, Skinner SA, Neul JL, Glaze DG (2011) Vitamin d deficiency is prevalent in girls and women with rett syndrome. J Pediatr Gastroenterol Nutr 53:569-574.

Motil KJ, Caeg E, Barrish JO, Geerts S, Lane JB, Percy AK, Annese F, McNair L, Skinner SA, Lee HS, Neul JL, Glaze DG (2012) Gastrointestinal And Nutritional Problems Occur Frequently Throughout Life In Girls And Women With Rett Syndrome. J Pediatr Gastroenterol Nutr.

Müller R, Van Campenhout H, Van Damme B, Van Der Perre G, Dequeker J, Hildebrand T, Rüegsegger P (1998) Morphometric analysis of human bone biopsies: a quantitative structural comparison of histological sections and micro-computed tomography. Bone 23:59-66.

Na ES, Monteggia LM (2011) The role of MeCP2 in CNS development and function. Horm Behav 59:364-368.

Nagy A (2000) Cre recombinase: the universal reagent for genome tailoring. Genesis 26:99-109.

Nagy A, Moens C, Ivanyi E, Pawling J, Gertsenstein M, Hadjantonakis AK, Pirity M, Rossant J (1998) Dissecting the role of N-myc in development using a single targeting vector to generate a series of alleles. Curr Biol 8:661-664.

Naim MM (2011) Histological assessment of zoledronic acid (Aclasta) in protection against induced osteoporosis in female albino rats. The Egyptian journal of Histology 34:129-138.

Nakamura I, Rodan GA, Duong lT (2003) Regulatory mechanism of osteoclast activation. J Electron Microsc (Tokyo) 52:527-533.

Nakashima T (2014) [Coupling and communication between bone cells]. Clin Calcium 24:853-861.

Nan X, Tate P, Li E, Bird A (1996) DNA methylation specifies chromosomal localization of MeCP2. Mol Cell Biol 16:414-421.

Nan X, Ng HH, Johnson CA, Laherty CD, Turner BM, Eisenman RN, Bird A (1998a) Transcriptional repression by the methyl-CpG-binding protein MeCP2 involves a histone deacetylase complex. Nature 393:386-389.

Nan X, Ng HH, Johnson CA, Laherty CD, Turner BM, Eisenman RN, Bird A (1998b) Transcriptional repression by the methyl-CpG-binding protein MeCP2 involves a histone deacetylase complex. Nature 393:386-389.

Nazarian A, von Stechow D, Zurakowski D, Müller R, Snyder BD (2008) Bone volume fraction explains the variation in strength and stiffness of cancellous bone affected by metastatic cancer and osteoporosis. Calcif Tissue Int 83:368-379.

Neul JL, Zoghbi HY (2004) Rett syndrome: a prototypical neurodevelopmental disorder. Neuroscientist 10:118-128.

Neul JL, Kaufmann WE, Glaze DG, Christodoulou J, Clarke AJ, Bahi-Buisson N, Leonard H, Bailey ME, Schanen NC, Zappella M, Renieri A, Huppke P, Percy AK, Consortium R (2010) Rett syndrome: revised diagnostic criteria and nomenclature. Ann Neurol 68:944-950.

Ng AH, Wang SX, Turner CH, Beamer WG, Grynpas MD (2007) Bone quality and bone strength in BXH recombinant inbred mice. Calcif Tissue Int 81:215-223.

Nguyen MV, Du F, Felice CA, Shan X, Nigam A, Mandel G, Robinson JK, Ballas N (2012) MeCP2 is critical for maintaining mature neuronal networks and global brain anatomy during late stages of postnatal brain development and in the mature adult brain. J Neurosci 32:10021-10034.

Nicolella DP, Bonewald LF, Moravits DE, Lankford J (2005) Measurement of microstructural strain in cortical bone. Eur J Morphol 42:23-29.

Nikitina T, Shi X, Ghosh RP, Horowitz-Scherer RA, Hansen JC, Woodcock CL (2007) Multiple modes of interaction between the methylated DNA binding protein MeCP2 and chromatin. Mol Cell Biol 27:864-877.

Niyibizi C, Eyre DR (1989) Bone type V collagen: chain composition and location of a trypsin cleavage site. Connect Tissue Res 20:247-250.

Niyibizi C, Eyre DR (1994) Structural characteristics of cross-linking sites in type V collagen of bone. Chain specificities and heterotypic links to type I collagen. Eur J Biochem 224:943-950.

Nomura Y (2005) Early behavior characteristics and sleep disturbance in Rett syndrome. Brain Dev 27 Suppl 1:S35-S42.

Nutt SL, Heavey B, Rolink AG, Busslinger M (1999) Commitment to the B-lymphoid lineage depends on the transcription factor Pax5. Nature 401:556-562.

O'Brien MJ, Keating NM, Elderiny S, Cerda S, Keaveny AP, Afdhal NH, Nunes DP (2000) An assessment of digital image analysis to measure fibrosis in liver biopsy specimens of patients with chronic hepatitis C. Am J Clin Pathol 114:712-718.

O'Connor RD, Zayzafoon M, Farach-Carson MC, Schanen NC (2009a) Mecp2 deficiency decreases bone formation and reduces bone volume in a rodent model of Rett syndrome. Bone 45:346-356.

O'Connor RD, Zayzafoon M, Farach-Carson MC, Schanen NC (2009b) Mecp2 deficiency decreases bone formation and reduces bone volume in a rodent model of Rett syndrome. Bone 45:346-356.

Oddy WH, Webb KG, Baikie G, Thompson SM, Reilly S, Fyfe SD, Young D, Anderson AM, Leonard H (2007) Feeding experiences and growth status in a Rett syndrome population. J Pediatr Gastroenterol Nutr 45:582-590.

Ogawa E, Inuzuka M, Maruyama M, Satake M, Naito-Fujimoto M, Ito Y, Shigesada K (1993) Molecular cloning and characterization of PEBP2 beta, the heterodimeric partner of a novel Drosophila runt-related DNA binding protein PEBP2 alpha. Virology 194:314-331.

Oldberg A, Franzén A, Heinegård D (1986) Cloning and sequence analysis of rat bone sialoprotein (osteopontin) cDNA reveals an Arg-Gly-Asp cell-binding sequence. Proc Natl Acad Sci U S A 83:8819-8823.

Olson CO, Zachariah RM, Ezeonwuka CD, Liyanage VR, Rastegar M (2014) Brain region-specific expression of MeCP2 isoforms correlates with DNA methylation within Mecp2 regulatory elements. PLoS One 9:e90645.

Otto F, Thornell AP, Crompton T, Denzel A, Gilmour KC, Rosewell IR, Stamp GW, Beddington RS, Mundlos S, Olsen BR, Selby PB, Owen MJ (1997) Cbfa1, a candidate gene for cleidocranial dysplasia syndrome, is essential for osteoblast differentiation and bone development. Cell 89:765-771.

Owen TA, Aronow M, Shalhoub V, Barone LM, Wilming L, Tassinari MS, Kennedy MB, Pockwinse S, Lian JB, Stein GS (1990) Progressive development of the rat osteoblast phenotype in vitro: reciprocal relationships in expression of genes associated with osteoblast proliferation and differentiation during formation of the bone extracellular matrix. J Cell Physiol 143:420-430.

Palle S, Chappard D, Vico L, Riffat G, Alexandre C (1989) Evaluation of the osteoclastic population in iliac crest biopsies from 36 normal subjects: a histoenzymologic and histomorphometric study. J Bone Miner Res 4:501-506.

Palmer A, Qayumi J, Ronnett G (2008) MeCP2 mutation causes distinguishable phases of acute and chronic defects in synaptogenesis and maintenance, respectively. Mol Cell Neurosci 37:794-807.

Parfitt AM (1994) Osteonal and hemi-osteonal remodeling: the spatial and temporal framework for signal traffic in adult human bone. J Cell Biochem 55:273-286.

Parfitt AM, Mundy GR, Roodman GD, Hughes DE, Boyce BF (1996) A new model for the regulation of bone resorption, with particular reference to the effects of bisphosphonates. J Bone Miner Res 11:150-159.

Pavalko FM, Norvell SM, Burr DB, Turner CH, Duncan RL, Bidwell JP (2003) A model for mechanotransduction in bone cells: the load-bearing mechanosomes. J Cell Biochem 88:104-112.

Pelka GJ, Watson CM, Radziewic T, Hayward M, Lahooti H, Christodoulou J, Tam PP (2006) Mecp2 deficiency is associated with learning and cognitive deficits and altered gene activity in the hippocampal region of mice. Brain 129:887-898.

Percy AK, Lee HS, Neul JL, Lane JB, Skinner SA, Geerts SP, Annese F, Graham J, McNair L, Motil KJ, Barrish JO, Glaze DG (2010) Profiling scoliosis in Rett syndrome. Pediatr Res 67:435-439.

Philippe C, Villard L, De Roux N, Raynaud M, Bonnefond JP, Pasquier L, Lesca G, Mancini J, Jonveaux P, Moncla A, Chelly J, Bienvenu T (2006) Spectrum and distribution of MECP2 mutations in 424 Rett syndrome patients: a molecular update. Eur J Med Genet 49:9-18.

Picard D (1994) Regulation of protein function through expression of chimaeric proteins. Curr Opin Biotechnol 5:511-515.

Pittenger MF, Mackay AM, Beck SC, Jaiswal RK, Douglas R, Mosca JD, Moorman MA, Simonetti DW, Craig S, Marshak DR (1999) Multilineage potential of adult human mesenchymal stem cells. Science 284:143-147.

Plöchl E, Sperl W, Wermuth B, Colombo JP (1996) [Carnitine deficiency and carnitine therapy in a patient with Rett syndrome]. Klin Padiatr 208:129-134.

Puchtler H, Waldrop FS, Valentine LS (1973) Polarization microscopic studies of connective tissue stained with picro-sirius red FBA. Beitr Pathol 150:174-187.

Quiros-Gonzalez I, Yadav VK (2014) Central genes, pathways and modules that regulate bone mass. Arch Biochem Biophys.

Rastegar M, Hotta A, Pasceri P, Makarem M, Cheung AY, Elliott S, Park KJ, Adachi M, Jones FS, Clarke ID, Dirks P, Ellis J (2009) MECP2 isoform-specific vectors with regulated expression for Rett syndrome gene therapy. PLoS One 4:e6810.

Rauchenzauner M, Schmid A, Heinz-Erian P, Kapelari K, Falkensammer G, Griesmacher A, Finkenstedt G, Högler W (2007) Sex- and age-specific reference curves for serum markers of bone turnover in healthy children from 2 months to 18 years. J Clin Endocrinol Metab 92:443-449.

Reichwald K, Thiesen J, Wiehe T, Weitzel J, Poustka WA, Rosenthal A, Platzer M, Strätling WH, Kioschis P (2000) Comparative sequence analysis of the MECP2-locus in human and mouse reveals new transcribed regions. Mamm Genome 11:182-190.

Reilly S, Cass H (2001) Growth and nutrition in Rett syndrome. Disabil Rehabil 23:118-128.

Reseland JE, Syversen U, Bakke I, Qvigstad G, Eide LG, Hjertner O, Gordeladze JO, Drevon CA (2001) Leptin is expressed in and secreted from primary cultures of human osteoblasts and promotes bone mineralization. J Bone Miner Res 16:1426-1433.

Rett A (1966) [On a unusual brain atrophy syndrome in hyperammonemia in childhood]. Wien Med Wochenschr 116:723-726.

Reznikov N, Shahar R, Weiner S (2014) Three-dimensional structure of human lamellar bone: the presence of two different materials and new insights into the hierarchical organization. Bone 59:93-104.

Rezzonico R, Cayatte C, Bourget-Ponzio I, Romey G, Belhacene N, Loubat A, Rocchi S, Van Obberghen E, Girault JA, Rossi B, Schmid-Antomarchi H (2003) Focal adhesion kinase pp125FAK interacts with the large conductance calcium-activated hSlo potassium channel in human osteoblasts: potential role in mechanotransduction. J Bone Miner Res 18:1863-1871.

Rho JY, Kuhn-Spearing L, Zioupos P (1998) Mechanical properties and the hierarchical structure of bone. Med Eng Phys 20:92-102.

Riise R, Brox JI, Sorensen R, Skjeldal OH (2011) Spinal deformity and disability in patients with Rett syndrome. Dev Med Child Neurol 53:653-657.

Roberts AP, Conner AN (1988) Orthopaedic aspects of Rett's syndrome: brief report. J Bone Joint Surg Br 70:674.

Robinson L, Guy J, McKay L, Brockett E, Spike RC, Selfridge J, De Sousa D, Merusi C, Riedel G, Bird A, Cobb SR (2012a) Morphological and functional reversal of phenotypes in a mouse model of Rett syndrome. Brain.

Robinson L, Guy J, McKay L, Brockett E, Spike RC, Selfridge J, De Sousa D, Merusi C, Riedel G, Bird A, Cobb SR (2012b) Morphological and functional reversal of phenotypes in a mouse model of Rett syndrome. Brain 135:2699-2710.

Roende G, Ravn K, Fuglsang K, Andersen H, Nielsen JB, Brøndum-Nielsen K, Jensen JE (2011a) DXA measurements in Rett syndrome reveal small bones with low bone mass. J Bone Miner Res 26:2280-2286.

Roende G, Ravn K, Fuglsang K, Andersen H, Vestergaard A, Brondum-Nielsen K, Jensen J-EB, Nielsen JB (2011b) Patients With Rett Syndrome Sustain Low-Energy Fractures. Pediatric Research 69:359-364.

Roende G, Petersen J, Ravn K, Fuglsang K, Andersen H, Nielsen JB, Brondum-Nielsen K, Jensen JE (2013a) Low bone turnover phenotype in Rett syndrome: Results of biochemical bone marker analysis. Pediatr Res.

Roende G, Petersen J, Ravn K, Fuglsang K, Andersen H, Nielsen JB, Brøndum-Nielsen K, Jensen JE (2013b) Low bone turnover phenotype in Rett syndrome: Results of biochemical bone marker analysis. Pediatr Res.

Roende G, Petersen J, Ravn K, Fuglsang K, Andersen H, Nielsen JB, Brøndum-Nielsen K, Jensen JE (2014) Low bone turnover phenotype in Rett syndrome: results of biochemical bone marker analysis. Pediatr Res 75:551-558.

Rossant J, Nagy A (1995) Genome engineering: the new mouse genetics. Nat Med 1:592-594.

Rossant J, McMahon A (1999) "Cre"-ating mouse mutants-a meeting review on conditional mouse genetics. Genes Dev 13:142-145.

Roux JC, Panayotis N, Dura E, Villard L (2010) Progressive noradrenergic deficits in the locus coeruleus of Mecp2 deficient mice. J Neurosci Res 88:1500-1509.

Rubin MA, Rubin J, Jasiuk I (2004) SEM and TEM study of the hierarchical structure of C57BL/6J and C3H/HeJ mice trabecular bone. Bone 35:11-20.

Samaco RC, Fryer JD, Ren J, Fyffe S, Chao HT, Sun Y, Greer JJ, Zoghbi HY, Neul JL (2008) A partial loss of function allele of methyl-CpG-binding protein 2 predicts a human neurodevelopmental syndrome. Hum Mol Genet 17:1718-1727.

Sato T, Hara T, Mori S, Shirai H, Minagi S (1998) Threshold for bone resorption induced by continuous and intermittent pressure in the rat hard palate. J Dent Res 77:387-392.

Sauer B (1998) Inducible gene targeting in mice using the Cre/lox system. Methods 14:381-392.

Sawyer A, Lott P, Titrud J, McDonald J (2003) Quantification of tartrate resistant acid phosphatase distribution in mouse tibiae using image analysis. Biotech Histochem 78:271-278.

Schmid RS, Tsujimoto N, Qu Q, Lei H, Li E, Chen T, Blaustein CS (2008) A methyl-CpG-binding protein 2-enhanced green fluorescent protein reporter mouse model provides a new tool for studying the neuronal basis of Rett syndrome. Neuroreport 19:393-398.

Schultz RJ, Glaze DG, Motil KJ, Armstrong DD, del Junco DJ, Hubbard CR, Percy AK (1993) The pattern of growth failure in Rett syndrome. Am J Dis Child 147:633-637.

Seeman E (2008a) Bone quality: the material and structural basis of bone strength. J Bone Miner Metab 26:1-8.

Seeman E (2008b) Bone quality: the material and structural basis of bone strength. J Bone Miner Metab 26:1-8.

Seeman E, Delmas PD (2006) Bone quality--the material and structural basis of bone strength and fragility. N Engl J Med 354:2250-2261.

Shahbazian M, Young J, Yuva-Paylor L, Spencer C, Antalffy B, Noebels J, Armstrong D, Paylor R, Zoghbi H (2002a) Mice with truncated MeCP2 recapitulate many Rett syndrome features and display hyperacetylation of histone H3. Neuron 35:243-254.

Shahbazian MD, Antalffy B, Armstrong DL, Zoghbi HY (2002b) Insight into Rett syndrome: MeCP2 levels display tissue- and cell-specific differences and correlate with neuronal maturation. Hum Mol Genet 11:115-124.

Shapiro F (2008) Bone development and its relation to fracture repair. The role of mesenchymal osteoblasts and surface osteoblasts. Eur Cell Mater 15:53-76.

Shapiro JR, Bibat G, Hiremath G, Blue ME, Hundalani S, Yablonski T, Kantipuly A, Rohde C, Johnston M, Naidu S (2010) Bone mass in Rett syndrome: association with clinical parameters and MECP2 mutations. Pediatr Res 68:446-451.

Sharir A, Barak MM, Shahar R (2008) Whole bone mechanics and mechanical testing. Vet J 177:8-17.

Sheng MH, Baylink DJ, Beamer WG, Donahue LR, Lau KH, Wergedal JE (2002) Regulation of bone volume is different in the metaphyses of the femur and vertebra of C3H/HeJ and C57BL/6J mice. Bone 30:486-491.

Singh J, Saxena A, Christodoulou J, Ravine D (2008) MECP2 genomic structure and function: insights from ENCODE. Nucleic Acids Res 36:6035-6047.

Singleton MK, Gonzales ML, Leung KN, Yasui DH, Schroeder DI, Dunaway K, LaSalle JM (2011) MeCP2 is required for global heterochromatic and nucleolar changes during activity-dependent neuronal maturation. Neurobiol Dis 43:190-200.

Sirianni N, Naidu S, Pereira J, Pillotto RF, Hoffman EP (1998) Rett syndrome: confirmation of X-linked dominant inheritance, and localization of the gene to Xq28. Am J Hum Genet 63:1552-1558.

Skene PJ, Illingworth RS, Webb S, Kerr AR, James KD, Turner DJ, Andrews R, Bird AP (2010) Neuronal MeCP2 is expressed at near histone-octamer levels and globally alters the chromatin state. Molecular cell 37:457-468.

Skerry TM (2008) The response of bone to mechanical loading and disuse: fundamental principles and influences on osteoblast/osteocyte homeostasis. Arch Biochem Biophys 473:117-123.

Skerry TM, Bitensky L, Chayen J, Lanyon LE (1989) Early strain-related changes in enzyme activity in osteocytes following bone loading in vivo. J Bone Miner Res 4:783-788.

Smith R, Francis MJ, Bauze RJ (1975) Osteogenesis imperfecta. A clinical and biochemical study of a generalized connective tissue disorder. Q J Med 44:555-573.

Smith RM, Sadee W (2011) Synaptic signaling and aberrant RNA splicing in autism spectrum disorders. Front Synaptic Neurosci 3:1.

Smrt RD, Eaves-Egenes J, Barkho BZ, Santistevan NJ, Zhao C, Aimone JB, Gage FH, Zhao X (2007) Mecp2 deficiency leads to delayed maturation and altered gene expression in hippocampal neurons. Neurobiol Dis 27:77-89.

Smyk M, Obersztyn E, Nowakowska B, Nawara M, Cheung SW, Mazurczak T, Stankiewicz P, Bocian E (2008) Different-sized duplications of Xq28, including MECP2, in three males with mental retardation, absent or delayed speech, and recurrent infections. Am J Med Genet B Neuropsychiatr Genet 147B:799-806.

Stancheva I, Collins AL, Van den Veyver IB, Zoghbi H, Meehan RR (2003) A mutant form of MeCP2 protein associated with human Rett syndrome cannot be displaced from methylated DNA by notch in Xenopus embryos. Mol Cell 12:425-435.

Suda T, Takahashi N, Udagawa N, Jimi E, Gillespie MT, Martin TJ (1999) Modulation of osteoclast differentiation and function by the new members of the tumor necrosis factor receptor and ligand families. Endocr Rev 20:345-357.

Suresh S (2001) Graded materials for resistance to contact deformation and damage. Science 292:2447-2451.

Suzuki H, Matsuzaka T, Hirayama Y, Sakuragawa N, Arima M, Tateno A, Tojo M, Suzuki Y (1986) Rett's syndrome: progression of symptoms from infancy to childhood. J Child Neurol 1:137-141.

Swaminathan R (2001) Biochemical markers of bone turnover. Clin Chim Acta 313:95-105.

Szulc P, Seeman E, Delmas PD (2000) Biochemical measurements of bone turnover in children and adolescents. Osteoporos Int 11:281-294.

Takahashi N, Yamana H, Yoshiki S, Roodman GD, Mundy GR, Jones SJ, Boyde A, Suda T (1988) Osteoclast-like cell formation and its regulation by osteotropic hormones in mouse bone marrow cultures. Endocrinology 122:1373-1382.

Takeda S, Elefteriou F, Levasseur R, Liu X, Zhao L, Parker KL, Armstrong D, Ducy P, Karsenty G (2002) Leptin regulates bone formation via the sympathetic nervous system. Cell 111:305-317.

Takuwa Y, Ohse C, Wang EA, Wozney JM, Yamashita K (1991) Bone morphogenetic protein-2 stimulates alkaline phosphatase activity and collagen synthesis in cultured osteoblastic cells, MC3T3-E1. Biochem Biophys Res Commun 174:96-101.

Tang B, Ngan AH, Lu WW (2007) An improved method for the measurement of mechanical properties of bone by nanoindentation. J Mater Sci Mater Med 18:1875-1881.

Tao J, Hu K, Chang Q, Wu H, Sherman NE, Martinowich K, Klose RJ, Schanen C, Jaenisch R, Wang W, Sun YE (2009) Phosphorylation of MeCP2 at Serine

80 regulates its chromatin association and neurological function. Proc Natl Acad Sci U S A 106:4882-4887.

Tarbell JM, Weinbaum S, Kamm RD (2005) Cellular fluid mechanics and mechanotransduction. Ann Biomed Eng 33:1719-1723.

Tashjian AH, Goltzman D (2008) On the interpretation of rat carcinogenicity studies for human PTH(1-34) and human PTH(1-84). J Bone Miner Res 23:803-811.

Tatsumi S, Ishii K, Amizuka N, Li M, Kobayashi T, Kohno K, Ito M, Takeshita S, Ikeda K (2007) Targeted ablation of osteocytes induces osteoporosis with defective mechanotransduction. Cell Metab 5:464-475.

Teitelbaum SL (2000) Bone resorption by osteoclasts. Science 289:1504-1508.

Temudo T, Ramos E, Dias K, Barbot C, Vieira JP, Moreira A, Calado E, Carrilho I, Oliveira G, Levy A, Fonseca M, Cabral A, Cabral P, Monteiro JP, Borges L, Gomes R, Santos M, Sequeiros J, Maciel P (2008) Movement disorders in Rett syndrome: an analysis of 60 patients with detected MECP2 mutation and correlation with mutation type. Mov Disord 23:1384-1390.

Temudo T et al. (2007) Stereotypies in Rett syndrome: analysis of 83 patients with and without detected MECP2 mutations. Neurology 68:1183-1187.

Terai K, Takano-Yamamoto T, Ohba Y, Hiura K, Sugimoto M, Sato M, Kawahata H, Inaguma N, Kitamura Y, Nomura S (1999) Role of osteopontin in bone remodeling caused by mechanical stress. J Bone Miner Res 14:839-849.

Thomas GP, Baker SU, Eisman JA, Gardiner EM (2001) Changing RANKL/OPG mRNA expression in differentiating murine primary osteoblasts. J Endocrinol 170:451-460.

Thomson BM, Saklatvala J, Chambers TJ (1986) Osteoblasts mediate interleukin 1 stimulation of bone resorption by rat osteoclasts. J Exp Med 164:104-112.

Tian QX, Huang GY, Zhou JL, Liu QH, DU XR (2007) [Effects of calcitonin on osteoblast cell proliferation and OPG/RANKL expression: experiment with mouse osteoblasts]. Zhonghua Yi Xue Za Zhi 87:1501-1505.

Trappe R, Laccone F, Cobilanschi J, Meins M, Huppke P, Hanefeld F, Engel W (2001) MECP2 mutations in sporadic cases of Rett syndrome are almost exclusively of paternal origin. Am J Hum Genet 68:1093-1101.

Tuchman S, Thayu M, Shults J, Zemel BS, Burnham JM, Leonard MB (2008) Interpretation of biomarkers of bone metabolism in children: impact of growth velocity and body size in healthy children and chronic disease. J Pediatr 153:484-490.

Turner CH (2006) Bone strength: current concepts. Ann N Y Acad Sci 1068:429-446.

van der Linden JC, Homminga J, Verhaar JA, Weinans H (2001) Mechanical consequences of bone loss in cancellous bone. J Bone Miner Res 16:457-465.

van der Rest M, Garrone R (1991) Collagen family of proteins. FASEB J 5:2814-2823.

Van Esch H, Bauters M, Ignatius J, Jansen M, Raynaud M, Hollanders K, Lugtenberg D, Bienvenu T, Jensen LR, Gecz J, Moraine C, Marynen P, Fryns JP, Froyen G (2005) Duplication of the MECP2 region is a frequent cause of severe mental retardation and progressive neurological symptoms in males. Am J Hum Genet 77:442-453.

Vashishth D (2008) Small animal bone biomechanics. Bone 43:794-797.

Vatsa A, Smit TH, Klein-Nulend J (2007) Extracellular NO signalling from a mechanically stimulated osteocyte. J Biomech 40 Suppl 1:S89-95.

Vatsa A, Semeins CM, Smit TH, Klein-Nulend J (2008) Paxillin localisation in osteocytes--is it determined by the direction of loading? Biochem Biophys Res Commun 377:1019-1024.

Vatsa A, Mizuno D, Smit TH, Schmidt CF, MacKintosh FC, Klein-Nulend J (2006) Bio imaging of intracellular NO production in single bone cells after mechanical stimulation. J Bone Miner Res 21:1722-1728.

Vezeridis PS, Semeins CM, Chen Q, Klein-Nulend J (2006) Osteocytes subjected to pulsating fluid flow regulate osteoblast proliferation and differentiation. Biochem Biophys Res Commun 348:1082-1088.

Waarsing JH, Day JS, Weinans H (2004) An improved segmentation method for in vivo microCT imaging. J Bone Miner Res 19:1640-1650.

Wakefield RI, Smith BO, Nan X, Free A, Soteriou A, Uhrin D, Bird AP, Barlow PN (1999) The solution structure of the domain from MeCP2 that binds to methylated DNA. J Mol Biol 291:1055-1065.

Wakita T, Taya C, Katsume A, Kato J, Yonekawa H, Kanegae Y, Saito I, Hayashi Y, Koike M, Kohara M (1998) Efficient conditional transgene expression in hepatitis C virus cDNA transgenic mice mediated by the Cre/loxP system. J Biol Chem 273:9001-9006.

Wallace JM, Rajachar RM, Allen MR, Bloomfield SA, Robey PG, Young MF, Kohn DH (2007) Exercise-induced changes in the cortical bone of growing mice are bone- and gender-specific. Bone 40:1120-1127.

Walsh BJ, Thornton SC, Penny R, Breit SN (1992) Microplate reader-based quantitation of collagens. Anal Biochem 203:187-190.

Wan M, Lee SS, Zhang X, Houwink-Manville I, Song HR, Amir RE, Budden S, Naidu S, Pereira JL, Lo IF, Zoghbi HY, Schanen NC, Francke U (1999) Rett syndrome and beyond: recurrent spontaneous and familial MECP2 mutations at CpG hotspots. Am J Hum Genet 65:1520-1529.

Wang X, Shen X, Li X, Agrawal CM (2002) Age-related changes in the collagen network and toughness of bone. Bone 31:1-7.

Weaving LS, Williamson SL, Bennetts B, Davis M, Ellaway CJ, Leonard H, Thong MK, Delatycki M, Thompson EM, Laing N, Christodoulou J (2003) Effects of MECP2 mutation type, location and X-inactivation in modulating Rett syndrome phenotype. Am J Med Genet A 118A:103-114.

Webb T, Latif F (2001) Rett syndrome and the MECP2 gene. J Med Genet 38:217-223.

Webb T, Clarke A, Hanefeld F, Pereira JL, Rosenbloom L, Woods CG (1998) Linkage analysis in Rett syndrome families suggests that there may be a critical region at Xq28. J Med Genet 35:997-1003.

Weinstein RS, Hutson MS (1987) Decreased trabecular width and increased trabecular spacing contribute to bone loss with aging. Bone 8:137-142.

Wellik DM, Capecchi MR (2003) Hox10 and Hox11 genes are required to globally pattern the mammalian skeleton. Science 301:363-367.

Wergedal JE, Ackert-Bicknell CL, Tsaih SW, Sheng MH, Li R, Mohan S, Beamer WG, Churchill GA, Baylink DJ (2006) Femur mechanical properties in the F2 progeny of an NZB/B1NJ x RF/J cross are regulated predominantly by genetic loci that regulate bone geometry. J Bone Miner Res 21:1256-1266.

Wesolowski G, Duong LT, Lakkakorpi PT, Nagy RM, Tezuka K, Tanaka H, Rodan GA, Rodan SB (1995) Isolation and characterization of highly enriched, prefusion mouse osteoclastic cells. Exp Cell Res 219:679-686.

Whittaker P, Kloner RA, Boughner DR, Pickering JG (1994) Quantitative assessment of myocardial collagen with picrosirius red staining and circularly polarized light. Basic Res Cardiol 89:397-410.

Witt Engerström I (1992) Age-related occurrence of signs and symptoms in the Rett syndrome. Brain Dev 14 Suppl:S11-20.

Wolpowitz D, Mason TB, Dietrich P, Mendelsohn M, Talmage DA, Role LW (2000) Cysteine-rich domain isoforms of the neuregulin-1 gene are required for maintenance of peripheral synapses. Neuron 25:79-91.

Wright M, Thursz M, Pullen R, Thomas H, Goldin R (2003) Quantitative versus morphological assessment of liver fibrosis: semi-quantitative scores are more robust than digital image fibrosis area estimation. Liver Int 23:28-34.

Xiang F, Zhang Z, Clarke A, Joseluiz P, Sakkubai N, Sarojini B, Delozier-Blanchet CD, Hansmann I, Edström L, Anvret M (1998) Chromosome mapping of Rett syndrome: a likely candidate region on the telomere of Xq. J Med Genet 35:297-300.

Xiao Z, Zhang S, Mahlios J, Zhou G, Magenheimer BS, Guo D, Dallas SL, Maser R, Calvet JP, Bonewald L, Quarles LD (2006) Cilia-like structures and

polycystin-1 in osteoblasts/osteocytes and associated abnormalities in skeletogenesis and Runx2 expression. J Biol Chem 281:30884-30895.

Xie Q, Ainamo A, Tilvis R (1997) Association of residual ridge resorption with systemic factors in home-living elderly subjects. Acta Odontol Scand 55:299-305.

Xinhua Bao, Shengling Jiang, Fuying Song, Hong Pan, Meirong Li, Wu XR (2008) X chromosome inactivation in Rett Syndrome and its correlations with MECP2 mutations and phenotype. J Child Neurol 23:22-25.

Yamaguchi A, Komori T, Suda T (2000) Regulation of osteoblast differentiation mediated by bone morphogenetic proteins, hedgehogs, and Cbfa1. Endocr Rev 21:393-411.

Yano S, Yamashita Y, Matsuishi T, Abe T, Yamada S, Shinohara M (1991) Four adult Rett patients at an institution for the handicapped. Pediatr Neurol 7:289-292.

Yasuda H, Shima N, Nakagawa N, Yamaguchi K, Kinosaki M, Mochizuki S, Tomoyasu A, Yano K, Goto M, Murakami A, Tsuda E, Morinaga T, Higashio K, Udagawa N, Takahashi N, Suda T (1998) Osteoclast differentiation factor is a ligand for osteoprotegerin/osteoclastogenesis-inhibitory factor and is identical to TRANCE/RANKL. Proc Natl Acad Sci U S A 95:3597-3602.

Yoshida H, Hayashi S, Kunisada T, Ogawa M, Nishikawa S, Okamura H, Sudo T, Shultz LD (1990) The murine mutation osteopetrosis is in the coding region of the macrophage colony stimulating factor gene. Nature 345:442-444.

You J, Yellowley CE, Donahue HJ, Zhang Y, Chen Q, Jacobs CR (2000) Substrate deformation levels associated with routine physical activity are less stimulatory to bone cells relative to loading-induced oscillatory fluid flow. J Biomech Eng 122:387-393.

Young JI, Hong EP, Castle JC, Crespo-Barreto J, Bowman AB, Rose MF, Kang D, Richman R, Johnson JM, Berget S, Zoghbi HY (2005) Regulation of RNA splicing by the methylation-dependent transcriptional repressor methyl-CpG binding protein 2. Proc Natl Acad Sci U S A 102:17551-17558.

Yuan F, Stock SR, Haeffner DR, Almer JD, Dunand DC, Brinson LC (2011) A new model to simulate the elastic properties of mineralized collagen fibril. Biomech Model Mechanobiol 10:147-160.

Zachariah RM, Rastegar M (2012) Linking epigenetics to human disease and Rett syndrome: the emerging novel and challenging concepts in MeCP2 research. Neural Plast 2012:415825.

Zhang X, Bao X, Zhang J, Zhao Y, Cao G, Pan H, Wei L, Wu X (2012) Molecular characteristics of Chinese patients with Rett syndrome. Eur J Med Genet 55:677-681.

Zhou Z, Hong EJ, Cohen S, Zhao WN, Ho HY, Schmidt L, Chen WG, Lin Y, Savner E, Griffith EC, Hu L, Steen JA, Weitz CJ, Greenberg ME (2006) Brain-specific phosphorylation of MeCP2 regulates activity-dependent Bdnf transcription, dendritic growth, and spine maturation. Neuron 52:255-269.

Ziv V, Weiner S (1994) Bone crystal sizes: a comparison of transmission electron microscopic and X-ray diffraction line width broadening techniques. Connect Tissue Res 30:165-175.

Zlatanova J (2005) MeCP2: the chromatin connection and beyond. Biochem Cell Biol 83:251-262.

Zysman L, Lotan M, Ben-Zeev B (2006) Osteoporosis in Rett syndrome: A study on normal values. ScientificWorldJournal 6:1619-1630.

.....